Thermal particle production in the early Universe

Dissertation

Submitted by:

Denis Besak

Fakultät für Physik,
Universität Bielefeld

June 2010

Referees: Prof.Dr.Dietrich Bödeker
Prof.Dr.Mikko Laine

Contents

Published work from thesis

The new results contained in this thesis are also published in the following articles:

[1] D.Besak, D.Bödeker, "Hard Thermal Loops with soft or collinear external momenta"
This article contains the derivation of the integral equation for the LPM effect in photon production. It serves to introduce the new method that is used in this work. This paper thus contains the essence of sections 3.3 and 3.4 as well as the relevant appendices.

[2] A.Anisimov, D.Besak, D.Bödeker, "The complete leading order high-temperature production rate of Majorana neutrinos"
This paper essentially contains what is presented in chapter 4 of this thesis. It presents the new results on the high-temperature particle production rate of Majorana neutrinos and compares them to the zero-temperature results.

1. Introduction

Who is in that house? I opened the door to see.
Who is up the stairs? I'm walking up foolishly.
Katie Melua - *The House*

The very early universe is a system of extraordinary complexity and very rich phenomenology, making it an ideal playground to test our understanding of the fundamental laws of nature and our ability to obtain precise answers to all the questions that we can ask within the framework of theoretical physics. If we knew everything that we need to know about the theories that govern the Universe in its present state and its history, then we could, provided we could somehow get the correct initial conditions, in principle make a simulation of everything that happened between the Big Bang and the present Universe–assuming sufficient machine power or patience to wait for the answer. However, Nature is still successful in limiting our knowledge, while our curiosity remains as unlimited as ever and we may hope that revealing all myths our Universe still has kept will only be a question of time.
At present however, it is fair to say that everything which happened before the time of Big Bang Nucleosynthesis (BBN) still has to be regarded as having speculative ingredients, with definite evidence still missing. Yet, there is a wide consensus that we know at least how to describe the fundamental interactions (strong, weak, electromagnetic and gravitational) and consequently we do have a theoretical framework to describe the evolution of the Universe starting at a time sufficiently far away from the Planck scale such that the lack of a consistent theory of quantum gravity is unproblematic and only a classical description in terms of General Relativity is needed.
Based on the vast observational data that was accumulated in the past decades and on their interpretation using our knowledge about the fundamental interactions, a 'mainstream' picture about the evolution of the Universe has emerged, sometimes called the 'Standard Model of Cosmology'. Within this standard paradigm, it is assumed that shortly after the Big Bang there was a period of *inflation* which lead to an exponential expansion of the Universe and left it in a state far from thermal equilbrium. After the period of inflation, the so-called *reheating* set in, which served to thermalize the constituents of the early universe and lead to a very hot and dense plasma. Its maximum temperature, the *reheating temperature*, is at present unknown. It can in principle be very high, e.g. something in the range of 10^9GeV $\sim 10^{22}$ K.
This moment in the evolution of the Universe is exactly where the phenomena that are considered in this work set in–particles which due to their weak coupling to the thermal bath have not yet come to equilibrium are very efficiently produced (and destroyed) via various decay and scattering processes involving the thermal bath, creating a population of these particles even if reheating was unable to do so, and eventually thermalizing them after a sufficiently long time. We speak of **thermal particle production**. It occurs not only in the early universe but also e.g. in heavy-ion collisions where it is believed that a quark-gluon plasma in thermal equilibrium is formed. Then thermal production of e.g. photons occurs and since they interact only very weakly with the constituents of the plasma, they can basically escape freely and give us information on the properties of the plasma that was formed. Computing thermal photon production from a quark-gluon plasma thus helps us to understand how the plasma is formed and how it behaves.
In the case of thermal particle production in the early universe the interest in quantitative predictions is a bit different, as they also help us to understand the state in which the Universe is now, when its temperature and density are so low that it can be thought of as a vacuum state instead of a hot and dense plasma. This is because it is crucial to understand and reproduce the observed amount of matter in the Universe from theoretical considerations. As explained in more detail in the introduction to chapter 4, the matter in the Universe consists predominantly of one (or several) unknown particle species, called *Dark Matter*, and of a smaller amount of baryonic matter whose nature is of course well understood. Dark Matter particles can be produced via various mechanisms in the early universe, one of them being thermal particle production. For baryonic matter, the striking feature is the *asymmetry* between baryons and antibaryons which is generated in the early universe by a mechanism called *baryogenesis* (for more details see again the introduction of chapter 4). There are various realizations of this mechanism, out of which we focus on *leptogenesis* where an asymmetry between leptons and antileptons is generated and later converted into a baryon asymmetry.

A successful implementation of leptogenesis requires the introduction of new particles, the *right-handed Majorana neutrinos* N_i, which are weakly coupled to the other particles in the plasma and are not in thermal equilibrium. They are thus produced via thermal particle production and computing their resulting number density is a necessary intermediate step in the computation of the final baryon asymmetry which can then be compared with what we observe. Chapter 4, which can be regarded as the main part of this thesis, precisely deals with calculating the number density of Majorana neutrinos produced in a hot thermal bath.
When doing such a calculation, one needs to take into account that the processes happen in a hot plasma and that in addition the particles have relativistic energies and that the interactions can only be described with quantum physics. The theoretical framework that is needed is thus *finite-temperature quantum field theory*, which differs from the 'ordinary' quantum field theory–needed e.g. for LHC phenomenology–that is valid in absence of a thermal bath. As the latter, it is inherently too complicated to allow for exact solutions to realistic problems and one has to resort to systematic approximations. Like for vacuum QFT, the method of choice is perturbation theory and it works in a similar way–one can still draw Feynman diagrams and translate them with a set of Feynman rules into mathematical expressions which can then be evaluated more or less straightforwardly. However, the presence of a thermal bath induces new features in the perturbative expansion that are not encountered at zero temperature and that render perturbation theory much more complicated. Because of this, no attempt is made in this work to do calculations beyond leading order in the relevant coupling constants. Even a leading order computation of the thermal production rate turns out to be a huge task because it already requires the resummation of a (countably) infinite set of Feynman diagrams. The physical phenomenon behind this is a quantum effect (with no classical analogue) which is known as **Landau-Pomeranchuk-Migdal (LPM) effect** after the people who described it more than 50 years ago in the context of cosmic rays [3, 4]. Its relevance for the thermal photon production rate in a quark-gluon plasma was discovered 10 years ago [5], and only one year later it was for the first time included in the computation of the thermal photon production rate [6, 7].
A treatment of the LPM effect in the production of other particles like DM candidates or the aforementioned Majorana neutrinos has not been performed so far. One of the main points of this work is to study the relevance of the LPM effect in the production of Majorana neutrinos as an example how the LPM effect modifies also the production rate of fermions. The method that is used to compute this modification is new, conceptually easier and much more general than the one introduced in [6]. It can also be used without conceptual modification to study how the LPM effect modifies the production rate of any other particles, e.g. possible DM candidates. The work presented here can thus be regarded as only a starting point for subsequent studies of particle production rates which are of phenomenological interest but which have been omitted here in order to keep the work at a reasonable length.

This thesis is organized as follows. Chapter 2 mostly serves as a brief introduction to quantum field theory in a thermal bath and the correct formulation of perturbation theory which is rendered more difficult than in vacuum due to IR and collinear divergences that appear frequently and require a reorganization of the perturbative series in order to obtain finite and thus physically meaningful results. The chapter also introduces the relevant set of Feynman diagrams needed for the computation of the LPM effect and puts them into a broader context, thus opening another door for possible future studies which could finally result in a new effective perturbation theory similar to the well-known HTL effective theory presented in section 2.2. Chapter 3 serves as a preparation for the computation in chapter 4. The master formula for the thermal production rate in terms of a retarded self-energy is explicitly derived and the connection to the Boltzmann equation is illustrated. Then the physics of the LPM effect is outlined and the relevance for the thermal particle production rate is established, thus making a connection to the presentation in section 2.3. Finally, everything is put together in section 3.3 where the new method to deal with the LPM effect is presented in detail (with some intermediate calculations moved to the appendix) and a general integral equation for the LPM effect is derived. As a consistency check, section 3.4 finally provides a proof that specifying the thermally produced particle to be a photon indeed leads to the equations already derived in [6]. The presentation culminates in chapter 4 where the complete leading-order thermal production rate of Majorana neutrinos is computed in the high-temperature limit $T \gg M_N$. The production rate includes both decay/recombination processes (section 4.3) where the LPM effect needs to be taken into account and $2 \leftrightarrow 2$ scattering processes (section 4.4) where it is irrelevant at leading order. Yet, these scattering processes also require some care due to IR divergences that occur and HTL resummation is needed to obtain meaningful results. The results for both parts of the production rate have never been reported in the literature so far. Subsequently, the Boltzmann equation is used to study the evolution of the number density of Majorana neutrinos. The results are in

addition compared with what would be obtained by neglecting all finite-temperature effects and performing all computations in vacuum, which is the approach chosen by many authors in leptogenesis calculations. In chapter 5 we finally summarize and give an outlook how the work presented here can be used as a basis for future investigations.
The appendices contain calculational details which would disturb the flow of reading if they were presented in the main text. In appendix B we derive the finite-temperature propagators for scalars, spin 1/2-fermions and gauge bosons in the kinematical limits that are needed for our purposes. Appendices C and D contain technical details needed to derive the integral equation for the LPM effect and appendices E and F finally contain some details that we need in order to obtain the production rate of Majorana neutrinos studied in chapter 4.

2. Quantum field theory in a hot thermal bath

36 Grad und es wird noch heißer.
2RAUMWOHNUNG - *36 Grad*

2.1. Perturbation theory at finite temperature

In this thesis we will be concerned with phenomena in the very early universe which is in a state of a *hot and dense plasma* in *thermal equilibrium*. The conventional Feynman rules that can be found in standard textbooks on quantum field theory [8] are valid in the vacuum and they need to be modified in the presence of a thermal bath. There are two major formalisms that have been set up to deal with such a situation.
In the *imaginary-time (Matsubara) formalism* one considers all fields as functions of imaginary time. This allows to use the conventional Feynman rules with only slight modifications. The disadvantage is that real-time observables then cannot be computed directly but have to be extracted via analytical continuation to the real time axis.
The *real-time (Schwinger-Keldysh) formalism* on the other hand is designed to compute everything in real time right away, thus avoiding the need for an analytical continuation to real values. However, for consistency it is necessary to double the degrees of freedom, thereby introducing 2x2 matrices as propagators and two different kinds of vertices, which makes the Feynman rules and calculations more involved.
Which formalism one chooses to perform computations in thermal equilibrium is merely a matter of personal taste while only the real-time formalism can be used for *nonequilibrium* phenomena. This is because the temperature, which plays a central role in the imaginary-time formalism, is never needed explicitly. For the phenomena that are the subject of this thesis, the imaginary-time formalism is sufficient and will be used throughout.
In section 2.1, we give a short review of the imaginary-time formalism, mostly in order to set the conventions and the notation that will be used throughout. In addition, we discuss important *momentum (energy) scales* in a thermal bath. Pedagogical introductions to the imaginary-time (and real-time) formalism in general can be found e.g. in [9, 10].

2.1.1. A short review of the imaginary-time formalism

The full information about a system of quantum fields is encoded in the set of all *n-point Green functions*

$$G^{(n)}(x_1,\ldots,x_n) \equiv \langle T_{\mathcal{C}}\,\{\phi(x_1)\ldots\phi(x_n)\}\rangle \tag{2.1}$$

where $\langle\cdots\rangle$ denotes a thermal average and the time ordering is along a complex time contour $\mathcal{C}$ [9]. In a thermal bath at temperature T which is described by the density matrix[1] $\hat{\rho} = \frac{1}{Z}e^{-\beta\hat{H}}$ with partition function $Z \equiv \mathrm{Tr}\, e^{-\beta\hat{H}}$, it has to start at some initial time t_i (usually chosen as $t_i = 0$) and go to a final time $t_f = t_i - i\beta$ where $\beta \equiv 1/T$ is the inverse temperature. The easiest possible contour for $\mathcal{C}$ is the *Matsubara contour*, which is just a straight line. Along this time path, only the imaginary part of the time varies, which explains the name 'imaginary-time formalism' already mentioned before. This formalism is by construction applicable only in thermal equilibrium with temperature T where the average that was written in (2.1) is given by

$$\langle A\rangle \equiv \mathrm{Tr}[\hat{\rho}A] = \frac{1}{Z}\,\mathrm{Tr}[e^{-\beta\hat{H}}A]. \tag{2.2}$$

The meaning of the average constitutes the crucial difference between quantum field theory in a thermal bath and quantum field theory in vacuum, where instead of (2.2) we only have a vacuum expectation value, $\langle A\rangle_{T=0} \equiv \langle 0|A|0\rangle$.

[1] The generalization to nonzero chemical potential is straightforward and can be found in the cited literature. It is irrelevant for the presentation here and we therefore always assume $\mu = 0$ for simplicity.

By interpreting $e^{-\beta\hat{H}}$ as time evolution operator in imaginary time, it is straightforward to derive a path integral expression for the Green functions:[2]

$$G^{(n)}(x_1,\ldots,x_n) = \frac{\int_{\phi(0,\vec{x}_i)=\phi(-i\beta,\vec{x}_i)} \mathcal{D}\phi\phi(x_1)\ldots\phi(x_n)e^{iS}}{\int_{\phi(0,\vec{x}_i)=\phi(-i\beta,\vec{x}_i)} \mathcal{D}\phi e^{iS}} \tag{2.3}$$

Because of the trace in (2.2), the path integral is restricted to field configurations that are *periodic* in imaginary time with period β.
We now take a closer look at the *propagator* (2-point function) in the Matsubara formalism. We can first define the *Wightman functions*

$$D^{>}(x,x') \equiv \langle\phi(x)\phi(x')\rangle, \quad D^{<}(x,x') \equiv \langle\phi(x')\phi(x)\rangle \tag{2.4}$$

which are both related due to the periodicity in imaginary time:

$$D^{>}(t,\vec{x};t',\vec{x}') = D^{<}(t+i\beta,\vec{x};t',\vec{x}') \tag{2.5}$$

This periodicity reflects the so-called *Kubo-Martin-Schwinger (KMS)* relation [11, 12]. The 'usual', real-time Feynman propagator would then be

$$D(x,x') \equiv \Theta(t-t')D^{>}(x,x') + \Theta(t'-t)D^{<}(x,x'). \tag{2.6}$$

In the Matsubara formalism, we define the *imaginary-time (Matsubara) propagator* by (suppressing the space dependence)

$$\Delta(\tau) \equiv D^{>}(-i\tau;0) \quad \tau\in[0;\beta]. \tag{2.7}$$

So far we have written everything in position space, but computations are like at zero temperature more conveniently performed in momentum space. Instead of the propagator (2.7) we should consider a propagator $\Delta(P)$ obtained by a Fourier transformation. Here the periodicity in imaginary time has an important consequence: For the time component of the momentum, we obtain *discrete values*, $p^0 = i\omega_n$ with *Matsubara frequencies* $\omega_n = 2\pi nT, n\in\mathbb{N}$. This also means that instead of a Fourier transformation w.r.t. time we get a discrete Fourier series while we still have a continous Fourier transformation for the spatial part. Consequently, the free (scalar) propagator is obtained as a straightforward generalization of the zero temperature result and reads

$$\Delta(P) = \frac{-1}{P^2-m^2} \tag{2.8}$$

where $P^\mu = (i\omega_n,\vec{p})$. Note that it differs from the zero-temperature propagator by a factor of i, as explained in appendix A. As the zeroth component only takes discrete values (which are in addition purely imaginary) the 'physical', real-time propagator is obtained after an *analytical continuation* to real and continuous values, which is described below.
It is useful to introduce the so-called *spectral function* which is defined in momentum space via (suppressing spatial components in the argument again)

$$\rho(p_0,\vec{p}) \equiv D^{>}(p_0,\vec{p}) - D^{<}(p_0,\vec{p}). \tag{2.9}$$

Using (2.5), which in momentum space becomes $D^{<}(p_0,\vec{p}) = e^{-\beta p_0}D^{>}(p_0,\vec{p})$, we obtain

$$D^{>}(p_0,\vec{p}) = (1+f_B(p_0))\rho(p_0,\vec{p}), \quad D^{<}(p_0,\vec{p}) = f_B(p_0)\rho(p_0,\vec{p}) \tag{2.10}$$

and by taking the Fourier transformation of (2.7) and inserting (2.10), we arrive at the *spectral representation* of the propagator,

$$\Delta(i\omega_n,\vec{p}) = \int_{-\infty}^{\infty}\frac{\mathrm{d}\omega}{2\pi}\frac{\rho(\omega,\vec{p})}{\omega-i\omega_n}, \tag{2.11}$$

that will prove useful later on. As it stands, the relation is valid for discrete values $p_0 = i\omega_n$, but it is also ideally suited for the analytical continuation to continuous, real values of p_0 obtained by merely replacing $i\omega_n \to p_0 \in \mathbb{R}$. In general, however, this continuation is *not* unique and an unambiguous result can only be obtained under the following assumptions:

[2] At the moment we focus on scalar fields and postpone the modifications for fermions and gauge bosons to the end of this subsection.

- For $p_0 \to \infty$, we have $|\Delta(p_0, \vec{p})| \to 0$
- Outside the real axis, the function $\Delta(p_0, \vec{p})$ is analytic

The proof involves complex analysis and is given in [13].
From the analytical continuation of (2.11), we can see that the spectral function is given by the *discontinuity* of the two-point function:

$$\rho(p_0, \vec{p}) = -i \,\mathrm{Disc}\, \Delta(p_0, \vec{p}) \equiv \Delta(p_0 + i\varepsilon, \vec{p}) - \Delta(p_0 - i\varepsilon, \vec{p}) \tag{2.12}$$

In order to see this, one only needs to recall the useful relation

$$\frac{1}{x \pm i\varepsilon} = \mathfrak{P}\left(\frac{1}{x}\right) \mp i\pi\delta(x) \tag{2.13}$$

where $\mathfrak{P}$ denotes the principal value and the limit $\varepsilon \to 0^+$ is implicitly understood. Defining the retarded propagator by $\Delta_{ret}(p_0, p) \equiv \lim_{\varepsilon \to 0^+} \Delta(p_0 + i\varepsilon, p)$, we can also write

$$\rho(p_0, \vec{p}) = 2 \,\mathrm{Im}\, \Delta_{ret}(p_0, \vec{p}). \tag{2.14}$$

This relation can be interpreted as a *fluctuation-dissipation relation* which is valid only in thermal equilibrium [14]. One can also easily deduce the spectral function of *free* scalar particles from (2.11):

$$\rho(p_0, \vec{p}) = 2\pi \,\mathrm{sgn}(p_0)\delta(P^2 - m^2) \tag{2.15}$$

Computing thermal sums

With the modification of the propagator (2.8) we are already more or less done with changing the Feynman rules compared to the $T = 0$ case. The essence of all vertex factors, remains unchanged, one only has to be careful that they contain an additional factor $-i$, as explained in appendix A. The only fundamental change is that as soon as we have loop diagrams, we need to perform a discrete sum over p^0 instead of an integral:

$$\int \frac{\mathrm{d}^4 P}{(2\pi)^4} \to T \sum_{p_0 = i\omega_n} \int \frac{\mathrm{d}^3 p}{(2\pi)^3} \tag{2.16}$$

We now turn to describe a method to deal with those so-called *thermal sums*. The most efficient way to

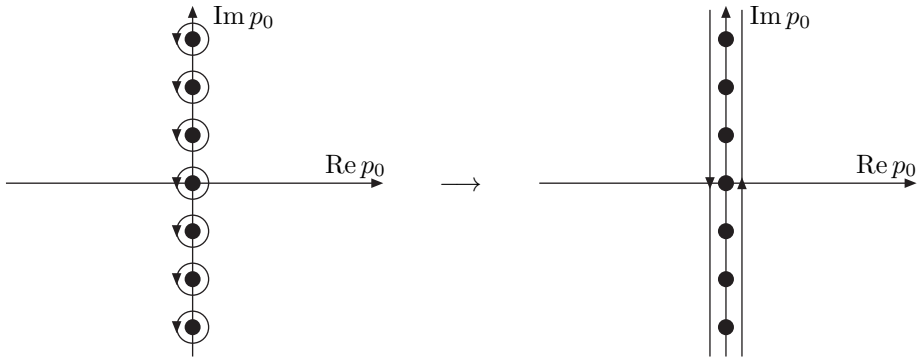

Figure 2.1.: Integration contour for the thermal summation formula (2.17).

compute thermal sums uses the method of residues to transform the sum into a complex contour integral. We obtain

$$T \sum_{p_0 = i\omega_n} g(p_0) = \int_C \frac{\mathrm{d}p_0}{2\pi i} \left(\frac{1}{2} + f_B(p_0)\right) g(p_0) \tag{2.17}$$

where the integration contour C is shown in figure 2.1 and consists of circles which enclose precisely one pole of the integrand each. It is easy to show that $\left(\frac{1}{2} + f_B(p_0)\right)$ indeed has poles with residue T whenever $p_0 = i\omega_n$, indicated by the blobs along the imaginary axis. The function $g(p_0)$ is assumed to be analytical

except for poles which lie on the *real* axis, and it has to vanish at infinity. Then we can deform the contour as indicated in the rightmost part of figure 2.1 and close it with large half-circles at infinity, thereby enclosing the poles of $g(p_0)$. The value of the integral is unchanged because the additional pieces of the integration contour do not contribute. Then only the poles coming from $g(p_0)$ contribute and the integral in (2.17) can easily be evaluated with the theorem of residues.
Let us look at some examples which will also be relevant for the calculations in this thesis. The easiest example is the case that we have to perform the sum (and subsequently also the loop integral over the spatial components) with one free propagator only. We take only a *massless* propagator, i.e. we set $m = 0$. This amounts to dropping terms of order m/T which is reasonable as long as $m \sim gT$ is a *thermal mass*.[3] In this case, we get

$$T\sum_{p_0}\int\frac{\mathrm{d}^3p}{(2\pi)^3}\Delta(P) = -\frac{T^2}{12} \tag{2.18}$$

which can easily be proved using (2.17).[4] The propagator has poles at $p^0 = \pm p$ and therefore we get

$$T\sum_{p_0}\int\frac{\mathrm{d}^3p}{(2\pi)^3}\Delta(P) = -\int\frac{\mathrm{d}^3p}{(2\pi)^3}\frac{1+2f_B(p)}{2p}.$$

The temperature independent part is in fact *UV-divergent* and one needs to apply the usual renormalization procedure to get a finite result. However, in this work we are exclusively interested in the high-temperature limit which means that such temperature-independent parts are negligible compared to the rest of the sum-integral, which behaves like T^2. We may therefore replace $1 + 2f_B(p) \to 2f_B(p)$ and assume that the zero-temperature part has been made finite by renormalization without the need to do this explicitly. It is only necessary to know that it is always possible–which is clear if the theory we consider (e.g. QCD or electroweak theory) is renormalizable. Performing the d^3p integration then leads to (2.18).
However, when dealing with loop diagrams we will typically have products of at least two propagators depending on p^0. An important technique to deal with such thermal sums is by using the *Saclay representation* of the propagators which is obtained via Fourier transformation w.r.t. imaginary time:

$$\Delta(\tau,\vec{p}) = T\sum_{p_0}e^{-p_0\tau}\Delta(p_0,\vec{p}); \quad \Delta(p_0,\vec{p}) = \int_0^\beta \mathrm{d}\tau e^{p_0\tau}\Delta(\tau,\vec{p}) \tag{2.19}$$

An explicit representation for $\Delta(\tau,\vec{p})$ can be derived by applying (2.17) to its definition:

$$\Delta(\tau,\vec{p}) = -\frac{1}{2E_{\vec{p}}}\left[(1+f_B(E_{\vec{p}}))e^{-E_{\vec{p}}\tau} + f_B(E_{\vec{p}})e^{E_{\vec{p}}\tau}\right] \tag{2.20}$$

This also allows for a clear physical interpretation of the propagator in *position space*: It describes the stimulated emission or absorption of scalar particles in a thermal bath and therefore clearly resembles its vacuum counterpart.[5]
The trick to compute thermal sum-integrals involving several propagators is now to replace them by their Saclay representations, which ultimately always leads to a trivial thermal sum of the form

$$T\sum_{p_0}e^{p_0(\tau-\tau')} = \delta(\tau-\tau'). \tag{2.21}$$

The 'price' for this simplification is that we have additional integrals over imaginary times. One of them is always trivial because of the delta function obtained from the thermal sum, but the rest has to be performed and can lead to cumbersome expressions if many propagators are involved. However, for the most important case of a product of two propagators, the computational effort is rather modest and one gets e.g. the following

[3] Examples for thermal masses will be shown in section 2.2 and 2.3.
[4] The minus sign comes from the definition (2.8). When comparing it e.g. to [9] where all computations are performed in *Euclidean space* instead of Minkowski space, one has to be careful because the overall sign of the propagator is different.
[5] Note that this interpretation is not restricted to the imaginary-time formalism–it also holds in real time.

result:

$$T\sum_{p_0}\int\frac{\mathrm{d}^3p}{(2\pi)^3}\Delta(P)\Delta(P-K)=\int\frac{\mathrm{d}^3p}{(2\pi)^3}\frac{1}{4E_1E_2}\Bigg[(1+f_B(E_1)+f_B(E_2))\left(\frac{1}{k^0-E_1-E_2}-\frac{1}{k^0+E_1+E_2}\right)$$
$$+(f_B(E_1)-f_B(E_2))\left(\frac{1}{k^0+E_1-E_2}-\frac{1}{k^0-E_1+E_2}\right)\Bigg] \tag{2.22}$$

An additional complication may arise due to powers of p_0, which come from the vertex factors, appearing in the numerator. This can be dealt with via an integration by parts, e.g.

$$p_0\Delta(p_0,\vec{k})=-\int_0^\beta e^{p_0\tau}\frac{\partial\Delta}{\partial\tau}\mathrm{d}\tau. \tag{2.23}$$

The surface term vanishes because of the periodicity properties of $\Delta(\tau,\vec{p})$. If we have p_0^n as prefactor, we get $(-1)^n$ times the n-th derivative of $\Delta(\tau,\vec{p})$ instead.
By using this additional trick, we can derive the following additional results that will be needed in this thesis, e.g. in appendix B:

$$T\sum_{p_0}\int\frac{\mathrm{d}^3p}{(2\pi)^3}p_0\Delta(P)\Delta(P-K)=-\int\frac{\mathrm{d}^3p}{(2\pi)^3}\frac{1}{4E_2}\Bigg[(1+f_B(E_1)+f_B(E_2))\left(\frac{1}{k^0-E_1-E_2}+\frac{1}{k^0+E_1+E_2}\right)$$
$$-(f_B(E_1)-f_B(E_2))\left(\frac{1}{k^0+E_1-E_2}+\frac{1}{k^0-E_1+E_2}\right)\Bigg] \tag{2.24}$$

$$T\sum_{p_0}\int\frac{\mathrm{d}^3p}{(2\pi)^3}p_0^2\Delta(P)\Delta(P-K)=\int\frac{\mathrm{d}^3p}{(2\pi)^3}\frac{E_1}{4E_2}\Bigg[(1+f_B(E_1)+f_B(E_2))\left(\frac{1}{k^0-E_1-E_2}-\frac{1}{k^0+E_1+E_2}\right)$$
$$+(f_B(E_1)-f_B(E_2))\left(\frac{1}{k^0+E_1-E_2}-\frac{1}{k^0-E_1+E_2}\right)\Bigg] \tag{2.25}$$

However, it can also happen that we need to compute 1-loop diagrams with *resummed* propagators, e.g. the HTL resummed propagators that are introduced in section 2.2. In this case, it is difficult to find the appropriate explicit representation that corresponds to (2.20). Therefore it is better to use the *spectral representation* (2.11) since spectral functions are easier to determine than explicit results for the Saclay representation of the full propagator. The dependence on p^0 is given only by simple rational functions then which also allows an efficient evaluation of thermal sums. It is also possible to combine the Saclay and spectral representation as is done e.g. in appendix F. Which method is the most efficient one depends on the concrete problem at hand and in the course of this thesis, all methods described here will be applied at least once.

Fermions

The formalism developed so far is only valid for *bosons*, more precisely for spin 0-particles. For spin 1 bosons, no fundamental changes are needed, only in the propagators we need to take the Lorentz structure into account, which is in general more complicated than in vacuum (see appendix B.3). For fermions, however, some fundamental changes arise that we finally need to describe. The basic change is that, as one can easily show [9], fermion fields need to be *antiperiodic* in imaginary time instead of periodic, i.e. $\psi(0,\vec{x})=-\psi(-i\beta,\vec{x})$. In the KMS relation (2.5), we then also obtain a minus sign on the rhs. Both of this ultimately results from the Grassmann nature of fermion fields. Therefore, we need to make the following modifications to the previous results:

- Replace the integer Matsubara frequencies by half-integer ones:

$$\omega_n\to\tilde{\omega}_n=2\pi\left(n+\frac{1}{2}\right)T \tag{2.26}$$

- Replace $f_B\to -f_F$ with Fermi-Dirac distribution f_F, e.g. in the formula (2.17) for the computation of thermal sums or the explicit examples considered thereafter. This also leads to a difference in the

sum-integral over one free propagator by a factor of -1/2:

$$T\sum_{\tilde{p}_0}\int\frac{\mathrm{d}^3p}{(2\pi)^3}\Delta(P)=\frac{T^2}{24} \tag{2.27}$$

With these two new rules for fermions, the modification of the Feynman rules is completed. However, in a thermal plasma new phenomena appear that lead to the breakdown of naive perturbation theory and require a more sophisticated treatment, which we turn to now.

2.1.2. Scales and effective theories

The naive perturbation theory described in section 2.1.1 only holds in certain kinematical regimes whereas there may be substantial modifications otherwise. This is due to the ubiquitious *IR and collinear divergences* that appear much more frequently in computations at finite temperature compared to the zero-temperature case (whereas there are no new UV divergences as already shown before). Their appearance signals a sensitivity to new physical phenomena, inherent to the hot and dense plasma, at a given order of perturbation theory.
In order to correctly describe particles in a hot thermal bath it is therefore necessary to modify perturbation theory more profoundly than outlined in the previous subsection. When doing so, one has to distinguish different momentum scales:

- The *hard* scale, $P\sim T, P^2\sim T^2$. This is the typical momentum scale of particles inside a plasma and the only one where the simple generalization of perturbation theory described before is fully valid. Particles with hard momenta are, at least at leading order in the perturbative expansion, not affected in their propagation by the thermal bath and move essentially as free particles, subject only to weak, perturbative interactions among themselves.

- The *soft* scale, $P\sim gT$ where $g\ll 1$ is the relevant coupling constant. This is the typical momentum scale of *collective excitations* in a plasma. For momenta on this scale, the propagation of particles is profoundly modified due to the interaction with the thermal bath which causes $\mathcal{O}(1)$ corrections compared to the case that the particles propagate in vacuum. For a scalar particle, the dispersion relation e.g. becomes $\omega^2=k^2+m^2$ where $m\sim gT$ is a *thermal mass*; for fermions and gauge bosons thermal masses appear as well but the dispersion relation is changed more drastically. Also vertices have to be replaced by effective vertices as soon as all momenta meeting at the vertex are soft. The corresponding effective theory is called *Hard Thermal Loop (HTL) resummed perturbation theory* and we will outline its basics in section 2.2. However, since interactions among soft particles are still perturbative, after one has performed the HTL resummation one can apply a (modified) perturbation theory approach again.

- The *ultrasoft* scale, $P\sim g^2T$. This is the scale of *magnetic screening*, i.e. transverse polarizations of gauge fields can be sensitive to this scale. At this scale, conventional perturbation theory breaks down and one can find observables that become *nonperturbative* [15]. This is because occupation numbers of (gauge) boson modes become $\sim 1/g^2$ and therefore very large which leads to a strong coupling among the ultrasoft degrees of freedom. It is still possible to formulate effective theories that describe physics at the ultrasoft scale [16, 17, 18], they usually need nonperturbative input, e.g. results from lattice simulations, however. We will not deal with effects at the ultrasoft scale here and do not further comment on the related effective theories.

- The *lightcone* scale, $P\sim T, P^2\sim g^2T^2$: If hard momenta approach the lightcone[6] such that $P^2\sim g^2T^2$, then caution is needed again. In this case, *collinear divergences* can occur and one needs to consider another sort of thermal masses, the so-called *asymptotic masses*, which modify the dispersion relation always in the simple way $\omega^2=k^2+m_\infty^2$. One has to be careful, however, that only for scalars thermal mass and asymptotic mass coincide. See section 2.3 and appendix B for details.

[6] Note that in this thesis, we will only be concerned with the case of *hard* momenta near the lightcone. For *soft* momenta near the lightcone, collinear singularities arise and the effective HTL perturbation theory has to be modified [19, 20]. This will not be needed here and bears little resemblance to our treatment.

The appearance of IR and collinear divergences has a striking effect on perturbative computations: Certain diagrams of higher order in the *loop expansion* turn out to be of the same order in the *coupling constant*. This phenomenon which is a characteristic feature of finite-temperature calculations appears in different contexts. The most prominent one is the *HTL effective theory* that we outline in section 2.2–in order to get the leading order expression for the propagator of a soft particle, self-energy insertions have to be resummed. However, such divergences do not exclusively appear at finite temperature. Even in zero-temperature QCD, IR and collinear divergences can occur if e.g. soft and/or collinear (with respect to the emitting source) gluons are radiated and they also require a resummation of Feynman diagrams to get finite results. Effective theories, e.g. the soft-collinear effective theory (SCET), which deals with a very similar kinematical setup as the one considered in this thesis [21, 22], need to be used and conventional perturbation theory becomes useless.

The next two sections describe the modification of perturbation theory needed for momenta at the soft scale (section 2.2) and near the lightcone (section 2.3).

2.2. Hard Thermal Loops (HTL)

For soft momenta, the naive perturbation theory described in the previous section fails to include all contributions of a given order in the coupling constant. Instead, propagators for particles with soft momenta and vertices where all ingoing momenta are soft need to be replaced by effective, resummed counterparts. To illustrate this phenomenon, we can look at a resummed scalar propagator with 1-loop self-energy insertions as in figure 2.2.[7]

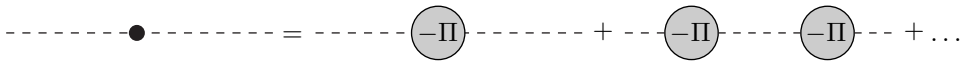

Figure 2.2.: Resummed scalar propagator with pure scalar self-interaction.

For a hard momentum $P \sim T$, the resummed propagator is obviously suppressed compared to the bare one, but for $P \sim gT$ [8], the resummed propagator is of the order

$$\Delta(P)(-\Pi(P))\Delta(P)\ldots \sim \frac{1}{(gT)^2}(gT)^2\frac{1}{(gT)^2}\ldots \sim \frac{1}{(gT)^2}$$

where we assume the loop momentum to be hard, such that $-\Pi(P) \sim g^2 \sum_{k_0} \int \mathrm{d}^3k \Delta(K) \sim g^2T^2$. It is obviously of the same order as the bare propagator and therefore the resummation needs to be taken into account. This is the easiest example of a so-called *Hard Thermal Loop (HTL)*. A more explicit computation can be found in appendix B.1.
HTLs in scalar theories are rather simple whereas gauge theories are more involved. A general power-counting to establish which Green functions in gauge theories exhibit HTLs and require a resummation was established in [23] while for Yukawa theories, HTLs were investigated in [24]. The power-counting for gauge theories is rather involved and one needs to distinguish different cases. We do not reproduce it here since we will not need the general framework, and only list the HTL corrections that are needed in gauge theories [9, 10, 23]:

- Scalar propagators, where the HTL is momentum-independent and contributes only a *thermal mass*, $\Pi(P) = \frac{g^2T^2}{4} \equiv m^2$.
- Fermion and gauge boson propagators with momentum-dependent HTL self-energies which modify the dispersion relations considerably (see below),
- N-gauge boson vertices and $(N-2)-$gauge boson + two-fermion vertices.

[7] Note that the diagrams always correspond to $-\Pi$ and not $+\Pi$. See appendix A for details.
[8] We assume a self-interaction of the form $g^2/4!\,\phi^4$ and denote the scalar self-coupling different from the usual conventions by g^2 to get a more direct analogy to gauge theories.

Note that N-photon vertices are not induced for $N \geq 3$.
In this thesis, we will never need the effective vertices and we can focus on the resummed propagators. The self-energies in the HTL approximation can be derived either by a field-theoretic calculation [9] or via a semi-classical approach using kinetic equations [14]. This dual approach is possible because the wavelength of the collective plasma excitations is typically $\lambda \sim (gT)^{-1}$, which is much larger than the thermal de Broglie wavelength $\lambda_T \sim T^{-1}$. Either calculation leads to the following results, that are derived with the field-theoretic approach in appendix B:

- The imaginary-time gauge boson propagator in a covariant gauge reads

$$-\Delta_{\mu\nu}(k_0, \vec{k}) = \frac{P^T_{\mu\nu}}{K^2 - \Pi_T(k_0, \vec{k})} + \frac{P^L_{\mu\nu}}{K^2 - \Pi_L(k_0, \vec{k})} + \frac{\xi}{K^2}\frac{K_\mu K_\nu}{K^2} \tag{2.28}$$

  with transverse and longitudinal projectors $P^{T/L}_{\mu\nu}$ and the corresponding self-energies

$$\Pi_L(k_0, \vec{k}) = -\frac{m_D^2 K^2}{k^2}\left(1 - xQ_0(x)\right), \quad \Pi_T(k_0, \vec{k}) = m_D^2 x\left[(1-x^2)Q_0(x) + x\right] \tag{2.29}$$

  where $x \equiv k_0/k$ and by

$$Q_0(x) \equiv \frac{1}{2}\ln\left|\frac{x+1}{x-1}\right| - \frac{i\pi}{2}\Theta(1-x^2)$$

  we denote the Legendre function of the second kind. For $K^2 < 0$, the self-energy has an imaginary part which is associated with *Landau damping*, the absorption and emission of the particle by the thermal bath. Finally, the thermal *Debye mass* is given by

$$m_D^2 = \frac{g^2T^2}{6}\left(C_2(r) + \frac{1}{2}N_f + \frac{1}{4}N_S\right) \tag{2.30}$$

  where N_f denotes the number of fermion flavours, N_S the number of scalar particles and $C_2(r)$ the Casimir invariant of the group representation r.

- The imaginary-time fermion propagator is given by

$$-S(p_0, \vec{p}) = \frac{1}{2}\Delta_+(p_0, \vec{p})(\gamma^0 - \gamma^i\hat{p}^i) + \frac{1}{2}\Delta_-(p_0, \vec{p})(\gamma^0 + \gamma^i\hat{p}^i) \tag{2.31}$$

  with

$$\Delta_\pm(p_0, \vec{p}) = \frac{1}{p_0(1 \mp x) - \frac{m_f^2}{2p}\left[(1 \mp x)\ln\left(\frac{1+x}{1-x}\right) \pm 2\right]} \tag{2.32}$$

  with x defined the same way as above and the HTL fermion mass

$$m_f^2 = \frac{g^2 C_2(r) T^2}{8}. \tag{2.33}$$

  It is defined such that the limit $p \to 0$ of the HTL propagator equals that of a bare fermion propagator with mass m_f.

The propagation of both fermions and gauge bosons is obviously drastically changed–they do not only get a mass like a scalar particle does, their dispersion relation becomes much more complicated. We will study this point in more detail for the fermions where some of the explicit results will be needed later on; for gauge bosons one would obtain qualitatively similar results.
The most striking feature is the appearance of *new fermionic excitations* described by eigenstates of $\gamma^0 + \gamma^i\hat{p}^i$. This means that their ratio of helicity and chirality is opposite to 'normal' fermions which are described by spinors that are eigenstates of $\gamma^0 - \gamma^i\hat{p}^i$.[9] The heat bath allows the presence of such *quasiparticles*, called

[9] Note that the presence of the thermal bath does not lead to a breakdown of chiral symmetry: The resummed fermion propagator still anticommutes with γ_5.

plasminos. The notion of quasiparticles can be understood by looking at the spectral function, which we first give explicitly for both types of particles since we will need it in section 4.4.3:

$$\tilde{\rho}_{\pm}(p_0,p) = 2\pi\left[Z_{\pm}(p)\delta(p_0-\omega_{\pm}(p)) + Z_{\mp}(p)\delta(p_0+\omega_{\mp}(p))\right] + \frac{\pi}{p}m_f^2(1\mp x)\Theta(1-x^2)$$
$$\left[\left(p(x\mp 1) - \frac{m_f^2}{2p}\cdot\left[(1\mp x)\ln\left|\frac{x+1}{x-1}\right| \pm 2\right]\right)^2 + \frac{\pi^2 m_f^4}{4p^2}(1\mp x)^2\right]^{-1} \tag{2.34}$$

where the residua are given by

$$Z_{\pm}(p) = \frac{\omega_{\pm}(p)^2 - p^2}{2m_f^2} \tag{2.35}$$

while the dispersion relations $p^0 = \pm\omega_{\pm}(p)$ follow from solving for the zeros of the denominator of $\Delta_{\pm}$. Analytical solutions for $\omega_{\pm}$ can be given in terms of Lambert W functions [25], a numerical plot is shown

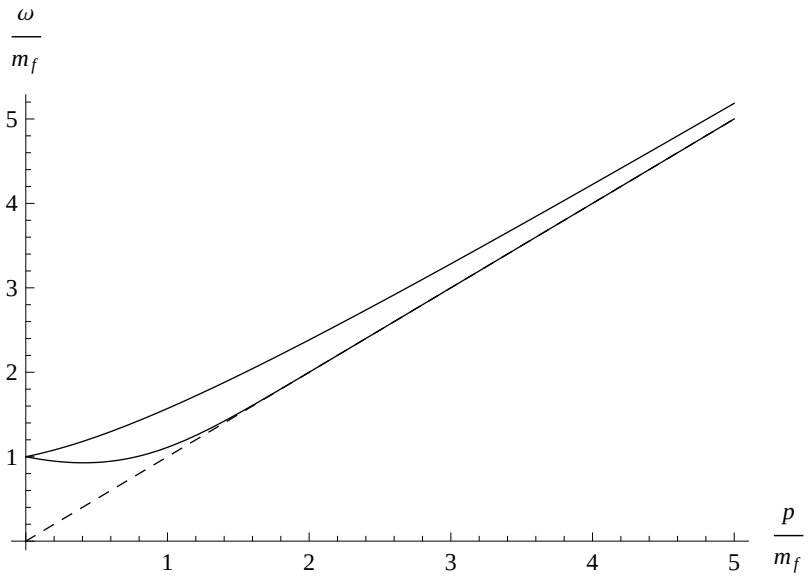

Figure 2.3.: Dispersion relations of soft fermions. The upper curve represents the solution $\omega(p) = +\omega_+(p)$ while the lower curve shows the solution $\omega(p) = -\omega_-(p)$. For comparison, the zero-temperature (massless) dispersion relation $\omega(p) = p$ is plotted as well (dashed line).

in figure 2.3 where we see that in the limit $p \gg m_f$ the dispersion relations approach the usual massless dispersion relation $\omega(p) = p$.

We want to take a closer look at the notion of quasiparticles following [14]. Free particles not subject to any interaction have a delta function-like spectral function, as shown in (2.15) (for free fermions, an additional factor $\not{p} \pm m$ appears). If we switch on interactions, the spectral function contains two parts, as can be seen from (2.34): A pole contribution and a continuum contribution. The question we want to tackle is in which sense we can still keep up a particle-like interpretation of the field excitations. For this purpose, we introduce

$$\tilde{\Gamma}(p_0,\vec{p}) \equiv \Sigma^{>}(p_0,\vec{p}) - \Sigma^{<}(p_0,\vec{p}) = 2\,\mathrm{Im}\,\Sigma_{ret}(p_0,\vec{p}) \tag{2.36}$$

where $\Sigma^{<,>}$ and Σ_{ret} are defined in analogy to $D^{<,>}, \Delta_{ret}$ given in section 2.1. Using (2.14), we can write the spectral function of a fermion as

$$\tilde{\rho}(p_0,\vec{p}) = \frac{\tilde{\Gamma}(p_0,\vec{p})}{(p_0^2 - E_{\vec{p}}^2 - \mathrm{Re}\,\Sigma_{ret}(p_0,\vec{p}))^2 + (\tilde{\Gamma}(p_0,\vec{p})/2)^2} \tag{2.37}$$

If the interactions are perturbative, then $\tilde{\Gamma}$ can be assumed to be 'small' (in a sense to be made precise below) and we can write [14]

$$\rho(p_0 \simeq E_{\vec{p}},\vec{p}) \simeq \frac{z_p}{2E_{\vec{p}}}\frac{2\gamma_p}{(p_0 - E_{\vec{p}})^2 + \gamma_p^2} \tag{2.38}$$

where

$$z_p \equiv 1 - \frac{1}{2E_{\vec{p}}} \left.\frac{\partial \Sigma_{ret}}{\partial p_0}\right|_{p_0=E_{\vec{p}}}, \quad \gamma_p \equiv \frac{z_p}{4E_{\vec{p}}}\tilde{\Gamma}(p_0 = E_{\vec{p}}, \vec{p}) \tag{2.39}$$

in the vicinity of $p_0 = E_{\vec{p}}$. The spectral function thus has a Lorentz shape and in the free-field limit $z_p \to 1, \gamma_p \to 0$ we recover a delta function. Note that to obtain this form, one has to assume that $\gamma_p \ll E_{\vec{p}}$ which makes the statement that $\tilde{\Gamma}$ has to be small more precise. The retarded propagator then becomes

$$\tilde{\Delta}_{ret}(p_0 \simeq E_{\vec{p}}, \vec{p}) \simeq \frac{z_p}{2E_{\vec{p}}} \frac{-1}{p_0 - E_{\vec{p}} + i\gamma_p}, \tag{2.40}$$

i.e. it has a pole at $p_0 = E_{\vec{p}} - i\gamma_p$. As long as z_p, γ_p are only perturbatively small corrections to the free-field values, one can see now that a particle-like description of the interacting degrees of freedom is still reasonable. This is what is referred to as *quasiparticles*. Note that in this interpretation, there is nothing more 'mysterious' about the plasminos compared to 'normal' fermions: both can in a well-defined sense be referred to as particle-like excitations.
Finally we remark that in order to perform perturbative calculations at the soft scale, one often writes down an *effective Lagrangian*, which then generates the HTLs at *tree-level*, i.e. one uses the Lagrangian

$$\mathcal{L} = \mathcal{L}_{eff} - \delta\mathcal{L} \tag{2.41}$$

where $\mathcal{L}_{eff} = \mathcal{L}_0 + \delta\mathcal{L}$ and the final term is treated as counterterm to avoid overcounting. Here, $\mathcal{L}_0$ can be e.g. the QCD Lagrangian and $\delta\mathcal{L}$ should be a gauge-invariant[10] HTL lagrangian. It was derived in [26, 27] and is given by

$$\delta\mathcal{L} = -m_D^2 \,\mathrm{Tr} \int \frac{\mathrm{d}\Omega}{4\pi} F^{\mu\alpha} \frac{\hat{K}_\mu \hat{K}_\alpha}{\hat{K}\cdot D} F^{\beta\mu} + i m_f^2 \bar{\psi} \int \frac{\mathrm{d}\Omega}{4\pi} \frac{\hat{\not{K}}}{\hat{K}\cdot D}\psi \tag{2.42}$$

with covariant derivative D_μ and $\hat{K} = (1, \hat{k})$. This effective Lagrangian is *nonlocal* due to the covariant derivative in the denominator. It also leads to *collinear divergences* and has to be modified when momenta approach the light-cone [20], but, as already mentioned, we do not go into detail here since these modifications will not be needed.
By using this effective theory, IR divergences and gauge dependent results for physical quantities that appeared in tree-level calculations could be successfully removed in many important applications. Examples are the gluon damping rate in a QCD plasma [28, 29] (this was historically one of the major triggers for the discovery of resummed perturbation theory), the production rates of photons [30] or the collisional energy loss of heavy fermions in a plasma [31]. The computation in chapter 4 will provide another example where the inclusion of HTL resummed propagators is crucial to obtain an IR finite result.

2.3. Perturbation theory close to the lightcone

2.3.1. Thermal width and asymptotic mass

In the previous section we have studied the modification of perturbation theory that is needed when momenta become soft. We have explicitly seen that bare propagators need to be replaced by their *resummed* counterparts which contain HTL self-energy insertions (cf. figure 2.2). However, for that to happen in fact we do not need to impose that all components of P^μ are of the order gT–all that is relevant is that $P^2 \sim g^2T^2$! This means that an analogous resummation is also needed for momenta on the *lightcone scale* $P \sim T, P^2 \sim g^2T^2$. The outcome of this resummation, however, is qualitatively different. For illustration, we take again a scalar particle. Its resummed propagator will be of the form

$$\Delta(K) = \frac{-1}{K^2 - \Pi(k_0, \vec{k})}. \tag{2.43}$$

It can be parametrized with two quantities, the *thermal width* $\Gamma(k_0, \vec{k})$ and the *thermal mass* m as

$$\Delta(K) = \frac{-1}{(k^0 + i\Gamma)^2 - \vec{k}^2 - m^2}. \tag{2.44}$$

[10] The HTLs in gauge theories obey tree-like Ward identities [9, 23], therefore one should have manifestly gauge-invariant HTL lagrangians.

Comparing (2.44) to (2.43), we obtain, imposing[11] $\Gamma^2 \ll m^2$,

$$\mathrm{Re}\,\Pi(k_0,\vec{k}) = m^2, \quad \mathrm{Im}\,\Pi(k_0,\vec{k}) = -2ik^0\Gamma(k_0,\vec{k}). \tag{2.45}$$

Since $\Pi \sim g^2T^2$, both m^2 and $k^0\Gamma$ are of the order g^2T^2 (which implies $\Gamma \sim g^2T$) and therefore they are equally important. However, for reasons that will become clear later, we can limit ourselves to *hard* loop momenta and it turns out that we will obtain a purely *real* self-energy then. This means that we only need to compute the asymptotic thermal mass. This is very fortunate because the thermal width turns out to be an IR divergent quantity [32] (see also [9, 33]) which is thus not well-defined without putting a cutoff on the loop integration that has to be cancelled by some other contribution. In our treatment in chapter 3.3 the width will indeed never appear alone but only together with terms coming from a certain class of Feynman diagrams, the so-called *ladder diagrams*, which will cancel the IR divergence and give us a finite and well-defined result. Because of the IR divergence, including the width alone at this stage is not very useful. By restricting ourselves to hard loop momenta, we can avoid this and deal only with well-defined quantities. The calculation in section 3.3 will provide us with a systematic attack on this problem and also with a more rigorous justification why we take only hard loop momenta.
All what was said so far basically applies also to fermions and gauge bosons. However, while for scalar particles there is only one thermal mass, for fermions and gauge bosons asymptotic thermal mass and HTL mass are *different* and one needs to be careful not to confuse them. Explicit computations for scalars and fermions are, like for the HTL resummed propagators studied before, moved to appendix B and here we list only the results:

- The scalar propagator becomes
$$\Delta(K) = \frac{-1}{K^2 - m^2} \tag{2.46}$$
with thermal mass m which equals the HTL thermal mass of a scalar particle (see section 2.2).

- The fermion propagator becomes
$$S(P) = -\frac{\not{P} - \frac{m_\infty^2}{2p_0}\gamma^0}{P^2 - m_\infty^2}. \tag{2.47}$$
The asymptotic thermal mass is *different* from the HTL mass (2.33) and given by
$$m_\infty^2 = \frac{g^2 C_2(r) T^2}{4}. \tag{2.48}$$
Both fermionic thermal masses thus differ by a factor $\sqrt{2}$.

For the calculation in section 3.3 the equivalent form (B.34) of the fermion propagator will turn out to be very useful. The gauge boson propagator at the lightcone scale will not be needed in this thesis and we omit it.
We have mentioned in section 2.2 that in order to formulate a consistent perturbation theory at the soft scale, one also needs to introduce *effective vertices* whenever all momenta that are involved are soft. This happens because one-loop corrections with a hard loop momentum are of the same order as the bare vertex and may therefore not be omitted. One may think that if all momenta meeting at a vertex are at the lightcone scale, one has to add 1-loop corrections to the vertices as well, as illustrated in figure 2.4. This, however, is *not* the case. This is easy to see for a generic hard loop momentum $Q \sim T, Q^2 \sim T^2$ because we get two additional powers of g and nothing can cancel them. Note that it does not help at all to assume that the loop momentum is at the lightcone scale $Q \sim T, Q^2 \sim g^2T^2$ because the enhancement due to the propagator is cancelled by a phase space suppression from the loop integral. The same happens if we consider a soft loop momentum $Q \sim gT$. The only interesting case is when all the momenta are not only at the lightcone scale, but also *collinear* in the sense that $Q \cdot P, Q \cdot K \sim g^2T^2$. In order to understand why this case is interesting, we need to establish a power-counting that will enable us to see at which order in g such diagrams contribute. This is what we turn to now.

[11] This condition is necessary to keep up a *quasiparticle* description of the interacting degrees of freedom in analogy to what we described in section 2.2. If Γ is large, than we are dealing with broad resonances that no longer allow an interpretation in terms of particles.

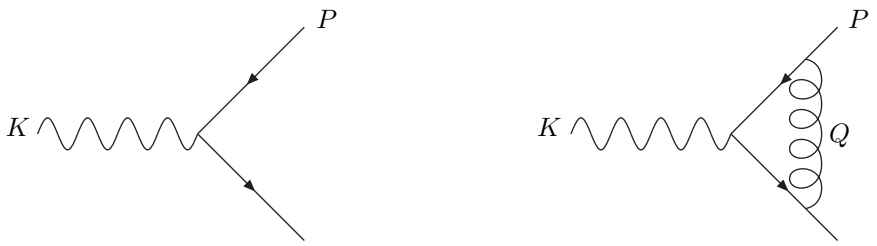

Figure 2.4.: Example for a bare vertex and a 1-loop vertex correction. If the external momenta are all soft, then both contributions are of the same order whereas for external momenta at the lightcone scale, the vertex correction is suppressed and need not be taken into account at leading order.

2.3.2. A new class of diagrams: Collinear Thermal Loops (CTL)

Now we turn to objects that we call **Collinear Thermal Loops (CTLs)** which should not be confused with the collinear limit of the HTLs that was studied in [20]. They correspond to a different kinematic situation, where the external momenta are not soft, as for the HTLs considered before, but rather at the lightcone scale $P_i \sim T, P_i^2 \sim g^2T^2$. For the moment, we consider only 1-loop diagrams as depicted in figure 2.5 which serve as a starting point for the construction of the full CTLs. The loop momentum is of the same kind, $K \sim T, K^2 \sim g^2T^2$, which means that the propagator is a resummed one of the form shown in section 2.3.1. Moreover, it is *collinear* with the external momentum, such that $K \cdot P_i \sim g^2T^2$. This explains why we refer to those objects as *Collinear Thermal Loops*: The loop momentum is hard and *collinear* with the external momenta. The collinearity will soon turn out to be the crucial feature, while a consistent computation at a given order in the coupling constant will force us to include diagrams with more than one loop where the additional loop momenta are *soft*. This will be shown for the example of the two-point function in section 2.3.4.
In order to describe this setup, we define a lightlike four-vector

$$V^\mu \equiv (1, \hat{v}) \tag{2.49}$$

and split up the momenta into components *parallel* to $\hat{v}$, denoted as $k_\parallel, p_{i,\parallel}$, and components *perpendicular* to $\hat{v}$, denoted by $\vec{k}_\perp, \vec{p}_{i,\perp}$. The collinearity of $\vec{k}$, $\vec{p}_i$ means that the longitudinal components are $\mathcal{O}(T)$ and the perpendicular ones $\mathcal{O}(gT)$. The angle between the vectors is then $\vartheta \sim \mathcal{O}(g)$ and the scalar product is $P_i \cdot K \sim g^2T^2$.[12] Finally, the fact that the momenta are nearly lightlike is expressed by demanding that $V \cdot K \sim g^2T$ and the same for the P_i. In summary, we consider 1-loop n-point functions which obey the

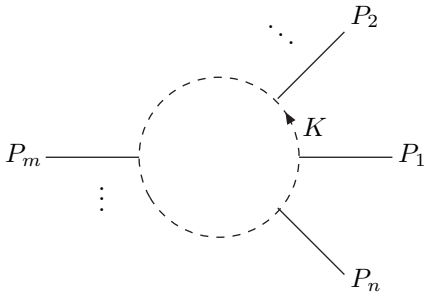

Figure 2.5.: Generic 1-loop contribution to CTL n-point functions with particles of arbitrary spin.

constraints

$$P_i, K \sim T, \quad V \cdot P_i \sim g^2T, \quad V \cdot K \sim g^2T, \quad P_i \cdot K \sim g^2T^2. \tag{2.50}$$

When dealing with such objects, it is very convenient to introduce *lightcone components* $p_\pm = p_0 \pm p_\parallel$ and describe the vector as

$$P^\mu \sim (p_+, p_-, \vec{p}_\perp). \tag{2.51}$$

[12] This follows easily by writing $K \cdot P_i = |\vec{k}||\vec{p}_i|(1 - \cos\vartheta) + \mathcal{O}(g^2T^2)$ where the additional terms depend on the thermal masses and are automatically $\mathcal{O}(g^2T^2)$, whereas for the first term it requires $\vartheta \sim g$.

This amounts to expanding the vector as

$$P^\mu = \frac{1}{2}\bar{V}\cdot P\, V^\mu + \frac{1}{2}V\cdot P\,\bar{V}^\mu + P_\perp^\mu = \frac{p_+}{2}V^\mu + \frac{p_-}{2}\bar{V}^\mu + P_\perp^\mu \tag{2.52}$$

with $\bar{V}^\mu \equiv (1,-\hat{v})$ and $P_\perp^\mu \equiv (0,p^1,p^2,0) = (0,\vec{p}_\perp,0)$. Clearly,

$$p_+ \sim T, \vec{p}_\perp \sim gT, p_- \sim g^2T, \tag{2.53}$$

thus providing us with a hierarchy of scales. This scale hierachy is reminiscent of the *soft-collinear effective theory (SCET)* already mentioned at the end of section 2.1.2. In a very broad sense, an effective CTL-resummed perturbation theory, once written down in analogy to the HTL-resummed perturbation theory mentioned at the end of section 2.2, could be interpreted as a finite-temperature analogue of SCET.
Note that any momentum which obeys $P \sim T, P^2 \sim g^2T^2$ can be described that way, it does not yet say anything about the *collinearity* of the momenta that are involved. Only the fact that the preferred vector V^μ which defines the parallel direction is *the same* for all momenta P_i and the loop momentum K guarantees that the diagrams obey the kinematics (2.50).
In most cases, however, such n-point functions will be suppressed compared to the bare n-point function or the case where the loop momentum is *not collinear* with the external momenta. This is because, although every propagator becomes of order $1/(g^2T^2)$ if (2.50) holds and is thus large, the loop integral and also the vertices will give additional powers of g which can overbalance the enhancement from the propagators and therefore result in an overall suppression of the CTL contribution. We thus first want to provide a general power-counting and determine for all n-point functions at which order in the coupling they contribute. This will also help us to tackle the issue raised at the end of section 2.3.1. Later on we will focus on the simplest case of the **CTL self-energy**, which is the most important one and which we will need in chapter 4 to calculate the impact of the *LPM effect* in thermal particle production. We will then finally also show that taking only the 1-loop diagrams shown in figure 2.5 is not sufficient if we want to get all relevant diagrams at a given order in perturbation theory. Finding all contributions of higher loop order that need to be resummed by a pure diagrammatic analysis will turn out to be an inefficient approach and difficulties will be outlined. An efficient strategy for the computation is presented in section 3.3.1 and then subsequently applied to the computation of the *discontinuity* of the CTL self-energy, whose relevance for physical applications is outlined in section 3.2.

2.3.3. A general power-counting for CTLs

We now want to establish power-counting rules for the CTLs in order to determine at which order in the coupling constant these diagrams contribute. It will prove convenient to absorb any possible Dirac and/or Lorentz structure pertinent to the propagators into the vertices, thus formally dealing with 'scalar propagators' only [13]. This will become clearer in the concrete calculation performed in section 3.3. The biggest difficulty will then be to determine at which order the *vertices* contribute. We will consider only spin 1/2 fermions and spin 1 gauge bosons as external particles because they are the only ones that are needed in this thesis.
We start with presenting the set of power-counting rules:

- The loop integral gives a g^4 suppression,
- Every propagator is of order $1/(g^2T^2)$,
- Every vertex involving a gauge boson gives an explicit factor of g,
- Every *trilinear vertex* is effectively suppressed by another factor of g.

Here, g is a gauge-boson coupling constant-either the strong coupling in a quark-gluon plasma or the weak or electromagnetic coupling if we consider an electroweak plasma instead. It is always assumed to be the *largest* coupling constant involved, which means that the photon coupling plays no role if we consider a QCD plasma since $g_s \gg g_{em}$.[14] Whenever we refer in general to 'gauge bosons' in the following, this slightly different role

[13] One obviously still has to take care of half-integer Matsubara frequencies when fermion propagators are involved.
[14] Numerically, other coupling constants like e.g. the top Yukawa coupling, can be equally large or even larger. One should therefore consider g to represent generically the set of coupling constants which are taken into account at leading order, and this can include more than only gauge coupling constants. For notational simplicity, we will always refer to this set of coupling constants with the letter g.

of photons has to be kept in mind. Note that we count only the powers of g but not those of other coupling constants that may be involved. This is because nothing changes w.r.t. those if we go from collinear to non-collinear momenta since collinearity is always defined in terms of g, like in equation (2.53).
Before we turn to the proof of the power-counting rules, let us summarize at which order in g a CTL N-point function with n vertices involving gauge bosons (as external particles or inside the loop) and $m = N - n$ additional vertices[15] contributes:

$$\Pi_{CTL}^{(n+m=N)} \sim g^4 \left(\frac{1}{g^2}\right)^N g^n g^N \sim g^{4-m} \tag{2.54}$$

It is very remarkable that the power of the gauge boson coupling constant is *independent* of the number of hard gauge boson vertices and only determined by all other particles. Setting $m = 2$, we obviously find that the CTL self-energies without gauge bosons in the loop that will be studied in detail soon are expected to be of second order w.r.t. the coupling constant–a result that will be confirmed with the explicit calculation in section 3.3.
With the help of (2.54) we are now also able to understand why the 1-loop vertex correction shown in figure 2.4 is not of the same order as the bare trilinear vertex. Naively, one would have concluded that it is, because one gets two explicit powers of g from the new vertices, an $(1/g^2)^3$ enhancement from the additional propagators and finally a g^4 phase space suppression. All additional powers of g thus seem to cancel. However, this simple approach misses to correctly count the powers of g due to the vertices. The bare trilinear vertex is suppressed by only one power of g, while the 1-loop correction is already suppressed by g^3, which immediately follows from (2.54) by setting $m = 1$. At leading order, the introduction of effective vertices analogous to those considered in the HTL resummed perturbation theory is therefore not necessary.

Now it is time to prove the power-counting rules. The second and third rule are rather obvious. For the phase space suppression belonging to the loop integral, one can use the lightcone components defined in (2.51) and write

$$\mathrm{d}^4K \sim \mathrm{d}k_+\mathrm{d}k_-\mathrm{d}^2k_\perp. \tag{2.55}$$

We have left out a factor $-i(1 \pm 2f(k^0))$ coming from the thermal sum (an additional factor of 2 arises due to the Jacobi determinant) since K is a hard momentum and even if we have $f_B(k^0)$ this will not affect the power-counting. The g^4 suppression now immediately follows from (2.53).

The vertices

Finally, we must prove the final rule, the suppression of trilinear vertices by one power of g.

- **External gauge bosons:** External, real gauge bosons couple always to two particles of the same spin and they have *transverse* polarizations only. This means that even if a vertex has contributions proportional to V^μ which according to (2.52) are $\mathcal{O}(1)$, when summed over the polarizations of the gauge boson this contribution will vanish. Only *transverse* components of the momenta can contribute and we directly see that we get an $\mathcal{O}(g)$ suppression if the particle in the loop is a scalar or fermion.
  If we couple it however to a gauge boson loop (which is obviously only possible if no photons are involved), then we must think a bit more carefully since every vertex involves a Lorentz tensor of rank 3. However, we already said that we can absorb any nontrivial Lorentz structure of the propagators into the vertices, which means that two out of three indices are contracted. In general, this does *not* imply that at leading order every vertex is proportional to V^μ, in which case only transverse momentum components contribute and we get the same $\mathcal{O}(g)$ again. If several external gauge bosons are involved, it can also happen that we get terms which involve $g^{\mu\nu}$ with μ, ν belonging to the external particles and not to the particles in the loop. Any such terms must, however, come with prefactors that involve scalar products of collinear momenta, which are of order $\mathcal{O}(g^2T^2)$. Although the separate vertices for themselves thus need not show any suppression, two of them grouped together will always be suppressed by two powers of g, thus resulting 'effectively' in an $\mathcal{O}(g)$ suppression of every vertex.
- **External spin 1/2-fermion:** External spin 1/2 fermions couple to two particles which differ by 1/2 in their spin, which means that one is again a spin 1/2 fermion and the other either a scalar or a gauge

[15] For this formula to hold in general every quadrilinear vertex has to be counted like *two* trilinear vertices. This is explained below.

boson. If we couple it to a fermion and a gauge boson, then there may be a contribution proportional to V^μ at a single vertex which is thus not suppressed by itself. But this contribution is contracted with another such vertex factor[16] and will finally result in something suppressed by two powers of g for the very same reason as above. Once more, effectively every vertex is suppressed by $\mathcal{O}(g)$ in the sense that every pair of vertices with external fermions involves a g^2 suppression.
Finally we must look at a Yukawa coupling involving a scalar particle in the loop. The only nontrivial structure comes from the numerator of the fermion propagator. Summing over the spins of the external fermions will result in a scalar product of collinear momenta and for every pair of external fermions, we will get a suppression by g^2 again.

It remains to have a look at the possible *quadrilinear* couplings with four gauge bosons or two gauge bosons and two scalars. They are momentum *independent* and involve only the metric tensor and the square of the corresponding coupling constant. Therefore, there is *no further suppression at the vertices*, no matter if we consider the loop momentum to be collinear or not with the external momenta. In order to get the powers of g right, they still have to be counted like *two trilinear vertices*, because quadrilinear vertices reduce the number of propagators by one each, thus removing one $(1/g^2)$ enhancement factor.

2.3.4. The CTL self-energy

After all the general considerations, we want to take a closer look at the simplest case, the CTL *two-point function*, i.e. a *self-energy* including a summation over external spin states. We want to show that what we looked at so far was still incomplete and that in order to get a consistent expression for a certain CTL n-point function at leading order in the coupling constants, it is *not* sufficient to consider only the one-loop diagrams shown in figure 2.5. In fact, there is an infinite set of additional diagrams, the so-called **ladder diagrams**, which contribute at the same order provided we respect the kinematical constraints (2.50). This is another example of the general statement about perturbation theory at finite temperature that we made at the end of section 2.1. The generalization to n-point functions is in principle straightforward, in detail subtleties might arise however. Since in this thesis, only the CTL self-energy will be needed we do not go into detail here.
In order to understand this phenomenon, let us look at the diagram shown in figure 2.6 with one additional virtual *soft* gauge boson.

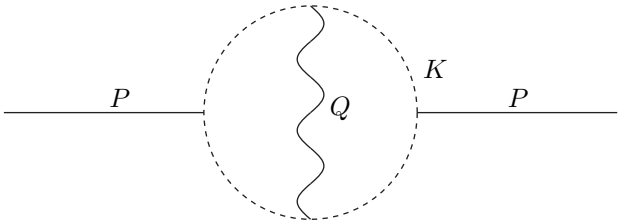

Figure 2.6.: Contribution to CTL self-energy with one soft gauge boson rung.

The expression for this diagram is

$$\Pi_{1rung} \sim g^2 T \sum_{p_0} \int \frac{\mathrm{d}^3 p}{(2\pi)^3} T \sum_{q_0} \int \frac{\mathrm{d}^3 q}{(2\pi)^3} V(P,K,Q)\Delta(P)\Delta(P-Q)\Delta(P-K+Q)\Delta(P-K)\Delta(Q)$$

with $V(P,K,Q)$ containing all the structure from the vertices (with possible Lorentz and/or spinor indices as always suppressed) and an explicit g^2 from the gauge boson vertices.[17] We now have to count the powers of g and compare with the diagram without the soft gauge boson:

- There is an explicit g^2 suppression from the new gauge boson vertices,

[16] Note that external fermions always come in pairs.
[17] We have chosen a scalar loop for simplicity, but for the power counting, nothing changes if we use fermions instead, only the expressions become more complicated.

- There is a $1/g^2$ enhancement from each new propagator, provided we choose Q such that $Q \cdot P \sim g^2 T$.
- For this choice of Q, there is a g^4 phase space suppression from each sum-integral.

There is of course still the g^2 suppression from $V(P,K,Q)$ which was discussed already at length in section 2.3.2. Note that there is no additional kinematical suppression at the soft gauge boson vertices because at leading order the longitudinal polarizations contribute. The difference compared to the hard gauge bosons studied in the power-counting scheme of section 2.3.3 is that a contraction of the form $V^\mu V^\nu \Delta_{\mu\nu}$ where $\Delta_{\mu\nu}$ is the HTL propagator (2.28) does *not* vanish at leading order.
The second point is the crucial one here. A generic soft momentum will, of course, not obey this constraint, but then the scalar propagators depending on Q will lack the $1/g^2$ enhancement and the resulting expression will be suppressed compared to the more special case where $Q \cdot P \sim g^2 T$.
Finally we must look at the phase space suppression coming from the sum-integral over Q because the power-counting proceeds a little bit different compared to the hard momentum K that we studied in 2.3.2. First of all, note that $Q \cdot P \sim g^2 T$ also implies $q_- \sim g^2 T$. Then we can write

$$T \sum_{q_0} \int \frac{\mathrm{d}^3 q}{(2\pi)^3} \sim \int \mathrm{d}q_+ \mathrm{d}q_- \left(\frac{1}{2} + f_B(q^0) \right) \int \mathrm{d}^2 q_\perp$$

and since $\vec{q}_\perp \sim gT, q_+ \sim gT, f_B(q^0) \sim 1/g$ we end up with four powers of g like for the hard momentum P. Obviously, the Bose function is crucial here-taking soft fermions instead will fail to give the same order as the 1-loop diagram.
Putting all powers of g together, we arrive at

$$\Pi_{1rung} \sim \underbrace{g^2}_{\text{explicit}} \underbrace{g^2}_{V(P,K,Q)} \underbrace{\left(\frac{1}{g^2}\right)^5}_{\text{propagators}} \underbrace{(g^4)^2}_{\text{phase space}} \sim g^2 \tag{2.56}$$

All additional powers of g have cancelled, leaving us with a contribution of second order in g again. The same will be true for an *arbitrary number of soft gauge boson rungs* as depicted in figure 2.7. Every additional

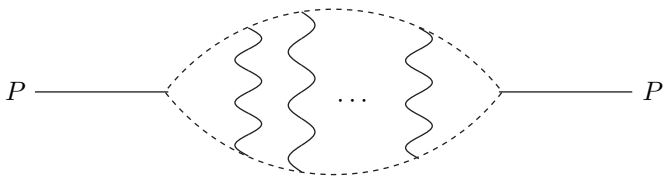

Figure 2.7.: Ladder diagrams to be taken into account in a consistent leading-order treatment.

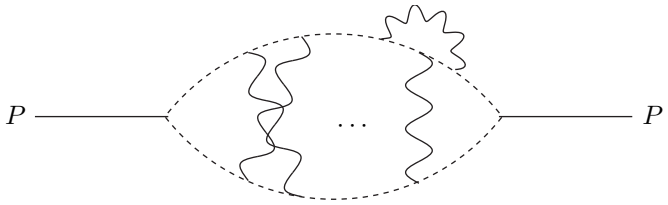

Figure 2.8.: Example for a diagram with crossed ladder rungs and vertex correction. Diagrams of that type will turn out to be irrelevant at leading order.

gauge boson rung will give a g^4 phase space suppression and introduce an additional explicit g^2 from the vertices, but this g^6 suppression gets cancelled by the three new propagators which appear and which give a $1/g^2$ enhancement each. This means that we need to include the complete set of such ladder diagrams with soft gauge boson rungs in order to get the complete $\mathcal{O}(g^2)$ expression. Note that this in fact leads to a multifold resummation because the propagators in fig. 2.7 are already resummed quantities themselves–the

momenta are either at the soft or at the lightcone scale!
However, at this stage it is not yet obvious that this is all we need to include. One could e.g. also imagine that diagrams with *crossed ladder rungs* or with additional vertex corrections as shown in figure 2.8 have to be included. Finally, what we did for a *soft* gauge boson momentum Q can also be done at any $Q \sim g^n T, n > 1$ and we would naively obtain that this is of order g^2. All those additional contributions are *suppressed*, but there is no intuitive argument that dictates this. Although it is possible to prove that the leading order only the ladder diagrams from figure 2.7 need to be taken into account [6], an analysis in terms of Feynman diagrams is rather tedious. We will address this problem in the course of the calculation in section 3.3 and in appendix D.

3. Thermal particle production and the LPM effect

Tell me
Why'd you have to go and make things so complicated?
Avril Lavigne - *Complicated*

3.1. Thermal particle production

Whenever we have a hot thermal bath and one particle species which is so weakly coupled that it is not in equilibrium with its surrounding medium, it can be produced via decays or scattering of particles from the thermal bath and then escape without substantial effects of the medium on its subsequent propagation. We refer to this situation as *thermal particle production* and it plays an important role both in heavy-ion collisions where a quark-gluon plasma may be formed [34, 35] and in the early universe. Well-studied examples are photon production in a quark-gluon plasma or the thermal production of dark matter candidates shortly after reheating in the early, radiation-dominated era of the cosmological evolution [6, 7, 36, 37, 38, 39].
The key quantity in this context is the *particle production rate* defined as the number of particles produced per volume and time. The subject of this thesis is to study this quantity for certain interesting examples, to leading order in the relevant coupling constants. Although this sounds like a rather straightforward task, a careful analysis reveals that it is in fact highly nontrivial. A consistent treatment requires a formalism to deal with the *Landau-Pomeranchuk-Migdal (LPM) effect*, a coherent quantum effect that will be explained in section 3.2. Before we do this, we first present a derivation of a master formula for the thermal particle production rate and outline the connection to the Boltzmann equation needed to study the time evolution of the particle number density.

3.1.1. Particle production rate

Here we give a first principles-derivation of a master formula for the thermal particle production rate. This derivation is usually not shown in the existing literature on the topic where the final result is often taken as starting point or derived in a less rigorous way by arguing on the basis of S-matrix elements [9, 40]. The presentation here basically follows [41].

General setting

The relevant hamiltonian is given by

$$H = H_{sys} + H_{\varphi} \tag{3.1}$$

where H_{sys} contains all particles in *full equilibrium* which provide the thermal bath, and φ is the weakly interacting particle whose production we want to study and which is *not* in equilibrium with the thermal bath. Its hamiltonian can be further split up into a free and an interaction contribution according to[1]

$$H_{\varphi} \equiv H_0 + H_{int} = \int \frac{\mathrm{d}^3 p}{(2\pi)^3} E_{\vec{p}} \sum_{\lambda} a^{\dagger}(\vec{p},\lambda) a(\vec{p},\lambda) + \left(\int \mathrm{d}^3 x \varphi(x) \cdot J(x) + h.c. \right). \tag{3.2}$$

We have used a compact notation where λ denotes the helicity states of fermions or gauge bosons (in case of real scalars, the sum actually contains only one term) and the product $\varphi(x) \cdot J(x)$ may involve a contraction

[1] We perform the calculations in Minkowski space although we are mainly interested in thermal particle production in the early universe. This is possible because the time-scale of interactions we will be interested in is $t \sim (g^2 T)^{-1}$ which is much shorter than the expansion time scale $H^{-1} \sim (\sqrt{g_*} T^2 / M_{Pl})^{-1}$ where $M_{Pl} = 2.4 \cdot 10^{18}$ GeV is the (reduced) Planck mass and $g_* = \mathcal{O}(100)$ is the number of relativistic d.o.f., because all processes we look at happen at temperatures $T/M_{Pl} \ll g^2$. This means that on the time scale of the interaction, the expansion of the Universe is irrelevant.

of Lorentz, spinor and/or internal group indices, if present. Furthermore, the coupling constant is absorbed in the definition of the interaction current $J(x)$. The addition of the hermitian conjugate is not needed if the current is hermitian by itself. As an example, in the case of a pure EM interaction we get $\int \mathrm{d}^3x\varphi(x)\cdot J(x) \equiv e\int \mathrm{d}^3x A_\mu(x)J^\mu(x)$ with $J^\mu = \bar{\psi}\gamma^\mu\psi$ which is hermitian. For the Yukawa interaction between Majorana neutrinos N_i, leptons ℓ_k and the Higgs ϕ (that will be studied in detail in chapter 4), we get $\int \mathrm{d}^3x\varphi(x)\cdot J(x) \equiv \sum_k \lambda_{ik}\int \mathrm{d}^3x\bar{N}_i(x)P_L\ell_k(x)\phi^\dagger(x)$ with lepton doublet ℓ_k (the indices i,k label fermion generations) and Higgs doublet ϕ. In this case, the '$+h.c.$' in (3.2) will be taken into account.
The density matrix of the system is time-dependent because we have a nonequilibrium problem. As initial condition at a time $t = 0$ it is assumed that

$$\hat{\rho}(t=0) \equiv \hat{\rho}_0 = \hat{\rho}_{sys}\otimes|0\rangle\langle 0|, \tag{3.3}$$

which means that initially we have no φ particles while the thermal bath is described with the canonical ensemble

$$\hat{\rho}_{sys} = \frac{1}{Z}e^{-\beta H_{sys}}. \tag{3.4}$$

The observable we want to study is described by the operator

$$\frac{\mathrm{d}N_\varphi}{\mathrm{d}^3x\mathrm{d}^3p} \equiv \frac{1}{V}\sum_\lambda a^\dagger(\vec{p},\lambda)a(\vec{p},\lambda). \tag{3.5}$$

Defining the *differential production rate* as

$$\frac{\mathrm{d}\Gamma_\varphi}{\mathrm{d}^3p} \equiv \frac{\mathrm{d}\langle N_\varphi\rangle}{\mathrm{d}^4x\mathrm{d}^3p}, \tag{3.6}$$

with the average being taken w.r.t. the full density matrix, we obtain

$$\frac{\mathrm{d}\Gamma_\varphi}{\mathrm{d}^3p} = \frac{1}{V}\frac{\mathrm{d}}{\mathrm{d}t}\,\mathrm{Tr}\left[\sum_\lambda a^\dagger(\vec{p},\lambda)a(\vec{p},\lambda)\hat{\rho}(t)\right]. \tag{3.7}$$

To continue, we need to solve for the time development of the density matrix. Its equation of motion is the usual von Neumann-equation

$$i\frac{\mathrm{d}\hat{\rho}_I(t)}{\mathrm{d}t} = [H_I(t),\hat{\rho}_I(t)] \tag{3.8}$$

with the formal solution[2]

$$\hat{\rho}_I(t) = \hat{\rho}_0 - i\int_0^t \mathrm{d}t'[H_I(t'),\hat{\rho}_0] + (-i)^2\int_0^t \mathrm{d}t'\int_0^{t'}\mathrm{d}t''[H_I(t'),[H_I(t''),\hat{\rho}_0]] + \ldots. \tag{3.9}$$

Here, we have transformed to the interaction picture

$$H_I \equiv e^{iH_0t}H_{int}e^{-iH_0t}, \quad \hat{\rho}_I \equiv e^{iH_0t}\hat{\rho}e^{-iH_0t}. \tag{3.10}$$

Upon inserting into (3.7), we see that the first two terms do not contribute. For the first term, it is obvious because it is constant in time, whereas the second one requires a closer inspection. Its contribution is of the form[3]

$$\mathrm{Tr}\left[\sum_\lambda a^\dagger(\vec{p},\lambda)a(\vec{p},\lambda)[H_I(t),|0\rangle\langle 0|]\right] = \langle 0|\sum_\lambda a^\dagger(\vec{p},\lambda)a(\vec{p},\lambda)H_I(t) - H_I(t)\sum_\lambda a^\dagger(\vec{p},\lambda)a(\vec{p},\lambda)|0\rangle = 0$$

where we used the cyclic invariance of the trace and the fact that all states containing at least one particle with arbitrary momentum are orthogonal to the vacuum state, such that finally only a vacuum expectation

[2] As discussed in [41], this series contains in general *secular terms* which grow with time and invalidate the perturbative expansion. This can be related to the fact that at a certain time $t = t_{eq}$ the particle φ has reached its equilibrium density. For larger times $t > t_{eq}$ the evolution of the number density has to be found by other means and the formula for the thermal production rate derived here is no longer valid. Its usage is limited to times $t \ll t_{eq}$ for which the density remains small.

[3] Here, the factor ρ_{sys} is irrelevant since it is independent of φ, therefore the trace can be factorized.

value remains. It vanishes due to the creation operator acting on the bra and the annihilation operator acting on the ket. The third term from (3.9) can be handled precisely the same way and we end up with (we write t' instead of t'' for simplicity)

$$\frac{\mathrm{d}\Gamma_\varphi}{\mathrm{d}^3p} = -\frac{1}{V}\left\langle \int_0^t \mathrm{d}t' \langle 0| \left[[\sum_\lambda a^\dagger(\vec{p},\lambda)a(\vec{p},\lambda), H_I(t)], H_I(t') \right] |0\rangle \right\rangle_\beta \tag{3.11}$$

with the thermal expectation value taken w.r.t. the equilibrium density matrix,

$$\langle \cdots \rangle_\beta \equiv \mathrm{Tr}[\cdots \hat{\rho}_{sys}]. \tag{3.12}$$

In order to evaluate this expression, it is necessary to expand the field φ in creation and annihilation operators (which is possible because on the time scale of the interaction the particle φ escapes freely and does not feel the presence of the medium) and insert this expression in $H_I(t)$. This means, we write

$$\begin{aligned} \varphi(x) &= \int \frac{\mathrm{d}^3p}{\sqrt{(2\pi)^3 2E_{\vec{p}}}} \sum_\lambda (a(\vec{p},\lambda)\chi(\vec{p},\lambda)e^{-iPx} + a^\dagger(\vec{p},\lambda)\omega(\vec{p},\lambda)e^{iPx}), \\ \bar{\varphi}(x) &= \int \frac{\mathrm{d}^3p}{\sqrt{(2\pi)^3 2E_{\vec{p}}}} \sum_\lambda (a^\dagger(\vec{p},\lambda)\bar{\chi}(\vec{p},\lambda)e^{iPx} + a(\vec{p},\lambda)\bar{\omega}(\vec{p},\lambda)e^{-iPx}), \end{aligned} \tag{3.13}$$

where $\bar{\varphi}$ is the conjugate field and the mode functions $\chi(\vec{p},\lambda), \omega(\vec{p},\lambda)$ may again contain Lorentz- or spinor indices.[4] For scalar particles, this function is unity, for fermions it is a spinor and for gauge bosons a polarization vector. The interaction hamiltonian then becomes

$$\begin{aligned} H_I(t) = \int \mathrm{d}^3x \int \frac{\mathrm{d}^3q}{\sqrt{(2\pi)^3 2E_{\vec{q}}}} \sum_{\lambda'} \big(&[a(\vec{q},\lambda')\chi(\vec{q},\lambda')e^{-iQx} + a^\dagger(\vec{q},\lambda')\omega(\vec{q},\lambda')e^{iQx}]\bar{J}(x) \\ &+ J(x)[a^\dagger(\vec{q},\lambda')\bar{\chi}(\vec{q},\lambda')e^{iQx} + a(\vec{q},\lambda')\bar{\omega}(\vec{q},\lambda')e^{-iQx}]\big), \end{aligned} \tag{3.14}$$

$$\begin{aligned} H_I(t') = \int \mathrm{d}^3y \int \frac{\mathrm{d}^3r}{\sqrt{(2\pi)^3 2E_{\vec{r}}}} \sum_{\lambda''} \big(&[a(\vec{r},\lambda'')\chi(\vec{r},\lambda'')e^{-iRy} + a^\dagger(\vec{r},\lambda'')\omega(\vec{r},\lambda'')e^{iRy}]\bar{J}(y) \\ &+ J(y)[a^\dagger(\vec{r},\lambda'')\bar{\chi}(\vec{r},\lambda'')e^{iRy} + a(\vec{r},\lambda'')\bar{\omega}(\vec{r},\lambda'')e^{-iRy}]\big), \end{aligned} \tag{3.15}$$

The distinction between J and $\bar{J}$ is very important if φ is a fermion while for production of e.g. photons, one could do with an easier notation. In fact, the second half of the terms in (3.14) and (3.15) is absent there because in the interaction hamiltonian we do not have any '+ h.c.'.
The evaluation of the vacuum expectation value in (3.11) looks like a rather horrible task, but it is greatly simplified by the fact that most terms vanish because they involve an annihilation operator acting on the ket or a creation operator acting on the bra. There are only two terms where only annihilation operators act on the bra and only creation operators on the ket, both of which have the number operator $\sum_\lambda a^\dagger(\vec{p},\lambda)a(\vec{p},\lambda)$ sandwiched between the hamiltonians, thus producing terms of the form $\langle 0|aa^\dagger aa^\dagger|0\rangle$ which are the only nonzero ones. These two terms come with a minus sign which cancels the overall minus sign in (3.11). With this in mind, one can immediately write down the following expression:

$$\frac{\mathrm{d}\Gamma_\varphi}{\mathrm{d}^3p} = \frac{1}{V}\left\langle \int_0^t \mathrm{d}t' \langle 0|H_I(t')\sum_\lambda a^\dagger(\vec{p},\lambda)a(\vec{p},\lambda)H_I(t) + H_I(t)\sum_\lambda a^\dagger(\vec{p},\lambda)a(\vec{p},\lambda)H_I(t')|0\rangle \right\rangle_\beta$$

[4] For Dirac fermions, the expression is of course not strictly correct since we should take into account that particles are distinct from their antiparticles and consequently we must distinguish between two different sets of creation and annihilation operators. However, here we will only be interested in the production of *Majorana* fermions which are their own antiparticles, such that the distinction is not necessary. The generalization to Dirac fermions is straightforward and only introduces slightly more complicated expressions.

To get the aforementioned nonzero contributions, we insert for $H_I(t), H_I(t')$ only those terms from (3.14) and (3.15) which produce the desired vacuum expectation values. This means, that we get

$$\begin{aligned}\frac{\mathrm{d}\Gamma_\varphi}{\mathrm{d}^3p} =&\frac{1}{V}\left\langle \int_0^t \mathrm{d}t' \int \mathrm{d}^3x\mathrm{d}^3y \int \frac{\mathrm{d}^3q}{\sqrt{(2\pi)^3 2E_{\vec{q}}}} \int \frac{\mathrm{d}^3r}{\sqrt{(2\pi)^3 2E_{\vec{r}}}} \sum_{\lambda,\lambda',\lambda''} \big[(\chi(\vec{r},\lambda'')\bar{J}(y) + J(y)\bar{\omega}(\vec{r},\lambda'')) \right.\\ &\langle 0|a(\vec{r},\lambda'')a^\dagger(\vec{p},\lambda)a(\vec{p},\lambda)a^\dagger(\vec{q},\lambda')|0\rangle(\omega(\vec{q},\lambda')\bar{J}(x) + J(x)\bar{\chi}(\vec{q},\lambda'))e^{i(Qx-Ry)} + (\chi(\vec{q},\lambda')\bar{J}(x) + J(x)\bar{\omega}(\vec{q},\lambda'))\\ &\left.\langle 0|a(\vec{q},\lambda')a^\dagger(\vec{p},\lambda)a(\vec{p},\lambda)a^\dagger(\vec{r},\lambda'')|0\rangle(\omega(\vec{r},\lambda'')\bar{J}(y) + J(y)\bar{\chi}(\vec{r},\lambda''))e^{-i(Qx-Ry)}\big] \right\rangle_\beta .\end{aligned}$$

Using the (anti-) commutation relations

$$[a(\vec{p},\lambda), a^\dagger(\vec{q},\lambda')]_\pm = \delta_{\lambda\lambda'}\delta(\vec{p}-\vec{q}), \tag{3.16}$$

we immediately see that the vacuum expectation values simply give a factor of $\delta_{\lambda\lambda'}\delta_{\lambda\lambda''}\delta(\vec{p}-\vec{q})\delta(\vec{p}-\vec{r})$ each, and we end up with

$$\begin{aligned}\frac{\mathrm{d}\Gamma_\varphi}{\mathrm{d}^3p} = \frac{1}{V}\frac{1}{(2\pi)^3 2E_{\vec{p}}}\left\langle \int_0^t \mathrm{d}t' \int \mathrm{d}^3x\mathrm{d}^3y \sum_\lambda \Big[(\chi(\vec{p},\lambda)\bar{J}(y) + J(y)\bar{\omega}(\vec{p},\lambda))(\omega(\vec{p},\lambda)\bar{J}(x) + J(x)\bar{\chi}(\vec{p},\lambda))e^{iP(x-y)}\right.\\ \left. +(\chi(\vec{p},\lambda)\bar{J}(x) + J(x)\bar{\omega}(\vec{p},\lambda))(\omega(\vec{p},\lambda)\bar{J}(y) + J(y)\bar{\chi}(\vec{p},\lambda))e^{-iP(x-y)}\Big] \right\rangle_\beta .\end{aligned} \tag{3.17}$$

This formula is valid for the more general case where the interaction current is not hermitian and the hermitian conjugate is added. Although it would be possible to apply this formula also e.g. to photon production, it appears easier to simplify it already at this stage. All the computational steps remain unchanged, we only have to omit all terms which involve the conjugate mode functions $\bar{\chi}, \bar{\omega}$ in the final result (cf. the remark after equation (3.15)) and write J instead of $\bar{J}$. The starting point valid for the case where the interaction hamiltonian is already hermitian by itself then becomes

$$\begin{aligned}\frac{\mathrm{d}\Gamma_{\varphi,hermit.}}{\mathrm{d}^3p} = \frac{1}{V}\frac{1}{(2\pi)^3 2E_{\vec{p}}}\left\langle \int_0^t \mathrm{d}t' \int \mathrm{d}^3x\mathrm{d}^3y \sum_\lambda \Big[\chi(\vec{p},\lambda)J(y)\omega(\vec{p},\lambda)J(x)e^{iP(x-y)}\right.\\ \left. +\chi(\vec{p},\lambda)J(x)\omega(\vec{p},\lambda)J(y)e^{-iP(x-y)}\Big] \right\rangle_\beta\end{aligned} \tag{3.18}$$

Up to now, the calculation was completely general. At this point, it is finally convenient to consider specific examples separately by specifying the mode functions and the current.

Production of photons

We first consider the production of photons[5], where we can start from (3.18). The mode functions carry a Lorentz index and are given by polarization vectors, $\chi(\vec{p},\lambda) \to \varepsilon^\mu(\vec{p},\lambda), \omega(\vec{p},\lambda) \to \varepsilon^{\nu *}(\vec{p},\lambda)$. Introducing the retarded current-current-correlator

$$e^2\Pi^<_{\mu\nu}(x) \equiv \langle J_\mu(0)J_\nu(x)\rangle_\beta , \tag{3.19}$$

we get, due to translational invariance,

$$\langle J_\mu(x)J_\nu(y)\rangle_\beta = e^2\Pi^<_{\mu\nu}(y-x). \tag{3.20}$$

A Fourier transform then yields

$$\langle J_\mu(x)J_\nu(y)\rangle_\beta = e^2\int\frac{\mathrm{d}^4Q}{(2\pi)^4}e^{-iQ(y-x)}\Pi^<_{\mu\nu}(Q), \quad \langle J_\mu(y)J_\nu(x)\rangle_\beta = e^2\int\frac{\mathrm{d}^4Q}{(2\pi)^4}e^{-iQ(x-y)}\Pi^<_{\mu\nu}(Q) \tag{3.21}$$

[5]Note that the production rate for scalar particles (which we will not be interested in) follows as a simple corollary by replacing $\varepsilon_\mu \to 1$ and omitting the Lorentz index on the currents.

which we insert into the result (3.18) and obtain

$$\frac{\mathrm{d}\Gamma_\gamma}{\mathrm{d}^3p} = \frac{e^2}{V}\frac{1}{(2\pi)^3 2E_{\vec{p}}}\sum_\lambda \varepsilon^\mu(\vec{p},\lambda)\varepsilon^{\nu *}(\vec{p},\lambda)\int\frac{\mathrm{d}^4Q}{(2\pi)^4}\Pi^<_{\mu\nu}(Q)\int_0^t \mathrm{d}t'\int \mathrm{d}^3x\mathrm{d}^3y(e^{i(P-Q)(x-y)}+e^{i(P-Q)(y-x)}). \tag{3.22}$$

The spatial integrals give a factor $(2\pi)^3V\delta(\vec{p}-\vec{q})$ each, and in the limit $t\to\infty$, the integral over t' over the sum of both gives another factor $2\pi\delta(E_{\vec{p}}-q^0)$.[6] Note that we need to integrate t' from $-\infty$ to $+\infty$ to obtain the delta function and not from 0 to ∞. This is achieved by taking $t'\to -t'$ in one of the two terms and then writing them as a single integral.
With this in mind and with the computation above, we arrive at the standard textbook result

$$\frac{\mathrm{d}\Gamma_\gamma}{\mathrm{d}^3p} = \frac{e^2}{(2\pi)^3 2E_{\vec{p}}}\sum_\lambda \varepsilon^\mu(\vec{p},\lambda)\varepsilon^{\nu *}(\vec{p},\lambda)\Pi^<_{\mu\nu}(P). \tag{3.23}$$

For practical calculations, it is often easier to use the following, equivalent formula:

$$\frac{\mathrm{d}\Gamma_\gamma}{\mathrm{d}^3p} = \frac{e^2}{(2\pi)^3 2E_{\vec{p}}}f_B(p^0)\sum_\lambda \varepsilon^\mu(\vec{p},\lambda)\varepsilon^{\nu *}(\vec{p},\lambda)\,\mathrm{Im}\,\Pi_{\mu\nu,ret}(P) \tag{3.24}$$

One therefore needs to compute the imaginary part of the retarded gauge boson self-energy. In order to show the equivalence, one first of all needs to remember that instead of the correlation function of currents, one can also use the self-energy. To see this, consider e.g. the path integral representation of the full propagator (omitting possible Lorentz indices):

$$D(x-y) = \langle\varphi(x)\varphi(y)\rangle = \int \mathcal{D}\varphi\varphi(x)\varphi(y)e^{-ig\int \mathrm{d}^4x J\cdot\varphi}e^{iS_0} \tag{3.25}$$

On the other hand, we have the geometric series which schematically looks like

$$D(P) = \Delta(P) + \Delta(P)(-i\Pi(P))\Delta(P) + \ldots. \tag{3.26}$$

Since only the term of order g^2 contributes to the production rate, we need to expand (3.25) to that order, which then yields two free propagators and the two-point correlation function of the currents. This can, using (3.26), be then identified with the self-energy of the φ field, which shows that the correlation function of currents can be replaced by the correlation function of the field itself. The final step is then to use the KMS relation which leads to the identity

$$\Pi_<(P) = f_B(p^0)\rho(p^0) \tag{3.27}$$

with spectral function $\rho(p^0)$ (again emitting possible Lorentz indices). The spectral function can be identified with twice the imaginary part of the retarded self-energy (see section 2.1.1), which completes the proof.

Production of Majorana neutrinos

Now we turn to the production of Majorana neutrinos which interact with leptons and Higgs bosons via

$$H_I = \lambda_{ik}\int \mathrm{d}^3x\bar{N}_i(x)P_L\ell_k(x)\phi^\dagger(x) + h.c. \tag{3.28}$$

where i,k label the fermion generations.[7] We will focus in the following on the production of the *lightest* Majorana neutrino N_1 because only this is relevant for the calculations in chapter 4. The index '1' will mostly be suppressed to make the notation less clumsy.
In this case, we need to distinguish between J and $\bar{J}$ and start from (3.17). The mode functions are given by $\chi(\vec{p},\lambda)\to u(\vec{p},s)$ and $\omega(\vec{p},\lambda)\to v(\vec{p},s)$. Nonzero correlation functions are only obtained with one J and one $\bar{J}$. To understand it, one may not forget that the interaction currents involve chiral projectors P_L (in J)

[6] The infinite time limit is to be understood in the sense that t is much larger than the timescale of interactions.
[7] The λ that appears here is of course the Yukawa coupling matrix and bears no relation to the summation variable λ (which is called s here) used before in the derivation of the photon production rate.

and P_R (in $\bar{J}$). Only expressions involving one P_L and one P_R are nonzero because they will lead to terms of the form $P_L \Sigma P_R$ where Σ is one of the correlation functions that are introduced in a moment. An expression like $P_L \Sigma P_L$ with two identical projectors is zero. This means that (3.17) becomes

$$\frac{\mathrm{d}\Gamma_{N_1}}{\mathrm{d}^3 p} = \frac{1}{V}\frac{1}{(2\pi)^3 2E_{\vec{p}}}\int_0^t \mathrm{d}t' \int \mathrm{d}^3x \mathrm{d}^3y \sum_s \Big[e^{iP(x-y)} \left(u(\vec{p},s)\bar{u}(\vec{p},s)\langle \bar{J}(y)J(x)\rangle_\beta + v(\vec{p},s)\bar{v}(\vec{p},s)\langle J(y)\bar{J}(x)\rangle_\beta \right) + e^{-iP(x-y)} \left(u(\vec{p},s)\bar{u}(\vec{p},s)\langle \bar{J}(x)J(y)\rangle_\beta + v(\vec{p},s)\bar{v}(\vec{p},s)\langle J(x)\bar{J}(y)\rangle_\beta \right) \Big]. \tag{3.29}$$

We can now perform the sum over the external spins which leads to the usual trace over gamma matrices. When doing so, again one may not forget that the interaction currents involve chiral projectors which 'kill' the mass term from the spin sums because $P_L m P_R = 0$. This means that for the summation over spins, it does not matter here whether we have u- or v-spinors. The remaining traces involve only two Dirac matrices each which means that γ_5 does not contribute and we may replace the remaining $P_{L,R}^2 \to \frac{1}{2}$. Therefore, it is more convenient to define the currents $j, \bar{j}$ via

$$J = \sum_k \lambda_{1k} \ell_k \phi^\dagger, \quad \bar{J} = \sum_k \lambda_{1k}^\dagger \bar{\ell}_k \phi \tag{3.30}$$

where the sum goes over the fermion generations, and to pull out an overall factor 1/2 from the chiral projectors. Then we can write

$$\frac{\mathrm{d}\Gamma_{N_1}}{\mathrm{d}^3 p} = \frac{1}{V}\frac{|\lambda|^2}{2(2\pi)^3 2E_{\vec{p}}}\int_0^t \mathrm{d}t' \int \mathrm{d}^3x \mathrm{d}^3y \int \frac{\mathrm{d}^4Q}{(2\pi)^4} \Big[\mathrm{Tr}[\not{P}\Sigma^>(Q)] \left(e^{i(P+Q)(x-y)} + e^{-i(P+Q)(x-y)} \right) - \mathrm{Tr}[\not{P}\Sigma^<(Q)] \left(e^{i(P+Q)(x-y)} + e^{-i(P+Q)(x-y)} \right) \Big]. \tag{3.31}$$

Here we set $|\lambda|^2 \equiv \sum_k (\lambda^\dagger \lambda)_{1k}$ and we introduced the current-current correlators

$$\langle j(x)\bar{j}(y)\rangle_\beta = \int \frac{\mathrm{d}^4Q}{(2\pi)^4} e^{-iQ(x-y)}\Sigma^>(Q), \tag{3.32}$$

$$\langle \bar{j}(x)j(y)\rangle_\beta = -\int \frac{\mathrm{d}^4Q}{(2\pi)^4} e^{-iQ(y-x)}\Sigma^<(Q). \tag{3.33}$$

Now we perform the integrals over $\mathrm{d}t, \mathrm{d}^3x$ and d^3y like we previously did for the production rate of photons. Due to the arising delta functions, we can integrate finally over d^4Q and obtain

$$\frac{\mathrm{d}\Gamma_{N_1}}{\mathrm{d}^3 p} = \frac{|\lambda|^2}{2(2\pi)^3 2E_{\vec{p}}} \left(\mathrm{Tr}[\not{P}\Sigma^>(-P)] - \mathrm{Tr}[\not{P}\Sigma^<(P)] \right). \tag{3.34}$$

The final step is again to replace the current-current correlators by the imaginary part of the retarded self-energy. This is done the same way as in the case of photon production, only that we must pay attention to the additional minus signs:

$$\Sigma^<(P) = -2f_F(p_0)\,\mathrm{Im}\,\Sigma_{ret}(P), \quad \Sigma^>(-P) = 2(1-f_F(-p_0))\,\mathrm{Im}\,\Sigma_{ret}(-P) = 2f_F(p_0)\,\mathrm{Im}\,\Sigma_{ret}(-P)$$

The final result for the production rate of Majorana neutrinos therefore is

$$\frac{\mathrm{d}\Gamma_{N_1}}{\mathrm{d}^3 p} = \frac{|\lambda|^2}{(2\pi)^3 2E_{\vec{p}}} \left(\mathrm{Tr}[\not{P}\,\mathrm{Im}\,\Sigma_{ret}(-P)] + \mathrm{Tr}[\not{P}\,\mathrm{Im}\,\Sigma_{ret}(P)] \right). \tag{3.35}$$

3.1.2. Particle abundances and Boltzmann equation

We now want to obtain an equation for the particle number density. Integrating (3.11) over d^3p, we obtain

$$\frac{\mathrm{d}\langle \hat{n}_\varphi \rangle}{\mathrm{d}t} = \mathscr{C}_\varphi \tag{3.36}$$

with the *collision term*

$$\mathscr{C}_\varphi \equiv \int \mathrm{d}^3p \frac{\mathrm{d}\Gamma_\varphi}{\mathrm{d}^3p} \tag{3.37}$$

and the particle density operator $\hat{n}_\varphi = \hat{N}_\varphi/V$. Due to the expansion of the Universe, $V = V_0 a^3$ and therefore computing the total time derivative, we obtain

$$\frac{\partial n}{\partial t} + 3Hn = \mathscr{C}_\varphi \tag{3.38}$$

with number density[8] $n \equiv \langle \hat{n}_\varphi \rangle$ and Hubble parameter $H \equiv \dot{a}/a$. This clearly resembles the usual (integrated) Boltzmann equation–provided we can identify the rhs with the conventional collision term [42]

$$\begin{aligned}\mathscr{C}_\varphi = \int \mathrm{d}\Pi \big[&|\mathcal{M}|^2_{i+j+\ldots\to\varphi+a+b+\ldots} f_i f_j \ldots (1 \pm f_a)(1 \pm f_b)\ldots(1 \pm f_\varphi) \\ &- |\mathcal{M}|^2_{\varphi+a+b+\ldots\to i+j+\ldots} f_a f_b \ldots f_\varphi (1 \pm f_i)(1 \pm f_j)\ldots \big] .\end{aligned} \tag{3.39}$$

Here, $\mathrm{d}\Pi$ denotes the relativistic phase space element and the f's are either Bose-Einstein or Fermi-Dirac distributions, except for f_φ which can be an arbitrary nonthermal distribution.
Both forms (3.37) and (3.39) are indeed equivalent under certain circumstances, as discussed at length in the classic paper [43] which we do not want to reproduce here and whose results we take for granted. In general, (3.39) contains more than the integral over the production rate does, however. Both lead to the same result provided

- Disappearance processes which reduce the number of φ particles are neglected,
- Pauli blocking/Bose enhancement factors $(1 \pm f_\varphi)$ are replaced by 1 such that one can use an integrated form of the Boltzmann equation instead of solving an integro-differential equation for the phase space density f_φ.

Both conditions are in accord with our assumptions that went into the derivation of (3.24) and (3.35)–we started with no φ particles at all and focused on early times $t \ll t_{eq}$, where t_{eq} denotes the time when φ reaches its equilibrium density. If we stay within that setup, then both inverse processes and Pauli blocking/Bose enhancement are indeed negligible.
We already remark that both expressions (3.37) and (3.39) will be used in the computations of chapter 4 because sometimes the one and sometimes the other formula is more convenient and it is useful to switch between both if this simplifies the computation.

3.2. The LPM effect and its role in thermal particle production

Whenever particles traverse a medium, their dynamics and properties may experience profound changes with respect to the vacuum. We have already described such cases in chapter 2 and now we want to turn to a very specific medium effect, named **Landau-Pomeranchuk-Migdal (LPM) effect** after the persons who first described it [3, 4]. First discovered in the context of electromagnetic showering in high-energy cosmic rays, it plays a role in many different contexts (for a review of experimental results and different theoretical approaches on the LPM effect see [44]), but we will focus only on its relevance on thermal particle production here. Since the discussion mostly borrows from [6, 45], all concrete statements will be about photon production from a QGP, but they are analogously valid for other cases, including the production of Majorana neutrinos from an electroweak plasma that will be studied in chapter 4.
Let us first recall how one usually deals with production and absorption of particles via decay and/or scattering. Typically one sets up a set of *Boltzmann equations*, either of the type (3.38) or a more general version where inverse processes are included and one solves for the phase-space density instead of the number density (see e.g. [42]). The collision term of the Boltzmann equation contains all *local* interaction processes that may

[8] The identification of the expectation value of a number density operator with the classical number density is allowed as long as occupation numbers of individual states do not become large. For the applications that are studied within this thesis, this does not happen.

occur and that change the number and/or momentum distribution of the particles that we look at. The crucial assumption is what Boltzmann has termed 'Stoßzahlansatz' in his original treatment: All particles move *freely* except for the moment they experience a collision. This implies that all collisions occur *sequentially* and cannot influence each other–the particles are uncorrelated and once they have interacted they move away from each other, ignorant to the subsequent evolution of their reaction partners. The very same assumptions have also been put in into our calculation in section 3.1. Even more so–the propagation of the particles in between two collisions is essentially *classical* and can be described by phase-space trajectories. This means, that, in prose,

$$\text{de Broglie wavelength} \ll \text{mean free path between collisions.}$$

This is indeed correct since the de Broglie wavelength scales with momentum like $1/p$ whereas the mean free path scales with the interaction cross section like $1/\sigma$. Already at leading order the mean free path is thus at most $1/(g^2T)$ and therefore much larger than the de Broglie wavelength, provided the momenta are larger than the ultrasoft scale, $p \gg g^2T$ which is a safe assumption in phenomenologically relevant considerations. In a hot plasma with gauge interactions, this simple picture in general breaks down. In order to understand why, we must note that there is a second condition for the applicability of the Boltzmann equation:

$$\text{scattering duration} \ll \text{mean free time between collisions}$$

This condition ensures that collisions can indeed be considered sequentially and there is no quantum interference between them. It is precisely this condition that in general is not fulfilled in gauge theories.
Let us look at an emission process $1 \to 2 + \varphi$. The masses are all assumed to be $m \lesssim gT$, which is no restriction if they are thermal masses. In that case, the emission occurs *collinearly*, with a relative angle of order $\vartheta \sim g$. In order to see this, we write

$$P^2 = m_1^2 = (Q + R)^2 = m_2^2 + m_\varphi^2 + 2Q \cdot R, \tag{3.40}$$

which implies $Q \cdot R \sim g^2T^2$ and thus $1 - \cos^2\vartheta \sim g^2 \Leftrightarrow \vartheta \sim g$. We thus precisely have the lightcone kinematics that we considered in section 2.3. Note that we have assumed the particles to be *on-shell* which is relevant e.g. for the production of Majorana neutrinos studied in chapter 4. If we look at the emission of photons instead, then $m_1 = m_2 = m_q \sim gT$ and $m_\varphi = m_\gamma \sim eT \ll m_q$. This process cannot occur unless we set $p^0 = E_{\vec{p}} + \delta E$ and require that $\delta E \sim g^2T$. The emitting quark is thus required to be *off-shell* and one can estimate the scattering duration (in this context also referred to as *formation time*) from the uncertainty principle to be $\tau \sim 1/\delta E \sim (g^2T)^{-1}$. This happens to be *of the same order as the mean free time between soft collisions*. This follows immediately if we remember that the *thermal width* due to soft scattering is $\Gamma \sim g^2T$, as explained in section 2.3.1.[9]
Having understood that the formation time of the photon is of the same order as the mean free time between soft collisions in the plasma, we know that it is impossible to treat emission and prior or subsequent scattering as independent processes. The usual Boltzmann picture of collisions breaks down here. This is illustrated in figure 3.1 which shows the overlap of photon and quark wavefunction during the emission process. The emitted photon still 'feels' the presence of the source, which undergoes soft scattering processes and may also emit another photon. The outgoing photons interfere with each other, thus modifying the emission rate. This is the LPM effect. For photon production, the interference turns out to be destructive on average and the LPM effect leads to a *suppression* of the production rate [7]. A central issue of chapter 4 is to study how the LPM effect influences the production rate of Majorana neutrinos, i.e. of (a special form of) *fermions*.

Now that we have completed the task of explaining what the LPM effect is and why it is relevant for thermal particle production we must explain how to compute it. If we want to keep a Boltzmann-like description, we certainly need to modify the collision term such that it incorporates the LPM effect. In terms of Feynman diagrams, the LPM effect manifests itself as nontrivial interference terms, as depicted in figure 3.2, with an arbitrary number of soft gauge boson scatterings. But such interference terms are precisely generated by cutting *ladder diagrams* of the form shown in figure 2.7. This means that in order to take the LPM effect into account, we need to compute the production rate by taking the imaginary part of the *CTL self-energy* that

[9] Note that due to the width, the scattering duration cannot be larger than $(g^2T)^{-1}$ even if the on-shell emission is kinematically allowed. This is because we must set $p^0 \to p^0 + i\Gamma$ and then even if $p^0 = \sqrt{\vec{p}^2 + m^2}$, the four momentum P is not on-shell and $P^2 \neq m^2$. This also means that there is no pole due to internal lines going on-shell, it is regulated by the thermal width, provided we compute it with an IR regulator which drops out at the end if all relevant diagrams have been included.

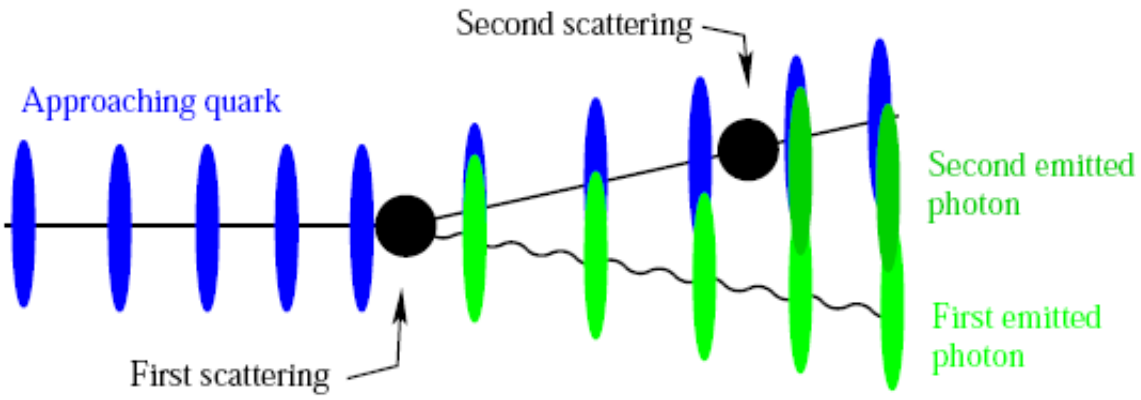

Figure 3.1.: Intuitive picture of the interference of produced photons due to the LPM effect. Picture taken from [46].

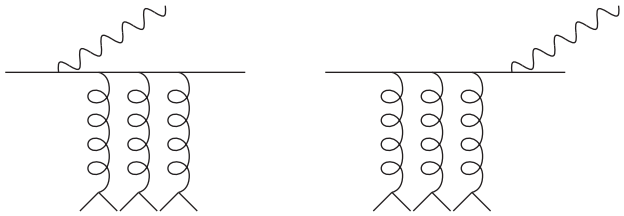

Figure 3.2.: Example for two processes which lead to a nontrivial interference term that needs to be taken into account for the leading order production rate of photons from a QGP. These interference terms are generated by cutting diagrams of the type 2.7.

was introduced in section 2.3.4.[10] Remember that there we have already shown that all ladder diagrams are of the same order w.r.t. the coupling constant, without explaining what the physics behind those diagrams is and what they are good for. In this section we have outlined an intuitive physical picture why they all contribute at leading order provided the momenta are collinear and lightlike–their imaginary part gives the particle production rate including the LPM effect, which as we have learned needs to be taken into account at leading order. What remains to be understood is why diagrams of the form shown in figure 2.8 do not contribute. The explicit calculation in section 3.3 and appendix D.1 proves that no such diagrams contribute

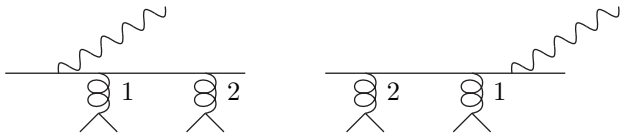

Figure 3.3.: Example for two processes whose interference term would be generated by cutting a ladder diagram with two crossed gluon rungs like in 2.8 but which do not interfere with each other. Time is running from left to right with the leftmost scattering event happening first. Adapted from figure 11 in [47].

at leading order, without providing an intuitive physical picture, however. At least for crossed ladder rungs, one can gain a physical intuition why they need not be taken into account [47]. Look at figure 3.3 which illustrates what kind of interference term would result from cutting a self-energy diagram with two crossed

[10] Note that in contrast to that approach, it is far from obvious how to modify the reaction amplitudes in the version (3.39) of the collision term in order to include the LPM effect. The approach via the relation (3.24) or (3.35) is much more straightforward here.

gluon rungs. The gluons have been labelled [11] in order to make the difference clear. We see that we would have an interference between two processes where the order of soft scattering events is opposite to each other. Such processes cannot interfere because the time scale between two interactions is $1/(g^2T)$ which is much larger than the time scale $1/(gT)$ over which soft gluons can at most interact due to Debye screening. This is indicated by the length scales that were chosen in the figure. Note that this of course only provides a very rough and qualitative picture of the complicated processes that happen in a hot plasma (a slightly more elaborate but still qualitative analysis is given in [47]), but it helps to get a feeling why only the ladder diagrams with uncrossed ladder rungs have to be included in the computation of the particle production rate. The explicit computation performed in [1, 6] as well as this thesis proves this statement at a quantitative level and thus confirmes that the intuitive picture that was put forth here is indeed reasonable.

3.3. An integral equation for the LPM effect

In the previous section we have shown that computing the leading order particle production rate in general requires taking the discontinuity of the CTL self-energy. Here we present its computation with some lengthy intermediate steps moved to appendices C and D.

3.3.1. The basic strategy

The crucial task is to set up a method how to perform the required resummation of ladder diagrams. Before we go into the details of the computation, let us first present the strategy:

1. Start with 1-loop diagrams with two particles of the kind we want to study and an arbitrary number of external soft gauge bosons[12] in the kinematical limit where the loop momentum and the external momenta are collinear, as explained in the previous section. Using approximations justified in this kinematical regime, it is possible to set up a recursion relation that relates a given n-point function to $(n-1)$-point functions where one of the gauge bosons has been removed. Only the 2-point function without any additional soft gauge bosons then needs to be computed explicitly for the case at hand.

2. Define a *current* as the first functional derivative of the generating functional which generates the 1-loop diagrams computed in the first step. The current is much more convenient than the diagrams themselves because one does not need to worry about summing over all possible permutations of external fields. It is given by the integral over all external momenta of the n-point functions, contracted with the external fields. It obeys an integral equation that can easily be found using the results from step 1.

3. Finally, integrate out the soft gauge boson background. The gauge bosons then only appear in self-energy insertions (which generates a *thermal width* for the hard particles in the loop) and as rungs in the ladder diagrams. This new current satisfies an integral equation that is straightforwardly obtained from the one found in step 2. By taking a functional derivative w.r.t. the external field, we finally get an integral equation for the CTL self-energy.

The rest of this section deals with precisely the program outlined above.

3.3.2. The two-point functions

In this section, we first compute the 2-point functions obeying the kinematical constraints (2.50), which serve as a starting point for the construction of the CTL self-energy. This simple case will already enable us to study the approximations that are allowed for the given kinematics.
Consider, then, the generic self-energy as depicted in figure 3.4. The thermal masses of the particles inside the loop are denoted by m_a and m_b, where $m_a = m_b$ is possible. It will be convenient to define a *reduced self-energy* by taking out the spatial loop integral and also the factor associated with the vertex on the right, where the momentum K 'starts'. The vertex factor is denoted by Φ_φ, with possible Lorentz, spinor and/or

[11] Since the gluons have different momenta, they are *not* indistinguishable particles.
[12] The gauge boson background contains also *hard* gauge bosons, but they are already assumed to be integrated out in this step. This leads to the appearance of *asymptotic thermal masses* which are studied in section 2.3.1 and appendix B.

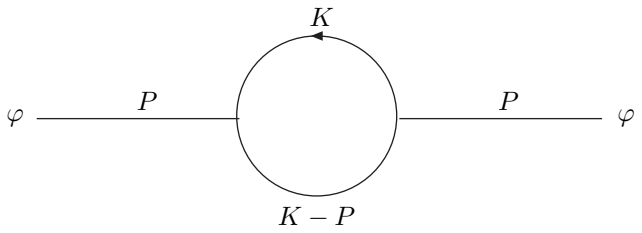

Figure 3.4.: Generic two-point function with hard, lightlike external momentum collinear to the loop momentum. The external particle is denoted by φ like in section 3.1.

group indices left implicit in order to be as general as possible. We then study the reduced self-energy $\hat{\Pi}(P,\vec{k})$ defined by[13]

$$\Pi(P) = -\int \frac{\mathrm{d}^3k}{(2\pi)^3}\,\mathrm{Tr}[\Phi_\varphi(K,K-P)\hat{\Pi}(P,\vec{k})] \tag{3.41}$$

where the trace goes over internal degrees of freedom.
Let us first look at the propagators. What we need are propagators for a hard, lightlike momentum which are dressed with an asymptotic mass. The corresponding propagators were already shown in section 2.3.1 and they are derived in appendix B: The scalar propagator is simply

$$\Delta(K) = -\frac{1}{K^2 - m^2} \tag{3.42}$$

whereas the fermion propagator can be related to the scalar propagator, as shown in equation (B.34). Diagrams with gauge boson propagators will not be needed in this thesis and are therefore not considered here. The nontrivial spinor structure of fermion propagators will for convenience be absorbed into the definition of the vertex factor Φ. Then we can always use propagators of the form (3.42) and only have to be careful whether we have integer or half-integer Matsubara frequencies.
The reduced self-energy is then given by

$$\hat{\Pi}(P,\vec{k}) = T\sum_{k_0^\sigma} \Phi_\varphi^\dagger(K,K-P)\Delta(K)\Delta(K-P). \tag{3.43}$$

Here we have introduced an index σ with $\sigma = 0$ for bosons (integer Matsubara frequencies) and $\sigma = 1$ for fermions (half-integer Matsubara frequencies). The thermal sum is performed via the usual complex integration procedure (2.17):

$$\hat{\Pi}(P,\vec{k}) = \int_C \frac{\mathrm{d}k_0}{2\pi i}\left(\frac{1}{2} + (-1)^\sigma f^\sigma(k_0)\right)\Phi_\varphi^\dagger(K,K-P)\Delta(K)\Delta(K-P). \tag{3.44}$$

The poles are located at $k_0 = \pm E_k$ and $k_0 = p_0 \pm E_{k-p}$. Then we can write

$$\begin{aligned}\hat{\Pi}(P,\vec{k}) = &\sum_{k_{0,pole}=\pm E_k}\left(\frac{1}{2} + (-1)^\sigma f^\sigma(k_{0,pole})\right)\left[\Phi_\varphi^\dagger(K,K-P)\Delta(K-P)(k_0 \pm E_k)^{-1}\right]\big|_{k_0=k_{0,pole}} \\ &+ \sum_{k_{0,pole}=p_0\pm E_{p-k}}\left(\frac{1}{2} + (-1)^\sigma f^\sigma(k_{0,pole})\right)\left[\Phi_\varphi^\dagger(K,K-P)\Delta(K)(k_0 - p_0 \pm E_{k-p})^{-1}\right]\big|_{k_0=k_{0,pole}}\end{aligned}$$

To obtain expressions for the propagators, we first of all approximate the energies using

$$E_k = \sqrt{k_\parallel^2 + k_\perp^2 + m^2} = \left|k_\parallel\right| + \frac{k_\perp^2 + m^2}{2\left|k_\parallel\right|} + \mathcal{O}(g^4T). \tag{3.45}$$

[13] A minus sign is inserted because with our conventions, the diagrams correspond to $-\Pi$ and not to Π, see appendix A. The reduced self-energy $\hat{\Pi}$ is then free of this additional minus sign.

We now look at the inverse propagator $(\Delta(K-P))^{-1}$ at $k_0 = \pm E_k$. We replace p_0 using $p_- = p_0 - p_\parallel$ and obtain

$$\begin{aligned}(\Delta(K-P))^{-1}\big|_{k_0=\pm E_k} &= -\left[(k_0-p_0)^2 - (\vec{k}-\vec{p})^2 - m_b^2\right] \\ &= -\left[E_k^2 + \left(p_- + p_\parallel\right)^2 \mp 2\left(p_- + p_\parallel\right)E_k - \vec{p}^2 - \vec{k}^2 + 2\vec{p}\cdot\vec{k} - m_b^2\right] \\ &\approx -\left[2p_\parallel(k_\parallel \mp |k_\parallel|) + 2p_-\left(p_\parallel \mp |k_\parallel|\right) \mp p_\parallel \frac{\vec{k}_\perp^2 + m_a^2}{|k_\parallel|} - (\vec{p}_\perp - \vec{k}_\perp)^2 + \vec{k}_\perp^2 + m_a^2 - m_b^2\right]\end{aligned}$$

where (3.45) was used and higher order terms were neglected. The first term is $\sim T^2$, whereas all other terms are $\sim g^2T^2$. In order to get an enhancement, we therefore have to impose the condition[14]

$$k_\parallel = \pm|k_\parallel|. \tag{3.46}$$

The inverse propagator is then given by

$$(\Delta(K-P))^{-1}\big|_{k_0=\pm E_k} \approx -\left[2p_-(p_\parallel - k_\parallel) - \frac{p_\parallel}{k_\parallel}(\vec{k}_\perp^2 + m_a^2) - (\vec{p}_\perp - \vec{k}_\perp)^2 + k_\perp^2 + m_a^2 - m_b^2\right]$$

and after some simple algebra we arrive at the result

$$\Delta(K-P))|_{k_0=\pm E_k} = \frac{\Theta(\pm k_\parallel)}{2(k_\parallel - p_\parallel)}\left[p_- - \frac{\vec{k}_\perp^2 + m_a^2}{2k_\parallel} + \frac{(\vec{k}_\perp - \vec{p}_\perp)^2 + m_b^2}{2(k_\parallel - p_\parallel)}\right]^{-1}. \tag{3.47}$$

A step function was included to guarantee the condition (3.46).
The procedure to approximate the other propagator is exactly the same and leads to the following result:

$$\Delta(K)|_{k_0=p_0\pm E_{p-k}} = -\frac{\Theta(\pm(k_\parallel - p_\parallel))}{2k_\parallel}\left[p_- - \frac{\vec{k}_\perp^2 + m_a^2}{2k_\parallel} + \frac{(\vec{k}_\perp - \vec{p}_\perp)^2 + m_b^2}{2(k_\parallel - p_\parallel)}\right]^{-1}. \tag{3.48}$$

The remaining factors in (3.45) can be easily evaluated. For the distribution functions we use that $e^{\beta p_0} = (-1)^{\sigma+\tau}$ where τ is an index of the same form as σ and refers to the particle with momentum $K-P$ in the loop. This leads, again dropping all higher order terms, to

$$(-1)^\sigma f^\sigma(\pm E_k) = (-1)^\sigma f^\sigma(k_\parallel); \quad (-1)^\sigma f^\sigma(p_0 \pm E_{k-p}) = \frac{(-1)^\sigma}{e^{\beta p_0}e^{\pm\beta E_{k-p}} - (-1)^\sigma} = (-1)^\tau f^\tau(k_\parallel - p_\parallel). \tag{3.49}$$

For the factors $(k_0 \pm E_k)^{-1}$ and $(k_0 - p_0 \pm E_{k-p})^{-1}$, we may use $k_0 = k_\parallel$, such that in the end the two factors lead to identical contributions. Summing over both of them then just has the effect to remove the step functions from the final result, since $\Theta(x) + \Theta(-x) = 1$.
For notational convenience, we will from now on use $D(K)$ and $D(K-P)$ defined as

$$\Delta(K) \equiv \frac{1}{2k_\parallel}D(K) \tag{3.50}$$

(and the same for $D(K-P)$) as propagators and absorb the prefactors into the function $\Phi_\varphi(K, K-P)$. The final result for the reduced 1-loop two-point function is then given by

$$\begin{aligned}\hat{\Pi}(P,\vec{k}) = &\left[\left(\frac{1}{2} + (-1)^\sigma f^\sigma(k_\parallel)\right)\Phi_\varphi^\dagger(K,K-P)\big|_{k_0=E_k} - \left(\frac{1}{2} + (-1)^\tau f^\tau(k_\parallel - p_\parallel)\right)\Phi_\varphi^\dagger(K,K-P)\big|_{k_0=p_0+E_{p-k}}\right] \\ &\epsilon_{ab}^{-1}(P,\vec{k})\end{aligned} \tag{3.51}$$

with a relative minus sign coming from (3.47) and (3.48). Here we defined

$$\epsilon_{ab}(P,\vec{k}) \equiv p_- - \frac{\vec{k}_\perp^2 + m_a^2}{2k_\parallel} + \frac{(\vec{k}_\perp - \vec{p}_\perp)^2 + m_b^2}{2(k_\parallel - p_\parallel)} \tag{3.52}$$

[14]Note that the sign refers to the sign of the two poles at $k_0 = \pm E_k$, otherwise the condition would be tautological.

for convenience because this factor will frequently reappear in the following computation and also in the final integral equation. It is nothing else but the difference of the pole locations of our two propagators and it is of order g^2T.
If we take the *discontinuity* w.r.t. p_0, the result becomes even easier because we get a delta function $\delta(\epsilon_{ab}(P,\vec{k}))$. This means that the difference between the pole locations vanishes and we can factor out $\Phi^\dagger$ as well. In that case, we obtain

$$\operatorname{Disc}\hat{\Pi}(P,\vec{k}) = 2i\operatorname{Im}\hat{\Pi}(p_0+i\varepsilon,\vec{p},\vec{k}) = \mathcal{F}(k_\parallel,p_\parallel)\ \Phi^\dagger_\varphi(K,K-P)\big|_{k_0=E_k}\ 2i\pi\delta(\epsilon_{ab}(P,\vec{k})). \tag{3.53}$$

The combination of distribution function that appears here has also been given a name:

$$\mathcal{F}(k_\parallel,p_\parallel) \equiv (-1)^\sigma f^\sigma(k_\parallel) - (-1)^\tau f^\tau(k_\parallel - p_\parallel) \tag{3.54}$$

In the following, we will write equations directly for $\hat{\Pi}$ and take the discontinuity only when we compute the particle production rate. Still, we will make simplifications allowed by taking the locations of the poles to vanish in order to get easier expressions. One has to keep in mind then that the integral equation we will finally obtain is not a strict equality but we may only use it if we are interested in $\operatorname{Disc}\hat{\Pi}$ only. This allows us to simply write

$$\hat{\Pi}(P,\vec{k}) = \mathcal{F}(k_\parallel,p_\parallel)\ \Phi^\dagger_\varphi(K,K-P)\big|_{k_0=E_k}\ \epsilon^{-1}_{ab}(P,\vec{k}). \tag{3.55}$$

We should finally remark that whenever we have only bosonic external particles, there may also be a *quadrilinear* vertex which leads to a totally different form of the self-energy. However, these diagrams have vertex factors which are *independent* of the external momentum and therefore they are not interesting for our purposes, although in a more complete treatment they should certainly be included.

3.3.3. The recursion relation for amplitudes

As outlined in section 3.3.1, the next step is to consider diagrams with n external gauge bosons as shown in figure 3.5 and to find a recursion relation that relates the amplitude with n external gauge bosons to the one with $n-1$ gauge bosons. The external gauge bosons are all taken to have *soft* momenta–except for the two photons in the case of the photon self-energy which always have hard, nearly lightlike momenta. In that case, we also assume one of the photons to have a momentum $K_m, 1 \le m \le n-1$, i.e. we never explicitly distinguish external photons and external gluons which proves to be unnecessary. To obtain a more compact notation, we have finally defined $\tilde{K}_l \equiv \sum_{j=0}^{l} K_j$.
The starting point for all the recursion relations is the following simple identity for the propagators, valid both for the bosonic and the fermionic (and also a mixed) case:

$$D(K)D(K-P) = \frac{D(K)-D(K-P)}{\epsilon_{ab}(P,\vec{k})} \tag{3.56}$$

It is proved in appendix B.4.
This result means that instead of the product of the two propagators meeting at the rightmost vertex in figure 3.5, we get two contributions where in each of them only one of the propagators has remained. This already suggests that one should try to relate the expression for the amplitude to the one with one of the external particles removed, such that in total, one propagator less occurs. And this is precisely what can be done.
First of all, we need to define a general amplitude including n soft gauge bosons with momenta K_i as a generalization of the previous definitions:

$$\Pi^{(n)a_1\ldots a_n}_{\mu_1\ldots\mu_n}(P,K_1,\ldots,K_n) = -\int\frac{\mathrm{d}^3k}{(2\pi)^3}\operatorname{Tr}\left[\Phi_\varphi(K,K-P)\hat{\Pi}^{(n)a_1\ldots a_n}_{\mu_1\ldots\mu_n}(P,K_1,\ldots,K_n,\vec{k})\right]. \tag{3.57}$$

Here, a_i and μ_i refer to the soft gauge bosons. For the photon polarization tensor, there is an additional Lorentz index in $\hat{\Pi}$ (and one in Φ_φ), which we simply assume to be one of the μ_i. This is because, as already mentioned, we do not want to specify which of the external gauge bosons are the photons and which ones are the gluons. Note that the gauge couplings are not written explicitly but instead are assumed to be absorbed in the gauge boson fields.
In the following we will only have to consider n-point diagrams of the form shown in figure 3.5. One can

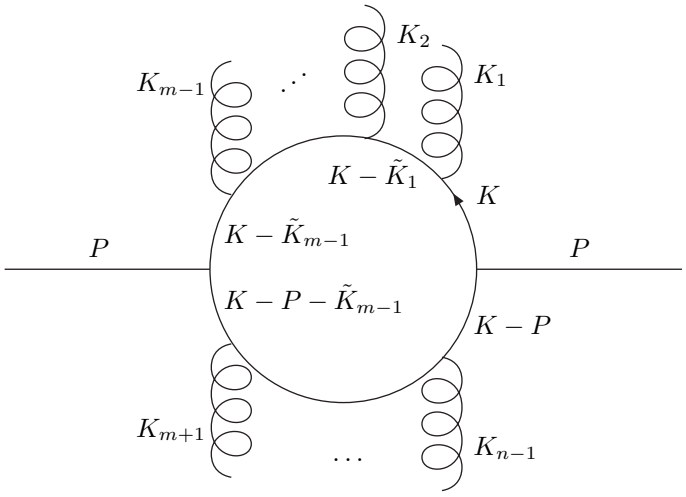

Figure 3.5.: Generic n-point function with soft external gauge bosons

Figure 3.6.: Diagrams involving seagull vertices are suppressed compared to diagrams with only trilinear vertices because one propagator is 'missing' and cannot give a $1/g^2$ enhancement. The same reasoning applies to four gauge boson-vertices.

of course also draw diagrams which involve a seagull vertex with soft gauge bosons or a four gauge boson vertex, but they are suppressed at leading order, as illustrated in figure 3.6.
Now we can formulate our recursion relation. Using (3.56), we get, starting from an amplitude with n gauge bosons, two terms proportional to amplitudes with $n-1$ gauge bosons. Obviously we need to remove the two external particles adjacent to the rightmost vertex, i.e. those with momenta K_1 and K_{n-1}, and in one case perform also a shift of the momentum (and summation variable), $K \to K - K_1$, as illustrated in figure 3.7. The resulting recursion relation is of the form

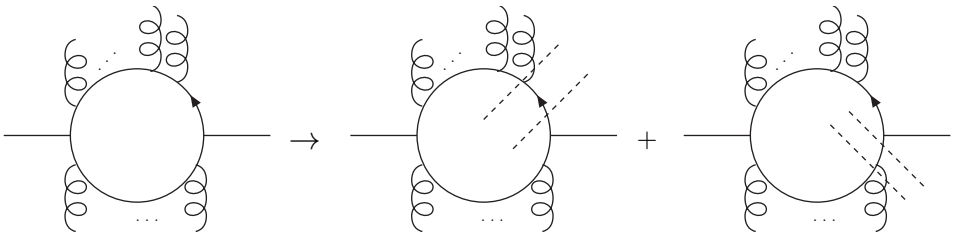

Figure 3.7.: Sketch of the desired recursion relation: A diagram with an arbitrary number n of external gauge bosons is related to the sum of two diagrams, each of them with one gauge boson removed.

$$\hat{\Pi}^{(n)a_1\ldots a_n}_{\mu_1\ldots\mu_n}(P,K_1,\ldots,K_n,\vec{k}) = \frac{1}{\epsilon_{ab}(P,\vec{k})}\Big[\hat{\Pi}^{(n-1)a_1\ldots a_{n-1}}_{\mu_1\ldots\mu_{n-1}}(P,K_1,\ldots,K_{n-1},\vec{k})\mathcal{V}^{a_n}_{\mu_n}(K-P,K-P+K_n) - \mathcal{V}^{a_1}_{\mu_1}(K-K_1,K)\hat{\Pi}^{(n-1)a_2\ldots a_n}_{\mu_2\ldots\mu_n}(P,K_2,\ldots,K_n,\vec{k}-\vec{k}_1)\Big] \tag{3.58}$$

where the factors $\mathcal{V}$ arise from the corresponding vertices with the external gluons that were removed and will be evaluated soon. They involve gauge bosons with a *soft* momentum and we denote them by $\mathcal{V}$ to avoid confusion with the vertex factors Φ_φ at the vertices with the particle whose production we want to study and which involves only *hard* momenta. This means that even if the external particle itself is a gauge boson, e.g. a photon, the factors $\mathcal{V}$ and Φ_φ are not the same (see appendix C).
Note that we always assume that the two external particles to be removed are soft gauge bosons. This raises the question how to deal with n-point amplitudes where all external soft gauge bosons couple to only one of the particles inside the loop, where either the first or the last external particle is of the type whose production we study and (3.56) suggests to remove one of them instead. This would not be a real problem if we consider photon production where Φ_φ and $\mathcal{V}$ have essentially the same structure (cf. appendix C) and we could just use Φ_φ in the recursion relation instead. But for the production of fermions, the corresponding factor Φ_φ is fundamentally different from $\mathcal{V}$ and one could be worried about how to formulate the recursion relation to cover that case as well. However, in appendix C.2 we will show that those contributions to the recursion relation where an external hard particle is removed can be left out at leading order. Thus (3.58) is the final result for the recursion relation.

The soft vertex factors

We now need expressions for the vertex factors $\mathcal{V}$ in (3.58). They always involve one gauge boson with soft momentum K_i and two other particles of identical spin, which are either scalars or spin 1/2 fermions and which have a hard momentum K or $K-P$. Other types of vertices may arise depending on the context (for the production of *gravitinos* one needs e.g. to consider also vertices with three gauge bosons), but they are not relevant for this thesis and will be omitted.
We denote the vertex factors involving hard scalars and fermions temporarily by $\mathcal{V}_{(S)}$ and $\mathcal{V}_{(F)}$, respectively. It will turn out that *at leading order* they are equal and there is only one soft vertex factor $\mathcal{V}$. The first one can be trivially written down exactly:

$$\mathcal{V}^{\mu_i}_{(S),a_i} = \frac{1}{2k_\parallel}\,(2K^{\mu_i})|_{k^0=k_\parallel}\,t^{a_i} \tag{3.59}$$

The prefactor $1/2k_\parallel$ can easily be understood by looking at (3.50) and (3.56). Depending on which part of the loop the i-th gluon is coupled to, K must eventually be replaced by $K-P$. To avoid unnecessary notational complications, we will always assume the hard momentum to be K in the following.
Determining the vertex factor for a fermion-antifermion-gauge boson vertex requires more work. As explained before, the spinor structure in the numerator of the fermion propagators (B.34) is always absorbed in the vertices such that we deal with propagators formally identical (up to the difference between integer and half-integer Matsubara frequencies) to those for scalars. Since thermal masses do not break the chiral symmetry, we may use, as explained in appendix B.2, spinors of *definite chirality* here, i.e. we consider left- and righthanded contributions seperately which amounts to using two-component spinors and replacing γ^μ by $\sigma^\mu=(\mathbb{1},\sigma^i)$ or $\bar{\sigma}^\mu=(\mathbb{1},-\sigma^i)$. The fermion trace then takes the form

$$\mathrm{Tr}\left[\eta(K)\eta^\dagger(K)\bar{\sigma}^{\mu_1}\eta(K-\tilde{K}_1)\eta^\dagger(K-\tilde{K}_1)\ldots\eta^\dagger(K-\tilde{K}_{n-2})\bar{\sigma}^{\mu_{n-1}}\eta(K-\tilde{K}_{n-1})\eta^\dagger(K-\tilde{K}_{n-1})\bar{\sigma}^{\mu}\right] +$$
$$\mathrm{Tr}\left[\chi(K)\chi^\dagger(K)\sigma^{\mu_1}\chi(K-\tilde{K}_1)\chi^\dagger(K-\tilde{K}_1)\ldots\chi^\dagger(K-\tilde{K}_{n-2})\sigma^{\mu_{n-1}}\chi(K-\tilde{K}_{n-1})\chi^\dagger(K-\tilde{K}_{n-1})\sigma^{\mu}\right]$$

where $\tilde{K}_l\equiv\sum_{i=1}^{l}K_i$ and both η and χ are left- or right-handed Weyl spinors defined as eigenspinors of $\vec{\sigma}\cdot\hat{k}$. Depending on the form of the interaction, it may also happen that only fermions of *one* chirality propagate in the loop and not both. This happens e.g. for the production of Majorana neutrinos studied in chapter 4. Since for the applications that we study, both chiralities (if present) give exactly the same result this does not affect the argument at all. For us it is always sufficient to take spinors of one chirality (say, the left-handed ones) and if necessary multiply the final result by 2. Thus, what we need to evaluate are expressions of the form $\eta^\dagger(K)\sigma^{\mu_i}\eta(K-K_i)$.[15] This is done in appendix C where we show that indeed at leading order

[15] Note that the trace has a cyclic invariance which allows to move the first spinor to the very end.

$\mathcal{V}_{(F)} = \mathcal{V}_{(S)}$ and we simply get

$$\mathcal{V}_a^\mu = V^\mu t_a + \mathcal{O}(g). \tag{3.60}$$

3.3.4. Integral equation for the CTL self-energy

With the help of the recursion relation (3.58), it is now possible to formulate equations for the *current*. It will give us a relatively simple method to *integrate out* the soft gauge bosons and therefore lead to the *ladder diagrams* shown in section 2.3.4 and also generate a thermal width for the particles in the loop. Once the soft gauge bosons are integrated out, the functional derivative of the new current gives us back the self-energy we are interested in.

The current

First of all, we need to define the current for our particle φ. We write it in the form

$$J_\varphi(P) \equiv -\int \frac{\mathrm{d}^3 k}{(2\pi)^3} \operatorname{Tr}[\Phi_\varphi(K, K-P)\hat{J}_\varphi(P,\vec{k})], \tag{3.61}$$

leaving possible Lorentz and/or spinor indices implicit. The reduced current $\hat{J}_\varphi$ is given by an expression of the form

$$\hat{J}_\varphi(P,\vec{k}) = \sum_{n=0}^{\infty}\prod_{i=1}^{n}\left(\int \frac{\mathrm{d}^4 K_i}{(2\pi)^4} W_{\mu_i}^{a_i}(K_i)\right)(2\pi)^4\delta(K-\tilde{K}_n)\hat{\Pi}^{(n)a_1\ldots a_n}_{\mu_1\ldots\mu_n}(K_1,\ldots,K_n,\vec{k}) \tag{3.62}$$

where the external gauge fields are collectively denoted by $W_\mu \equiv t^a W_\mu^a$ and we used the notation $\tilde{K}_l \equiv \sum_{i=1}^{l} K_i$ again. The form above with only gauge fields appearing as external fields is valid for the photon current, in general one of the external fields needs to be replaced by the corresponding fermion field φ instead (for photons, φ is one of the gauge fields W_μ).
Using the recursion relations (3.58) and the explicit result (3.55) for the two-point function, we can write down an integral equation for the reduced current. The explicit result for the two-point function is needed because the recursion relation is only valid if there are more than two external fields. We get the following integral equation:

$$\hat{J}_\varphi(P,\vec{k}) = \frac{1}{\epsilon_{ab}(P,\vec{k})}\left\{\mathcal{C}_\varphi(K,P)\cdot\varphi(P) + \int_Q\left[\hat{J}_\varphi(P-Q,\vec{k})V^\mu W_\mu(Q) - V^\mu W_\mu(Q)\hat{J}_\varphi(P-Q,\vec{k}-\vec{q})\right]\right\} \tag{3.63}$$

where due to (3.55), we have

$$\mathcal{C}_\varphi(K,P) \equiv \mathcal{F}(k_\parallel,p_\parallel)\Phi_\varphi^\dagger(K,K-P) \tag{3.64}$$

and we used (3.60). Furthermore, we wrote Q instead of K_1 as in (3.58) and we introduced the compact notation

$$\int_Q \equiv T\sum_{q_0}\int\frac{d^3q}{(2\pi)^3}. \tag{3.65}$$

A subtlety arises again in the equation for the photon current since we treated photons and gauge bosons on the same footing. It is related to the issue of removing external fermion lines raised after equation (3.58) and is treated in passing in appendix C.2 where we show that only contributions where a *soft* external gauge boson is removed contribute at leading order. This is why we need only the equation which has an explicit photon field A_μ in the inhomogeneous term, and under the integral, we then only have gluon fields.

Integrating out the soft gauge boson background

The final step is to *integrate out* the soft gauge bosons. By this procedure, they disappear as external particles and appear only in propagators, thereby generating the ladder diagrams introduced in 2.3.4 and also the *thermal widths* of the hard particles inside the loop. Both of these two contributions taken for themselves would be IR divergent, but combined together they will lead to a finite result.
Integrating out the soft gauge bosons means that we consider now the current

$$\left\langle \hat{J}_\varphi[\varphi]\right\rangle = \int \mathcal{D}W_\mu e^{iS[W_\mu,\varphi]}\hat{J}_\varphi[W_\mu,\varphi] \tag{3.66}$$

where for clarity we have written the currents as functionals of the fields instead of functions of momenta. In order to formulate an equation for the current (3.66), we first iterate equation (3.63) once by inserting the rhs under the integral. We throw away terms which have both an explicit field φ and an explicit gauge boson W_μ which no longer corresponds to a current of real φ fields in a soft gauge boson background; those terms would give no contribution after performing the path integral anyway. Therefore, what remains is

$$\begin{aligned}\hat{J}_\varphi(P,\vec{k}) = \frac{1}{\epsilon_{ab}(P,\vec{k})}\Bigg\{\mathcal{C}_\varphi(K,P)\cdot\varphi(P) + \int_Q\int_{Q'}\Bigg[\frac{1}{\epsilon_{ab}(P-Q,\vec{k})}\Big(\hat{J}_\varphi(P-Q-Q',\vec{k})V^\mu W_\mu(Q')- \\ V^\mu W_\mu(Q')\hat{J}_\varphi(P-Q-Q',\vec{k}-\vec{q}')\Big)V^\mu W_\mu(Q) - V^\mu W_\mu(Q)\frac{1}{\epsilon_{ab}(P-Q,\vec{k}-\vec{q})}\cdot \\ \Big(\hat{J}_\varphi(P-Q-Q',\vec{k}-\vec{q})V^\mu W_\mu(Q') - V^\mu W_\mu(Q')\hat{J}_\varphi(P-Q-Q',\vec{k}-\vec{q}-\vec{q}')\Big)\Bigg]\Bigg\}.\end{aligned}$$

Now it is advantageous to take the trace over the group generators according to the definition of the currents, because this allows to perform cyclic permutations and put the factors $V^\mu W_\mu$ together such that they can be factored out:

$$\begin{aligned}\mathrm{Tr}\,\hat{J}_\varphi(P,\vec{k}) = \frac{1}{\epsilon_{ab}(P,\vec{k})}\Bigg\{d(r)\mathcal{C}_\varphi(K,P)\cdot\varphi(P) + \int_Q\int_{Q'}\frac{1}{\epsilon_{ab}(P-Q,\vec{k})}\,\mathrm{Tr}\,[V^\mu W_\mu(Q)V^\mu W_\mu(Q') \\ \Big(\hat{J}_\varphi(P-Q-Q',\vec{k}) - \hat{J}_\varphi(P-Q-Q',\vec{k}-\vec{q}')\Big)\Big] - \frac{1}{\epsilon_{ab}(P-Q,\vec{k}-\vec{q})}\cdot \\ \mathrm{Tr}\left[V^\mu W_\mu(Q)V^\mu W_\mu(Q')\left(\hat{J}_\varphi(P-Q-Q',\vec{k}-\vec{q}) - \hat{J}_\varphi(P-Q-Q',\vec{k}-\vec{q}-\vec{q}')\right)\right]\Bigg\}.\end{aligned}$$

Here, $d(r)$ results from the trace over a unit matrix and is the dimension of the corresponding group representation.
Now it is time to integrate out the soft gauge bosons. In a very sketchy notation, leaving out all irrelevant factors, we will get something like

$$\mathrm{Tr}\langle\hat{J}_\varphi\rangle = \mathcal{C}_\varphi\cdot\varphi + \int_Q \mathrm{Tr}\langle WW\hat{J}_\varphi\rangle$$

where the final term has two contributions:

$$\langle WW\hat{J}_\varphi\rangle = \langle WW\rangle\langle\hat{J}_\varphi\rangle + \langle WW\hat{J}_\varphi\rangle_{connected} \tag{3.67}$$

The connected part is precisely made out of those contributions that cannot be factored into a W-propagator and the current itself and it contributes to diagrams with *crossed ladder rungs* which we do not need. In fact, at leading order, this part gives a vanishing contribution and can be left out. Details can be found in appendix D.1.
We therefore discard the connected part and obtain, using the propagator[16]

$$\langle W^a_\mu(Q)W^b_\nu(Q')\rangle = g^2\delta^{ab}\delta(Q+Q')\Delta_{\mu\nu}(Q) \tag{3.68}$$

and the Casimir invariant $t^a t^a = C_2(r)\mathbb{1}$, the following simplified form where the integral over Q' which is now trivial due to (3.68) is already performed:

$$\begin{aligned}\mathrm{Tr}\langle\hat{J}_\varphi(P,\vec{k})\rangle = \frac{1}{\epsilon_{ab}(P,\vec{k})}\Bigg\{d(r)\mathcal{C}_\varphi(K,P)\cdot\varphi(P) + C_2(r)g^2\int_Q V^\mu V^\nu\Delta_{\mu\nu}(Q) \\ \left(\frac{1}{\epsilon_{ab}(P-Q,\vec{k})} + \frac{1}{\epsilon_{ab}(P-Q,\vec{k}-\vec{q})}\right)\mathrm{Tr}\left[\langle\hat{J}_\varphi(P,\vec{k})\rangle - \langle\hat{J}_\varphi(P,\vec{k}-\vec{q})\rangle\right]\Bigg\}.\end{aligned} \tag{3.69}$$

Note that due to the propagator, the gauge coupling that was always left implicit so far now reappears.
This can still be simplified. Although in (3.52) all terms are of the same order, we still need to keep only

[16] The compact notation hides the fact that there may be several gauge bosons that contribute, as e.g. for the production of Majorana neutrinos where both external weak gauge bosons and external photons may play a role. Therefore, when dealing with specific cases one has to state carefully what kind of gauge bosons $\Delta_{\mu\nu}$ stands for.

$1/(p_- - q_-)$ here. In order to understand this, we can explicitly look at the thermal sum over q_0, where the dominant contribution would be from the pole at $q_0 = q_\parallel$. If we keep the additional terms in (3.52), their only effect would be to shift the pole to $q_0 = q_\parallel + X$, where $X \sim g^2 T$. Since $q_\parallel \sim gT \gg X$, we can neglect this contribution at leading order.[17] For this it is crucial that the integrand, including the gauge boson propagator, separately depends on q^0 and $q_\parallel$ and not just on q_-. Therefore, we may finally write

$$\begin{aligned}\mathrm{Tr}\langle \hat{J}_\varphi(P,\vec{k})\rangle = \frac{1}{\epsilon_{ab}(P,\vec{k})}\Bigg\{ & d(r)\mathcal{C}_\varphi(K,P)\cdot\varphi(P) + 2C_2(r)g^2\int_Q \frac{V^\mu V^\nu \Delta_{\mu\nu}(Q)}{p_- - q_-} \\ & \mathrm{Tr}\left[\langle \hat{J}_\varphi(P,\vec{k})\rangle - \langle \hat{J}_\varphi(P,\vec{k}-\vec{q})\rangle\right]\Bigg\}. \end{aligned} \tag{3.70}$$

The integrand still depends on the HTL resummed gauge boson propagator and is therefore rather complicated. It is possible to find a much more explicit form for it, which requires a rather long and tedious calculation that we show in appendix D.2. The final result then is

$$\begin{aligned}\mathrm{Tr}\langle \hat{J}_\varphi(P,k_\parallel,\vec{k}_\perp)\rangle = \frac{1}{\epsilon_{ab}(P,\vec{k})}\Bigg\{ & d(r)\mathcal{C}_\varphi(K,P)\cdot\varphi(P) + ig^2 C_2(r) T\int \frac{\mathrm{d}^2 q_\perp}{(2\pi)^2}\mathcal{K}(\vec{q}_\perp) \\ & \mathrm{Tr}\left[\langle \hat{J}_\varphi(P,k_\parallel,\vec{k}_\perp)\rangle - \langle \hat{J}_\varphi(P,k_\parallel,\vec{k}_\perp-\vec{q}_\perp)\rangle\right]\Bigg\} \end{aligned} \tag{3.71}$$

with the kernel

$$\mathcal{K}(\vec{q}_\perp) \equiv \frac{1}{q_\perp^2} - \frac{1}{q_\perp^2 + m_D^2} \tag{3.72}$$

which depends on the *Debye mass* m_D defined in (B.81).[18] Using this form, it is now easy to see that the apparent logarithmic IR-divergence is in fact cancelled by the vanishing difference of the two currents. Each of them separately, however, would lead to an IR divergence. Note that one can interpret those two terms as generating self-energy insertions and therefore a width for the hard loop particle (first term) and the ladder diagrams with soft gauge boson rungs (second term), respectively. This shows that both the width and the ladder diagrams taken for themselves are not physically meaningful and only taken together give a well-behaved result. For more details on the IR safeness of the integral equation and other general properties see the discussion in [6] that we do not want to repeat here.
Finally, we can write an equation for the reduced self-energy by taking a functional derivative w.r.t. the external field:

$$\hat{\Pi}_\varphi = \frac{\delta\langle \mathrm{Tr}\,\hat{J}_\varphi\rangle}{\delta\varphi} \tag{3.73}$$

This leads to

$$\hat{\Pi}_\varphi(P,k_\parallel,\vec{k}_\perp) = \frac{1}{\epsilon_{ab}(P,\vec{k})}\left\{ d(r)\mathcal{C}_\varphi(K,P) + ig^2 C_2(r) T\int \frac{\mathrm{d}^2 q_\perp}{(2\pi)^2}\mathcal{K}(\vec{q}_\perp)\left[\hat{\Pi}_\varphi(P,k_\parallel,\vec{k}_\perp) - \hat{\Pi}_\varphi(P,k_\parallel,\vec{k}_\perp-\vec{q}_\perp)\right]\right\}. \tag{3.74}$$

This equation is the main result of this section. It is still completely general, but we can now easily specify certain cases by computing the explicit form of $\mathcal{C}_\varphi$ which depends on the external vertex factor Φ_φ.

Before we apply (3.74) in a context where the LPM effect has not been studied before, we finally want to reproduce the equations for the production of photons from a quark-gluon plasma. This will serve as a consistency check of our new method.

3.4. Photon production from a quark-gluon-plasma

Here we want to show that for photon production from a quark-gluon plasma the integral equation (3.74) is equivalent to the one derived in [6, 47]. We will not review the computation of the complete leading-order thermal production rate of photons which can be found in [7]. Rather we want to provide a consistency check

[17] Note, however, that p_- may not be simply left out, even after the analytical continuation of p^0, because we need to take the discontinuity, i.e. set $p^0 \to p^0 \pm i\varepsilon$.

[18] If there are several gauge bosons that contribute, e.g. photons and weak gauge bosons in the case of Majorana neutrino production, we need to sum over all possibilities and take the different Debye masses into account.

that the new method to deal with the LPM effect leads to the correct result in a case where we already know what it looks like before applying it to the production of Majorana neutrinos in the following chapter.
In this case, the external particle is represented by a Lorentz four-vector field A^μ and the reduced amplitude as well as the vertex factor Φ both have a Lorentz index. Inside the loop, we have a pair of quarks, i.e. spin 1/2 fermions. Therefore, equation (3.74) can be written more explicitly as

$$\begin{aligned}\hat{\Pi}_\nu(P,k_\parallel,\vec{k}_\perp) = \frac{1}{\epsilon(P,\vec{k})}\Bigg\{ & d(r)\mathcal{F}(k_\parallel,p_\parallel)\Phi_\nu^\dagger(K,K-P) + ig^2C_2(r)T\int\frac{\mathrm{d}^2q_\perp}{(2\pi)^2}\mathcal{K}(\vec{q}_\perp) \\ & \left[\hat{\Pi}_\nu(P,k_\parallel,\vec{k}_\perp) - \hat{\Pi}_\nu(P,k_\parallel,\vec{k}_\perp-\vec{q}_\perp)\right]\Bigg\}.\end{aligned} \tag{3.75}$$

with $\mathcal{F}(k_\parallel,p_\parallel) = f_F(k_\parallel) - f_F(k_\parallel - p_\parallel)$ and $\epsilon(P,\vec{k}) \equiv \epsilon_{q\bar{q}}(P,\vec{k})$.
The computation of $\Phi_\nu^\dagger(K-P,K)$ is done in appendix C where we show that in the circular basis $\Phi_{L,R} \equiv \frac{1}{\sqrt{2}}(\Phi_1 \pm i\Phi_2)$, we get

$$\Phi_L(K,K-P) = \frac{k_L}{k_\parallel - p_\parallel}, \quad \Phi_R(K,K-P) = \frac{k_R}{k_\parallel}. \tag{3.76}$$

We want to write (3.75) in a form as close as possible to the one in [6, 47]. For this purpose, we define a quantity $\vec{f}$ via

$$\hat{\Pi}_\perp \equiv id(r)\mathcal{F}(k_\parallel,p_\parallel)\vec{f}. \tag{3.77}$$

Why we take only the perpendicular components will become clear in a moment. Using this definition, we can recast the integral equation in the form

$$\vec{\Phi}_\perp^\dagger(K,K-P) = i\epsilon(P,\vec{k})\vec{f}(P,k_\parallel,\vec{k}_\perp) + g^2C_2(r)T\int\frac{\mathrm{d}^2q_\perp}{(2\pi)^2}\mathcal{K}(q_\perp)\left[\vec{f}(P,k_\parallel,\vec{k}_\perp) - \vec{f}(P,k_\parallel,\vec{k}_\perp-\vec{q}_\perp)\right]. \tag{3.78}$$

In order to show that this is indeed equivalent to the equations in [6, 47], we look at the production rate (3.24). Using

$$\Pi_{\mu\nu}(P) = -\int\frac{\mathrm{d}^3p}{(2\pi)^3}\Phi_\mu(K,K-P)\hat{\Pi}_\nu(K,\vec{p}), \tag{3.79}$$

together with (3.77) and summing over the external polarizations, equation (3.24) becomes

$$\frac{\mathrm{d}\Gamma}{\mathrm{d}^3p} = \frac{d(r)e^2}{(2\pi)^3 2p_\parallel}f_B(p_\parallel)\int\mathrm{d}^3k\mathcal{F}(k_\parallel,p_\parallel)\,\mathrm{Re}(\vec{\Phi}_\perp(K,K-P)\cdot\vec{f}(P,\vec{k})). \tag{3.80}$$

Here we explicitly see that we only need the perpendicular components of $\hat{\Pi}$, or equivalently the two-dimensional vector $\vec{f}$.
Because of rotational symmetry, it is clear that

$$\vec{f}(P,\vec{k}) = \Psi(P,\vec{k})\vec{\Phi}_\perp^\dagger(K,K-P) \tag{3.81}$$

with a *scalar* function Ψ. Inserting the ansatz (3.81) and using the result (C.9) finally yields

$$\frac{\mathrm{d}\Gamma}{\mathrm{d}^3p} = \frac{d(r)\alpha_{EM}}{\pi^2 p_\parallel}f_B(p_\parallel)\int\frac{\mathrm{d}^3k}{(2\pi)^3}A_\gamma(k_\parallel,p_\parallel)k_\perp^2\,\mathrm{Re}\,\Psi(P,\vec{k}) \tag{3.82}$$

with the kinematical factor

$$A_\gamma(k_\parallel,p_\parallel) = \frac{k_\parallel^2 + (k_\parallel-p_\parallel)^2}{2k_\parallel^2(k_\parallel-p_\parallel)^2}\mathcal{F}(k_\parallel,p_\parallel). \tag{3.83}$$

We have multiplied by 2 to take both chiralities of the quark into account.
As one can now easily see, this is indeed equivalent to the equations from [6, 47] if we identify their quantity $\vec{f}_{AMY}$ in terms of our quantity Ψ as $\vec{f}_{AMY}(P,\vec{k}) \equiv 2\vec{k}_\perp\Psi(P,\vec{k})$.

4. Thermal production of Majorana neutrinos

Who are you my tiny alien?
What are you here to do?
Katie Melua - *Tiny Alien*

4.1. The origin of matter in the Universe: Baryogenesis

Modern cosmological observations have provided us with rather precise figures about the composition of the Universe. Its dominant contributions are Dark Energy, Dark Matter and baryonic matter with small additional amounts of radiation (photons, neutrinos). From measurements, we infer the following fractions of the energy density[48]:

$$\Omega_\Lambda = 0.734 \pm 0.029, \quad \Omega_{DM} = 0.222 \pm 0.026, \quad \Omega_b = 0.0449 \pm 0.0028 \tag{4.1}$$

There is an additional tiny amount Ω_{rad} of radiation with a large relative uncertainty because of the cosmic neutrino background which is largely inaccessible to observation.
While the composition of the Universe is rather well understood, we still have no clear understanding of the figures (4.1). In fact it is fair to say that $\Omega_{tot} - \Omega_{rad} \approx 1$ is still a mystery and requires physics beyond the SM. For baryonic matter whose nature is–in contrast to (nonbaryonic) Dark Matter–well understood this may appear suprising, but its origin is no less mysterious than that of Dark Matter. In fact, one can only understand the number if we assume a tiny *asymmetry between baryons and antibaryons* because in a baryon-symmetric universe one would expect a freeze-out abundance of baryons and antibaryons with the value [42]

$$\frac{n_b}{n_\gamma} = \frac{n_{\bar{b}}}{n_\gamma} \approx 7 \cdot 10^{-20}. \tag{4.2}$$

In a Universe with such a small amount of baryons, the structures we observe would have never formed and our Universe would be radically different. The observed value is larger by about 10 orders of magnitude: [49]

$$\frac{n_B}{n_\gamma} = (6.21 \pm 0.16) \cdot 10^{-10} \tag{4.3}$$

Therefore we need an asymmetry between baryons and antibaryons-for roughly every $6 \cdot 10^6$ antibaryons there should be $6 \cdot 10^6 + 1$ baryons. This asymmetry must be generated after reheating since inflation exponentially dilutes any preexisting asymmetry which then may be assumed to vanish. We are obviously in need of a mechanism to dynamically create such an asymmetry after the period of inflation.
Providing a theoretical model that can successfully explain the measured baryon-to-photon ratio is a challenging task although there are only three basic conditions needed to create a baryon asymmetry, as outlined by Sakharov in his seminal paper [50]. Several different scenarios how to realize the Sakharov conditions have been invented since then (for a review, see e.g. [51, 52]). In the last decade, *leptogenesis* [53] has become the most popular and most widely used scenario. The basic idea of most leptogenesis models is to enlarge the particle content of the SM with *right-handed Majorana neutrinos* that in the simplest realization interact with the SM particles only via a Yukawa coupling to left-handed leptons and the Higgs boson:

$$\mathcal{L}_{int} = \lambda_{ik} N_i P_L \ell_k \tilde{\phi}^\dagger + h.c. \tag{4.4}$$

With N_i we denote the Majorana neutrinos (the indices i, j label the fermion generations) and ℓ and ϕ are the lepton doublet and the Higgs doublet, respectively. Since only left-handed leptons couple to the Majorana neutrino, a chiral projector P_L was inserted. The contraction of SU(2) doublets in (4.4) is to be performed with the 'SU(2) metric' ϵ_{ab}, i.e. (suppressing the additional generation index) $\ell\tilde{\phi}^\dagger \equiv \epsilon_{ab}\ell_a\phi_b$ with $a, b \in \{1, 2\}$. Finally, λ_{ik} is the Yukawa coupling matrix which in general need not be diagonal.

The Majorana neutrinos are unstable and decay into leptons and antileptons, $N_i \to \ell_k + \phi^\dagger, N_i \to \bar{\ell_k} + \phi$, creating an asymmetry between leptons and antileptons because CP is not conserved. The resulting asymmetry is converted into a baryonic asymmetry via the sphalerons that conserve $B - L$ but violate $B + L$ [54]. Finally the departure from thermal equilibrium occurs because the Yukawa coupling is small and therefore the interaction rates of the Majorana neutrino are small compared to the expansion rate of the Universe, which prevents the Majorana neutrino from thermalizing with the electroweak plasma. All three Sakharov conditions are thus fulfilled and the model can be used to effectively create a baryon asymmetry.[1] The computations of the resulting baryon-to-photon ratio have been performed with increasing complexity in the past [56], taking more and more phenomena into account. The key parameter is the *efficiency of leptogenesis* $0 < \eta < 1$ defined by

$$\eta \equiv \frac{n_B(T \ll M_N)}{n_{B,max}(T \ll M_N)} \tag{4.5}$$

where

$$n_{B,max}(T \ll M_N) = c_{sph} \epsilon \, n_N(T \gg M_N). \tag{4.6}$$

Here, c_{sph} is the sphaleron conversion factor[2] and ϵ is the value of the *CP asymmetry* in the decay of the lightest Majorana neutrino $N \equiv N_1$, which we assume to be the dominant source of lepton asymmetry.
The computation of the efficiency for a given set of masses and coupling constants is performed by solving a set of Boltzmann equations with collision terms that encode all relevant decay and scattering process that can create and partially erase the lepton asymmetry. Due to the related complexity, the vast majority of work published on this subject neglects finite-temperature effects coming from the hot electroweak plasma that sets the stage for the decay and scattering processes . The cross sections are computed at zero temperature and the distribution functions are usually assumed to be a Maxwell-Boltzmann distribution [56]. The collision terms obtained that way can only be a rough approximation whose accuracy is a priori unknown.
The impact of finite-temperature effects on the computation of the collision term therefore calls for a thorough investigation. There have been some attempts in the past to include finite-temperature effects, e.g. [57, 58], but a completely rigorous, first principles treatment of thermal leptogenesis in a hot plasma is still an unfulfilled task. It is currently even under debate whether the evolution of the lepton asymmetry can be reliably tracked with the (classical) Boltzmann equation and whether quantum kinetic equations (e.g. Kadanoff-Baym equations) should preferrably be used [59, 60, 61]. In this thesis, we will not attempt at providing a fully fledged computation of the efficiency of leptogenesis taking all relevant finite temperature effects into account–this is clearly an enormous task and progress needs to be done step by step. We focus on calculating the production rate of a Majorana neutrino in a hot electroweak plasma that is fully equilibrated. We restrict the computation to the leading order in the gauge coupling constant g, with g being either the SU(2) or U(1) gauge coupling, and in the top quark Yukawa coupling constant λ_t. Also we perform the computations in the high-temperature regime where $M_N \ll T$ such that all masses can formally be treated as being (at most) of order $\sim gT$, although the Majorana mass is not a thermal mass. This will also require a treatment of the LPM effect using the method outlined in the previous chapter. We perform the complete leading-order computation of the production rate and then solve the Boltzmann equation for the number density of Majorana neutrinos with the collision term obtained via the integral (3.37) over the production rate. Like the quantum kinetic approach, our approach thus relies on first principles. A comparison of the final results obtained with both approaches, although it would be very interesting, will not be performed here since it goes beyond the scope of this thesis.

4.2. Production rate and leading order contributions

As an application of the general formalism from the previous chapters, we will now compute the leading order thermal production rate of the lightest Majorana neutrino N whose decay creates the lepton asymmetry. We assume a high temperature $T \gg M_N$ since the thermal effects are dominant in this regime whereas their influence becomes more and more negligible for smaller values of T/M_N [58]. In contrast to the thermal production of Dark Matter candidates where the leading order scattering contributions are already known

[1] Note that by using this scenario one can also naturally explain the small neutrino masses via the *seesaw (type I) mechanism* [55] that we do not explain in detail here. This twofold virtue, explaining both the baryon asymmetry and the smallness of the neutrino masses, is what makes leptogenesis particularly appealing.
[2] For the SM, its value is e.g. $c_{sph} = 28/79$.

(e.g. [36, 39]), none of the analogous contributions to the production rate of the Majorana neutrinos has ever been consistently computed within the full framework of thermal field theory.
The production rate of Majorana neutrinos with momentum p is given by[3]

$$\frac{\mathrm{d}\Gamma_N}{\mathrm{d}^3 p} = \frac{|\lambda|^2}{(2\pi)^3 p_0} f_F(p_0)\,\mathrm{Im}\,\mathrm{Tr}\left[(\not{P} + M_N)\Sigma_{N,ret}(p_0,\vec{p})\right] \tag{4.7}$$

where $\Sigma_{N,ret}(p_0,\vec{p})$ is the retarded, proper self-energy and $|\lambda|^2 \equiv \sum_j |\lambda_{1j}|^2$. This follows from (3.35) because both terms contribute the same due to symmetry under time reflection. Among the leading order contributions

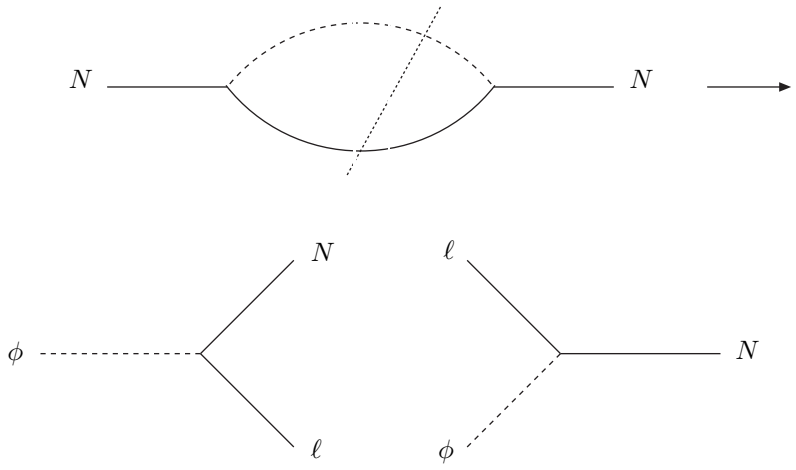

Figure 4.1.: Decay and recombination contributions to Majorana neutrino production and the 1-loop self-energy whose cuts give the corresponding tree-level diagrams.

are, on the one hand, decay and recombination processes as depicted in figure 4.1. The Higgs decay is only allowed if $m_\phi \geq M_N + m_\ell$ whereas for the recombination we need $M_N \geq m_\phi + m_\ell$. At most one of the conditions can be fulfilled which means that at a given temperature, only one of the two processes can happen and for $m_\phi - m_\ell < M_N < m_\phi + m_\ell$, both of them are forbidden. They are both characterized by the momenta of the particles being *collinear* in the sense that the relative angle is small, $\vartheta \sim g$. This is due to the fact that the masses that are involved are all (at most) of order gT and was already explained in section 3.2. The Yukawa vertex is therefore effectively suppressed by a factor of g and the rate for the process is already suppressed by two powers of the gauge coupling, as explained in section 2.3.3. It can also easily be seen by inserting the self-energy shown in figure 4.1 into (4.7) and taking the trace. This means that it is sensitive to the LPM effect and one has to treat this contribution with the formalism from section 3.3. The lepton and the Higgs boson undergo an arbitrary number of scatterings off soft gauge bosons during the 'emission' of the Majorana neutrino which still feels the presence of its 'source'. This leads to nontrivial interference terms analogous to the ones shown in figure 3.2. In order to take this into account, one has to resum an infinite set of diagrams, like in [6, 1, 47] for the case of photon production from a quark-gluon plasma. This will be dealt with in section 4.3.
In addition, there are various $2 \leftrightarrow 2$ scattering processes that can create a population of Majorana neutrinos. They are shown in figure 4.2. For those processes, the LPM effect plays no role at leading order. However, the computation is still not straightforward. In a naive treatment, IR divergences can occur if particles are exchanged in the t- or u-channel. The correct treatment is due to Braaten and Yuan [62] and is performed by introducing a *cutoff* $gT \ll q_* \ll T$ for the relative momenta. For relative momenta smaller than q_*, we have to replace the bare propagator by a HTL resummed propagator which takes the modified dispersion relation

[3] Note that while we denoted the self-energy by Π in the general framework of section 3.3, here we stick to the usual convention of denoting the self-energy of a fermion by Σ. Further note that in the literature, the production rate of a fermion is quoted with an analogous expression, only with an opposite overall sign [36, 37, 38]. Our expression is consistent with those, however, because the diagrams correspond to $-\Sigma$, as explained in appendix A.

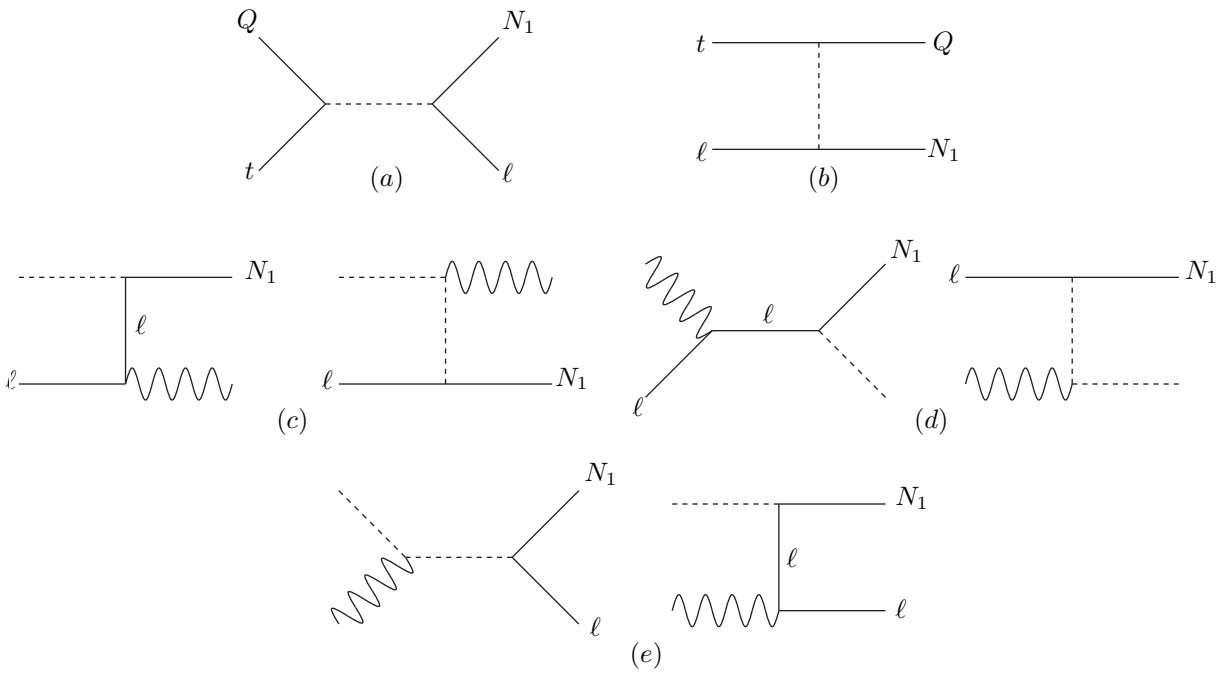

Figure 4.2.: Scattering contributions to Majorana neutrino production. Higgs bosons are denoted with a dashed line and gauge bosons with a wiggled line. Fermions are represented by solid lines and bear a label to distinguish leptons, quarks and Majorana neutrinos.

due to the interaction with the thermal bath into account (see section 2.2). External momenta are always assumed to be hard and HTL effective vertices are therefore never needed. For relative momenta larger than q_*, we may limit ourselves to bare propagators. We then obtain two contributions of the form

$$\begin{aligned}\left(\frac{\mathrm{d}\Gamma}{\mathrm{d}^3p}\right)_{q\geq q_*} &= A_{hard}(E) + B(E)\ln\frac{T}{q_*}\\ \left(\frac{\mathrm{d}\Gamma}{\mathrm{d}^3p}\right)_{q<q_*} &= A_{soft}(E) + B(E)\ln\frac{q_*}{m}.\end{aligned} \tag{4.8}$$

where the coefficients on the rhs are, like the production rate on the lhs, in fact only functions of the energy $E = p^0$.
Both contributions alone would be divergent in the limit $q_* \to 0$, but if we sum them up before taking the limit $q_* \to 0$, we obtain a finite result where the IR divergence is cut off by a thermal mass. This is done in section 4.4 for the processes shown in figure 4.2.

4.3. Decay and recombination

We start with the decay and recombination contribution which involves also the suppression due to the LPM effect. For this purpose, we have to formulate the general equation (3.74) for Majorana neutrinos interacting with Higgs bosons and leptons via the Lagrangian (4.4). The LPM effect is described by an integral equation of the form (3.74) where the self-energy carries a spinor index α. The two-point function contains a loop with a boson and a fermion, which means that

$$\mathcal{F}(k_\parallel, p_\parallel) = f_B(k_\parallel) + f_F(k_\parallel - p_\parallel). \tag{4.9}$$

The vertex factor is easy to write down because the vertex itself is a Yukawa vertex which has a trivial structure and we only need to take the spinor for the lepton in the loop into account. The correct factor explicitly reads

$$\Phi^\dagger_\alpha(K-P,K) = \frac{1}{\sqrt{2k_\parallel}}\eta^\dagger_\alpha(K-P) \tag{4.10}$$

where α is a spinor index and η a Weyl spinor. In order to get this form, we have used (B.34) for the lepton propagator. In contrast to the vertex factor (C.6) for external photons, the factor (4.10) is not dimensionless. The difference comes from the fact that a photon self-energy has dimension 2 while a fermion self-energy only has dimension 1. This means that (3.57) and (3.74) are only consistent if the dimensions of Φ and $\hat{\Pi}$ are $-1/2$ and $-3/2$, respectively.
Using this information, we can cast the integral equation in a form which closely resembles the one given in section 3.4 and previously derived in [6, 47] for the production of photons from a quark-gluon plasma:

$$\eta_\alpha^\dagger(K-P) = i\epsilon(P,\vec{k}) f_\alpha(P,\vec{k}) + \sum_{a=0}^{3} g_a^2 C_2(r) T \int \frac{d^2 q_\perp}{(2\pi)^2} \mathcal{K}_a(\vec{q}_\perp) \left[f_\alpha(P,\vec{k}) - f_\alpha(P, k_\parallel, \vec{k}_\perp - \vec{q}_\perp) \right] \tag{4.11}$$

The kernel is given by

$$\mathcal{K}_a(\vec{q}_\perp) = \frac{1}{\vec{q}_\perp^2} - \frac{1}{\vec{q}_\perp^2 + m_{D,a}^2} \tag{4.12}$$

with $a = 0$ referring to U(1) and $a = 1, 2, 3$ to SU(2) gauge bosons, and we have defined

$$\hat{\Pi}_\alpha(P,\vec{k}) = \frac{i d(r) \mathcal{F}(k_\parallel, p_\parallel)}{\sqrt{2k_\parallel}} f_\alpha(P,\vec{k}) \tag{4.13}$$

in analogy to equation (3.77). Finally, $\epsilon \equiv \epsilon_{\ell\phi}$.
Once the equation for f_α has been solved, we can compute the production rate (4.7) which can be written as

$$\frac{\mathrm{d}\Gamma_N}{\mathrm{d}^3 p} = -\frac{4N_f |\lambda|^2}{(2\pi)^3 p_0} f_F(p_0) \int \frac{\mathrm{d}^3 k}{(2\pi)^3} \frac{f_B(k_\parallel) + f_F(k_\parallel - p_\parallel)}{2k_\parallel} \mathrm{Re}\left[(\sigma \cdot P)_{\alpha\beta} \eta_\beta (K-P) f_\alpha(P,\vec{k}) \right]. \tag{4.14}$$

where β is again a spinor index. Since only fermions of one chirality participate in the interaction, we wrote everything consistently in two-component form and replaced $\not{P} \to \sigma \cdot P$. A factor $4N_f$ which counts the number of distinct contributions to the self-energy has been explicitly pulled out and written as a prefactor of the integral. This factor takes into account that there are N_f generation of fermions, every lepton and Higgs has an antiparticle and finally that the Majorana neutrino interacts with the left-handed particle doublets, which means there are in total four contributions (neutrino,antineutrino,charged lepton,charged antilepton) for every fermion generation.

4.3.1. Tree-level contribution

Before we attempt at solving the full integral equation (4.11), we look at the contribution of the *tree-level* decay and recombination processes shown in figure 4.1. This will allow us to study the importance of the bremsstrahlung and multiple rescattering contribution to the production rate. The tree-level contribution is found by solving (4.11) without the integral term, i.e. it satisfies a purely algebraic equation with the simple solution

$$f_{\alpha,tree-level}(P,\vec{k}) = \frac{-i}{\epsilon(P,\vec{k})} \eta_\alpha^\dagger(K-P). \tag{4.15}$$

We can insert this into (4.14) and take the real part, which amounts to taking the imaginary part of $1/\epsilon(P,\vec{k})$ according to the formula (2.13). We can use the emerging delta function to integrate over $\mathrm{d}^2 k_\perp = \pi \mathrm{d}(k_\perp^2)$. Writing

$$\epsilon(P,\vec{k}) = \alpha(k_\parallel, p_\parallel) + \beta(k_\parallel, p_\parallel) k_\perp^2,$$

where α and β can be read off from (3.52), we get

$$\frac{\mathrm{d}\Gamma_N}{\mathrm{d}^3 p} = \frac{N_f |\lambda|^2}{2(2\pi)^4 p_0} f_F(p_0) \int \mathrm{d}k_\parallel \frac{f_B(k_\parallel) + f_F(k_\parallel - p_\parallel)}{k_\parallel (k_\parallel - p_\parallel)} \frac{1}{|\beta(k_\parallel, p_\parallel)|} \left(K\cdot P - M_N^2 - \frac{m_\ell^2}{2(k_\parallel - p_\parallel)} p_\parallel \right) \Bigg|_{\vec{k}_\perp^2 = -\alpha/\beta} \tag{4.16}$$

where (B.33) was used to compute the trace and the factor $1/|\beta|$ and the condition $\vec{k}_\perp^2 = -\alpha/\beta$ both come from $\delta(\epsilon(P,\vec{k}))$. We have assumed that the delta function indeed contributes which means that $\epsilon(P,\vec{k}) = 0$ has a positive solution for $k_\perp^2$. This constraint will translate into nontrivial integration limits for the remaining

integral over the parallel component which we will turn to in a moment. Before that, we have to simplify the expression:

$$\left(K\cdot P - M_N^2 - \frac{m_\ell^2}{2(k_\parallel - p_\parallel)}p_\parallel\right)\Big|_{\vec{k}_\perp^2=-\alpha/\beta} \equiv (Ak_\perp^2 + B)\big|_{\vec{k}_\perp^2=-\alpha/\beta} = B - A\frac{\alpha}{\beta}$$

where to leading order

$$A = \frac{p_\parallel}{2k_\parallel}, \quad B = \left(\frac{k_\parallel}{2p_\parallel} - 1\right)M_N^2 + p_\parallel\left(\frac{m_\phi^2}{2k_\parallel} - \frac{m_\ell^2}{2(k_\parallel - p_\parallel)}\right).$$

Inserting the explicit definitions of A, B, α, β and performing some algebraic manipulations finally yields

$$\frac{\mathrm{d}\Gamma_N}{\mathrm{d}^3 p} = \frac{N_f|\lambda|^2}{2(2\pi)^4 p_\parallel^2} f_F(p_\parallel)\int \mathrm{d}k_\parallel \frac{f_B(k_\parallel) + f_F(k_\parallel - p_\parallel)}{|k_\parallel - p_\parallel|}\left[(m_\phi^2 - M_N^2)(k_\parallel - p_\parallel) - m_\ell^2 k_\parallel\right]. \tag{4.17}$$

This is apparently singular at $k_\parallel = p_\parallel$, but that point lies outside the integration range. To see this, we must determine the integration limits. They are determined by the following two conditions:

- The equation $\epsilon(P, \vec{k}) = 0$ must have a positive solution for $k_\perp^2$,
- The energy of the lepton must be positive.

The second condition means that for the Higgs decay $\phi^\dagger \to \ell + N$ where the lepton momentum is $K - P$, we must have $k_\parallel \geq p_\parallel$, whereas for the recombination process $\phi^\dagger + \ell \to N$ where the lepton momentum is $P - K$, we get $0 \leq k_\parallel \leq p_\parallel$.
The first condition is a bit harder to study. Solving for $k_\perp^2$ with the help of (3.52), we get the condition

$$k_\perp^2 = \frac{\frac{M_N^2}{p_\parallel}k_\parallel^2 + (m_\phi^2 - m_\ell^2 + M_N^2)k_\parallel - m_\phi^2 p_\parallel}{k_\parallel} \geq 0. \tag{4.18}$$

Since $k_\parallel > 0$, the numerator of the rhs must be positive which can be translated into an allowed integration range for $k_\parallel$. Solving the resulting inequalities gives the integration range

$$\frac{X - \sqrt{Y}}{2M_N^2}p_\parallel \leq k_\parallel \leq \frac{X + \sqrt{Y}}{2M_N^2}p_\parallel \tag{4.19}$$

where

$$X \equiv m_\phi^2 + M_N^2 - m_\ell^2, \quad Y \equiv (m_\phi + m_\ell + M_N)(m_\phi - m_\ell + M_N)(m_\phi + m_\ell - M_N)(m_\phi - m_\ell - M_N) \tag{4.20}$$

It is easy to see that $Y \geq 0$ if either $m_\phi \geq M_N + m_\ell$ or $M_N \geq m_\phi + m_\ell$, in perfect agreement with the general remarks from section 4.2. In addition, the lower integration limit is bigger than $p_\parallel$ for all temperatures where the Higgs decay/recombination is allowed–thus the singular point of the integrand lies outside the integration range and the expression is well-defined.[4]
The expressions above are rather cumbersome if we keep a nonzero Majorana mass M_N. If we set $M_N \to 0$, then only the Higgs decay is allowed and the integration range simply becomes

$$k_\parallel \geq \frac{m_\phi^2}{m_\phi^2 - m_\ell^2}p_\parallel \tag{4.21}$$

with no upper bound on $k_\parallel$.

[4] If we simultaneously take $k_\parallel \to 0, p_\parallel \to 0$ then we do have a logarithmic divergence of the differential production rate $\mathrm{d}\Gamma_N/\mathrm{d}p_\parallel$, which is harmless however because the integral over a logarithm is finite and the total production rate has no divergence left.

4.3.2. Multiple rescattering and LPM effect

The full integral equation for f_α can only be solved numerically. It is an integral equation for the two components of a Weyl spinor and it is convenient to consider the two equations for the upper and lower components separately because then we deal only with two scalar quantities and do not have to worry about having a spinor integral equation to solve. It turns out to be most convenient to define the components ψ and χ via

$$f(\vec{k}_\perp) = \begin{pmatrix} \psi(\vec{k}_\perp) \\ -\frac{\chi(\vec{k}_\perp)}{4(k_\parallel - p_\parallel)} \end{pmatrix} \tag{4.22}$$

In order to simplify the notation, we will from now on only write the perpendicular component $\vec{k}_\perp$ explicitly as argument of the function for which we want to solve. Using (4.22) and (C.3), we obtain the two integral equations

$$1 = i\epsilon(\vec{k}_\perp)\psi(\vec{k}_\perp) + \sum_{a=0}^{3} g_a^2 C_2(r_a) T \int \frac{\mathrm{d}^2 q_\perp}{(2\pi)^2} \mathcal{K}_a(\vec{q}_\perp) \left[\psi(\vec{k}_\perp) - \psi(\vec{k}_\perp - \vec{q}_\perp)\right] \tag{4.23}$$

$$2(k_x + ik_y) = i\epsilon(\vec{k}_\perp)\chi(\vec{k}_\perp) + \sum_{a=0}^{3} g_a^2 C_2(r_a) T \int \frac{\mathrm{d}^2 q_\perp}{(2\pi)^2} \mathcal{K}_a(\vec{q}_\perp) \left[\chi(\vec{k}_\perp) - \chi(\vec{k}_\perp - \vec{q}_\perp)\right]. \tag{4.24}$$

The production rate (4.14) can easily be expressed in terms of ψ and χ using once more (4.22) and (C.3):

$$\frac{\mathrm{d}\Gamma_N}{\mathrm{d}^3 p} = -\frac{4N_f|\lambda|^2}{(2\pi)^3 p_0} f_F(p_0) \int \frac{\mathrm{d}^3 k}{(2\pi)^3} \frac{f_B(k_\parallel) + f_F(k_\parallel - p_\parallel)}{2k_\parallel} \left[p_- \operatorname{Re}\psi(\vec{k}_\perp) + \frac{p_+}{8(k_\parallel - p_\parallel)^2} \operatorname{Re}((k_x - ik_y)\chi(\vec{k}_\perp))\right] \tag{4.25}$$

In order to solve (4.23) and (4.24) and then evaluate (4.25), it is very helpful to transform the integral equations via a Fourier transformation into differential equations. The procedure how to do this and how to solve the resulting ODE numerically is explained in appendix E. Plots of the numerical results both for the tree-level contribution (4.17) and the rate (4.25) which includes bremsstrahlung and the LPM effect will be presented in section 4.6.

Note that (4.25) contains only the contribution to the LPM effect but not the tree-level contribution. This is because the small imaginary part that was needed to get the tree-level result (using (2.13)) is never included in the derivation of the differential equations for ψ and h. This amounts to discarding the imaginary part of $1/\epsilon$ which means that the tree-level contribution is not included.

4.4. $2 \leftrightarrow 2$ scattering contribution

Next we study the scattering contributions from figure 4.2. The production rate for a process of the form

$$1 + 2 \to 3 + N$$

can be written in general as [5] [42, 43]

$$\frac{\mathrm{d}\Gamma}{\mathrm{d}^3 p} = \frac{1}{(2\pi)^3 2E} \int \frac{\mathrm{d}\Omega_p}{4\pi} \prod_{i=1}^{3} \left(\int \frac{\mathrm{d}^3 p_i}{(2\pi)^3 2E_i} \right) (2\pi)^4 \delta(P_1 + P_2 - P_3 - P) f_1 f_2 (1 \pm f_3) \overline{|\mathcal{M}|^2} \tag{4.26}$$

where $f_i \equiv f(E_i)$. Since we start with a negligible density of Majorana neutrinos, we can neglect disappearance processes and the Pauli blocking factor $1 - f_N(E)$ can be approximated by unity, in accord with the general statements from section 3.1.2. The amplitude squared can be calculated using zero-temperature field theory as usually done in previous treatments of leptogenesis (for a review see e.g. [56]).

Formula (4.26) is only used for the hard contribution to (4.8) where the master formula (4.7) would require the computation of the imaginary part of two-loop self-energy diagrams which is a very complicated task. It is important to point out that the Braaten-Yuan prescription (4.8) is only needed for diagrams with a *lepton*

[5] We have added an angular average which gives only a factor of 1 on the lhs because the production rate depends only on the energy of the Majorana neutrinos. This additional integral will soon prove to be convenient to perform the phase space integration.

in the t- or u-channel which means that always $m \equiv m_\ell$. In fact, in the limit where all masses are negligible w.r.t. the momenta, we find that only the diagrams with an intermediate lepton contribute and the sum of the amplitude squared with intermediate Higgs and the interference term vanishes. This is easy to see from the explicit results with nonzero mass of the Majorana neutrino[63]: [6]

$$\overline{|\mathcal{M}_{(a)}(s)|^2} = 6|\lambda|^2\lambda_t^2 \frac{s(s-M_N^2)}{(s-m_\phi^2)^2} \to 6|\lambda|^2\lambda_t^2, \tag{4.27a}$$

$$\overline{|\mathcal{M}_{(b)}(t)|^2} = 6|\lambda|^2\lambda_t^2 \frac{t(t-M_N^2)}{(t-m_\phi^2)^2} \to 6|\lambda|^2\lambda_t^2, \tag{4.27b}$$

$$\overline{|\mathcal{M}_{(c)}(s,t)|^2} = 4g^2|\lambda|^2 C_2(r)\left[\frac{t+u}{t} + \frac{u(u-M_N^2)}{(u-m_\phi)^2} + \frac{t^2+s(t+2M_N^2)}{t(u-m_\phi)^2}\right] \to -4g^2|\lambda|^2 C_2(r)\frac{s}{t}, \tag{4.27c}$$

$$\overline{|\mathcal{M}_{(d)}(s,t)|^2} = 4g^2|\lambda|^2 C(r)\left[\frac{s+u}{s} + \frac{u(u-M_N^2)}{(u-m_\phi^2)^2} + \frac{s^2+t(s+2M_N^2)}{s(u-m_\phi^2)}\right] \to -4g^2|\lambda|^2 C_2(r)\frac{t}{s} \tag{4.27d}$$

$$\overline{|\mathcal{M}_{(e)}(s,t)|^2} = -4g^2|\lambda|^2 C(r)\left[\frac{s+t}{t} + \frac{s-M_N^2}{s} + \frac{t^2+u(t+2M_N^2)}{st}\right] \to -4g^2|\lambda|^2 C_2(r)\left(1+\frac{s}{t}\right). \tag{4.27e}$$

Here λ_t denotes the top quark Yukawa coupling, which is by far the largest of all quark Yukawa couplings. Furthermore, g is either the U(1) or the SU(2) gauge coupling constant. To obtain the massless limit, we have benefited from the relation $s+t+u=0$.

4.4.1. Processes involving quarks

First we start with processes (a) and (b) where the prescription (4.8) is not necessary since no IR divergence appears. In fact, we have seen that the amplitudes are both equal and just a constant which makes the phase space integration in (4.26) rather simple. We present some of the technical details in appendix F and only give the most relevant intermediate steps here.
We start from (4.26) and follow the procedure introduced in [36]. The key point is to use the momentum in the CM frame,

$$\vec{q} = \vec{p} + \vec{p}_3 \tag{4.28}$$

as integration variable. Writing

$$\vec{q} = q\begin{pmatrix}0\\0\\1\end{pmatrix}, \quad \vec{p} = E\begin{pmatrix}0\\\sin\vartheta\\\cos\vartheta\end{pmatrix}, \quad \vec{p}_2 = E_2\begin{pmatrix}\cos\varphi\sin\chi\\\sin\varphi\sin\chi\\\cos\chi\end{pmatrix}, \tag{4.29}$$

we obtain

$$\mathrm{d}\Omega_p = \mathrm{d}\Phi\mathrm{d}\cos\vartheta \tag{4.30}$$

$$\frac{\mathrm{d}^3p_1}{(2\pi)^3 2E_1}\delta(P_1+P_2-P_3-P) = \frac{\Theta(E+E_3-E_2)}{(2\pi)^3 2qE_2}\delta\left(\cos\chi - \frac{E_2^2+q^2-(E+E_3-E_2)^2}{2qE_2}\right) \tag{4.31}$$

$$\frac{\mathrm{d}^3p_2}{(2\pi)^3 2E_2} = \frac{E_2}{2(2\pi)^3}\mathrm{d}E_2\mathrm{d}\varphi\mathrm{d}\cos\chi \tag{4.32}$$

$$\frac{\mathrm{d}^3p_3}{(2\pi)^3 2E_3} = \frac{\Theta(E_3)}{2(2\pi)^3}\frac{q}{E}\delta\left(\cos\vartheta - \frac{E^2-E_3^2+q^2}{2qE}\right)\mathrm{d}E_3\mathrm{d}q\mathrm{d}\Omega_q. \tag{4.33}$$

Performing all integrals that are now trivial leads to

$$\frac{\mathrm{d}\Gamma_{N,2\leftrightarrow2}^{(quark)}}{\mathrm{d}^3p} = \frac{1}{16(2\pi)^6E^2}\int \mathrm{d}E_2\mathrm{d}E_3\mathrm{d}q\Omega(q,E,E_2,E_3)f_F(E+E_3-E_2)f_F(E_2)(1-f_F(E_3))\overline{|\mathcal{M}|^2}. \tag{4.34}$$

[6] If we keep a nonzero M_1 it is necessary to use a massive Higgs propagator since otherwise further IR divergences from the contributions with intermediate Higgs bosons arise. They are always of the generic form $M_1^2\ln(1/m_\phi^2)$ and therefore vanish in the limit $M_1^2, m_\phi^2 \to 0$.

where $\overline{|\mathcal{M}|^2} = 12|\lambda|^2\lambda_t^2$. The function $\Omega(q, E, E_2, E_3)$ gathers all restrictions imposed onto the phase space due to the conditions $|\cos\vartheta| \leq 1, |\cos\chi| \leq 1$. A straightforward calculation shown in appendix F reveals that

$$\Omega(q, E, E_2, E_3) = \Theta(E_2)\Theta(E_3)\Theta(E + E_3 - E_2)\Theta(q - |E - E_3|)\left(\Theta(E + E_3 - q) - \Theta(|2E_2 - E_3 - E| - q)\right). \tag{4.35}$$

Performing the remaining integrals is now a straightforward, but tedious computation which can only be partially done analytically and leads to the result

$$\begin{aligned}\frac{\mathrm{d}\Gamma_{N,2\leftrightarrow 2}^{(quark)}}{\mathrm{d}^3p} = \frac{3|\lambda|^2\lambda_t^2 f_F(E)}{4(2\pi)^6\beta^2E^2}\Bigg[\frac{\pi^2}{3\beta}\left(\beta E + \ln\frac{2}{e^{\beta E}-1}\right) + 4\int_E^\infty \mathrm{d}E'(f_B(E') + f_F(E'-E)) \\ \left(2\,\mathrm{Li}_2\left(-e^{\frac{\beta E'}{2}}\right) - \mathrm{Li}_2\left(-e^{\beta E'}\right) - \frac{\beta^2E'^2}{8}\right)\Bigg]\end{aligned} \tag{4.36}$$

with $E' \equiv E + E_3$. The function Li_2 is the dilogarithm or Spence function defined as

$$\mathrm{Li}_2(x) \equiv \sum_{k=1}^\infty \frac{x^k}{k^2} = -\int_0^x \mathrm{d}t\frac{\ln(1-t)}{t}.$$

The remaining integral in (4.36) has to be subjected to a numerical treatment and we therefore leave it as it stands.

4.4.2. Processes involving gauge bosons: hard contribution

The processes (c) and (e) have internal fermions in the t-channel and therefore require the Braaten-Yuan prescription for a consistent treatment. Process (d) is free of this problem but still it is advantageous to treat it in the same way because in the soft contribution that will be computed subsequently we cannot easily distinguish between the separate processes and automatically obtain the sum over all three.
The procedure to compute the production rate starting from (4.26) is very similar to the previous subsection. The crucial difference is that we introduce a *cutoff* $gT \ll q^* \ll T$ by adding another step function $\Theta(|\vec{p}_1 - \vec{p}_3| - q^*)$. Because of this, it is convenient to introduce here the relative momentum

$$\vec{q} = \vec{p}_1 - \vec{p}_3 \tag{4.37}$$

as integration variable. We then use a coordinate system in which

$$\vec{q} = q\begin{pmatrix}0\\0\\1\end{pmatrix}, \quad \vec{p} = E\begin{pmatrix}0\\\sin\vartheta\\\cos\vartheta\end{pmatrix}, \quad \vec{p}_3 = E_3\begin{pmatrix}\cos\varphi\sin\chi\\\sin\varphi\sin\chi\\\cos\chi\end{pmatrix} \tag{4.38}$$

such that in analogy to above

$$\mathrm{d}\Omega_p = \mathrm{d}\Phi\mathrm{d}\cos\vartheta \tag{4.39}$$

$$\frac{\mathrm{d}^3p_1}{(2\pi)^3 2E_1} = \frac{\Theta(E_1)}{2(2\pi)^3}\frac{q}{E_3}\delta\left(\cos\chi - \frac{E_1^2 - E_3^2 - q^2}{2qE_3}\right)\mathrm{d}E_3\mathrm{d}q\mathrm{d}\Omega_q \tag{4.40}$$

$$\frac{\mathrm{d}^3p_2}{(2\pi)^3 2E_2}\delta(P_1 + P_2 - P_3 - P) = \frac{\Theta(E + E_3 - E_1)}{(2\pi)^3 2qE}\delta\left(\cos\vartheta - \frac{E^2 + q^2 - (E + E_3 - E_1)^2}{2qE}\right) \tag{4.41}$$

$$\frac{\mathrm{d}^3p_3}{(2\pi)^3 2E_3} = \frac{E_3}{2(2\pi)^3}\mathrm{d}E_3\mathrm{d}\varphi\mathrm{d}\cos\chi. \tag{4.42}$$

Now the amplitudes squared depend on the Mandelstam variables s and t, which in our coordinate system take the form[7]

$$s = 2EE_3(1 - \sin\vartheta\sin\chi\sin\varphi - \cos\vartheta\cos\chi), \quad t = (E_1 - E_3)^2 - q^2. \tag{4.43}$$

[7]Note the unusual feature that s depends on the angles whereas t does not.

This means that we cannot trivially perform the integral over φ here but instead have the following starting point:

$$\frac{\mathrm{d}\Gamma^{(gauge)}_{N,2\leftrightarrow 2}}{\mathrm{d}^3p} = \frac{1}{16(2\pi)^7 E^2}\int \mathrm{d}\varphi \mathrm{d}E_1 \mathrm{d}E_3 \mathrm{d}q \tilde{\Omega}(q,E,E_1,E_3) f(E_1) f(E+E_3-E_1)(1\pm f(E_3))\overline{|\mathcal{M}(s,t)|^2} \quad (4.44)$$

with (see appendix F)

$$\begin{aligned}\tilde{\Omega}(q,E,E_1,E_3) \equiv & \Theta(2E+E_3-E_1-q)\Theta(E_1)\Theta(E_3)\Theta(E+E_3-E_1) \\ & \Big[\Theta(q-q^*)\left(\Theta(q^*-|E_1-E_3|)-\Theta(q^*-E_1-E_3)\right) \\ & +\Theta(q-|E_1-E_3|)\Theta(|E_1-E_3|-q^*)-\Theta(q-E_1-E_3)\Theta(E_1+E_3-q^*)\Big]\end{aligned} \quad (4.45)$$

This function follows from the same argument as the function Ω did, only that in addition we haved traded as many q's for a q_* as possible by cleverly combining the step functions. With the help of (4.43) (and the cosines determined by the delta functions), the integrals over φ and q can be performed and are still free of logarithmic divergences. The divergence shows up in the integral over E_1 which has integration limits depending on q_*.
Now we consider each of the three processes (c)-(e) separately.

Process (c)

The combination of distribution functions appearing here is denoted by

$$f_{FBB} \equiv f_F(E_1) f_B(E+E_3-E_1)(1+f_B(E_3)). \quad (4.46)$$

Performing the integrals over φ and q using (4.43) results in

$$\frac{\mathrm{d}\Gamma_{(c)}}{\mathrm{d}^3p} = \frac{g^2|\lambda|^2 C_2(r)}{4(2\pi)^6 E^2}\int_0^\infty \mathrm{d}E_3 \int_0^\infty \mathrm{d}E_1 \Theta(E+E_3-E_1)\omega(q^*,E,E_1,E_3) f_{FBB} \quad (4.47)$$

where $\omega(q^*,E,E_1,E_3)$ sums the different contributions due to (4.45). It consists of two pieces,

$$\omega(q^*,E,E_1,E_3) = \omega_1(q^*,E,E_1,E_3) + \omega_2(q^*=0,E,E_1,E_3). \quad (4.48)$$

The first part leads to a logarithmic dependence on the cutoff q^* and would therefore diverge in the limit $q^* \to 0$, whereas in the second part we may set $q^*=0$. Explicitly, we get

$$\omega_1(q^*,E,E_1,E_3) = \left[\frac{2E_1(E+E_3-E_1)}{E_1-E_3}\Theta(E_1-E_3) - \frac{2EE_3}{E_1-E_3}\Theta(E_3-E_1)\right]\Theta(|E_1-E_3|-q^*) \quad (4.49)$$

and

$$\omega_2(q^*=0,E,E_1,E_3) = 4EE_3\delta(E_1-E_3) - 2(E-E_1)\Theta(E-E_1). \quad (4.50)$$

The finite terms which are gathered in ω_2 come from the middle line in (4.45) and the last term of (4.45). The delta function arises because $\Theta(q^*-|E_1-E_3|)$ enforces $E_1=E_3$ in the limit $q^*\to 0$ and the step function in (4.50) guarantees that $2E+E_3-E_1 \geq E_1+E_3$.[8]
Now it only remains to compute the integrals over E_1.[9] The logarithmic dependence on q^* is extracted via integration by parts, using

$$\frac{1}{E_1-E_3} = \frac{\mathrm{d}}{\mathrm{d}E_1}\ln\frac{|E_1-E_3|}{E_3}.$$

[8] This has to be imposed because a function of the form $\Theta(a-x)\Theta(x-b)$ vanishes everywhere if the condition $a \geq b$ is violated.
[9] When looking at intermediate results, one might be worried at a first look because there is apparently a divergence in the integral over E_3 coming from the singular behaviour of the Bose function at $E_3 \to 0$. However, an expansion of the complete integrand in powers of E_3 shows that it behaves at worst as $\ln E_3$ for small values of E_3 and all singular terms are cancelled, although many individual terms would diverge seperately. For this reason, it is better to leave the complete integral as it is and not try to evaluate parts of it analytically. See also the discussion in section 4.5.

The integral over ω_2 then only contributes to A_{hard} in (4.8) whereas the integral over ω_1 contributes both to A_{hard} and B. Explicitly, we obtain

$$\left(\frac{\mathrm{d}\Gamma_{(c)}}{\mathrm{d}^3p}\right)_{\omega_2} = \frac{g^2|\lambda|^2C_2(r)}{2(2\pi)^6E^2}\int_0^\infty \mathrm{d}E_3 f_F(E+E_3)(1+f_B(E_3))\left[2EE_3(1-f_F(E_3)+f_B(E))+\right.$$
$$\left.\frac{\pi^2}{12\beta^2}+\frac{E}{\beta}\ln\frac{2}{e^{-\beta(E+E_3)}-1}+\frac{1}{\beta^2}\left(\mathrm{Li}_2(-e^{\beta E})-\mathrm{Li}_2(e^{-\beta E_3})+\mathrm{Li}_2(e^{-\beta(E+E_3)})\right)\right] \tag{4.51}$$

from the part where we may set $q^*\to 0$. The part involving the logarithmic dependence on q^* can first be written as

$$\left(\frac{\mathrm{d}\Gamma_{(c)}}{\mathrm{d}^3p}\right)_{\omega_1} = \frac{g^2|\lambda|^2C_2(r)}{2(2\pi)^6E}\int_0^\infty \mathrm{d}E_3(1+f_B(E_3))f_F(E+E_3)\left[\int_{E_3+q_*}^{E+E_3}\mathrm{d}E_1\frac{g_1(E,E_1,E_3)}{E_1-E_3}\right.$$
$$\left.+\int_0^{E_3-q_*}\mathrm{d}E_1\frac{g_2(E,E_1,E_3)}{E_1-E_3}\right]. \tag{4.52}$$

where

$$g_1(E,E_1,E_3)\equiv E_1(E+E_3-E_1)(1-f_F(E_1)+f_B(E+E_3-E_1)),$$
$$g_2(E,E_1,E_3)\equiv -EE_3(1-f_F(E_1)+f_B(E+E_3-E_1)).$$

Performing the integration by parts as mentioned above then turns the expression into

$$\left(\frac{\mathrm{d}\Gamma_{(c)}}{\mathrm{d}^3p}\right)_{\omega_1} = -\frac{g^2|\lambda|^2C_2(r)}{2(2\pi)^6E^2}\left[2Ef_B(E)\int_0^\infty \mathrm{d}E_3(1+f_B(E_3))f_F(E_3)E_3\ln\frac{q_*}{E_3}\right.$$
$$-\int_0^\infty \mathrm{d}E_3 f_F(E+E_3)(1+f_B(E_3))\left(\frac{E+E_3}{\beta}\ln\frac{E}{E_3}\right.$$
$$\left.\left.-\int_{E_3}^{E+E_3}\mathrm{d}E_1\frac{\partial g_1}{\partial E_1}\ln\frac{E_1-E_3}{E_3}-\int_0^{E_3}\mathrm{d}E_1\frac{\partial g_2}{\partial E_1}\ln\frac{E_3-E_1}{E_3}\right)\right]. \tag{4.53}$$

where we set $q^*\to 0$ everywhere where no divergence occurs.
The first term will then give a contribution to B and all the rest contributes to A_{hard}. Since

$$-\frac{g^2|\lambda|^2C_2(r)f_B(E)}{(2\pi)^6E}\int_0^\infty \mathrm{d}E_3(1+f_B(E_3))f_F(E_3)E_3\ln\frac{q_*}{E_3} = \frac{g^2|\lambda|^2C_2(r)f_B(E)}{2^9\pi^4\beta^2E}\left(\ln\frac{T}{q_*}+\frac{1}{3}\ln 16\pi^3+12\zeta'(-1)\right),$$

this means that

$$B_{(c)} = \frac{g^2|\lambda|^2C_2(r)f_B(E)}{32(2\pi)^4\beta^2E}. \tag{4.54}$$

Process (d)

Process (d) is easier to handle because it has the lepton in the s-channel and therefore does not show any dependence on q^*. The expression for the rate is given by

$$\frac{\mathrm{d}\Gamma_{(d)}}{\mathrm{d}^3p} = \frac{g^2|\lambda|^2C_2(r)}{4(2\pi)^6E^2}\int_0^\infty \mathrm{d}E_3\int_0^\infty \mathrm{d}E_1\Theta(E+E_3-E_1)\omega(E,E_1,E_3)f_F(E_1)f_B(E+E_3-E_1)(1+f_B(E_3)) \tag{4.55}$$

with $\omega(E,E_1,E_3)=2E\frac{E+E_3-E_1}{E+E_3}-2(E-E_1)\Theta(E-E_1)$ and it contributes only to A_{hard}. Explicitly, we get

$$\frac{\mathrm{d}\Gamma_{(d)}}{\mathrm{d}^3p} = \frac{g^2|\lambda|^2C_2(r)}{2(2\pi)^6\beta^2E^2}\int_0^\infty \mathrm{d}E_3(1+f_B(E_3))f_F(E+E_3)\left[\frac{\pi^2}{12}\frac{2E+E_3}{E+E_3}-\beta^2E(E+E_3)\right.$$
$$+\beta E\ln\frac{(1+e^{\beta E})(e^{\beta(E+E_3)}-1)}{1-e^{-\beta E_3}}+\beta^2E^2\ln\frac{(1+e^{\beta E})(e^{\beta(E+E_3)}-1)}{e^{\beta E_3}-1}$$
$$\left.+\mathrm{Li}_2(-e^{\beta E})-\mathrm{Li}_2(e^{-\beta E_3})+\frac{1}{E+E_3}\left(E_3\,\mathrm{Li}_2(e^{-\beta(E+E_3)})-E\,\mathrm{Li}_2(-e^{\beta(E+E_3)})\right)\right]. \tag{4.56}$$

Process (e)

Finally there is process (e) which has a different combination of distribution functions denoted by

$$f_{BBF} \equiv f_B(E_1) f_B(E + E_3 - E_1)(1 - f_F(E_3)). \tag{4.57}$$

It has the same logarithmic dependence on q^* as process (c) but is free of the problem caused by $f_B(E_3)$ that was mentioned in the footnote above since $f_F(0) = 1/2$ is not divergent. Here, we get

$$\frac{\mathrm{d}\Gamma_{(e)}}{\mathrm{d}^3 p} = \frac{g^2|\lambda|^2 C_2(r)}{4(2\pi)^6 E^2} \int_0^\infty \mathrm{d}E_3 \int_0^\infty \mathrm{d}E_1 \Theta(E + E_3 - E_1)\tilde{\omega}(q^*, E, E_1, E_3) f_{BBF} \tag{4.58}$$

where $\tilde{\omega}$ again has two parts, in analogy to ω from process (c). The explicit results here are

$$\tilde{\omega}_1(q^*, E, E_1, E_3) = \left[\frac{2E_3(E + E_3 - E_1)}{E_1 - E_3}\Theta(E_1 - E_3) - \frac{2EE_1}{E_1 - E_3}\Theta(E_3 - E_1)\right]\Theta(|E_1 - E_3| - q^*) \tag{4.59}$$

and

$$\tilde{\omega}_2(q^* = 0, E, E_1, E_3) = 4EE_3\delta(E_1 - E_3). \tag{4.60}$$

The finite part is explicitly given by

$$\left(\frac{\mathrm{d}\Gamma_{(e)}}{\mathrm{d}^3 p}\right)_{\tilde{\omega}_2} = \frac{g^2|\lambda|^2 C_2(r)}{2(2\pi)^6 E} \int_0^\infty \mathrm{d}E_3 f_B(E + E_3)(1 - f_F(E_3))2E_3(1 + f_B(E_3) + f_B(E)). \tag{4.61}$$

The part with the logarithmic cutoff dependence can be written the same way as for process (c) if we just replace $g_{1,2}$ by the functions

$$\begin{aligned}
\tilde{g}_1(E, E_1, E_3) &\equiv E_3(E + E_3 - E_1)(1 + f_B(E_1) + f_B(E + E_3 - E_1)), \\
\tilde{g}_2(E, E_1, E_3) &\equiv -EE_1(1 + f_B(E_1) + f_B(E + E_3 - E_1)).
\end{aligned}$$

The contribution to B then turns out to be exactly the same, i.e.

$$B_{(e)} = B_{(c)} = \frac{g^2|\lambda|^2 C_2(r) f_B(E)}{32(2\pi)^4 \beta^2 E}. \tag{4.62}$$

4.4.3. Processes involving gauge bosons: soft contribution

To find the contribution to (4.8) with soft lepton momenta, we need to compute the imaginary part of the following self-energy with a HTL resummed lepton propagator: [10] This gives the expression

$$\Pi_N(p_0, \vec{p}) \equiv -\sum_{spin} \bar{u}_N(P)\Sigma_N(p_0, \vec{p})u_N(P) = |\lambda|^2 T \sum_{q^0} \int \frac{\mathrm{d}^3 q}{(2\pi)^3}\Delta(P - Q) \sum_{spin} \bar{u}_N(P) S^{HTL}(Q) P_L u_N(P) \tag{4.63}$$

[10] At first sight, one might be worried that this would also contribute to a decay or recombination process with soft lepton momentum which has to be subtracted by hand to isolate the soft contribution to the scattering rates. However, such a decay or recombination process is kinematically forbidden as one can see by repeating calculation (3.40) with a soft momentum Q:

$$P^2 = m_\phi^2 = (K + Q)^2 = M_N^2 + m_\ell^2 + 2k_\parallel(q^0 - |\vec{q}|\cos\vartheta)$$

This would imply $q^0 - |\vec{q}|\cos\vartheta \sim g^2 T$, which however is impossible. To see this, we write

$$q^0 - |\vec{q}|\cos\vartheta = |\vec{q}|\left(\sqrt{1 + \frac{m_\ell^2}{|\vec{q}|^2}} - \cos\vartheta\right)$$

The term in brackets cannot be of order $\mathcal{O}(g)$ because the cosine is at most one and the square root is larger than one by a an amount of order $\mathcal{O}(1)$ since $m_\ell/|\vec{q}|$ is $\mathcal{O}(1)$ if Q is a soft momentum. Only if $|\vec{q}| \sim T$ the process is kinematically allowed then while for $|\vec{q}| \sim gT$ it cannot occur and there is no overcounting. If, however, *all* momenta are soft, then the situation changes because then $k_\parallel, q^0, \vec{q} \sim gT$ and the condition on the angle is just $\cos\vartheta \sim 1$. Such a decay/recombination processes is allowed and the momenta are no longer collinear, which means the LPM effect is irrelevant at leading order [25]. Such processes are not considered in this thesis where we focus on Majorana neutrinos with *hard* momenta.

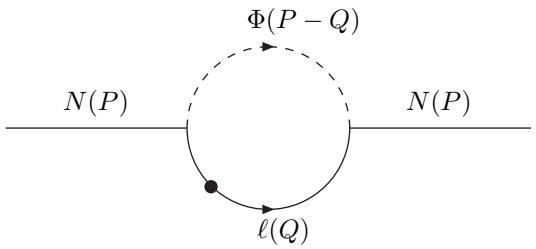

Figure 4.3.: One-loop self-energy diagram of the Majorana neutrino. The black dot indicates that the propagator is HTL resummed.

where the resummed fermion propagator is given by (2.31). Performing the spin sum then results in

$$\Pi_N(p_0,\vec{p}) \equiv |\lambda|^2 \int \frac{\mathrm{d}^3q}{(2\pi)^3}[p^0(S_+ + S_-) - \vec{p}\cdot\hat{q}(S_+ - S_-)) \tag{4.64}$$

where

$$S_\pm \equiv T\sum_{q^0} \Delta_\pm(Q)\Delta(P-Q). \tag{4.65}$$

Computing the thermal sums directly is an almost forbidding task, but fortunately, we will only need the imaginary part. Let us define

$$S(\tilde{\omega}_n) \equiv T\sum_{\tilde{\omega}_n} \Delta_1(i\tilde{\omega}_n,\vec{q})\Delta_2(i(\omega-\omega_n),\vec{k}) \tag{4.66}$$

which is exactly of the form required for $S_\pm$ if $\vec{k} = \vec{p} - \vec{q}$. The basic formula we need is

$$\mathrm{Disc}\, S(p^0) = 2i\,\mathrm{Im}\, S(p^0+i\varepsilon) = -2\pi i\left(e^{\beta p^0}+1\right)\int_{-\infty}^{\infty}\frac{\mathrm{d}k^0}{2\pi}\int_{-\infty}^{\infty}\frac{\mathrm{d}q^0}{2\pi}f_F(q^0)f_B(k^0)\tilde{\rho}_1(q^0,\vec{q})\rho_2(k^0,\vec{k})\delta(p^0-q^0-k^0) \tag{4.67}$$

where $p_0 = i\omega$ and we introduced the *spectral functions* $\rho_{1,2}$ of the corresponding propagators. The proof is given in appendix F.
We can now apply this to $S_\pm$. The spectral functions are given by (2.15) and (2.34). Inserting them and using the scalar spectral function to perform the trivial integral over k^0, we get

$$\mathrm{Disc}\, S_\pm(p^0) = \frac{-i}{f_F(p^0)}\frac{f_B(E_\phi)}{2E_\phi}\int_{-\infty}^{\infty}\mathrm{d}q^0 f_F(q^0)\rho_\pm(q^0,q)\delta(p^0-q^0-E_\phi) \tag{4.68}$$

where $E_\phi \equiv \sqrt{k^2+m_\phi^2} \approx |\vec{k}|$. We have thus arrived at the expression

$$\begin{aligned}\mathrm{Disc}\,\Pi_N(p_0,\vec{p}) = \frac{-i|\lambda|^2}{f_F(p^0)}\int\frac{\mathrm{d}^3q}{(2\pi)^3}\frac{f_B(|\vec{k}|)}{2|\vec{k}|}\int_{-\infty}^{\infty}\mathrm{d}q^0 f_F(q^0)\,\big[p^0(\rho_+(q^0,q)+\rho_-(q^0,q))\\ -\vec{p}\cdot\hat{q}(\rho_+(q^0,q)-\rho_-(q^0,q))\big]\,\delta(p^0-q^0-|\vec{k}|).\end{aligned} \tag{4.69}$$

It remains to put the cutoff q^* in the integral over q and extract the analytic dependence on q^*. First we can replace the distribution function inside the integral by $1/2$ since the momentum is soft. Then we rewrite the delta function in (4.69) in such a way that it allows us to perform the angular integral over $\mathrm{d}\Omega_q$, whereas we do not yet perform the integral over q^0 (the same procedure was used in a different context in [62]). To achieve this, we use that $\vec{q} = \vec{p} - \vec{k}$ is soft, but $\vec{k}, \vec{p}$ are hard. Then we may write $|\vec{k}| = |\vec{p}-\vec{q}| \approx |\vec{p}| - \hat{p}\cdot\vec{q}$ and therefore

$$p^0 - |\vec{k}| \approx \hat{p}\cdot\vec{q}.$$

Writing ω instead of q^0 to avoid confusion, we get

$$\begin{aligned}\mathrm{Disc}\,\Pi_N(p_0,\vec{p}) = \frac{-i|\lambda|^2}{2f_F(p^0)}\int\frac{\mathrm{d}^3q}{(2\pi)^3}\frac{f_B(|\vec{p}|-\hat{p}\cdot\vec{q})}{2(|\vec{p}|-\hat{p}\cdot\vec{q})}\int_{-\infty}^{\infty}\mathrm{d}\omega\,\big[p^0(\rho_+(\omega,q)+\rho_-(\omega,q))-\\ \vec{p}\cdot\hat{q}(\rho_+(\omega,q)-\rho_-(\omega,q))\big]\,\delta(\omega-\hat{p}\cdot\vec{q}).\end{aligned} \tag{4.70}$$

Next we perform the angular integrals by setting $\cos\vartheta \equiv \hat{p}\cdot\hat{q}$, which leads to

$$\operatorname{Disc}\Pi_N(p_0,\vec{p}) = \frac{-i|\lambda|^2}{2(2\pi)^2 f_F(p^0)}\frac{f_B(|\vec{p}|)}{2|\vec{p}|}\int_0^{q^*}\mathrm{d}q q\int_{-q}^{q}\mathrm{d}\omega\left[p^0(\rho_+(\omega,q)+\rho_-(\omega,q)) - |\vec{p}|\frac{\omega}{q}(\rho_+(\omega,q)-\rho_-(\omega,q))\right]. \tag{4.71}$$

We now need to integrate over ω using sum rules for the fermion spectral functions [9]:

$$\int_{-\infty}^{\infty}\frac{\mathrm{d}\omega}{2\pi}\rho_\pm(\omega,q) = 1 \tag{4.72a}$$

$$\int_{-\infty}^{\infty}\frac{\mathrm{d}\omega}{2\pi}\omega\rho_\pm(\omega,q) = \pm q, \tag{4.72b}$$

To leading order, we can set $p^0 = |\vec{p}| = E$ because we neglect all masses. Since the structure of the integral is then the same as in [30], we can follow the procedure there. In the integration range $-q \le \omega \le q$, only the continuum part from (2.34) contributes while the pole contributions do not because of the delta functions.[11] Integrating directly over the continuum part of the spectral functions is difficult. One can however use the following trick: for $\omega > q$, the continuum contributions $\rho_{\pm,cont.}$ vanish due to the step function in (2.34). Then we can integrate between $-\infty$ and ∞ instead and only have to subtract the contribution with $|\omega| > q$, which is simple because only the pole contributions in (2.34) survive. Using the sum rules (4.72) we easily see that the integral taken from $-\infty$ to ∞ over the integrand vanishes and only the subtracted part for $|\omega| > q$ contributes. Using (2.34) and (2.35), we finally get

$$\operatorname{Disc}\Pi_N(P) = \frac{-i|\lambda|^2}{8\pi f_F(p^0)}\frac{f_B(|\vec{p}|)}{m_\ell^2}\int_0^{q^*}\mathrm{d}q\left[(\omega_+^2(q)-q^2)(\omega_+(q)-q) - (\omega_-^2(q)-q^2)(q+\omega_-(q))\right]. \tag{4.73}$$

We can use that [30]

$$\frac{(\omega_\pm^2-q^2)(\omega_\pm \mp q)}{m_\ell^2} = \omega_\pm - q\frac{\mathrm{d}\omega_\pm}{\mathrm{d}q} \tag{4.74}$$

and that [9, 30]

$$\omega_+(q)-\omega_-(q) \overset{q\ll m_\ell}{=} \frac{2q}{3}, \quad \omega_+(q)-\omega_-(q) \overset{q\gg m_\ell}{=} \frac{m_\ell^2}{q}. \tag{4.75}$$

Inserting (4.74) into (4.73) and integrating by parts, we obtain

$$\frac{1}{m_\ell^2}\int_0^{q^*}\mathrm{d}q\left[(\omega_+^2(q)-q^2)(\omega_+(q)-q) - (\omega_-^2(q)-q^2)(q+\omega_-(q))\right] = 2\int_0^{q^*}\mathrm{d}q\,(\omega_+(q)-\omega_-(q)) - m_\ell^2,$$

where (4.75) was used for the boundary term. To extract the logarithmic divergence, we add zero in the form

$$0 = m_\ell^2\ln\left(\frac{q^*}{m_\ell}\right)^2 - 2m_\ell^2\int_0^{q^*}\frac{\mathrm{d}q}{q+m_\ell}$$

where for the integral we set $q^*+m_\ell \approx q^*$. Then we get the final result (cf. [30]):

$$\operatorname{Disc}\Pi_N(p_0,\vec{p}) = \frac{-i|\lambda|^2 f_B(|\vec{p}|)}{8\pi f_F(p^0)}m_\ell^2\left[2\ln\left(\frac{q^*}{m_\ell}\right) - 1 + 2\int_0^{\infty}\mathrm{d}q\left(\frac{\omega_+(q)-\omega_-(q)}{m_\ell^2} - \frac{1}{q+m_\ell}\right)\right]. \tag{4.76}$$

The upper integration limit was replaced by infinity since the integrand vanishes between q^* and ∞ (up to higher order corrections) due to (4.75).
The soft contribution to the production rate is obtained by supplying the necessary factors und using that $\operatorname{Disc}\Pi_N(P) = 2i\operatorname{Im}\Pi_N(p^0+i\varepsilon,\vec{p})$:

$$\frac{\mathrm{d}\Gamma_{soft}}{\mathrm{d}^3p} = \frac{|\lambda^2|g^2C_2(r)f_B(E)}{32(2\pi)^4\beta^2E}\left[2\ln\left(\frac{q^*}{m_\ell}\right) - 1 + 2\int_0^{\infty}\mathrm{d}q\left(\frac{\omega_+(q)-\omega_-(q)}{m_\ell^2} - \frac{1}{q+m_\ell}\right)\right]. \tag{4.77}$$

For the factor in front of the bracket, we also explicitly inserted the HTL fermion mass (B.45). The result for B is then consistent with the one obtained from the hard contribution.

[11] Note that this is in perfect agreement with the previous footnote because the pole contributions would precisely correspond to decay and recombination contributions involving leptonic quasiparticles.

4.4.4. Computation of A_{hard}, A_{soft} and B

It is now straightforward to compute A_{hard} and A_{soft} by gathering all results. The soft part can trivially be read off from (4.77) to be

$$A_{soft}(E) = \frac{|\lambda|^2 g^2 C_2(r) f_B(E)}{32(2\pi)^4 \beta^2 E}\left[2\int_0^\infty \mathrm{d}q \left(\frac{\omega_+(q)-\omega_-(q)}{m_\ell^2} - \frac{1}{q+m_\ell}\right) - 1\right]. \tag{4.78}$$

The coefficient B is also easy to read off from the previous results that consistently give

$$B(E) = \frac{|\lambda|^2 g^2 C_2(r) f_B(E)}{16(2\pi)^4 \beta^2 E}. \tag{4.79}$$

The most cumbersome expression is obtained for A_{hard} for which we need to sum all contributions which are finite for $q^* \to 0$:

$$\begin{aligned}
A_{hard}(E) = {} & \frac{g^2|\lambda|^2 C_2(r) f_B(E)}{16(2\pi)^4\beta^2 E}\left(\frac{1}{3}\ln 16\pi^3 + 12\zeta'(-1)\right) + \frac{g^2|\lambda|^2 C_2(r)}{2(2\pi)^6 E^2}\left\{\int_0^\infty \mathrm{d}E_3 f_F(E+E_3)(1+f_B(E_3))\right. \\
& \left[2EE_3(1-f_F(E_3)+f_B(E)) + \frac{\pi^2}{12\beta^2} + \frac{E}{\beta}\ln\frac{2}{1-e^{-\beta(E+E_3)}} + \frac{1}{\beta^2}\left(\mathrm{Li}_2(-e^{\beta E}) - \mathrm{Li}_2(e^{-\beta E_3})\right.\right. \\
& \left.\left. + \mathrm{Li}_2(e^{-\beta(E+E_3)})\right) + \frac{E+E_3}{\beta}\ln\frac{E}{E_3} - \int_{E_3}^{E+E_3}\mathrm{d}E_1 \frac{\partial g_1}{\partial E_1}\ln\frac{E_1-E_3}{E_3} - \int_0^{E_3}\mathrm{d}E_1\frac{\partial g_2}{\partial E_1}\ln\frac{E_3-E_1}{E_3}\right. \\
& + \frac{\pi^2}{12\beta^2}\left(1+\frac{E}{E+E_3}\right) - E(E+E_3) + \frac{E}{\beta}\ln\frac{(1+e^{\beta E})(e^{\beta(E+E_3)}-1)}{1-e^{-\beta E_3}} + \frac{1}{\beta^2}\left(\mathrm{Li}_2(-e^{\beta E}) - \mathrm{Li}_2(e^{-\beta E_3})\right) \\
& \left. + E^2\ln\frac{(1+e^{\beta E})(e^{\beta(E+E_3)}-1)}{e^{\beta E_3}-1} + \frac{1}{\beta^2(E+E_3)}\left(E_3\,\mathrm{Li}_2(e^{-\beta(E+E_3)}) - E\,\mathrm{Li}_2(-e^{\beta(E+E_3)})\right)\right] \\
& + \int_0^\infty \mathrm{d}E_3 f_B(E+E_3)(1-f_F(E_3))\left[2EE_3(1+f_B(E_3)+f_B(E)) + \frac{E_3}{\beta}\ln\frac{E}{E_3}\right. \\
& \left.\left. - \int_{E_3}^{E+E_3}\mathrm{d}E_1\frac{\partial\tilde{g}_1}{\partial E_1}\ln\frac{E_1-E_3}{E_3} - \int_0^{E_3}\mathrm{d}E_1\frac{\partial\tilde{g}_2}{\partial E_1}\ln\frac{E_3-E_1}{E_3}\right]\right\}
\end{aligned} \tag{4.80}$$

Now we can evaluate some of the integrals and also reorganize the remaining terms into a more compact expression. With $w = \beta E_1, x = \beta E_3, y = \beta E$, we can then finally write

$$\begin{aligned}
A_{hard}(y) = {} & \frac{g^2|\lambda|^2 C_2(r) f_B(y)}{16(2\pi)^4\beta y}\left(1+\frac{1}{3}\ln 16\pi^3 + 12\zeta'(-1)\right) + \frac{g^2|\lambda|^2 C_2(r)}{2(2\pi)^6\beta y^2}\left\{\int_0^\infty \mathrm{d}x f_F(x+y)(1+f_B(x))\right. \\
& \left[y\ln\frac{2(1+e^y)(e^{x+y}-1)}{(1-e^{-x})(1-e^{-(x+y)})} + 2\,\mathrm{Li}_2(-e^y) - 2\,\mathrm{Li}_2(e^{-x}) + \mathrm{Li}_2(e^{-(x+y)}) + (x+y)\ln\frac{y}{x}\right. \\
& - \int_x^{x+y}\mathrm{d}w\frac{\partial g_1}{\partial w}\ln\frac{w-x}{x} - \int_0^x \mathrm{d}w\frac{\partial g_2}{\partial w}\ln\frac{x-w}{x} + \frac{\pi^2}{12}\left(2+\frac{y}{x+y}\right) - y(x+y) \\
& \left. + y^2\ln\frac{(1+e^y)(e^{x+y}-1)}{e^x-1} + \frac{1}{(x+y)}\left(x\,\mathrm{Li}_2(e^{-(x+y)}) - y\,\mathrm{Li}_2(-e^{x+y})\right)\right] \\
& \left. + \int_0^\infty \mathrm{d}x f_B(x+y)(1-f_F(x))\left[x\ln\frac{y}{x} - \int_x^{x+y}\mathrm{d}w\frac{\partial\tilde{g}_1}{\partial w}\ln\frac{w-x}{x} - \int_0^x\mathrm{d}w\frac{\partial\tilde{g}_2}{\partial w}\ln\frac{x-w}{x}\right]\right\}
\end{aligned} \tag{4.81}$$

where now $g_1 = w(x+y-w)(1-f_F(w)+f_B(x+y-w))$ etc. and $f_B(x)$ etc. is a sloppy notation for $1/(e^x-1)$ etc. The remaining integrals have to be done numerically.

4.5. Collision term and yield of Majorana neutrinos

4.5.1. The leading-order collision term

With the results of the previous sections, we are now in a position to compute the evolution of the Majorana neutrino number density $n_N(t)$. Its time dependence is governed by the Boltzmann equation (3.38). By using

this integrated form of the Boltzmann equation which emerges naturally in our approach (see the discussion in section 3.1.2), we have implicitly assumed kinetic equilibrium which was indeed recently shown to be a good approximation for the evolution of the Majorana neutrinos [64].
The collision term is obtained from summing up contributions (4.17), (4.25), (4.8) (with the coefficients given by (4.78), (4.79) and (4.80)) and (4.36), and integrating over the energy of the Majorana neutrinos:

$$\mathscr{C}_N = \mathscr{C}_N^{1\to 2,2\to 1} + \mathscr{C}_N^{LPM} + \mathscr{C}_N^{2\leftrightarrow 2,quarks} + \mathscr{C}_N^{2\leftrightarrow 2,gauge} \tag{4.82}$$

with

$$\mathscr{C}_N = 4\pi \int_0^\infty \mathrm{d}E E^2 \frac{\mathrm{d}\Gamma}{\mathrm{d}^3 p} = \frac{4\pi}{\beta^3}\int_0^\infty \mathrm{d}y y^2 \frac{\mathrm{d}\Gamma}{\mathrm{d}^3 p}. \tag{4.83}$$

where we use the dimensionless variable $y = \beta E$.[12] The decay and recombination contribution has been splitted into two parts: The tree-level contribution where we neglect the multiple rescattering off soft gauge bosons and a part termed 'LPM' which precisely includes the multiple rescattering. This will allow us to work out the impact of the LPM effect on the production of Majorana neutrinos.
First we look at the $2 \leftrightarrow 2$ scattering contributions and start with processes (a) and (b) which involve external quarks. After integrating (4.36) over y, we obtain

$$\mathscr{C}_N^{2\leftrightarrow 2,quarks} = \frac{3|\lambda|^2\lambda_t^2}{2(2\pi)^5\beta^4} c_{quark} \tag{4.84}$$

with the result

$$c_{quark} = \frac{\pi^2}{36}(\pi^2 + 6\ln^2 2) - 1.80556 = 1.69056, \tag{4.85}$$

with the analytical part coming from the simple integral and the numerical value from the double integral involved.[13]
Now we look at the part involving gauge bosons. Here, we can first write the result in the form

$$\mathscr{C}_N^{2\leftrightarrow 2,gauge} = \frac{4\pi}{\beta^3}\int_0^\infty \mathrm{d}y y^2 \left(A_{hard}(y) + A_{soft}(y) + B(y)\ln\frac{T}{m_\ell}\right). \tag{4.86}$$

The by far easiest integral is the one over $B(y)$ which due to (4.79) gives

$$\frac{4\pi}{\beta^3}\int_0^\infty \mathrm{d}y y^2 B(y) = \frac{g^2|\lambda|^2 C_2(r)}{8(2\pi)^3\beta^4}\int_0^\infty \mathrm{d}y \frac{y}{e^y - 1} = \frac{g^2|\lambda|^2 C_2(r)}{384\pi\beta^4}. \tag{4.87}$$

The integral over A_{soft} is complicated by the fact that it contains a subintegral where the integrand is not given in terms of elementary functions. This integral only changes the prefactor while the integral over y is the same as the one above. Thus, we can write

$$\frac{4\pi}{\beta^3}\int_0^\infty \mathrm{d}y y^2 A_{soft}(y) = \frac{g^2|\lambda|^2 C_2(r)}{384\pi\beta^4} c_{soft} \tag{4.88}$$

and from (4.78) we can read off that

$$c_{soft} = \int_0^\infty \mathrm{d}q \left(\frac{\omega_+(q) - \omega_-(q)}{m_\ell^2} - \frac{1}{q + m_\ell}\right) - \frac{1}{2} = \int_0^\infty \mathrm{d}u \left(f_+(u) - f_-(u) - \frac{1}{u+1}\right) - \frac{1}{2} \tag{4.89}$$

where $q = m_\ell u$ and $\omega_\pm = m_\ell f_\pm$ to obtain dimensionless quantities. The integrand is determined by the solution to the equation (cf. (2.32))

$$f(u) - u - \frac{1}{2u}\left[\left(1 - \frac{f(u)}{u}\right)\ln\frac{f(u)+u}{f(u)-u} + 2\right] = 0 \tag{4.90}$$

which has the two solutions $f(u) = \pm f_\pm(u)$ that can be given analytically in terms of Lambert W functions [25]. The result of the integration is

$$c_{soft} = -0.653. \tag{4.91}$$

[12] For the decay and recombination contribution, we have $y = \beta p_\parallel$ instead to be consistent with the notation used before. For a hard momentum P, both are of course equivalent at leading order.
[13] Numerical errors for the integrals are negligibly small throughout and will thus not be quoted.

Finally we come to the integral over A_{hard} which is probably the most complicated one, not only because it involves many terms but also because some of them would by themselves lead to divergent integrals and only taken together give a finite result. Since the cancellation takes place between double (over E, E_3) and triple (over E, E_3, E_1) integrals, the expression has to be slightly rewritten first in order to get all terms under the integral over E_1.[14] For this purpose, one can simply "undo" integrals, i.e one reads e.g. the line

$$\int_0^E (E-E_1)(1-f_F(E_1)+f_B(E+E_3-E_1)) = \frac{\pi^2}{12\beta^2} + \frac{E}{\beta}\ln\frac{2}{e^{-\beta(E+E_3)}-1} + \frac{1}{\beta^2}\left(\mathrm{Li}_2(-e^{\beta E}) - \mathrm{Li}_2(e^{-\beta E_3}) + \mathrm{Li}_2(e^{-\beta(E+E_3)})\right)$$

that appears in (4.51) from right to left. The surface term from the partial integrations that shows up in (4.53) can also be put under the integral over E_1 by adding a dummy integration of the form

$$1 = \int_0^E \frac{\mathrm{d}E_1}{E}.$$

Finally, out of two remaining triple integrals in (4.53) only the one going from E_3 to $E+E_3$ is superficially divergent whereas the other is unproblematic. After performing the shift $E_1 \to E_1 + E_3$, the integration interval is mapped into $[0, E]$ and all superficially divergent integrals can be combined to the expression

$$\int_0^y \mathrm{d}w \left[w - y + \frac{x+y}{y}\ln\frac{y}{x} - \left(\frac{\partial g_1}{\partial w}\right)\Big|_{w\to w+x} \ln\frac{w}{x}\right]$$

where we switched back to the dimensionless variables w, x, y.
A Taylor expansion of the integrand around the problematic point $x = 0$ shows that the leading term is a constant w.r.t. x which might be dangerous because multiplied with $1 + f_B(x) \approx 1/x$ and integrated over x it would diverge at the lower integration. However, the integral of this term over w is exactly zero, as can be shown analytically. This means that we may even subtract it from our expression without changing the final value, thereby removing the singular behaviour of the integrand and allowing a stable numerical evaluation. The final outcome of this computation is

$$\frac{4\pi}{\beta^3}\int_0^\infty \mathrm{d}y y^2 A_{hard}(y) = \frac{g^2 C_2(r)|\lambda|^2}{(2\pi)^5\beta^4} c_{hard} \tag{4.92}$$

where

$$c_{hard} = 2.752 + 1.429 - 0.088 = 4.093 \tag{4.93}$$

with the three contributions due to processes (c),(d) and (e).
Putting it all together, we can write the complete Boltzmann collision term for $2 \leftrightarrow 2$ scattering as

$$\mathscr{C}_N^{2\leftrightarrow 2} = \left[\alpha\lambda_t^2 + \frac{g_1^2+3g_2^2}{768\pi}\ln\frac{\beta^{2\leftrightarrow 2}}{g_1^2+3g_2^2}\right]|\lambda|^2 T^4 \tag{4.94}$$

with the numerical constants

$$\alpha = 2.590\cdot 10^{-4}, \quad \beta^{2\leftrightarrow 2} = 11.882. \tag{4.95}$$

In order to get the numerical values, we use that $C_2(r) = 3/4$ for SU(2) and $C_2(r) = 1/4$ for U(1) and then have to compare coefficients in the equation

$$\left(\frac{c_{hard}}{(2\pi)^5} + \frac{c_{soft}}{384\pi} + \frac{1}{768\pi}\ln\frac{T^2}{m_\ell^2}\right)\frac{g_1^2+3g_2^2}{4} = \frac{g_1^2+3g_2^2}{768\pi}\ln\frac{\beta^{2\leftrightarrow 2}}{g_1^2+3g_2^2}$$

with m_ℓ given by (B.45).
Now we turn to the tree-level decay/recombination contribution $\mathscr{C}_N^{1\to 2,2\to 1}$. Here things are slightly different because the lower integration limit in (4.19) introduces a logarithmic dependence on T in addition to the

[14] As remarked before, this additional difficulty only concerns the contributions from process (c). Those from processes (d) (where all integrals over E_1 can be done analytically and only double integrals remain) and (e) (which does not show superficially divergent behaviour since the problematic Bose function is replaced by a Fermi function) can be treated straightforwardly.

overall T^4 which has to appear for dimensional reasons. This means that if we want to write the corresponding collision term in the same way as for scattering, the coefficients are not be constant but still have a nontrivial dependence on temperature:

$$\mathscr{C}_N^{1\to 2,2\to 1} = \left(\alpha_H(z)\Lambda + \alpha_t^{1\to 2,2\leftrightarrow 1}(z)\lambda_t^2 + (g_1^2+3g_2^2)\beta^{1\to 2,2\to 1}(z) - z^2(\mathcal{J}_{01}(z)-\mathcal{J}_{10}(z)\right)|\lambda|^2 T^4, \tag{4.96}$$

with Higgs self-coupling Λ and the integrals

$$\mathcal{J}_{mn}(z) \equiv \frac{N_f}{8\pi^3}\int_0^\infty \mathrm{d}\tilde{p}\tilde{p}^m f_F(\tilde{p}) \int_{\tilde{k}_{min}(z)}^{\tilde{k}_{max}(z)} \mathrm{d}\tilde{k}\tilde{k}^n \frac{f_B(\tilde{k})+f_F(\tilde{k}-\tilde{p})}{|\tilde{k}-\tilde{p}|} \tag{4.97}$$

where we have introduced rescaled quantities

$$\tilde{k} \equiv \frac{k_\parallel}{T}, \quad \tilde{p} \equiv \frac{p_\parallel}{T}, \quad z \equiv \frac{M_N}{T} \tag{4.98}$$

to make everything dimensionless. In terms of those integrals, the coefficients in (4.96) are given by

$$\alpha_H(z) = \frac{1}{2}(\mathcal{J}_{01}(z)-\mathcal{J}_{10}(z)), \quad \alpha_t^{1\to 2,2\leftrightarrow 1}(z) = \frac{1}{2}\alpha_H(z), \quad \beta^{1\to 2,2\to 1}(z) = -\frac{1}{16}\mathcal{J}_{10}(z). \tag{4.99}$$

In order to obtain this form, we have used the asymptotic Higgs and lepton masses (B.18) and (B.44) and inserted them into (4.19). Comparing coefficients in front of the couplings then allows to deduce the expressions given above.
Finally there is the multiple rescattering contribution that we have to add. Using (E.4) and introducing the same rescaled momenta as above leads to

$$\mathscr{C}_N^{LPM} = -\frac{N_f}{2\pi^3}|\lambda|^2 T^4 \int_0^\infty \mathrm{d}\tilde{p}\tilde{p} f_F(\tilde{p}) \int_0^\infty \mathrm{d}\tilde{k} \frac{f_B(\tilde{k})+f_F(\tilde{k}-\tilde{p})}{\tilde{k}} \lim_{b\to 0}\left[\frac{z^2}{2\tilde{p}}\,\mathrm{Re}\,\psi(b;\tilde{k},\tilde{p}) + \frac{\tilde{p}}{2(\tilde{k}-\tilde{p})^2}\,\mathrm{Im}\,h(b;\tilde{k},\tilde{p})\right]. \tag{4.100}$$

The functions ψ and h are solutions of differential equations which are given in appendix E.

4.5.2. Solution of the Boltzmann equation

Now we can finally solve the Boltzmann equation (3.38) with the collision term (4.82) which we write as $\mathscr{C}_N(T) \equiv \tilde{\mathscr{C}}_N|\lambda|^2T^4$ in order to scale out the dominant temperature dependence. As usual, we introduce the quantity

$$Y_N \equiv \frac{n_N}{s} \tag{4.101}$$

where $s \sim T^3$ is the entropy density in a radiation-dominated FRW universe [42]. Since $H(T) \sim T^2$, we have $\mathrm{d}t = -\mathrm{d}T/(H(T)T)$ and the Boltzmann equation becomes

$$\frac{\mathrm{d}Y_N(T)}{\mathrm{d}T} = -|\lambda|^2 \frac{\tilde{\mathscr{C}}_N(T)T^4}{H(T)s(T)T} = -|\lambda|^2 \frac{\tilde{\mathscr{C}}_N(T)}{s_0 H_0 T^2} \tag{4.102}$$

where $s(T) = s_0T^3, H(T) = H_0T^2$. The constants s_0, H_0 are given by [42]

$$s_0 = \frac{4\pi^2}{90}g_{*S}, \quad H_0 = \sqrt{\frac{\pi^2}{90}g_*}\frac{1}{M_{Pl}} \tag{4.103}$$

with (reduced) Planck mass $M_{Pl} = (8\pi G_N)^{-1/2} = 2.4\cdot 10^{18}$ GeV. The number of (entropy) degrees of freedom, $g_*(g_{*S})$ depends on the particle content of the thermal bath; for the SM, we have $g_* = 106.75$ and in the early universe we have $g_{*S} = g_*$.
We switch to $z = M_N/T$, which was already introduced in (4.98), as evolution variable which is more intuitive because z grows with time whereas the temperature drops and higher values of T would correspond to earlier times. The solution can be obtained by simply integrating over z:

$$Y_N(z) = \frac{|\lambda|^2}{M_N s_0 H_0}\int_{z_R}^z \tilde{\mathscr{C}}_N(z')\mathrm{d}z' \tag{4.104}$$

As initial temperature, we have chosen the *reheating temperature* T_R , and we defined $z_R \equiv M_N/T_R$. The solution depends on $|\lambda|, M_N$ and z_R which have to be treated as free parameters.
The quantity $\tilde{\mathscr{C}}_N$ contains different contributions depending on the value of z because not all processes are kinematically allowed at a given temperature. More explicitly, we can write

$$Y_N(z) = \frac{|\lambda|^2}{M_N s_0 H_0} \int_{z_R}^{z} [\tilde{\mathscr{C}}_N^{1\to 2}(z')\Theta(z_- - z') + \tilde{\mathscr{C}}_N^{2\to 1}(z')\Theta(z' - z_+) + \tilde{\mathscr{C}}_N^{LPM}(z') + \tilde{\mathscr{C}}_N^{2\leftrightarrow 2}(z')]\mathrm{d}z' \quad (4.105)$$

where by $z_\pm$ we denote the inverse temperature where the Higgs decay ceases to be kinematically allowed and where the recombination sets in, respectively. They can be determined by solving the equations

$$z_\pm = z_\phi(z_\pm) \pm z_\ell(z_\pm) \quad (4.106)$$

with $z_{\phi,\ell} \equiv m_{\phi,\ell}/T$ and the thermal masses given by (B.18) and (B.44). As a rough approximation, one has $z_- \approx 0.2$ and $z_+ \approx 0.7$; more precise values can only be found numerically.

4.5.3. RG running of coupling constants

The final ingredient that is needed in order to get numerical values are the renormalization group (RG) equations for the coupling constants which must be evaluated at an appropriate scale. While the gauge coupling constants obey very simple RG equations that can (at leading order) even be solved analytically, the corresponding equations for the top Yukawa and Higgs self-coupling are more involved and require a numerical treatment. The full set of renormalization group equations for the SM can be found e.g. in [65, 66] with the former giving more general and the latter slightly simpler equations where the Yukawa couplings of the first and second fermion generation are dropped. We use the equations as given in [66] and drop also the tau and bottom Yukawa coupling because they are much smaller than the other couplings. The relevant equations at 1-loop order are

$$u_1'(\tau) = \frac{41}{10}\frac{u_1^2(\tau)}{8\pi^2} \quad (4.107a)$$

$$u_2'(\tau) = -\frac{19}{6}\frac{u_2^2(\tau)}{8\pi^2} \quad (4.107b)$$

$$u_3'(\tau) = -7\frac{u_3^2(\tau)}{8\pi^2} \quad (4.107c)$$

$$u_t'(\tau) = \frac{u_t(\tau)}{8\pi^2}\left(\frac{9}{2}u_t(\tau) - 8u_3(\tau) - \frac{9}{4}u_2(\tau) - \frac{17}{20}u_1(\tau)\right) \quad (4.107d)$$

$$\Lambda'(\tau) = \frac{1}{16\pi^2}\left(\frac{27}{200}u_1^2(\tau) + \frac{9}{20}u_1(\tau)u_2(\tau) + \frac{9}{8}u_2^2(\tau) - \frac{9}{5}u_1(\tau)\Lambda(\tau) - 9u_2(\tau)\Lambda(\tau) - 6u_t^2(\tau) + 12u_t(\tau)\Lambda(\tau) + 24\Lambda^2(\tau)\right) \quad (4.107e)$$

where $u_i \equiv g_i^2, u_t \equiv \lambda_t^2$ and $\tau \equiv \ln(\mu/\mu_0)$ with an arbitrary reference scale μ_0. The scale where the coupling constants are evaluated is chosen as $\mu = 2\pi T$ [58]. The running of the Majorana neutrino coupling λ is not taken into account because its value is unknown (not even its order of magnitude) and has to be treated as free parameter anyway. This means that we are ignorant of the correct initial conditions for its RG equation and in order to simplify the computation, we thus assume its temperature dependence to be negligible.
In order to solve this system, we impose initial conditions at $\mu = M_Z$ given by [67]

$$\alpha_{EM}(M_Z) = 1/128, \quad \alpha_s(M_Z) = 0.117, \quad \sin^2\vartheta_W = 0.23, \quad m_t = 171\mathrm{GeV}, \quad v = 246\mathrm{GeV} \quad (4.108)$$

For the bare Higgs mass, we take for definiteness a value of $m_H = 150$ GeV, which lies within the experimentally allowed range [67].
The values above can be translated into initial conditions for the functions in (4.107) as follows:

$$u_1(\tau_0) = \frac{4\pi\alpha_{EM}(M_Z)}{\cos^2\vartheta_W}, \quad u_2(\tau_0) = \frac{4\pi\alpha_{EM}(M_Z)}{\sin^2\vartheta_W}, \quad u_3(\tau_0) = 4\pi\alpha_s(M_Z), \quad u_t(\tau_0) = \frac{2m_t^2}{v^2}, \quad \lambda(\tau_0) = \frac{m_H^2}{2v^2} \quad (4.109)$$

where $\tau_0 \equiv \ln(M_Z/2\pi T_R)$, i.e. we choose the reference scale to be the reheating temperature. Evaluating the coupling constants at $\mu = 2\pi T_R$ then means we must determine the value at $\tau = 0$.

4.6. Numerical results

In this section, we finally present some numerical solutions. We start in 4.6.2 with plotting the differential production rate for the different contributions (decay/recombination with and without LPM effect, scattering). We then go in section 4.6.3 to the integrated rate which gives the collision term in the Boltzmann equation and finally in section 4.6.4 we give plots for the yield $Y_N(z)$ of Majorana neutrinos. The main two points of this analysis are the following:

- To investigate how large the corrections due to the finite-temperature effects on the yield of Majorana neutrinos are,
- To study whether leaving out the LPM effect in the finite-temperature computation introduces a significant error or whether it is numerically pretty much irrelevant.

As mentioned after equation (4.104), there are three free parameters in the solution: The Majorana mass M_N, the Yukawa coupling $|\lambda|^2$ and the reheating temperature T_R. For the complete numerical analysis, we will fix the reheating temperature to the sample value $T_R = 10^9$ GeV and the coupling constant (when needed) will be taken as $|\lambda|^2 = 10^{-8}$. For the Majorana mass M_N, we will take several sample values to study the dependence of the solutions on M_N.

Before we show plots of the numerical solutions, we will make a short insertion with some preceding remarks about approximate solutions of the Boltzmann equation.

4.6.1. Approximate solutions

Before we dive into the details of the full solution, we want to mention two ways of obtaining an approximate solution, both of which do not provide a control of the quantitative accuracy and only serve to illustrate certain specific aspects.

Trivial temperature dependence

In order to study some qualitative features of the solution, we can as a rough approximation pretend that the only temperature dependence of the collision term is the overall factor T^4 and assume $\mathscr{C}_N(T)$ to be constant by evaluating it e.g. at $T = T_R$ and taking that value for all temperatures. This approximation is relatively good if we consider only very light Majorana neutrinos such that we always have $z \ll 1$ [15] and we can set $M_N \to 0$ in the computation of the decay and scattering rates. Then $\tilde{\mathscr{C}}_N$ depends on z only via the running coupling constants, but this is only a very mild dependence. This means that if we take z to be small enough, then we get the approximate solution

$$Y_N(z) \approx \frac{|\lambda|^2 \tilde{\mathscr{C}}_N}{M_N s_0 H_0} (z - z_R) . \tag{4.110}$$

We can use (4.110) to study qualitative features of the solution. First of all, compared to the analogous result for gravitino production [36, 37], we clearly observe a different temperature dependence. Whereas $Y_{\tilde{G}}$ is proportional to T_R and essentially constant, Y_N grows with z and consequently with time. This is because for gravitino production, which proceeds via a nonrenormalizable interaction, the collision term is proportional to T^6/M_{Pl}^2 instead of T^4. Another feature we can recognize is that the solution is inversely proportional to M_N, which means that the lighter the Majorana neutrinos are, the bigger the yield will be and the faster they will reach their equilibrium value. All other parameters being fixed, lighter particles are easier to produce than heavier ones, as one would intuitively expect.

[15] One has to remember that the equations we write are only valid as long as the number density of Majorana neutrinos is small. If the equilibrium density is already reached at $z \ll 1$, then it makes no sense to integrate the Boltzmann equation (3.38) until $z \sim 1$ where most of the lepton asymmetry is generated. Inverse processes which reduce the number of Majorana neutrinos would have to be included then and instead of the integrated Boltzmann equation (3.38) one would have to solve an integro-differential equation for the phase space density f_N. This complicates the computation considerably and is beyond the scope of this thesis.

Neglecting finite-temperature effects

While the previous approximative approach only served to illustrate some qualitative features without aiming at reliable quantitative estimates, we now look at another approximate approach which does aim at doing so. The approximation merely consists of neglecting all finite-temperature effects when computing the collision term and this approximation is very common in the existing literature (for a review, see either [56] or chapter 4 of [63] and references therein). It means that

- decay and scattering rates are computed in vacuum with no thermal effects (thermal masses etc.) taken into account,
- one uses Maxwell-Boltzmann statistics for all particles .

This results in a very simple set of Boltzmann equations where even inverse processes and the full dependence of the scattering rates on M_N can be relatively easily investigated. In order to compare the results with our finite-temperature approach, we will again drop all inverse processes with N_1 in the initial state and compute the scattering rates with the amplitudes given in (4.27) where all masses are set to zero.
Taking these limitations into account, the Boltzmann collision term can be written as [16] [63]

$$\mathscr{C}_N^{T=0} = n_N^{eq}\langle\Gamma\rangle + \langle\sigma\rangle \tag{4.111}$$

where

$$\langle\Gamma\rangle \equiv \frac{K_1(z)}{K_2(z)}\Gamma \tag{4.112}$$

with total decay rate

$$\Gamma = \frac{|\lambda|^2}{8\pi}M_N \tag{4.113}$$

and equilibrium number density (here computed with a Maxwell-Boltzmann distribution)

$$n_N^{eq} = \frac{T^3 z^2 K_2(z)}{\pi^2}, \tag{4.114}$$

and where $K_{1,2}$ denote Bessel functions of the second kind. Furthermore,

$$\langle\sigma\rangle \equiv \frac{T}{32\pi^4}\int_0^\infty \mathrm{d}s\sqrt{s}K_1\left(\frac{\sqrt{s}}{T}\right)\hat{\sigma}(s) \tag{4.115}$$

where $\hat{\sigma}(s)$ denotes the *reduced cross section*

$$\hat{\sigma}(s) = \frac{1}{8\pi s}\int_{t_{min}}^{t_{max}} \mathrm{d}t\overline{|\mathcal{M}|^2}. \tag{4.116}$$

Since we neglect the masses of external particles, $t_{min} = -s$ and $t_{max} = 0$.
For the scattering processes with a massless lepton in the t-channel we face the same IR divergence as in our finite-temperature approach. In the zero-temperature framework there is no consistent way to remove it; we choose to proceed as in [63, 68] where the thermal lepton mass was put in as a regulator by replacing $t \to t - m_\ell^2$ whereever one would otherwise get IR divergent terms.
Putting everything together and proceeding as in section 4.5.2 leads to

$$Y_N^{T=0}(z) = \frac{|\lambda|^2}{M_N s_0 H_0}\int_{z_R}^{z} \mathrm{d}z'\tilde{\mathscr{C}}_N^{T=0}(z') \tag{4.117}$$

where

$$\tilde{\mathscr{C}}_N^{T=0}(z) = \frac{z^3 K_1(z)}{8\pi^3} + \frac{3}{16\pi^5}\lambda_t^2 - \frac{g_1^2+3g_2^2}{256\pi^5}\int_0^\infty \mathrm{d}\xi\xi^2 K_1(\xi)\left[1 - 4\ln\frac{\xi^2 + z_\ell^2(z)}{z_\ell^2(z)}\right] \tag{4.118}$$

[16] Note that $T = 0$ as superscript always refers to thermal effects being neglected. For the evolution of $Y_N(z)$ we obviously do not set $T \to 0$ which would mean that $z \to \infty$.

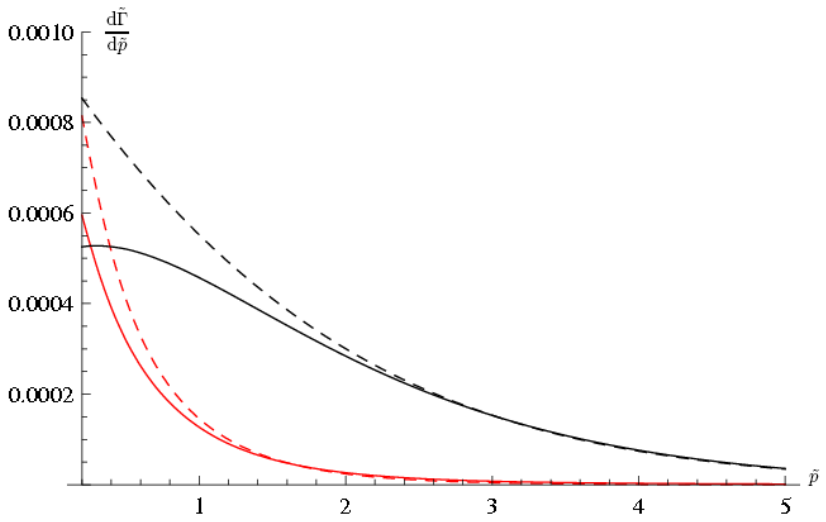

Figure 4.4.: Differential production rate due to decay of Higgs bosons (red, $z = 0.1$) and recombination of Higgs bosons and leptons (black, $z = 0.75$)). Dashed lines give the production rate without the inclusion of the LPM effect while the solid curves present the full solution.

with $\xi \equiv \sqrt{s}/T$ and $z_\ell \equiv m_\ell/T$ as before.[17] The first term is due to the recombination[18] while the other two clearly stem from scattering off quarks and off gauge bosons with the amplitudes given in (4.27).
In sections 4.6.3 and 4.6.4 we will include also the collision term (4.118) as well as the yield obtained with that collision term as source in the Boltzmann equation, thereby checking how accurate neglecting the finite-temperature effects actually is.

4.6.2. The differential production rate

We start with plotting the differential production rates for the different processes that are involved. We use a fixed Majorana mass of $M_N = 10^7$ GeV and we plot the dimensionless quantity

$$\frac{\mathrm{d}\tilde{\Gamma}}{\mathrm{d}\tilde{p}} \equiv 4\pi|\lambda|^{-2}T^{-3}\tilde{p}^2\frac{\mathrm{d}\Gamma}{\mathrm{d}^3p} \tag{4.119}$$

which is also divided by the square of the unknown Yukawa coupling λ. The plots are given only for two sample values of z, namely $z = 0.1$, where the Higgs decay occurs together with the $2 \leftrightarrow 2$ scattering processes, and $z = 0.75$ where the scattering processes are accompanied by the recombination of Higgs bosons and leptons. The full temperature dependence will only be considered in section 4.6.3, where we study the collision terms which are functions of temperature (or equivalently z) only. The plots do not show the region where $\tilde{p} \ll 1$ because this would correspond to *soft* Majorana neutrinos and one can expect substantial modifications to the rates that are computed here, especially for the scattering rates where we could no longer neglect the masses of the external particles. For $\tilde{p} \gg 1$ the rates become strongly suppressed and this region is not of great interest. Therefore we have chosen to plot the differential production rates for the region $0.2 \leq \tilde{p} \leq 5.0$.
In figure 4.4 we show the rates due to decay or recombination and in figure 4.5 we present a plot of the differential production rate due to $2 \leftrightarrow 2$ scattering.
Let us first look at figure 4.4. We observe an overall *suppression* of the production rate due to the LPM effect, like for photon production in a quark-gluon plasma [7]. The suppression is most pronounced for small momenta, $\tilde{p} < 1$, while for large momenta $\tilde{p} > 1$ it becomes weaker and weaker and finally even turns into a slight enhancement. However, this enhancement occurs in a region where the rate has already become small and thus it is clear that the collision term which is the integral over the differential rate will be smaller with the LPM effect than without it. Another thing one can already see is that the recombination process

[17] The remaining integral can be given analytically in terms of the so-called *Meijer G function*, which is not very illuminating however and for practical purposes a numerical integration is to be preferred.
[18] Note that the Higgs decay is now always forbidden since we neglect thermal masses.

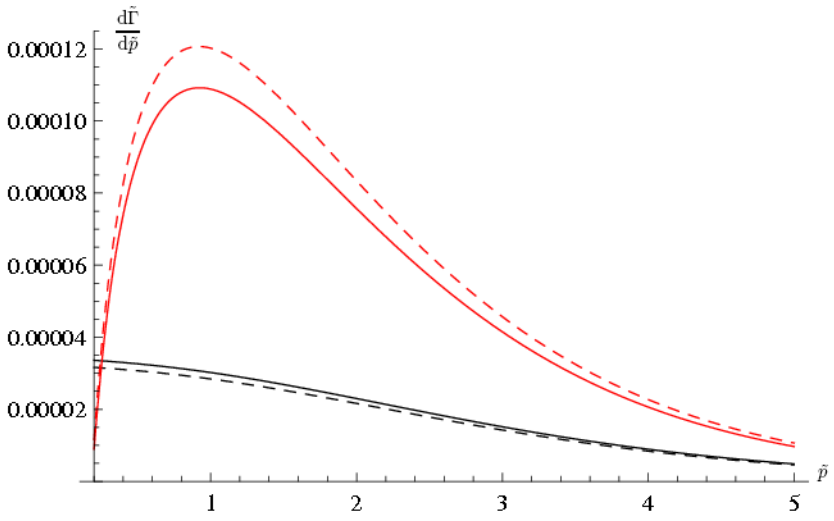

Figure 4.5.: Differential production rate due to scattering off gauge bosons (red) and quarks (black). Dashed lines give the production rate for high temperatures ($z = 0.1$) while the solid lines refer to low temperatures ($z = 0.75$).

dominates over the decay of Higgs bosons. This will be even more apparent when we look at the collision terms in section 4.6.3.
Now let us look at figure 4.5. First of all, we observe that the differential production rate due to scattering is smaller than the production rate due to decay or recombination by up to one order of magnitude. This indicates that of all the processes, the most important is the recombination of Higgs bosons and leptons. This qualitatively agrees with what was found in the finite-temperature treatment of [58], but differs from what is typically found in a zero-temperature treatment [63]. However, it is still too early to neglect the scattering processes since they can occur at any temperature while decay and recombination cannot, at least at tree-level (including the multiple rescattering off gauge bosons, they can, however). Especially at high temperatures, the scattering off gauge bosons still gives a sizable contribution to the collision term because the rate does not drop as fast with increasing momentum as the Higgs decay does.
Comparing the two classes of scattering processes with each other, we observe a remarkable qualitative difference: while the production rate due to scattering off quarks goes to a constant for $\tilde{p} \ll 1$, the production rate due to scattering off gauge bosons drops rapidly and tends towards zero. Why this happens can be understood by looking at (4.45): If we set $E \to 0$, then the function vanishes identically since only step functions which give contradicting conditions on q remain. For the scattering off quarks, this does not happen, but it is a bit subtle to see from (4.35). It is helpful to write down explicit inequalities. Then one finds that if $E > E_3$ and $2E_2 - E - E_3 < 0$, then $\Theta(q - |E - E_3|)\Theta(2E_2 - E - E_3 - q)$ gives the condition $E - E_3 \leq q \leq E + E_3 - 2E_2 \Leftrightarrow 2E_2 \leq 2E_3$, which is consistent with $\Theta(E + E_3 - E_2)$ from (4.35) in the limit $E \to 0$. Thus there is still some phase space available for scattering off quarks even for $E \to 0$, while this is not the case for scattering off gauge bosons.

4.6.3. The Boltzmann collision term

Now we turn to the Boltzmann collision terms which are obtained by integrating the differential rate over all momenta. We will plot the quantity $\tilde{\mathscr{C}}_N$ defined in section 4.5.2 because it is dimensionless and independent of the unknown Yukawa coupling $|\lambda|^2$.
Before presenting the complete collision term, we want to study how much it depends on the concrete value of the Majorana mass M_N. For this it is sufficient to keep only tree-level processes and avoid the numerically expensive computation of the LPM contribution for different masses M_N. In fact, one should expect only relatively small changes because $\tilde{\mathscr{C}}_N$ can, for dimensional reasons, depend only on z and not on M_N alone. As long as we look at the same range of values for z, we should see only a minor change which is solely due to the running coupling constants which depend not on z but rather on T/T_R. This variation is at most logarithmic

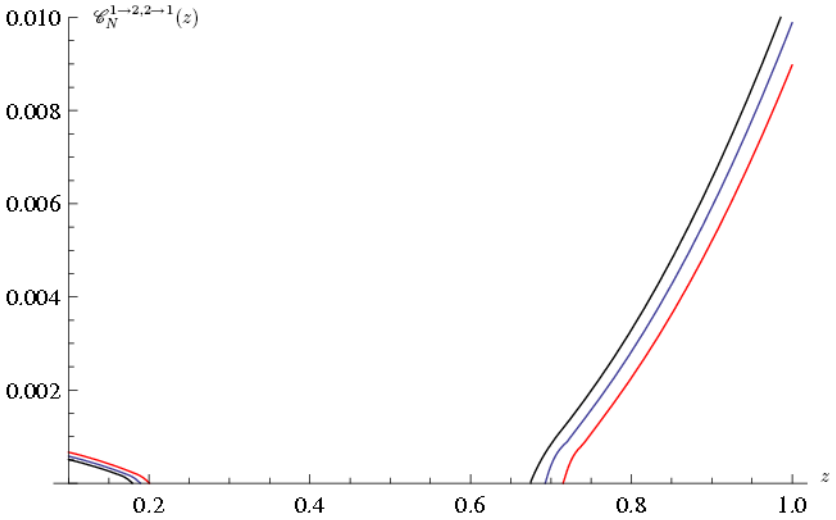

Figure 4.6.: Variation of the dimensionless collision term due to tree-level decay/recombination processes with the Majorana mass M_N. The curves show the results for $M_N = 10^6$ GeV (red), $M_N = 10^7$ GeV (blue) and $M_N = 10^8$ GeV (black).

and should be irrelevant compared to the linear dependence on M_N that we see in (4.104). Therefore, for the solution of the Boltzmann equation one should expect that computing the collision term once and using this for all values of the mass M_N is a relatively good approximation.
Looking at the plots 4.6 and 4.7, we indeed see our expectations confirmed. Even varying the Majorana mass by a factor of 100 induces only an $\mathcal{O}(1)$ change in the collision term for a fixed value of z. Therefore it is sufficient to compute the collision term for one value of the mass, say $M_N = 10^7$ GeV and use this result to solve the Boltzmann equation. This saves a lot of computational time since computing the collision term for one value of M_N can already take several hours, depending on the machine power.
We also see that the Higgs decay and $2 \leftrightarrow 2$ scattering are more efficient for light Majorana neutrinos while the recombination of Higgs bosons and leptons becomes more efficient if the mass of the Majorana neutrino increases. Especially for the decay and recombination contributions, this is perfectly reasonable because a light Majorana neutrino gives a large phase space for the decay while a heavy Majorana neutrino does the same for the recombination process.
Now we can take all contributions into account and plot the complete collision term for $0.1 \leq z \leq 1$. For values $z \approx 1$, the results for $2 \leftrightarrow 2$ scattering cannot be fully trusted any more since we have completely neglected all $\mathcal{O}(z)$ corrections in our computation in section 4.4. That is also why the contribution to $\tilde{\mathscr{C}}_N$ from scattering almost does not vary with z, as can be seen in figure 4.7. The full result together with the result where the LPM effect is neglected is shown in figure 4.8. For comparison, we also plot the zero-temperature result (4.118) (dotted line). We clearly see that, depending on the temperature, the inclusion of the LPM effect can either lead to a suppression (for small or high temperatures where the tree-level decay and recombination processes are kinematically allowed) or an enhancement (in the temperature regime where otherwise only $2 \leftrightarrow 2$ scattering would occur). The suppression is most pronounced for small temperatures $z \approx 1$ and one should expect the biggest effect on the yield of Majorana neutrinos there. However, as we already mentioned, for z close to 1 the $2 \leftrightarrow 2$ scattering contribution (4.94) only gives a rough approximation because terms of order $\mathcal{O}(z)$ have been neglected. It cannot be excluded that the correct result is substantially larger and since it is unaffected by the LPM effect, the overall relative suppression would be much smaller. For $z \ll 1$ the suppression is milder and mostly lies in the range of $10 - 20$ % .
Finally we observe that the zero-temperature result is only a rough approximation to the correct result. For very high temperatures or for temperatures $T \approx M_N$, it is too small by a factor of 2 or more, while for the intermediate regime where the tree-level decay and recombination are kinematically forbidden, it slightly overestimates the correct production rate. We should thus not expect the zero-temperature treatment to be a very accurate approximation and the explicit solutions of the Boltzmann equation that we turn to now will

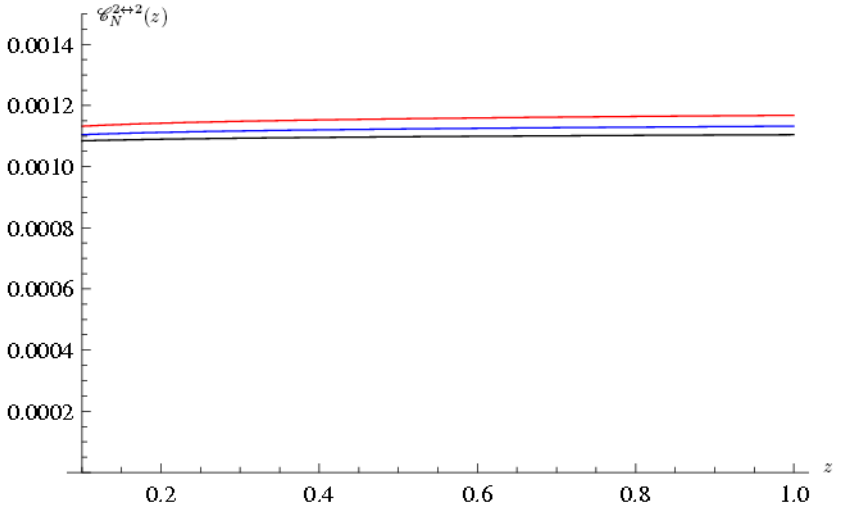

Figure 4.7.: Variation of the dimensionless collision term due to $2 \leftrightarrow 2$ scattering processes with the Majorana mass M_N. The curves show the results for $M_N = 10^6$ GeV (red), $M_N = 10^7$ GeV (blue) and $M_N = 10^8$ GeV (black).

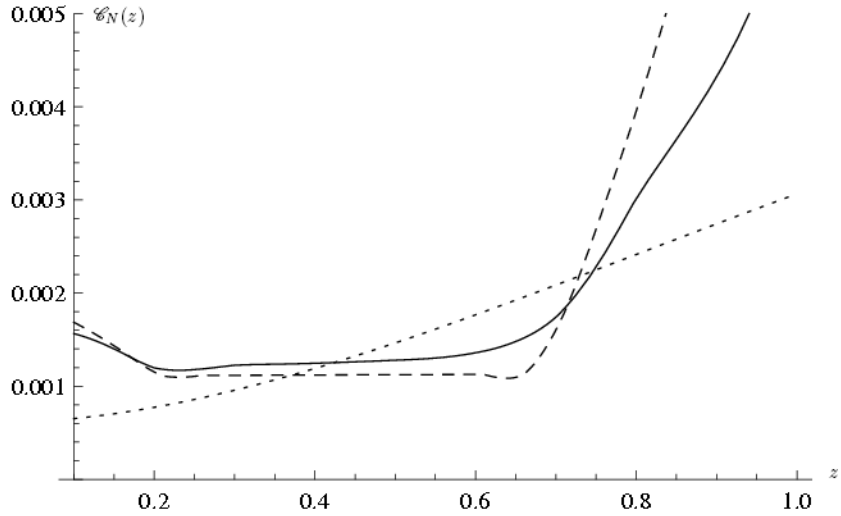

Figure 4.8.: Complete collision term for $M_N = 10^7$ GeV. The solid line represents the collision term (4.82) which sums all finite-temperature contributions, while the dashed line gives the collision term without the LPM effect. The dotted line finally gives the zero-temperature collision term (4.118).

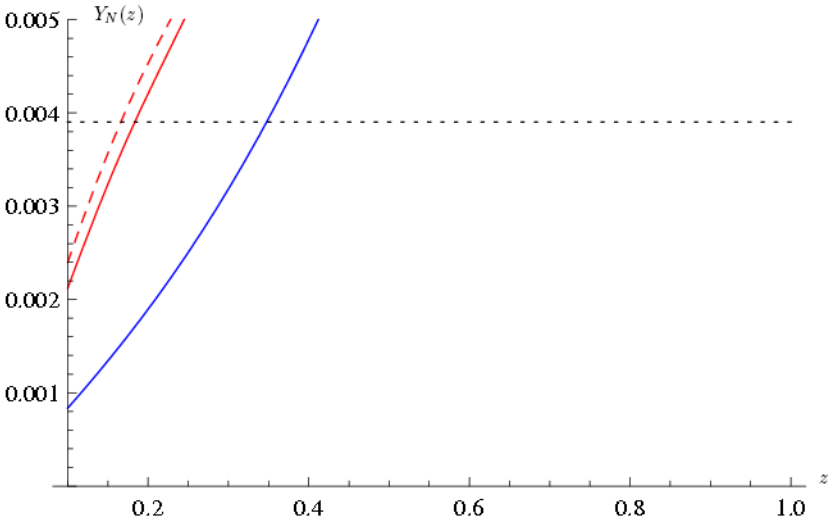

Figure 4.9.: Yield of Majorana neutrinos for $M_N = 10^7$ GeV and $|\lambda| = 10^{-4}$. The red lines give the solution using the finite-temperature collision term (dashed: without LPM effect, solid: with LPM effect) and the blue line the solution with the zero-temperature collision term. The dotted line gives the equilibrium yield for comparison.

confirm that.

4.6.4. The yield of Majorana neutrinos

Below we finally show plots of $Y_N(z)$ and compare with the value Y_N^{eq} which would be obtained if the Majorana neutrinos had already reached thermal equilibrium and which is given by $Y_N^{eq} = n_N^{eq}/s$ where (the factor of 2 takes the spin degrees of freedom into account)

$$n_N^{eq}(T) = 2\int \frac{\mathrm{d}^3 p}{(2\pi)^3} f_F(p) = \frac{3\zeta(3)}{2\pi^2} T^3 \tag{4.120}$$

with $\zeta(3) = 1.202$. Note that since we consider only the production of Majorana neutrinos with hard momenta and at temperatures where $z \lesssim 1$, we have neglected the mass in the argument of the Fermi function. For the coupling we take the value $|\lambda| = 10^{-4}$ to get concrete numbers. Obviously, the true value of that coupling is unknown. One can still at least compare solutions e.g. with and without the LPM effect because the unknown coupling always occurs as on overall factor $|\lambda|^2$ which is the same for all contributions. As soon as the yield of Majorana neutrinos exceeds the equilibrium value $Y_N^{eq} \approx 0.0039$, the approximation to neglect inverse processes with Majorana neutrinos in the initial state, which we used throughout, breaks down. That is why we show the solutions only in a very limited temperature range.
We start in figure 4.9 with the solution for a mass of $M_N = 10^7$ GeV, which we used most of the time. In this case, the equilibrium yield is already reached at $z \approx 0.2$ and the production occurs almost exclusively in the region where both Higgs decay and $2 \leftrightarrow 2$ scattering occurs. The suppression due to the LPM effect is relatively small which means that its inclusion is only necessary if one aims at a precision better than about 10% . The solution using the zero-temperature collision term (4.118) is much smaller, as could already be expected from looking at figure 4.8, and cannot be trusted.
Slightly more interesting is the case of a heavier Majorana neutrino where the equilibrium yield is reached later and we also enter the temperature regime where recombination occurs. This is shown in figure 4.10 where the solution is plotted for $M_N = 10^8$ GeV. We see that the LPM effect only gives a minor correction, except for small temperatures $z \approx 1$ where it gives a relatively large suppression of about 20% and more. However, in this region $\mathcal{O}(z)$ corrections to the scattering contribution become important and might change the relative suppression noticeably. In lack of a result for the rate due to scattering processes which gives the full dependence on M_N (and therefore z) one cannot at present say whether the correct solution would show

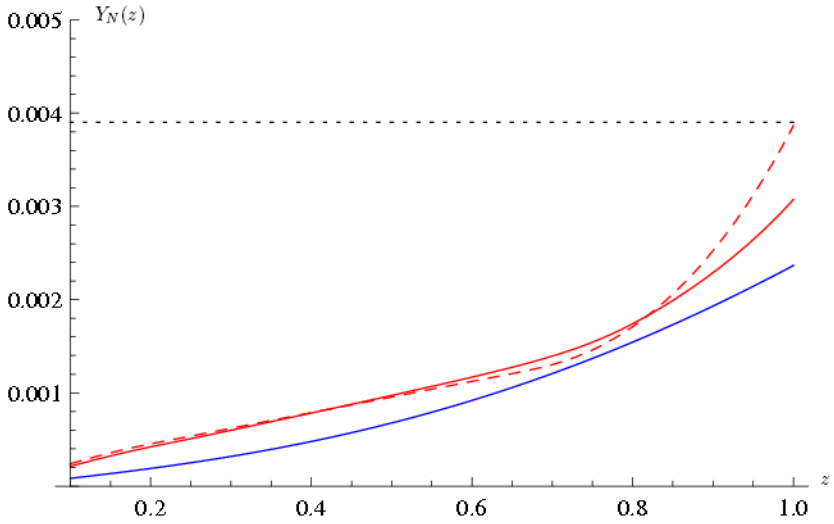

Figure 4.10.: Yield of Majorana neutrinos for $M_N = 10^8$ GeV and $|\lambda| = 10^{-4}$. The meaning of the curves is identical to the previous plot.

a stronger or weaker suppression than the one we can see here. Yet, one can already at this stage conclude that totally ignoring the LPM effect while aiming at quantitative (and not just qualitative) predictions will certainly introduce an error which is not negligible.
Finally, we see that using the zero-temperature collision term (4.118) gives indeed the correct qualitative behaviour of the solution, but quantitatively it is inaccurate and underestimates the obtained yield of Majorana neutrinos. Leaving out finite-temperature effects completely while aiming at quantitative is thus not the right approach. [19]

[19] Interesting enough, including the LPM effect has however brought the two curves closer together, in particular for $z \approx 1$.

5. Summary and Outlook

Don't tell me that it's over, it's only just begun.
Amy McDonald - *Don't tell me that it's over*

5.1. Summary – what has been done already

In this thesis, we have investigated the **thermal particle production rate** of right-handed Majorana neutrinos, which are an essential ingredient of most successful leptogenesis models, to leading order in the relevant coupling constants. A central point of the investigation was the inclusion of the **Landau-Pomeranchuk-Migdal (LPM) effect**, a coherent quantum phenomenon that constitutes a leading-order contribution to the production rate. It requires a relatively sophisticated treatment and developing a formalism which is conceptually more straightforward and more general than the one which was used in [6, 7, 47] to compute the impact of the LPM effect in thermal photon and gluon production is the main conceptual task performed in this work.
We started with an analysis of perturbation theory in a thermal bath, using the imaginary-time formalism. Naive perturbation theory is of very limited use and a reorganization of perturbation theory is often needed. Diagrams of higher order in the loop expansion turn out to be of the same order in the coupling constant expansion and a resummation program is needed. We have explicitly described the necessary resummation at the *soft (momentum) scale* which leads to the well-known *Hard Thermal Loop (HTL)* resummation [23, 26, 27]. In addition, we have studied perturbation theory for hard momenta near the lightcone, which we have termed *lightcone scale*. Propagators need to be resummed again which leads to the appearance of *asymptotic masses*, while vertices need not be replaced by effective counterparts.
For the study of the self-energy with the external momenta at the lightcone scale, a new class of diagrams appears which we have called *Collinear Thermal Loops (CTL)* because the leading-order contribution comes from loop momenta which are *collinear* with the external momenta, $P_i \cdot K_i \sim g^2 T^2$ where $g \ll 1$ generically denotes the relevant set of coupling constants. A resummation of multiloop-diagrams is needed to get the complete leading-order result. The identification of the complete set of contributions by a purely diagrammatic analysis was shown to be inefficient and a computation with the help of Feynman diagrams is hopelessly complicated. Yet, it is possible to compute the CTL self-energy in a relatively simple and transparent way by breaking the computation in several steps and studying the *current* (first derivative of the generating functional) instead of individual diagrams. One first *integrates out* the background of hard gauge bosons, which generates the aforementioned asymptotic masses but not the IR divergent *thermal widths* which are only generated after *soft* gauge bosons have been integrated out. One can therefore avoid to deal with the thermal width from the beginning, which is not the case in the framework that was introduced in [6, 47]. The resulting current, which still contains external soft gauge bosons, satisfies an integral equation that can be derived with relatively little computational effort. Then in the next step one integrates out also the soft gauge boson background, which generates thermal widths for the hard particles in the loop, but also *ladder diagrams* with soft gauge boson rungs. Both taken together are free of IR and collinear divergences, while the two individual contributions are not. This procedure thus generates the complete set of contributions to the CTL self-energy which cannot be given explicitly, but as the solution to an integral equation. The external particle only needs to be specified at the very end, as soon as one wants to solve the integral equation, and no explicit reference to it is made in its derivation.
As we have shown explicitly, in order to include the LPM effect in the computation of thermal particle production rates, one precisely needs to take the *discontinuity* of the CTL self-energy. As an application of the general formalism, we study the thermal production rate of right-handed Majorana neutrinos in the early universe, as an example how the LPM effect affects the production rate of spin 1/2 fermions. The computation of that rate is an important intermediate step to a full finite-temperature treatment of thermal leptogenesis which is still missing to date. The Majorana neutrinos N can on the one hand be produced via the decay of Higgs bosons or the recombination of Higgs bosons and leptons. Both processes are at leading order sensitive to the LPM effect, provided we focus on high temperatures where $M_N \ll T$ such that the momenta

of the particles are collinear and at the lightcone scale. They thus require the new general formalism that was set up in this thesis. In addition we have studied $2 \leftrightarrow 2$ scattering processes involving external quarks or external gauge bosons which can also produce the right-handed Majorana neutrinos. While the former turned out to be straightforward to compute, the latter require more care to obtain IR finite results. None of those processes has ever been consistently computed within the framework of finite-temperature quantum field theory. Previous treatments have either ignored corrections due to the thermal bath [56] or they were only partially included [58]. The presentation here provides for the first time a systematic finite-temperature approach.
After establishing the relevant equations, we perform numerical studies of the production rate and we compute the obtained yield of Majorana neutrinos by solving the Boltzmann equation, which is greatly simplified by neglecting both disappearance processes and Pauli blocking/Bose enhancement factors. The results are then compared to those obtained previously in the literature and we show that neglecting finite-temperature effects certainly does not lead to correct results. We also show that the LPM effect is indeed numerically relevant and although it increases the complexity and the required computational effort consideraly, it may not be omitted if one wants to get accurate results. However, since the most pronounced effect occurs for temperatures $T \approx M_N$ a more complete analysis which takes the full dependence of the scattering rates on the Majorana mass into account would be needed to derive more solid conclusions. Yet, already with our treatment we can show that ignoring the LPM effect introduced an error which is large enough not to be irrelevant for quantitative predictions.

5.2. Outlook – what can be done next

The work that was performed here is only a starting point and can be generalized and extended in various ways:

- An immediate extension is to include the results obtained here in a consistent finite-temperature treatment of thermal leptogenesis. A consistent first-principles computation of the resulting lepton asymmetry is believed to require the usage of nonequilibrium quantum field theory [59, 60, 61, 69]. A consistent incorporation of gauge interactions in this framework is at present not available and the results obtained here can be used to improve the recent investigations.

- Because the new approach to the computation of the LPM effect is sufficiently general, we can use it to study the relevance of the LPM effect in the production of other particles, e.g. Dark Matter candidates like gravitinos or axinos (see below). This will improve previous treatments [38, 70] that failed to include the LPM effect and can thus not be expected to provide accurate results.

- From a theoretical perspective, an interesting extension would be to compute not only the discontinuity of the CTL self-energy as was done here, but to derive full expressions for the CTL n-point functions with $n \geq 2$ and thus develop an effective perturbation theory at the lightcone scale, comparable to the HTL effective perturbation theory valid at the soft scale. This does not require a completely new concept because in the first steps of the computation in section 3.3, we in fact only assumed the external momenta to be lightlike and collinear. Only in the final step we took exactly two momenta to be in addition hard and all the rest to be soft, but nothing forced us to do so. One could take an arbitrary finite number $n \geq 2$ of external momenta to be hard and after integrating out the soft gauge bosons one would obtain an equation for the CTL n-point function. While there is no immediately obvious example where CTL n-point functions with $n > 2$ would be relevant at leading order, they might be needed as soon as computations are pushed beyond leading order.
  If one attempts at finding an effective Lagrangian that works in the same spirit as (2.42) and generates CTL n-point functions at 1-loop order, then a conceptually different approach would be needed, however, since in our approach it is not clear how such an effective lagrangian could be found.

- Finally, all calculations that were performed here are only valid if we have a thermal bath in full equilibrium. Genuine nonequilbrium situations, as they occur e.g. in heavy-ion collisions, cannot be treated within the framework that was established here. In order to generalize our equations to nonequilibrium systems, the first step would be to translate the results from the imaginary-time formalism that was used here to the real-time formalism which is not restricted to systems in thermal equilibrium.

We finally want to provide a short and qualitative discussion of the second point mentioned above because it is the subject of currently still ongoing research. At leading order, gravitinos[1] are produced via $2 \leftrightarrow 2$ scattering processes, which contribute at $\mathcal{O}(g^2 M_{Pl}^{-2})$. Decay and recombination processes, e.g. involving a gluon and a gluino, contribute only at higher order and are $\mathcal{O}(g^4 M_{Pl}^{-2})$. This is easily understood: Since the interaction is *nonrenormalizable* and comes from a dimension 6-operator suppressed by M_{Pl}^{-2}, there must be two more powers of the momenta in the numerator if we compare e.g. with the results for right-handed Majorana neutrinos. Because of Lorentz invariance, only the square of one momentum or the scalar product of two momenta can appear and because all masses are again $\lesssim gT$,the momenta are at the lightcone scale and the additional factor gives a g^2 suppression compared to the analogous results derived in this thesis. For gravitinos, the LPM effect thus constitutes a higher-order phenomenon and one might think it is negligible and not worth the computational effort.
This, however, is not true. In [38], tree-level decay processes of gluons into a gluino and a gravitino were investigated and it was found that although formally of higher order, they are still numerically relevant and give sizable corrections that were later on included in phenomenological studies [71]. This is because numerical prefactors are relative large and the strong coupling constant is not very small even at high temperatures. Including only tree-level decay processes and neglecting the LPM effect which is of the same order is not a consistent procedure and the conclusions that were drawn thus need to be checked by a more complete analysis. Such an analysis should certainly attempt also at studying NLO corrections to the $2 \leftrightarrow 2$ scattering processes which arise already at $\mathcal{O}(g^3 M_{Pl}^{-2})$ and should be expected as soon as one studies e.g. the production of *soft* gravitinos or NLO corrections to the gluon and gluino propagators, while a complete analysis of the $\mathcal{O}(g^4 M_{Pl}^{-2})$ (NNLO) contributions would be tremendously complicated and might require new conceptual developments. Studying the NLO corrections together with corrections due to the LPM effect (as an important subclass of NNLO contributions) is the subject of ongoing studies and results will be presented in a future publication.

[1] All the qualitative statements that are made in this paragraph equally apply to axinos, one only has to replace the Planck mass M_{Pl} by the Peccei-Quinn scale f_a.

A. Notation and conventions

'Cos the line between wrong and right is the width of a thread from a spider's web.
Katie Melua - *Spider's Web*

In this first appendix we want to summarize important conventions and explain our notation. We are doing computations in the imaginary-time formalism of finite-temperature quantum field theory where some of the usual 'ingredients' of perturbative computations differ from their zero-temperature counterparts by constant factors. Therefore one has to be careful not to introduce inconsistencies in the calculation which could lead e.g. to a wrong sign of certain terms.
We do not perform the calculations in Euclidean space as often done in the literature and in textbooks [9, 10] but instead in Minkowski space. We use a metric with signature $(+,-,-,-)$, such that for on-shell particles $P^2 = +m^2$ and the denominator of a propagator takes the form $P^2 - m^2$, where $p^0 = i\omega_n$ with discrete Matsubara frequency ω_n. As one can see here, four-momenta are labelled by capital letters whereas their components are referred to by small letters; in particular, $p = |\vec{p}|$.
Now we describe important relative factors between the imaginary-time expressions and their zero-temperature QFT counterparts. They appear because the action becomes

$$S = \int \mathrm{d}^4x\mathcal{L} \to -i\int_0^\beta \mathrm{d}\tau \int \mathrm{d}^3x\mathcal{L} \tag{A.1}$$

with imaginary time $\tau = it$ and the lagrangian $\mathcal{L}$ like at $T = 0$. The additional factor of $-i$ has two immediate consequences:

- Compared to their zero-temperature counterparts, *vertex factors* get an additional factor $-i$,
- For propagators, which are given by the *inverse* of the quadratic part of the action, the relative factor compared to the zero-temperature form is $+i$.

The second point explains why in this thesis, propagators do not have the usual factor i in the numerator, but rather -1, as e.g. in (2.8). This also has an important consequence for the self-energy: It is given by (-1) *times the Feynman diagrams*. In order to understand this, one has to use the well-known formula for the geometric series:

$$\frac{-1}{P^2-\Pi} = -\left(\frac{1}{P^2} + \frac{1}{P^2}\Pi\frac{1}{P^2} + \frac{1}{P^2}\Pi\frac{1}{P^2}\Pi\frac{1}{P^2} + \dots\right) = \frac{-1}{P^2} + \frac{-1}{P^2}(-\Pi)\frac{-1}{P^2} + \frac{-1}{P^2}(-\Pi)\frac{-1}{P^2}(-\Pi)\frac{-1}{P^2} + \dots \tag{A.2}$$

For the vertex factors, one can look in any textbook on zero-temperature QFT (e.g. [8]) and only has to multiply with $-i$. For the vertices involving gauge bosons, there is one final convention that has to be fixed, which concerns the covariant derivative. We choose it always with a minus sign, [1]

$$D_\mu\psi = (\partial_\mu - igA^a_\mu t^a)\psi. \tag{A.3}$$

In this case, the fermion-antifermion-gauge boson vertex is always positive:

$$e^{iS} = e^{i(-i)\int_0^\beta \mathrm{d}\tau \int \mathrm{d}^3x(i\bar{\psi}\not{D}\psi)} \Rightarrow \text{vertex factor } i(-i)i(-ig) = +g$$

The same applies to scalar-gauge boson vertices since they involve $i(-i)|D_\mu\phi|^2$ which is again positive.

[1] Note that in [8] the conventions are different for abelian gauge bosons which have a $+ieA_\mu$ and nonabelian gauge bosons which have a $-igA^a_\mu t^a$. Especially in chapter 4 it would be inconvenient to use such different conventions because both abelian and nonabelian external gauge bosons occur.

B. Finite-temperature propagators

I'll be marching through the morning,
marching through the night,
moving 'cross the borders,
of my secret life
Leonard Cohen - *In my secret life*

In this appendix we will study the finite-temperature resummed propagators for scalars, spin 1/2-fermions and gauge bosons including all 1-loop self-energy insertions. We do this both for soft as well as hard and lightlike external momenta.

B.1. Scalar propagator and asymptotic thermal mass

We start with the resummed scalar propagator, which in this thesis we will need only for the case of a hard and lightlike external momentum. Still we will easily be able to point out the result for a soft external momentum and show explicitly that for scalars, the obtained thermal masses coincide. We will specify the computation to the self-energy of a *Higgs boson* because it is relevant for the computation in chapter 4.
The resummed scalar propagator can be written as

$$\Delta(K) = \frac{-1}{K^2 - \Pi(k_0, \vec{k})}. \tag{B.1}$$

We need the self-energy $\Pi(k_0, \vec{k})$ at 1-loop level to determine the resummed propagator. As already explained in the main text (equation (2.44)), we can parametrize it with two quantities, the *thermal width* $\Gamma_\phi(k_0, \vec{k})$ and the *thermal mass* m_ϕ. Focusing on *hard* loop momenta, the self-energy is expected to be purely *real* and just give the asymptotic mass m_ϕ. The explicit computation will indeed show that for hard loop momenta the imaginary part vanishes and therefore also the thermal width. In the language of section 3.3, the thermal width is only generated by integrating out gauge bosons, fermions and scalars with soft momenta and therefore it never appears explicitly in 3.3. The same is true for the fermions and gauge bosons treated in the following sections.
The interaction lagrangian for the Higgs boson in the early universe with unbroken gauge symmetry is given by

$$\mathcal{L}_{int} = \Lambda(\phi^\dagger\phi)^2 + |D_\mu\phi|^2 + \left(\sum_{f=l,q} \lambda_f \bar{f} P_L \phi f + h.c.\right) \tag{B.2}$$

where the sum runs over all fermions (both leptons and quarks) and the covariant derivative (for hypercharge $Y = 1/2$) is given by

$$D_\mu = \partial_\mu - i g_W \frac{\sigma^a}{2} W_\mu^a - i \frac{g_Y}{2} B_\mu \tag{B.3}$$

with the Pauli matrices σ^a.
There are several one-loop diagrams that contribute to the self-energy of the Higgs boson, as shown in figure B.1. We start with the easiest contribution including the Higgs self-coupling, which is given by

$$-\Pi_\phi(k_0, \vec{k}) = 6T \sum_{q_0} \int \frac{\mathrm{d}^3 q}{(2\pi)^3} \Delta(Q). \tag{B.4}$$

In order to get the overall multiplicity right, one has to take care that the field ϕ is a SU(2) doublet $(\phi)_i, i = 1, 2$ and count the number of possible Wick contractions in an expression containing the field structure

$$\phi_i^\dagger \phi_j (\phi_k^\dagger \phi_k)(\phi_l^\dagger \phi_l).$$

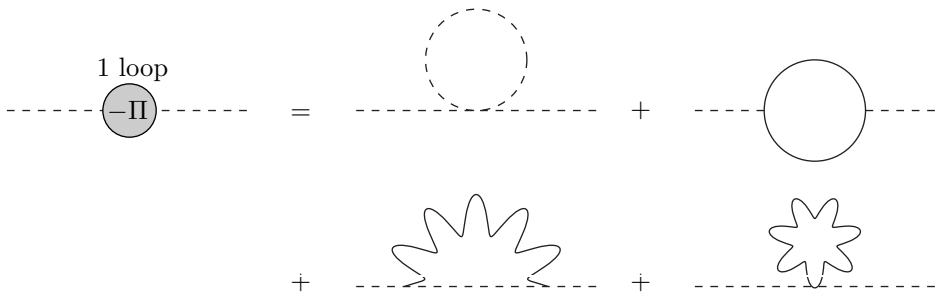

Figure B.1.: One-loop Higgs self-energy

It is indeed found to be six:

$$\delta_{ik}\delta_{jl}\delta_{kl} + \delta_{il}\delta_{jk}\delta_{kl} + \delta_{ik}\delta_{jk}\delta_{ll} + \delta_{il}\delta_{jl}\delta_{kk} = 6\delta_{ij}$$

The sum-integral is of course easily performed using (2.18) and we are left with

$$\Pi_\phi(k_0, \vec{k}) = \frac{\Lambda}{2}T^2. \tag{B.5}$$

This holds exactly and is independent of the external momentum K.
Now we turn to the gauge boson contribution. For simplicity, we work in Feynman gauge where the gauge boson propagator reads

$$\Delta^{ab}_{\mu\nu}(Q) = -g_{\mu\nu}\delta^{ab}\Delta(Q). \tag{B.6}$$

The sum of both diagrams leads to the expression

$$-\Pi_V(k_0, \vec{k}) = g_V^2 t_V^a t_V^b T \sum_{q_0} \int \frac{\mathrm{d}^3 q}{(2\pi)^3} \left[(2K-Q)^\mu \Delta^{ab}_{\mu\nu}(Q)(2K-Q)^\nu \Delta(K-Q) + \frac{1}{2}\cdot(-2g^{\mu\nu})\Delta^{ab}_{\mu\nu}(Q) \right] \tag{B.7}$$

where the factor $1/2$ is again a symmetry factor. We have chosen a compact notation where V denotes either a SU(2) or a U(1) gauge boson and g_V, t_V denote the corresponding coupling constant and generator matrices, respectively. Using (B.6), this simplifies to

$$-\Pi_V(k_0, \vec{k}) = g_V^2 C_2(r) T \sum_{q_0} \int \frac{\mathrm{d}^3 q}{(2\pi)^3} \left[4\Delta(Q) - (2K-Q)^2 \Delta(K-Q)\Delta(Q) \right] \tag{B.8}$$

with Casimir invariant $C_2(r)$.
Now we consider a hard and lightlike external momentum K. Writing

$$(2K-Q)^2 = 2K^2 - Q^2 + 2(K-Q)^2,$$

we get

$$\Pi_V(k_0, \vec{k}) = -g_V^2 C_2(r) T \sum_{q_0} \int \frac{\mathrm{d}^3 q}{(2\pi)^3} \left[2\Delta(Q) - 2K^2 \Delta(Q)\Delta(K-Q) + \Delta(K-Q) \right]. \tag{B.9}$$

The term proportional to K^2 can be neglected[1] and the result reads

$$\Pi_V(k_0, \vec{k}) = -g_V^2 C_2(r) T \sum_{q_0} \int \frac{\mathrm{d}^3 q}{(2\pi)^3} \left[2\Delta(Q) + \Delta(K-Q) \right] = \frac{g_V^2 C_2(r)}{4} T^2. \tag{B.10}$$

Had we considered a soft external momentum instead, then $(2K-Q)^2 \approx Q^2$ and we would have got

$$\Pi_V(k_0, \vec{k}) = -g_V^2 C_2(r) T \sum_{q_0} \int \frac{\mathrm{d}^3 q}{(2\pi)^3} \left[4\Delta(Q) - \Delta(K-Q) \right] \tag{B.11}$$

[1] If one wants to be very precise then one should first do the thermal sum, perform the analytical continuation to real values and only then argue that certain terms are suppressed. This is overly pedantic however because it is clear that this part will remain proportional to K^2 which, after the analytical continuation of k^0 to the real axis, is of order g^2T^2. Such terms will then always be immediately dropped to avoid unnecessary computations of thermal sums.

which leads to the same result.
Finally, we must take the diagram with a fermion loop into account. Defining $N_{c,l} = 1, N_{c,q} = 3$ as the number of "colors", we get

$$-\Pi_f(k_0,\vec{k}) = -\lambda_f^2 N_{c,f} T \sum_{\tilde{q}_0} \int \frac{\mathrm{d}^3 q}{(2\pi)^3} \,\mathrm{Tr}[P_L \not{Q}(\not{Q}-\not{K})]\Delta(Q)\Delta(Q-K) \tag{B.12}$$

with a minus sign from the closed fermion loop. The trace gives a contribution of

$$\mathrm{Tr}[P_L \not{Q}(\not{Q}-\not{K})] = 2Q\cdot(Q-K) = Q^2 + (Q-K)^2 - K^2$$

and the expression for the self-energy becomes

$$-\Pi_f(k_0,\vec{k}) = -\lambda_f^2 N_{c,f} T \sum_{\tilde{q}_0} \int \frac{\mathrm{d}^3 q}{(2\pi)^3} [\Delta(Q) + \Delta(Q-K) - K^2\Delta(Q)\Delta(Q-K)]. \tag{B.13}$$

Again, we may neglect the term proportional to K^2 and we are left with

$$\Pi_f(k_0,\vec{k}) = \lambda_f^2 N_{c,f} T \sum_{\tilde{q}_0} \int \frac{\mathrm{d}^3 q}{(2\pi)^3} [\Delta(Q) + \Delta(Q-K)] = \lambda_f^2 N_{c,f} \frac{T^2}{12}, \tag{B.14}$$

where the sum over half-integer Matsubara frequencies introduces a factor of -2 compared to the bosonic sum-integral considered before, as one can see in (2.27). In the HTL approximation, the trace would give just $2Q^2$ and the result would be

$$\Pi_f(k_0,\vec{k}) = 2\lambda_f^2 N_{c,f} T \sum_{\tilde{q}_0} \int \frac{\mathrm{d}^3 q}{(2\pi)^3} \Delta(Q-K) \tag{B.15}$$

which once more leads to the same result as for hard and lightlike momenta.
To finally get the thermal mass, we must add up all contributions. We neglect the contribution due to all fermions except for the top quark because the other Yukawa couplings are too small to be relevant. The Casimir invariants are easily computed:

$$t_Y = \frac{1}{2}\mathbb{1} \Rightarrow C_2(r_Y) = \frac{1}{4} \tag{B.16}$$

$$t_W^a = \frac{1}{2}\sigma^a \Rightarrow C_2(r_W) = \frac{3}{4} \tag{B.17}$$

This leads to the final expression

$$m_\phi^2 = \frac{8\Lambda + 4\lambda_t^2 + 3g_W^2 + g_Y^2}{16} T^2. \tag{B.18}$$

B.2. Fermion propagator

In this section we deal with the resummed fermion propagator both for soft and for hard and lightlike external momenta. In contrast to the scalar case treated before, the masses in those two different kinematical regimes will turn out to be different and for a soft external momentum we will also find a momentum-dependent self-energy leading to the *HTL fermion propagator* (2.31).

B.2.1. The resummed finite-temperature fermion propagator

We start with general considerations about the resummed fermion propagator at finite temperature. The general expression is

$$S(P) = \frac{-1}{\not{P} - \Sigma(p_0,\vec{p})} \tag{B.19}$$

with the self-energy $\Sigma(p_0,\vec{p})$ which is considered at one-loop level like for the scalar case treated previously. We can make an ansatz [72]

$$\Sigma(p_0,\vec{p}) = \tilde{a}(p_0,\vec{p})\not{P} + \tilde{b}(p_0,\vec{p})\not{u} \tag{B.20}$$

where u^μ is the four-velocity of the plasma. We perform the calculation in the plasma rest frame where $u^\mu = (1, \vec{0})$ and the expression simplifies to

$$\Sigma(p_0, \vec{p}) = \tilde{a}(p_0, \vec{p})\not{P} + \tilde{b}(p_0, \vec{p})\gamma^0. \tag{B.21}$$

The inverse propagator is thus given by

$$-S^{-1}(P) = (1 - \tilde{a}(p_0, \vec{p}))\not{P} - \tilde{b}(p_0, \vec{p})\gamma^0. \tag{B.22}$$

The propagator itself can be written as

$$-S(P) = \frac{(1 - \tilde{a}(p_0, \vec{p}))\not{P} - \tilde{b}(p_0, \vec{p})\gamma^0}{D} \tag{B.23}$$

where the denominator D is determined by $S^{-1}(P)S(P) = \mathbb{1}$. Explicitly, we get

$$-S(P) = \frac{(1 - \tilde{a}(p_0, \vec{p}))\not{P} - \tilde{b}(p_0, \vec{p})\gamma^0}{(1 - \tilde{a}(p_0, \vec{p}))^2 P^2 + \tilde{b}^2(p_0, \vec{p}) - 2\tilde{b}(p_0, \vec{p})(1 + \tilde{a}(p_0, \vec{p}))p^0}. \tag{B.24}$$

Up to now we have been completely general, but now we want to consider the two specific cases that we need: hard lightlike momenta ($P \sim T, P^2 \sim g^2T^2$) and soft momenta ($P \sim gT$).

B.2.2. Propagator for lightlike momenta, asymptotic thermal mass

We start with the case that the momentum P is hard and lightlike. We need not keep all the terms in (B.24) if we are just interested in the leading order expression. Since $\Sigma(p_0, \vec{p}) \sim g^2T$, we have (from (B.21)) $\tilde{a}(p_0, \vec{p}) \sim g^2 \ll 1$ and we may replace $(1 - \tilde{a}(p_0, \vec{p}))$ by 1. The other coefficient is of the order $\tilde{b}(p_0, \vec{p}) \sim g^2T$ and the terms linear in $\tilde{b}(p_0, \vec{p})$ cannot be neglected but $\tilde{b}^2(p_0, \vec{p})$ can. In the denominator this is obvious because $P^2 \sim g^2T^2$. In the numerator, it is less obvious but from taking traces with other quantities one may encounter terms that go like $\not{P}^2 = P^2 \sim g^2T^2$ and therefore it is necessary to keep the additional term in the numerator. Therefore, we use the approximate propagator

$$S(P) \approx (\not{P} - \tilde{b}(p_0, \vec{p})\gamma^0)\Delta(P) \tag{B.25}$$

with

$$\Delta(P) = \frac{-1}{P^2 - 2\tilde{b}(p_0, \vec{p})p^0}. \tag{B.26}$$

As for scalars, we should reproduce the standard form

$$\Delta(P) = \frac{-1}{(p^0 + i\Gamma)^2 - \vec{p}^2 - m_\infty^2} \tag{B.27}$$

which fixes $\tilde{b}(p_0, \vec{p})$:

$$\tilde{b}(p_0, \vec{p}) = \frac{m_\infty^2}{2p^0} - i\Gamma(p_0, \vec{p}). \tag{B.28}$$

As for scalars, we have imposed $\Gamma^2 \ll m_\infty^2$. The real part of $\tilde{b}(p_0, \vec{p})$ is then connected to the *asymptotic thermal mass* which we denote here by m_∞ and the imaginary part gives the thermal width. However, as for scalars, the width is due to the interaction with *soft* gauge bosons and does therefore not appear in the propagators used in section 3.3. The subsequent explicit computation will also show that $\tilde{b}(p_0, \vec{p})$ is purely real.

Taking the above into account, the fermion propagator can then be written as

$$S(P) = -\frac{\not{P} - \frac{m_\infty^2}{2p_\parallel}\gamma^0}{P^2 - m_\infty^2}. \tag{B.29}$$

where we set $p^0 = p_\parallel$ and dropped higher-order corrections.

For the recursion relations in section 3.3.3, it will prove convenient to rewrite this expression. First of all, one can notice that since chiral symmetry is left unbroken, we may consider left- and right-handed fermions

separately. We then choose to consider only left-handed fermions; for photon production where both chiralities contribute, we have to multiply by 2 at the end. Focusing on one chirality allows to replace γ^μ by σ^μ and use two-component Weyl spinors. If the term $m_\infty^2/2p_\parallel\,\sigma^0$ would not appear, we could immediately write the numerator in the convenient form $\sigma\cdot P$. In order to write the numerator in this simple form, we define

$$\tilde{P}=\begin{pmatrix} p^0-\frac{m_\infty^2}{2p_\parallel} \\ \vec{p}\end{pmatrix} \tag{B.30}$$

which allows us to write

$$S(P)=-\frac{\sigma\cdot\tilde{P}}{P^2-m_\infty^2}. \tag{B.31}$$

Now we can introduce a Weyl spinor $\eta(\tilde{P})$ as a normalized eigenspinor of $\vec{\sigma}\cdot\hat{p}$ with negative eigenvalue and another such Weyl spinor $\chi(\tilde{P})$, only with positive eigenvalue. Since σ^0 is diagonal, they are also eigenspinors of $\sigma\cdot\tilde{P}$:

$$\sigma\cdot\tilde{P}\eta(\tilde{P})=(\tilde{p}^0+|\vec{p}|)\eta(\tilde{P});\quad \sigma\cdot\tilde{P}\chi(\tilde{P})=(\tilde{p}^0-|\vec{p}|)\chi(\tilde{P}) \tag{B.32}$$

It is now crucial, that the eigenvalue of $\chi(\tilde{P})$ is zero (up to corrections of order $\mathcal{O}(g^4T)$), because $\tilde{P}^2=0$ [2], whereas $P^2\sim g^2T^2$ and the same type of reasoning that we use here would fail if the spinors would depend on P. But then we can write

$$\sigma\cdot\tilde{P}=(\tilde{p}^0+|\vec{p}|)\eta(\tilde{P})\eta^\dagger(\tilde{P})+\mathcal{O}(g^4T)=2|\vec{p}|\eta(\tilde{P})\eta^\dagger(\tilde{P})+\mathcal{O}(g^4T), \tag{B.33}$$

i.e. we represent the matrix $\sigma\cdot\tilde{P}$ in the basis of its eigenspinors and neglect the g^4T contribution due to $\chi(\tilde{P})$. The asymptotic fermion propagator can then finally be written as

$$S(P)=2|\vec{p}|\eta(\tilde{P})\eta^\dagger(\tilde{P})\Delta(P)=\eta(\tilde{P})\eta^\dagger(\tilde{P})D(P) \tag{B.34}$$

where at leading order, we have set $|\vec{p}|=p_\parallel$ and we used (3.50).

As shown in section 3.3.3, the difference between P and $\tilde{P}$ is irrelevant for the recursion relations because the soft vertex factors are always needed to order T, whereas the difference $p^0-\tilde{p}^0\sim g^2T$. There we may thus set $\tilde{P}\to P$. For the trace over the fermion propagators, however, it is crucial not to leave out these g^2T corrections since due to the collinearity all contributions to the trace turn out to be of that order. This means that the hard vertex factor Φ must be computed using $\tilde{P}$ and not P.

Asymptotic thermal mass

The asymptotic thermal mass m_∞ still has to be determined, which means that we have to compute the coefficient $\tilde{b}(p_0,\vec{p})$ explicitly. To determine it, we first define the traces (the factors of 1/4 are inserted for convenience)

$$T_1\equiv\frac{1}{4}\,\mathrm{Tr}[\not{P}\Sigma(p_0,\vec{p})] \tag{B.35}$$

$$T_2\equiv\frac{1}{4}\,\mathrm{Tr}[\gamma^0\Sigma(p_0,\vec{p})]. \tag{B.36}$$

With the help of (B.21), we easily find that $T_1=\tilde{a}(p_0,\vec{p})P^2+\tilde{b}(p_0,\vec{p})p^0$ and $T_2=\tilde{a}(p_0,\vec{p})p^0+\tilde{b}(p_0,\vec{p})$. This gives a 2x2 system of linear equations for the unknown functions $\tilde{a}(p_0,\vec{p})$ and $\tilde{b}(p_0,\vec{p})$ with the solution

$$\tilde{a}(p_0,\vec{p})=-\frac{1}{|\vec{p}|^2}(T_1-p^0T_2) \tag{B.37}$$

$$\tilde{b}(p_0,\vec{p})=\frac{1}{|\vec{p}|^2}(p^0T_1-P^2T_2). \tag{B.38}$$

Since $P^2\sim g^2T^2$, the second term in (B.38) can be omitted and we only need to compute T_1 using the one-loop self-energy given in figure B.2. We use Feynman gauge (B.6) again and the self-energy is given by

[2] A subtlety arises here when we look at the two-point function where we have to perform a thermal sum and we get two different pole contributions. Apparently, our reasoning only works for the pole coming from $\Delta(P)$, whereas the other propagator gives a different value for p^0 and $\tilde{p}^0-|\vec{p}|$ seems not to vanish any longer but rather get a nonzero g^2T contribution. However, this potentially harmful difference in the pole locations is nothing else but the quantity $\epsilon(P,\vec{k})$ defined in (3.52). Due to (3.56) we know that the discontinuity w.r.t. p^0 that we need for the computation of the production rate will be proportional to $\delta(\epsilon(P,\vec{k}))$ which means that $\tilde{p}^0-|\vec{p}|$ still vanishes and the reasoning we applied here is indeed correct, provided we look only at the discontinuity of the self-energy.

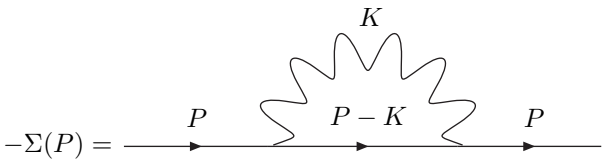

Figure B.2.: One-loop fermion self-energy

$$\Sigma(P) = g^2 C_2(r) T \sum_{k_0} \int \frac{\mathrm{d}^3 k}{(2\pi)^3} \gamma^\mu (\not{P} - \not{K}) \gamma_\mu \Delta(K) \Delta(P-K). \tag{B.39}$$

Then we have

$$T_1 = -\frac{g^2}{2} C_2(r) T \sum_{k_0} \int \frac{\mathrm{d}^3 k}{(2\pi)^3} \operatorname{Tr}[\not{P}(\not{P} - \not{K})] \Delta(K) \Delta(P-K) \tag{B.40}$$

and with the help of

$$\operatorname{Tr}[\not{P}(\not{P} - \not{K})] = 4(P^2 - P \cdot K) = 2(P^2 + (P-K)^2 - K^2),$$

we can rewrite this as

$$T_1 = -g^2 C_2(r) T \sum_{k_0} \int \frac{\mathrm{d}^3 k}{(2\pi)^3} \left[P^2 \Delta(K) \Delta(P-K) + \Delta(K) - \Delta(P-K) \right]. \tag{B.41}$$

The first term is non-leading since $P^2 \sim g^2 T^2$ and for the other two we can use the standard results (2.18) and (2.27) again. Then we get from (B.38) the following result:

$$\tilde{b}(p_0, \vec{p}) = \frac{p^0}{|\vec{p}|^2} g^2 C_2(r) \frac{T^2}{8} \tag{B.42}$$

From (B.28) and (B.42) we obtain, using that for lightlike momenta the difference between 1 and $(p^0)^2/|\vec{p}|^2$ is

$$1 - \frac{(p^0)^2}{|\vec{p}|^2} = \frac{P^2}{|\vec{p}|^2} \sim g^2$$

and therefore negligible, finally the value of the asymptotic mass:

$$m_\infty^2 = \frac{g^2 C_2(r) T^2}{4} \tag{B.43}$$

Since $C_2(r) = 1/4$ for the gauge group U(1) and $C_2(r) = 3/4$ for the gauge group SU(2), we get as asymptotic thermal lepton mass in total

$$m_{\ell,\infty}^2 = \frac{3g_W^2 + g_Y^2}{16} T^2. \tag{B.44}$$

B.2.3. HTL fermion propagator and HTL mass

Now we redo the computation assuming the external momentum P to be soft. In this case, we have to use the full expression (B.24) since $\Sigma(p_0, \vec{p}) \sim gT$ and therefore $\tilde{a}(p_0, \vec{p}) = \mathcal{O}(1)$ and $\tilde{b}(p_0, \vec{p}) \sim gT$, such that no term is negligible and we need to compute both traces $T_{1,2}$. The result for T_1 remains unchanged, i.e.

$$T_1 = \frac{g^2 C_2(r) T^2}{8} \equiv m_\ell^2 \tag{B.45}$$

where we have introduced the HTL thermal mass m_ℓ which will prove convenient later on. Although it appears somehow arbitrary at this stage, it is reasonable to define the HTL thermal mass exactly that way (and not e.g. larger by a factor of 2) because it turns out that in the limit $\vec{p} \to 0$, the HTL propagator reduces to the form of a bare fermion propagator with mass m_ℓ. It is important to note that due to that

definition, it is in contrast to scalar particles *different* from the asymptotic thermal mass (B.44) by a factor of $\sqrt{2}$!
For T_2 we obtain from (B.39) the following thermal sum-integral to be performed:

$$T_2 = -2g^2C_2(r)T\sum_{k_0}\int\frac{\mathrm{d}^3k}{(2\pi)^3}(p^0-k^0)\Delta(K)\Delta(P-K) \approx 2g^2C_2(r)T\sum_{k_0}\int\frac{\mathrm{d}^3k}{(2\pi)^3}k^0\Delta(K)\Delta(P-K),$$

The thermal sum we need here is given by (2.24) with $p^0 \leftrightarrow k^0$ and $f_B(E_2) \to -f_F(E_2)$:

$$T\sum_{k^0}\int\frac{\mathrm{d}^3k}{(2\pi)^3}k^0\Delta(K)\Delta(P-K) = -\int\frac{\mathrm{d}^3k}{(2\pi)^3}\frac{1}{4E_2}\Bigg[(1+f_B(E_1)-f_F(E_2))\left(\frac{1}{p^0-E_1-E_2}+\frac{1}{p^0+E_1+E_2}\right) \\ -(f_B(E_1)+f_F(E_2))\left(\frac{1}{p^0+E_1-E_2}+\frac{1}{p^0-E_1+E_2}\right)\Bigg] \tag{B.46a}$$

In order to proceed, we need to extract the leading-order contribution. First of all,

$$E_1 = k, E_2 = |\vec{p}-\vec{k}| = \sqrt{k^2-2kp\cos\vartheta+p^2} \approx k - p\cos\vartheta \tag{B.47}$$

since in the HTL approximation $p/k \ll 1$ and masses for the particles inside the loop would only give higher-order corrections which we drop. From this also follows after a Taylor expansion

$$f_B(E_1) = f_B(k), f_F(E_2) = f_F(k) - p\cos\vartheta\frac{\mathrm{d}f_F(k)}{\mathrm{d}k}. \tag{B.48}$$

In addition,

$$\frac{1}{p^0-E_1-E_2}+\frac{1}{p^0+E_1+E_2} = \frac{1}{p^0-2k}+\frac{1}{p^0+2k} = -\frac{p^0}{2k^2} \sim \frac{g}{T}$$

is subleading compared to

$$\frac{1}{p^0+E_1-E_2}+\frac{1}{p^0-E_1+E_2} = \frac{1}{p^0+p\cos\vartheta}+\frac{1}{p^0-p\cos\vartheta} \sim \frac{1}{gT}.$$

Therefore we only need to take the term multiplying the sum of the two distribution functions into account. Then we simply get

$$T_2 = 2g^2C_2(r)\int\frac{\mathrm{d}^3k}{(2\pi)^3}\frac{f_B(k)+f_F(k)}{4k}\left(\frac{1}{p^0+p\cos\vartheta}+\frac{1}{p^0-p\cos\vartheta}\right). \tag{B.49}$$

The only remaining task is to evaluate the integrals. The two terms in the bracket can be combined by replacing $\cos\vartheta \to -\cos\vartheta$ in the second term. We then finally obtain

$$T_2 = \frac{g^2C_2(r)T^2}{8p}Q_0(x) \tag{B.50}$$

with $x \equiv p_0/p$ and the Legendre function of the second kind, $Q_0(x) \equiv \frac{1}{2}\ln\frac{x+1}{x-1}$.
With the solutions at hand, we obtain for the two coefficients $\tilde{a}(p_0,\vec{p}), \tilde{b}(p_0,\vec{p})$ the following expressions:

$$\tilde{a}(p_0,\vec{p}) = \frac{m_\ell^2}{p^2}(1-xQ_0(x)), \quad \tilde{b}(p_0,\vec{p}) = -\frac{m_\ell^2}{p}(x+(1-x^2)Q_0(x)) \tag{B.51}$$

Instead of blindly inserting this into (B.24) which produces rather tedious expressions, it is much easier to reproduce the standard textbook result for the self-energy first, which can be written as

$$\Sigma(p_0,\vec{p}) = (ap^0+b)\gamma^0 - a\vec{\gamma}\cdot\vec{p} = \frac{m_\ell^2}{p}\left[Q_0(x)\gamma^0+(1-xQ_0(x))\vec{\gamma}\cdot\hat{p}\right]. \tag{B.52}$$

The inverse propagator (B.22) then becomes

$$-S^{-1}(P) = A_0\gamma^0 - A_S\vec{\gamma}\cdot\hat{p} \tag{B.53}$$

where we adopted the notation from [9] with

$$A_0 \equiv p^0 - \frac{m_\ell^2}{p^2}(1 - xQ_0(x)), \quad A_S \equiv p + \frac{m_\ell^2}{p}(1 - xQ_0(x)). \tag{B.54}$$

To show that the fermion propagator can indeed be written in the conventional form (2.31), one only needs to multiply with the inverse propagator determined above and define (2.32) as $\Delta_\pm(P) \equiv (A_0 \mp A_S)^{-1}$. With some basic Dirac algebra one can easily prove that this particular form of the fermion propagator is indeed equivalent to the one that was explicitly calculated here.

B.3. Gauge boson propagator

Finally we have to address the gauge boson propagator at finite temperature. Its tensor structure is in general much more complicated than at zero temperature and to avoid unnecessary complications, we will immediately focus on *covariant gauges* and go to the plasma rest frame: [3]

$$\Delta_{\mu\nu}(K) = P^T_{\mu\nu}\Delta_T(K) + P^L_{\mu\nu}\Delta_L(K) + \xi\frac{K_\mu K_\nu}{K^2}\Delta(K) \tag{B.55}$$

with scalar (timelike) propagator $\Delta(K)$, the longitudinal/transverse propagators

$$\Delta_T(K) = \frac{-1}{K^2 - \Pi_T(k_0, \vec{k})} \tag{B.56}$$

$$\Delta_L(K) = \frac{-1}{K^2 - \Pi_L(k_0, \vec{k})} \tag{B.57}$$

with the corresponding self-energies and finally the transverse and longitudinal projectors

$$P^T_{ij} = \delta_{ij} - \hat{k}_i\hat{k}_j; P^T_{\mu 0} = 0$$
$$P^L_{\mu\nu} = \frac{K_\mu K_\nu}{K^2} - g_{\mu\nu} - P^T_{\mu\nu}.$$

In order to compute the resummed gauge boson propagator at a given order in perturbation theory, we first define the *polarization tensor*

$$\Pi_{\mu\nu}(k_0, \vec{k}) \equiv \Delta^{-1}_{\mu\nu}(K) - \Delta^{-1}_{\mu\nu,0}(K) \tag{B.58}$$

where the index 0 indicates the *free* propagator and the inverse propagators are defined by $\Delta^{\mu\alpha}\Delta^{-1}_{\alpha\nu} = g^\mu{}_\nu$. The polarization tensor has the same tensor structure as the propagator (B.55), only in addition it obeys the Ward identity $K^\mu\Pi_{\mu\nu}(K) = 0$ which is only consistent if we can write

$$-\Pi_{\mu\nu}(k_0, \vec{k}) = \Pi_T(k_0, \vec{k})P^T_{\mu\nu} + \Pi_L(k_0, \vec{k})P^L_{\mu\nu}. \tag{B.59}$$

This explains why there are only two self-energy functions and the gauge-dependent term in (B.55) receives no self-energy corrections.[4]

As soon as we have found an expression for the polarization tensor, we can then use (B.59) to determine the transverse and longitudinal self-energy. By setting either $\mu = \nu = 0$ or by contracting with P^T_{ij}, it is simple to deduce from (B.59) the following explicit representations:

$$\Pi_L(k_0, \vec{k}) = -\frac{K^2}{k^2}\Pi_{00}(k_0, \vec{k}), \tag{B.60}$$

$$\Pi_T(k_0, \vec{k}) = -\frac{1}{2}(\delta^{ij} - \hat{k}^i\hat{k}^j)\Pi_{ij}(k_0, \vec{k}) \tag{B.61}$$

The task is now to compute Π_{00} and Π_{ij}. There are in total six one-loop diagrams that contribute, as shown in figure B.3, two with scalar loops, two with gauge boson loops and one with ghost or fermion loop each.

[3] A very general discussion of gauge boson propagators at finite temperature for arbitrary plasma four-velocity u^μ and for a wide class of gauge fixing conditions can be found in [73].

[4] Note that at $T = 0$, things are even easier since $\Pi_L = \Pi_T$ and the tensor structure is given by $g_{\mu\nu} - \frac{K_\mu K_\nu}{K^2}$, but at finite temperature, both self-energies are independent functions and need not be the same.

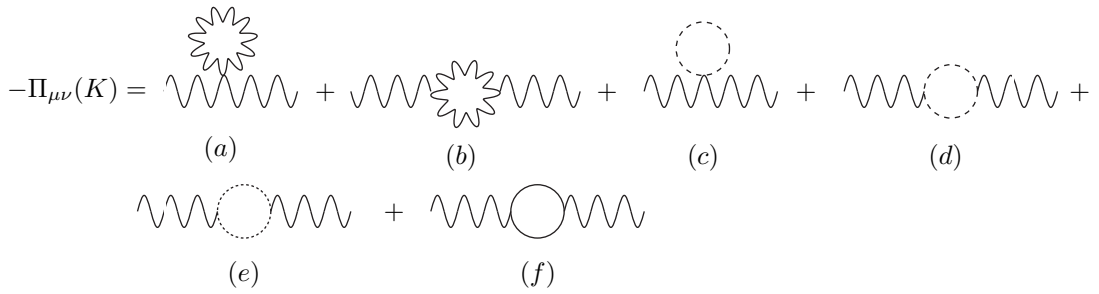

Figure B.3.: One-loop gauge boson polarization tensor

B.3.1. HTL gauge boson propagator

Now we do the concrete calculation for a soft external momentum $K \sim gT$. We go through all contributions separately, labelling them with letters (a)-(f) as indicated in figure B.3 and using Feynman gauge for gauge boson propagators.
The tadpole diagram gives a contribution of

$$-\Pi^{(a)}_{\mu\nu}(k_0,\vec{k}) = \frac{g^2}{2} T \sum_{q_0} \int \frac{\mathrm{d}^3 q}{(2\pi)^3} (-g^{\rho\sigma}\Delta(Q)) \delta^{cd} \left[f^{ace} f^{bde} (g_{\mu\nu} g_{\rho\sigma} - g_{\mu\sigma} g_{\nu\rho}) + f^{ade} f^{bce} (g_{\mu\nu} g_{\rho\sigma} - g_{\mu\rho} g_{\nu\sigma}) \right] \tag{B.62}$$

where we have left out the term containing f^{cde} because its contraction with δ^{cd} vanishes. The prefactor $1/2$ is a symmetry factor. We can now simplify the expression above using

$$\delta^{cd} f^{ace} f^{bde} = f^{ace} f^{bce} = C_2(r)\delta^{ab}; \quad \delta^{cd} f^{ade} f^{bce} = f^{ace} f^{bce} = C_2(r)\delta^{ab}.$$

Then we get, after performing the contraction of metric tensors,

$$\Pi^{(a)}_{\mu\nu}(k_0,\vec{k}) = 3g^2 C_2(r) \delta^{ab} g_{\mu\nu} T \sum_{q_0} \int \frac{\mathrm{d}^3 q}{(2\pi)^3} \Delta(Q). \tag{B.63}$$

We now turn to the second diagram involving the three gauge boson-vertex. The related vertex factor can be simplified because we may neglect the external momentum K w.r.t. to the hard loop momentum Q. When writing down the two vertex factors, it is important to pay attention to all momenta being *incoming* which introduces some additional minus signs. Then we obtain (there is again a symmetry factor of $1/2$)

$$-\Pi^{(b)}_{\mu\nu}(k_0,\vec{k}) = \frac{g^2}{2} f^{acd} f^{bcd} T \sum_{q_0} \int \frac{\mathrm{d}^3 q}{(2\pi)^3} \Delta(Q)\Delta(Q-K) \left[2Q_\mu g_{\rho\sigma} - Q_\rho g_{\mu\sigma} - Q_\sigma g_{\mu\rho} \right] \left[Q^\rho g^\sigma{}_\nu + Q^\sigma g^\rho{}_\nu - 2Q_\nu g^{\rho\sigma} \right]. \tag{B.64}$$

The contraction of the structure constants gives the same result as for the tadpole diagram, only with an additional minus sign due to the antisymmetricity of f^{bcd}. Contracting the metric tensors finally results in

$$\Pi^{(b)}_{\mu\nu}(k_0,\vec{k}) = -g^2 C_2 \delta^{ab} T \sum_{q_0} \int \frac{\mathrm{d}^3 q}{(2\pi)^3} (Q^2 g_{\mu\nu} + 5Q_\mu Q_\nu) \Delta(Q)\Delta(Q-K). \tag{B.65}$$

Now we turn to the diagrams with scalar loops. The tadpole diagram gives

$$-\Pi^{(c)}_{\mu\nu}(k_0,\vec{k}) = \frac{1}{2} \cdot (-2g^2 g_{\mu\nu}) \,\mathrm{Tr}[t^a t^b] N_S T \sum_{q_0} \int \frac{\mathrm{d}^3 q}{(2\pi)^3} \Delta(Q) \tag{B.66}$$

where N_S denotes the number of scalars that contribute and we have a symmetry factor $1/2$ again. The trace over the generator matrices simply gives

$$\mathrm{Tr}[t^a t^b] = \frac{1}{2}\delta^{ab}$$

and we get

$$\Pi^{(c)}_{\mu\nu}(k_0,\vec{k}) = g^2 g_{\mu\nu}\delta^{ab}\frac{N_S}{2}T\sum_{q_0}\int\frac{\mathrm{d}^3q}{(2\pi)^3}\Delta(Q). \tag{B.67}$$

The second diagram with a scalar loop contributes

$$\Pi^{(d)}_{\mu\nu}(k_0,\vec{k}) = -2g^2\delta^{ab}\frac{N_S}{2}T\sum_{q_0}\int\frac{\mathrm{d}^3q}{(2\pi)^3}Q_\mu Q_\nu\Delta(Q)\Delta(Q-K) \tag{B.68}$$

where we used the approximation $(2Q-K)_\mu(2Q-K)_\nu \approx 4Q_\mu Q_\nu$ and there is once more a symmetry factor of $1/2$.
Finally, there is only one contribution with scalar propagators left, the ghost diagram (e):

$$-\Pi^{(e)}_{\mu\nu}(k_0,\vec{k}) = -g^2 f^{acd}f^{bcd}T\sum_{q_0}\int\frac{\mathrm{d}^3q}{(2\pi)^3}Q_\mu Q_\nu\Delta(Q)\Delta(Q-K). \tag{B.69}$$

The external momentum was again neglected w.r.t. Q. Note that there is an additional minus sign due to the loop over anticommuting fields. Contracting the structure constants finally gives

$$\Pi^{(e)}_{\mu\nu}(k_0,\vec{k}) = g^2 C_2\delta^{ab}T\sum_{q_0}\int\frac{\mathrm{d}^3q}{(2\pi)^3}Q_\mu Q_\nu\Delta(Q)\Delta(Q-K). \tag{B.70}$$

Finally we have to deal with the fermion loop. Denoting by N_f the number of fermion flavours, we get (again there is an additional minus sign due to the closed fermion loop)

$$-\Pi^{(f)}_{\mu\nu}(k_0,\vec{k}) = -g^2 N_f\,\mathrm{Tr}[t^a t^b]T\sum_{\tilde{q}_0}\int\frac{\mathrm{d}^3q}{(2\pi)^3}\,\mathrm{Tr}[\gamma_\mu\not{Q}\gamma_\nu(\not{Q}-\not{K})]\Delta(Q)\Delta(Q-K) \tag{B.71}$$

Now $\mathrm{Tr}[\gamma_\mu\not{Q}\gamma_\nu(\not{Q}-\not{K})] \approx \mathrm{Tr}[\gamma_\mu\not{Q}\gamma_\nu\not{Q}] = -4(Q^2 g_{\mu\nu} - 2Q_\mu Q_\nu)$ and therefore

$$\Pi^{(f)}_{\mu\nu}(k_0,\vec{k}) = -2g^2 N_f\delta^{ab}T\sum_{\tilde{q}_0}\int\frac{\mathrm{d}^3q}{(2\pi)^3}(Q^2 g_{\mu\nu} - 2Q_\mu Q_\nu)\Delta(Q)\Delta(K-Q). \tag{B.72}$$

The complete one-loop HTL contribution to the gauge boson self-energy then is

$$\begin{aligned}\Pi_{\mu\nu}(k_0,\vec{k}) = 2g^2\delta^{ab}\Bigg[&\left(C_2(r)+\frac{N_S}{4}\right)T\sum_{q_0}\int\frac{\mathrm{d}^3q}{(2\pi)^3}(Q^2 g_{\mu\nu} - 2Q_\mu Q_\nu)\Delta(Q)\Delta(Q-K)\\ &-N_f T\sum_{\tilde{q}_0}\int\frac{\mathrm{d}^3q}{(2\pi)^3}(Q^2 g_{\mu\nu} - 2Q_\mu Q_\nu)\Delta(Q)\Delta(K-Q)\Bigg].\end{aligned} \tag{B.73}$$

We now need to extract the HTL part of the sum-integrals. What we need for (B.60) and (B.61) is the HTL part of I_{00} and $\frac{1}{2}(\delta^{ij}-\hat{k}^i\hat{k}^j)I_{ij}$ (and the corresponding quantities with fermion propagators) where

$$I_{\mu\nu} \equiv -T\sum_{q_0}\int\frac{\mathrm{d}^3q}{(2\pi)^3}(Q^2 g_{\mu\nu} - 2Q_\mu Q_\nu)\Delta(Q)\Delta(Q-K) \tag{B.74}$$

Using (2.18), we can rewrite this as

$$I_{\mu\nu} = \frac{T^2}{12}g_{\mu\nu} + 2T\sum_{q_0}\int\frac{\mathrm{d}^3q}{(2\pi)^3}Q_\mu Q_\nu\Delta(Q)\Delta(Q-K). \tag{B.75}$$

For the remaining sum-integrals, we use (2.22) and (2.25). We then obtain

$$I_{00} = \int \frac{\mathrm{d}^3q}{(2\pi)^3}\frac{E_1}{2E_2}\left[(1+f_1+f_2)\left(\frac{1}{k^0-E_1-E_2}-\frac{1}{k^0+E_1+E_2}\right)\right.$$
$$\left.+(f_1-f_2)\left(\frac{1}{k^0+E_1-E_2}-\frac{1}{k^0-E_1+E_2}\right)\right]+\frac{T^2}{12} \tag{B.76}$$

$$I_{ij} = \int \frac{\mathrm{d}^3q}{(2\pi)^3}\frac{q_iq_j}{2E_1E_2}\left[(1+f_1+f_2)\left(\frac{1}{k^0-E_1-E_2}-\frac{1}{k^0+E_1+E_2}\right)\right.$$
$$\left.+(f_1-f_2)\left(\frac{1}{k^0+E_1-E_2}-\frac{1}{k^0-E_1+E_2}\right)\right]+\frac{T^2}{12}\delta_{ij} \tag{B.77}$$

where $f_i \equiv f_B(E_i)$. The analogous results with fermion propagators are obtained as usual by replacing $f_B \to -f_F$.
We now separately extract the HTL contribution to the transverse and the longitudinal part.

Transverse self-energy

We first approximate the expression for I_{ij} in the same way as we did in section B.2.3 for the HTL fermion propagator by setting

$$E_1 = q, \quad E_2 = q - k\cos\vartheta; \quad f_1 = f_B(q), \quad f_2 = f_B(q) - k\cos\vartheta\frac{\mathrm{d}f_B(q)}{\mathrm{d}q}.$$

where $\cos\vartheta \equiv \hat{k}\cdot\hat{q}$. Then we can write I_{ij} as

$$I_{ij} = \frac{T^2}{12}\delta_{ij} + \int\frac{\mathrm{d}^3q}{(2\pi)^3}\frac{q_iq_j}{2q^2}\left[(1+2f_B(q))\left(\frac{1}{k^0-2q}-\frac{1}{k^0+2q}\right)+k\cos\vartheta\frac{\mathrm{d}f_B(q)}{\mathrm{d}q}\left(\frac{1}{k^0+k\cos\vartheta}-\frac{1}{k^0-k\cos\vartheta}\right)\right].$$

Dropping higher order corrections and temperature-independent terms, this simplifies to

$$I_{ij} = \frac{T^2}{12}\delta_{ij} + \int\frac{q^2\mathrm{d}q\mathrm{d}\Omega}{(2\pi)^3}\hat{q}_i\hat{q}_j\left[\frac{k\cos\vartheta}{k^0+k\cos\vartheta}\frac{\mathrm{d}f_B(q)}{\mathrm{d}q}-\frac{f_B(q)}{q}\right] \tag{B.78}$$

Performing the radial integral and contracting with $\frac{1}{2}(\delta^{ij}-\hat{k}^i\hat{k}^j)$ because of (B.61) gives

$$\frac{1}{2}(\delta^{ij}-\hat{k}^i\hat{k}^j)I_{ij} = \frac{T^2}{12}\left[1-\frac{1}{8\pi}\int\mathrm{d}\Omega(1-\cos^2\vartheta)\left(2\frac{\cos\vartheta}{x+\cos\vartheta}+1\right)\right] \tag{B.79}$$

where $x \equiv k^0/k$. Looking at (B.78) where radial and angular integrations are completely decoupled, it is easy to see that the result with fermion propagators where we have $-f_F$ instead of f_B will give the same result, up to a global factor of $-1/2$ due to the radial integral. Then it is easy to deduce the final result for the transverse self-energy after performing the final angular integral and inserting the result into (B.73):

$$\Pi_T(k_0,\vec{k}) = m_D^2x[(1-x^2)Q_0(x)+1], \quad x = \frac{k^0}{k} \tag{B.80}$$

with *Debye mass*

$$m_D^2 = \frac{g^2T^2}{6}\left(C_2(r)+\frac{N_f}{2}+\frac{N_s}{4}\right) \tag{B.81}$$

and the usual Legendre function of the second kind Q_0.

Longitudinal self-energy

Now we can treat I_{00} the same way. Without further explanation, we can write down the analogue of (B.78):

$$I_{00} = \frac{T^2}{12} + \int\frac{q^2\mathrm{d}q\mathrm{d}\Omega}{(2\pi)^3}\left[\frac{k\cos\vartheta}{k^0+k\cos\vartheta}\frac{\mathrm{d}f_B(q)}{\mathrm{d}q}-\frac{f_B(q)}{q}\right] \tag{B.82}$$

Again, radial and angular integrations are decoupled and changing $f_B \to -f_F$ will only introduce an overall factor of $-1/2$. After doing the radial integrals, we are left with

$$I_{00} = \frac{T^2}{12}\left[1 - \frac{1}{4\pi}\int \mathrm{d}\Omega \left(2\frac{\cos\vartheta}{x+\cos\vartheta}+1\right)\right].$$

Performing the angular integrals, inserting into (B.73) and multiplying with K^2/k^2 from (B.60) gives the final result

$$\Pi_L(k_0,\vec{k}) = -\frac{m_D^2 K^2}{k^2}(1 - xQ_0(x)), \quad x = \frac{k^0}{k} \tag{B.83}$$

with the Debye mass as defined in (B.81).

B.4. Proof of (3.56)

Here we finally want to prove (3.56) which lies at the heart of the recursion relation formulated in section 3.3. We will approximate the propagators immediately here, even *before performing the thermal sum*, although this strictly speaking undermines the power counting arguments that were used to isolate the leading order terms. We will comment below why this is still possible.
We use the lightcone components already introduced in section 2.3.3 and write the propagators as[5]

$$\Delta(K) = \frac{-1}{k_+k_- - \vec{k}_\perp^2 - m^2} \tag{B.84}$$

and the same for $\Delta(K-P)$, only eventually with a different mass. Since $k_- \sim g^2T$, we have to leading order $k_+ \approx 2k_\parallel \sim T$, since we may replace k^0 by $k_\parallel$, up to higher order corrections. Then we simply write

$$\Delta(K) = \frac{1}{2k_\parallel}\frac{-1}{k_- - \frac{\vec{k}_\perp^2+m^2}{2k_\parallel}} = \frac{1}{2k_\parallel}D(K). \tag{B.85}$$

Of course, we have 'lost' one pole that would contribute to the thermal sum and at first sight the procedure of approximating the propagators before performing the thermal sum appears dubious. However, the second pole arises when $k_+ = 0$, which would give $k_- = -2k_\parallel \sim T$. The second propagator would then behave like T^{-2} instead of $(gT)^{-2}$, which means that two powers of g would be missing in total and the expression would be suppressed by g^2 compared to the leading order result we are interested in. This means that we may neglect this additional pole contribution and use the approximate form (B.85), which has only one pole left. The same argument applies to $\Delta(K-P)$ which can be approximated the same way.
With this in mind, it is now very simple to prove (3.56). The product of the propagators is given by

$$D(K)D(K-P) = \frac{1}{ab}$$

where $a \equiv k_- - \frac{\vec{k}_\perp^2+m_1^2}{2k_\parallel}, b \equiv k_- - p_- - \frac{(\vec{k}_\perp-\vec{p}_\perp)^2+m_2^2}{2(k_\parallel-p_\parallel)}$. The only thing that remains is to use the partial fractioning

$$\frac{1}{ab} = \frac{1}{a-b}\left(\frac{1}{b}-\frac{1}{a}\right).$$

Then (3.56) is already proved and it is also clear that the quantity $\epsilon(K,\vec{p})$ is just the difference of the pole locations of the two propagators.
Note that we could have used the same type of reasoning to provide a shortcut for the computation of the two-point function in section 3.3.2 and it is easy to see that we would have obtained the same result. We chose not to do so in order to show explicitly that a more careful calculation where we do perform the thermal sum leads to the same result which strengthens the confidence in the procedure used here. For the recursion relation, we do not want to do the thermal sum and use (3.56) only at the pole locations, because this results in lengthy calculations with rather tedious intermediate results, which then seem to 'miraculously' simplify to a very compact recursion formula. Using (3.56) provides us with a much faster and more elegant approach.

[5] For the following derivation it is completely irrelevant whether we have integer or half-integer Matsubara frequencies as we do not perform any thermal sums. The results then trivially hold for the denominators of both scalar and fermion propagators.

C. Some details for the recursion relation

C.1. The vertex factors for external gauge bosons and fermion loop

Here we compute the vertex factors Φ_μ and $\mathcal{V}$ needed for the vertices with external, transverse gauge bosons. We take the case of a fermion loop; for a scalar loop, the result equals the soft vertex factor found in (3.60) and it is trivial to see this. If we have a fermion loop, then we need to use (B.34) which means that we need the spinor $\eta(K)$. According to the definition, it is given by

$$\vec{\sigma}\cdot\hat{k}\eta(K) = -|\vec{k}|\eta(K). \tag{C.1}$$

Inserting the explicit form of the Pauli matrices and choosing $\hat{v}$ along the 3-direction, we get the system of equations

$$\begin{aligned} k_\parallel\eta_1 + (k_1 - ik_2)\eta_2 &= -|\vec{k}|\eta_1 \\ (k_1 + ik_2)\eta_1 - k_\parallel\eta_2 &= -|\vec{k}|\eta_2 \end{aligned} \tag{C.2}$$

with the normalized solution

$$\eta(K) = \begin{pmatrix} \eta_1 \\ \eta_2 \end{pmatrix} = \begin{pmatrix} 1 \\ -\frac{k_1 - ik_2}{2k_\parallel} \end{pmatrix}. \tag{C.3}$$

The vertex factor for a gauge boson with momentum K_i coupling to two hard fermions with momenta K and $K - K_i$ is given by $\eta^\dagger(K - K_i)\bar{\sigma}^\mu(K)t^a$. This holds both for the photon and the gluon vertices. The difference between the soft (gluon) vertex factor $\mathcal{V}_a^\mu$ and the external (photon) vertex factor Φ^μ is on the one hand that the momentum K_i is in one case soft and therefore negligible whereas it is hard and not negligible in the other. Besides that, the generator matrix t^a is a unit matrix at the photon vertex. Finally, at the gluon vertices longitudinal polarizations contribute while the photon only has transverse polarizations. Because of that, the leading order contribution to $\mathcal{V}_a^\mu$ is $\mathcal{O}(1)$ while the leading order contribution to Φ^μ is $\mathcal{O}(g)$.

Soft vertex factor

For the leading order contribution to the soft vertex factor, one can neglect the gluon momentum K_i and we get

$$\mathcal{V}_a^\mu = \eta^\dagger(K)\bar{\sigma}^\mu\eta(K)t^a. \tag{C.4}$$

With our choice of the parallel direction, the leading order contribution which follows from (2.52) is found to be

$$\mathcal{V}_a^\mu = \frac{1}{2}\eta^\dagger(K)(\sigma^0 + \sigma^3)\eta(K)t^a. \tag{C.5}$$

Inserting (C.3), we immediately get (3.60).

Vertex factor for hard transverse gauge bosons

The hard vertex factor for transverse gauge bosons, which is needed for the photon production rate in section 3.4 is given by

$$\Phi_\mu^\dagger(K, K - P) = \eta^\dagger(K - P)\bar{\sigma}_\mu\eta(K) \tag{C.6}$$

where now $\mu = 1$ or $\mu = 2$. Inserting the result (C.3) results in ugly expressions, but if we go to *circular polarizations* by using the external polarization vectors $\epsilon_{L,R} \equiv (\epsilon_1 \pm i\epsilon_2)/\sqrt{2}$ and consequently define[1]

$$p_{L,R} \equiv \frac{1}{\sqrt{2}}(p_1 \pm ip_2), \quad \Phi_{L,R} \equiv \frac{1}{\sqrt{2}}(\Phi_1 \pm i\Phi_2) \tag{C.7}$$

[1] A notation with $\pm$ instead of L, R would look nicer, however it bears the danger of confusing it with the lightcone components of the momenta that were defined in section 2.3.3.

then we get rather simple results:

$$\Phi_L(K, K-P) = \frac{k_L}{k_\parallel - p_\parallel}, \quad \Phi^R(K, K-P) = \frac{k_R}{k_\parallel} \tag{C.8}$$

With this explicit result, it is simple to prove the relation

$$\begin{aligned}\vec{\Phi}_\perp(K, K-P) \cdot \vec{\Phi}^\dagger_\perp(K, K-P) &= \Phi^\dagger_L(K, K-P)\Phi_R(K, K-P) + \Phi^\dagger_R(K, K-P)\Phi_L(K, K-P) \\ &= \frac{k_\parallel^2 + (k_\parallel - p_\parallel)^2}{k_\parallel(k_\parallel - p_\parallel)} k_\perp^2\end{aligned} \tag{C.9}$$

needed in section 3.4 by inverting the defining equations for $\Phi_{L,R}$ and using that $k^\dagger_{L,R} = k_{R,L}$ as well as $2k_L k_R = k_\perp^2$.

C.2. No need to remove external fermions

Here we come back to the issue raised after equation (3.58). If we consider production of fermions, then

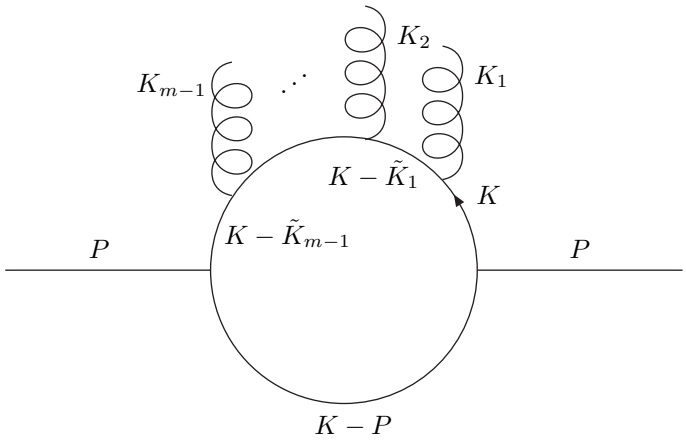

Figure C.1.: Example for a problematic n-point function which might spoil the simple recursion relation (3.58)

(3.58) is only valid if we exclude diagrams of the form shown in figure C.1 where all external gauge bosons couple only to one of the particles in the loop. This is because in such a case, we need to remove one of the external fermions and one of the loop particles, leaving us with an unphysical diagram and seemingly spoiling the recursion relation and the resulting, simple integral equation for the current. However, as we will show here, there is no such problem in fact because all such problematic terms do not contribute to the integral equation (3.63).

We start with looking explicitly at the production of photons because we deal only with well-defined diagrams here. If we remove one external hard photon instead of a soft gluon, then (3.63) remains valid. All fields appearing on the rhs are now soft gluon fields, however, and also the external momentum $p_\parallel$ is soft. We can call this current $\hat{J}_0$ and the current we have looked at in section 3.4 would then be $\hat{J}_1$.[2] The point is to show that we can write an equation for $\hat{J}_1$ (which is the current we are ultimately interested in) alone, without a need for an additional equation for $\hat{J}_0$ which is coupled to the equation for $\hat{J}_1$. Now in the equation for $\hat{J}_0$ the inhomogeneous term is suppressed by one power of g because for a soft $p_\parallel$ the leading order term in $\mathcal{F}(k_\parallel, p_\parallel)$ cancels. But then the whole solution for $\hat{J}_0$ is also suppressed. This is because an integral equation of the form

$$J(P) = f(P) - \int_Q F(Q) J(P-Q) \tag{C.10}$$

[2]Note that $\hat{J}_n$ generates diagrams with $n+1$ external photons, because the interaction is of the form $J_\mu A^\mu$.

has the iterative solution $J(P) = \sum_{N=0}^{\infty} J_N(P)$ where

$$
\begin{aligned}
J_0(P) &= f(P) \\
J_1(P) &= f(P) - \int_Q F(Q) f(P-Q) \\
J_2(P) &= f(P) - \int_Q F(Q) \left[f(P-Q) - \int_{Q'} F(Q') f(P-Q-Q') \right],
\end{aligned}
$$

and so on, i.e. every term in the sequence that converges to the solution is manifestly of at least linear order in the inhomogeneity. Therefore, it is really sufficient to consider only $\hat{J}_1$, as we did in section 3.4.
Now that we have understood what happens if we remove external hard photons, all that remains is to understand why removing an external fermion is essentially the same. Again we can call the current with no (one) explicit fermion field appearing on the rhs $\hat{J}_0$ ($\hat{J}_1$). Of course, $\hat{J}_0$ is not a physically well-defined object in this case because n-point functions with only one external fermion do not exist–which would make it even worse if they would appear in our equations. However, since we have removed one of the loop particles, the function $\mathcal{F}(k_\parallel, p_\parallel)$ is now again a difference of either Bose or Fermi functions and since one of the soft gauge bosons has taken the role of the fermion, the momentum $p_\parallel$ is soft, as it was in the case considered before. Then the leading order term in $\mathcal{F}$ vanishes again and the inhomogeneous term and thus the solution for $\hat{J}_0$ is suppressed again. Such disturbing and physically meaningless terms therefore do not appear in the equation for the current $\hat{J}_1$ which we need and we do not have to worry about them.

D. Remarks on the integral equation for the current

D.1. Connected and disconnected contributions

Here we show that when integrating out the soft gauge boson background, we only need to keep the disconnected part in (3.67). It generates only the ladder diagrams shown in fig. 2.7, but no diagrams with crossed ladder rungs or vertex corrections as illustrated in figure 2.8. This means that those diagrams do not contribute at leading order, as mentioned in section 2.3.4.
If one performs the integrals over the gluon momenta in the imaginary time formalism, only the poles in the spectral representation for the propagators contribute at leading order and for the thermal sum, the dependence on spatial momenta is irrelevant. Therefore, for the present discussion, we may study the simplified equation

$$p^- \hat{J}_\varphi(P,\vec{k}) = \mathcal{C}_\varphi(P,K)\varphi(P) + \int_Q V\cdot W(Q)\hat{J}_\varphi(P-Q,\vec{k}). \tag{D.1}$$

One can write down a formal solution using the iterative procedure already described in the previous subsection:

$$p^- \hat{J}_\varphi(P,\vec{k}) = \sum_{N=0}^{\infty}\prod_{m=1}^{N}(-1)^N\left(V\cdot W(Q_m)\frac{1}{p_m^-}\right)\mathcal{C}_\varphi(P_m,K)\varphi(P_m) \tag{D.2}$$

where $P_m \equiv P - \sum_{j=1}^{m} q_j$.
If we now integrate out the external soft gauge bosons, then we get delta functions $\delta(k_l + k_M)$ with $l, M \leq N$ from the propagators. There are two distinct contributions that we have to discriminate:

- We only have terms such that $M = l+1$.
- There are delta functions for which $M > l+1$.

Without loss of generality we have assumed $M > l$; otherwise we only have to relabel indices. The first case means that only neighbouring soft gauge boson fields are contracted. This is precisely the disconnected piece $\langle WW\rangle\left\langle \hat{J}_\varphi\right\rangle$ that we have kept in section 3.3.4. The second case corresponds to the connected piece and we want to show that it vanishes at leading order. For simplicity, let us pick $l = 1$ and look only at the thermal sum over q_1^0; for other choices of l the following argument remains unchanged. In this case, a thermal sum of the form

$$\left(T\sum_{q_1^0}\frac{V^\mu V^\nu \Delta_{\mu\nu}(Q_1)}{p_1^-}\frac{1}{p_2^-}\cdots\frac{1}{p_{M-1}^-}\right)\frac{1}{(P-Q_2-\ldots Q_{M-1})^-}\cdot\ldots \tag{D.3}$$

needs to be computed, with $M-1$ denominators depending on q_1^0. Performing the thermal sum is relatively easy if one uses the spectral representation (2.11) for the gauge boson propagator and then applies (2.17). We obtain contributions from each of the M poles, but only the one at $q_1^0 = \omega \sim gT$ needs to be kept since the Bose function then gives a $1/g$ enhancement, $f_B(\omega) \approx T/\omega \sim 1/g$, whereas at all other poles (coming from the denominators p_m^-) there is no such enhancement and their contributions are therefore suppressed by one power of the small coupling. When the thermal sum is performed, we may also analytically continue p^0 to the real axis and write $p^- = \mathrm{Re}(p^-) + i\varepsilon$. The expression (D.3) has then finally become

$$\left(\int\frac{\mathrm{d}\omega}{2\pi i}\,\mathrm{Disc}\,\Delta_{\mu\nu}(\omega,\vec{k}')\frac{T}{\omega}\frac{1}{p_1^- + i\varepsilon}\frac{1}{p_2^- + i\varepsilon}\cdots\frac{1}{p_{M-1}^- + i\varepsilon}\right)\frac{1}{(P-Q_2-\ldots Q_{M-1})^-}\cdots \tag{D.4}$$

All poles in the integrand lie above the real axis.[1] Now we close the integration contour with a half-circle at $\omega \to -i\cdot\infty$. If $M > 2$, which means that the denominator is at least quadratic in ω, we immediately see

[1] There is no pole at $\omega = 0$ since $\mathrm{Disc}(\omega,\vec{k}) = 0$ for $\omega = 0$.

that the result is zero. The half-circle gives no contribution because the integrand falls off rapidly enough at infinity. The additional dependence of Disc $\Delta_{\mu\nu}$ on the integration variable does not spoil the argument, since at leading order we may replace ω by $q_{1,\parallel}$ in the argument of Disc $\Delta_{\mu\nu}$, their difference being only of the order of g^2T.[2] If, however, we have $M = 2$, then there is only one power in the denominator and the integrand does not fall rapidly enough at infinity, so the argument fails. In fact, we will show in the next section through an explicit computation that for this disconnected part we obtain a nonvanishing result.
The only thing that remains to be done is to establish a connection to the diagrammatic picture from section 2.3.4 and thus understand why only ladder diagrams (and self-energy insertions) are generated and nothing of the form shown in figure 2.8. To understand that, it is useful to iterate the integral equation (D.1) using (3.67) repeatedly. Since we have proved that only the disconnected part contributes, this will result in an integral term of the form

$$\int_{q_1,q_2,\ldots} \langle WW\rangle_1 \langle WW\rangle_2 \langle WW\rangle_3 \ldots \left\langle \hat{J}_\varphi \right\rangle$$

with the gauge fields depending on different momenta (due to the delta function in the resulting gauge boson propagator (3.68), every correlator depends only on one independent momentum). In every step, a new pair of gauge fields appears which are contracted among each other. Since the current has to obey the integral equation (D.1) and the number of possible iterations is unlimited, it is intuitively clear that $\left\langle \hat{J}_\varphi \right\rangle$ cannot contain crossed ladder rungs or vertex corrections because this would mean it contains contractions of non-adjacent gauge fields. For illustration, a possible iteration sequence is shown in figure D.1.
In conclusion, we have proved that at leading order, only the disconnected part in (3.67) contributes and that this generates precisely those diagrams that are needed for the computation of the LPM effect. We now turn to its computation.

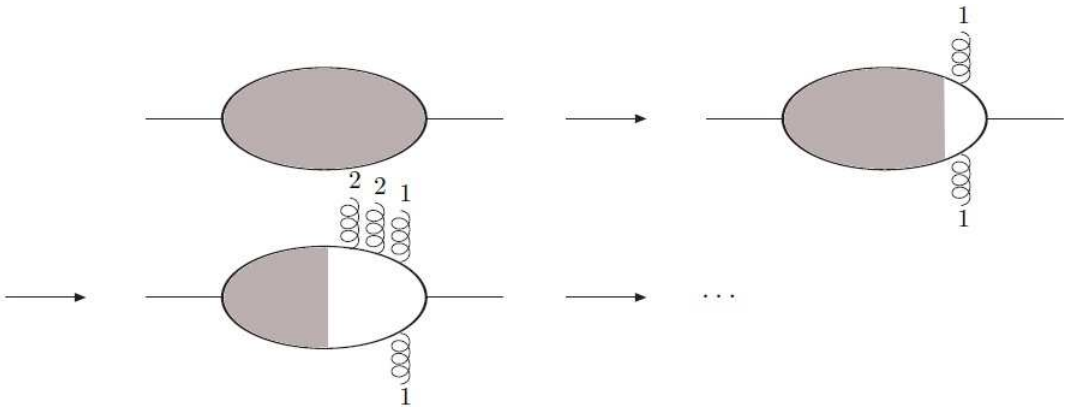

Figure D.1.: Example for an iteration sequence of the integral term in equation (D.1). The shaded area represents the current which still contains an infinite sum of diagrams. Adjacent gauge fields that are contracted with each other are labelled by a common number.

D.2. Towards an easier integral equation

Here we present the computation that leads from the rather complicated integral expression found in (3.70) to the easier one in (3.71). What we need to prove is that

$$\int_Q \frac{V^\mu V^\nu \Delta_{\mu\nu}(Q)}{p_- - q_-} = \frac{i}{2} T \int \frac{\mathrm{d}^2 q_\perp}{(2\pi)^2} \mathcal{K}(\vec{q}_\perp) \tag{D.5}$$

with the kernel

$$\mathcal{K}(q_\perp) = \frac{1}{\vec{q}_\perp^2} - \frac{1}{\vec{q}_\perp^2 + m_D^2}. \tag{D.6}$$

The proof proceeds in three steps.

[2] We already mention that in the following section we will encounter a delta function which forces us to do the same replacement, up to higher order corrections that are negligible.

Step 1: Computation of the thermal sum

As in the previous section, we use the spectral representation of the HTL propagator,

$$\Delta_{\mu\nu}(Q) = \int \frac{\mathrm{d}\omega}{2\pi i} \frac{1}{\omega - q_0} \operatorname{Disc} \Delta_{\mu\nu}(\omega, \vec{q}), \tag{D.7}$$

and then need to perform the following thermal sum:

$$\mathcal{T} \equiv T \sum_{q_0} \int \frac{\mathrm{d}\omega}{2\pi i} \operatorname{Disc} \Delta_{\mu\nu}(\omega, \vec{q}) \frac{1}{q_0 - \omega} \frac{1}{q_0 - q_\parallel - p_-} \tag{D.8}$$

It can be evaluated, like before, via complex contour integration using (2.17). The poles are at $q_0 = \omega$ and at $q_0 = q_\parallel + p_-$. As explained before, we may approximate $f_B(\omega) \approx T/\omega \gg 1$ and the other pole then gives a $\mathcal{O}(1)$ contribution and is negligible. Writing q_0 instead of ω for the integration variable, we get

$$\mathcal{T} = \int \frac{\mathrm{d}q_0}{2\pi i} \operatorname{Disc} \Delta_{\mu\nu}(Q) \frac{1}{q_0 - q_\parallel - p_-} \frac{T}{q_0}. \tag{D.9}$$

The expression has become easier since we now only need the *discontinuity* of the gauge boson propagator. We will deal with it in the next step. In addition, we need the discontinuity of $\Pi(p^0 + i\varepsilon)$ for the production rate. Then we set $p_- = \mathrm{Re}(p_-) \pm i\varepsilon$ and use (2.13) to get

$$\frac{1}{q_0 - q_\parallel - p_- - i\varepsilon} = \mathfrak{P}\left(\frac{1}{q_0 - q_\parallel - p_-}\right) + i\pi\delta(q_0 - q_\parallel).$$

The real part does not contribute to the q_0-integral[3], therefore we are allowed to replace the denominator under the integral by the delta function and we get

$$\int_Q \frac{V^\mu V^\nu \Delta_{\mu\nu}(Q)}{p_- - q_-} = \frac{1}{4\pi} \int \mathrm{d}q_0 \int \mathrm{d}q_\parallel \frac{T}{q_0} \delta(q_0 - q_\parallel) \int \frac{\mathrm{d}^2 q_\perp}{(2\pi)^2} V^\mu V^\nu \operatorname{Disc} \Delta_{\mu\nu}(Q) \tag{D.10}$$

where we have written q_0 again instead of ω.

Step 2: Computing the discontinuity of the gauge boson propagator

Here we profit from the results that were collected in section 2.2. Using the decomposition (2.28), we get

$$V^\mu V^\nu \operatorname{Disc} \Delta_{\mu\nu}(Q) = \left(1 - \frac{q_0^2}{q^2}\right) (\operatorname{Disc} \Delta_L(Q) - \operatorname{Disc} \Delta_T(Q)). \tag{D.11}$$

This is because

$$V^\mu V^\nu P^T_{\mu\nu} = 1 - \frac{(\hat{v} \cdot \vec{q})^2}{q^2} = 1 - \frac{q_\parallel^2}{q^2} = 1 - \frac{q_0^2}{q^2} \tag{D.12}$$

where the last equality is due to the delta function in (D.10), and

$$V^\mu V^\nu P^L_{\mu\nu} = \frac{(V_\mu Q^\mu)^2}{Q^2} - V^2 - \left(1 - \frac{q_0^2}{q^2}\right) = -\left(1 - \frac{q_0^2}{q^2}\right) \tag{D.13}$$

since the first term vanishes again due to the delta function and the second one according to the definition of V^μ. Finally, the last term in (2.28) gives no contribution due to the delta function in (D.10).
Since

$$\Delta_{L,T}(Q) = \frac{-1}{Q^2 - \Pi_{L,T}(Q)}, \tag{D.14}$$

we have

$$\operatorname{Disc} \Delta_{L,T}(Q) = 2i \operatorname{Im} \Delta_{L,T}(Q) = -2i |\Delta_{L,T}(Q)|^2 \operatorname{Im} \Pi_{L,T}(Q). \tag{D.15}$$

[3]Note that we may also here replace q^0 by $q_\parallel$ in the propagators even if there is no explicit delta function because we are only interested in those momenta Q for which the difference $q^0 - q_\parallel \sim g^2 T$ is negligible. For the same reason, we can neglect p_- inside the delta function-at leading order, it is irrelevant if we set $q^0 = q_\parallel$ or $q^0 = q_\parallel + p_-$ because $p_- \sim g^2 T \ll q_\parallel \sim gT$.

D. Remarks on the integral equation for the current

The HTL self-energies to 1-loop order are well-known and we have shown the results already in (2.29). We could use the explicit results to compute the integral kernel, which would result (after some algebraic rearrangements) in the integral equations as they were written down e.g. in [6, 47]. There is, however, an easier form of the integral kernel found later [74, 75], where only integrals only over the perpendicular components remain, but those over the longitudinal and the zero-component can be evaluated explicitly. We will use that approach and therefore note as new intermediate step the following:

$$\int_Q \frac{V^\mu V^\nu \Delta_{\mu\nu}(Q)}{p_- - q_-} = -\frac{i}{2\pi} T \int \frac{\mathrm{d}q_0}{q_0} \int \mathrm{d}q_\parallel \delta(q_0 - q_\parallel) \int \frac{\mathrm{d}^2 q_\perp}{(2\pi)^2} \left(1 - \frac{q_0^2}{q^2}\right) \\ \left(|\Delta_L(Q)|^2 \operatorname{Im}\Pi_L(q_0 + i\varepsilon, \vec{q}) - |\Delta_T(Q)|^2 \operatorname{Im}\Pi_T(q_0 + i\varepsilon, \vec{q})\right) \tag{D.16}$$

Step 3: Performing the integrals over q_0 and $q_\parallel$

It remains to do two of the remaining integrals analytically. The integral over $q_\parallel$ is of course trivial due to the delta function. The procedure to find an analytic result for the integral over q_0 was already presented in [75] and shall only be sketched here. We first introduce the integration variable $x \equiv q_0/|\vec{q}|$ and use the Jacobian

$$\left(1 - \frac{q_0^2}{q_0^2 + q_\perp^2}\right) \frac{\mathrm{d}q_0}{q_0} = \frac{\mathrm{d}x}{x}.$$

for which it is important to remember that after integrating over $q_\parallel$, the delta function enforces $q_0 = q_\parallel$.[4] Once this is done, we can write

$$\int_Q \frac{V^\mu V^\nu \Delta_{\mu\nu}(Q)}{p_- - q_-} = -\frac{i}{2\pi} T \int \frac{\mathrm{d}^2 q_\perp}{(2\pi)^2} \int_{-1}^{1} \frac{\mathrm{d}x}{x} \left(\frac{\operatorname{Im}\Pi_L(x, \vec{q})}{(q_\perp^2 + \operatorname{Re}\Pi_L(x, \vec{q}))^2 + (\operatorname{Im}\Pi_L(x, \vec{q}))^2} \right. \\ \left. - \frac{\operatorname{Im}\Pi_T(x, \vec{q})}{(q_\perp^2 + \operatorname{Re}\Pi_T(x, \vec{q}))^2 + (\operatorname{Im}\Pi_T(x, \vec{q}))^2} \right) \tag{D.17}$$

The limits are such because for $|x| > 1$ the imaginary part of the HTL self-energies (2.29) vanishes. The integral can be evaluated with the sum rule

$$\frac{2}{\pi} \int_0^1 \frac{\mathrm{d}x}{x} \frac{\operatorname{Im}\Pi(x)}{(z + \operatorname{Re}\Pi(x))^2 + (\operatorname{Im}\Pi(x)^2)} = \frac{1}{z + \operatorname{Re}\Pi(\infty)} - \frac{1}{z + \operatorname{Re}\Pi(0)} \tag{D.18}$$

that was proved in [74]. The integral from -1 to 0 gives exactly the same as from 0 to 1 which introduces an overall factor of 2. We can then directly apply this to our expression and only need the results (2.29) for the HTL self-energies in order to read off that

$$\operatorname{Re}\Pi_L(x = 0, \vec{q}) = m_D^2, \quad \operatorname{Re}\Pi_T(x = 0, \vec{q}) = 0 \\ \frac{1}{q_\perp^2 + \operatorname{Re}\Pi_L(x \to \infty, \vec{q})} - \frac{1}{q_\perp^2 + \operatorname{Re}\Pi_T(x \to \infty, \vec{q})} = 0 \tag{D.19}$$

where the *Debye mass* m_D is given by (2.30). Putting the results together, we have proved (D.5).

[4] Note that the current in fact depends only on $\vec{q}_\perp$ and not on $q_\parallel$, which can be neglected w.r.t $k_\parallel$.

E. Solving the equation for the LPM effect numerically

One and one is two,
And the one for me is you
SARAH CONNOR - *1 + 1 = 2*

E.1. Formulation in Fourier space

Although it would be possible to solve the integral equations (4.23) and (4.24) directly by adopting the approach used in [7], it is easier to go to *Fourier space* and then solve a *differential equation* instead of an integral equation. This approach was pursued in [74, 75] and we can largely follow it.[1] In fact, it is even possible to write the equation (4.24) in a way which makes its analogy to the equation for production of transversely polarized photons explicit. In order to do that, we introduce the auxilliary vector

$$\vec{u} = \begin{pmatrix} 1 \\ i \end{pmatrix} \tag{E.1}$$

which allows us to write $k_x + ik_y = \vec{u} \cdot \vec{k}_\perp$. We can then introduce also a vector quantity $\vec{f}(\vec{k}_\perp)$ by $\vec{u} \cdot \vec{f} \equiv \chi$. The equation (4.24) has now taken the form

$$2\vec{k}_\perp = i\epsilon(\vec{k}_\perp)\vec{f}(\vec{k}_\perp) + \sum_{a=0}^{3} g_a^2 C_2(r_a) T \int \frac{\mathrm{d}^2 q_\perp}{(2\pi)^2} \mathcal{K}_a(\vec{q}_\perp) \left[\vec{f}(\vec{k}_\perp) - \vec{f}(\vec{k}_\perp - \vec{q}_\perp)\right]. \tag{E.2}$$

This is identical in form to the equation that one has to solve for the production rate of transverse photons in a quark-gluon plasma [74, 75]. If $\vec{f}$ is a solution of this equation, then obviously $\vec{u} \cdot \vec{f}$ solves the original equation for the component χ.
Following [74, 75], we now make a Fourier transformation [2]

$$\psi(\vec{k}_\perp) \equiv \int \mathrm{d}^2 b e^{-i\vec{k}_\perp \cdot \vec{b}} \psi(\vec{b}), \tag{E.3}$$

and the same for $\vec{f}(\vec{k}_\perp)$. This will allow us to get rid of the integral over $\mathrm{d}^2 k_\perp$ in (4.25) because $\vec{k}_\perp$ only appears in an exponential and the integral then gives a delta function. The factors k_x and k_y can be removed by replacing $k_i \to i\frac{\mathrm{d}}{\mathrm{d}b_i}$ and integrating by parts. We obtain

$$\int \frac{\mathrm{d}^2 k_\perp}{(2\pi)^2} \operatorname{Re} \psi(\vec{k}_\perp) = \operatorname{Re} \int \mathrm{d}^2 b \delta(\vec{b}) \psi(b) = \lim_{b \to 0} \operatorname{Re} \psi(b)$$

and

$$\begin{aligned}
\int \frac{\mathrm{d}^2 k_\perp}{(2\pi)^2} \operatorname{Re}[(k_x - ik_y)\chi(\vec{k}_\perp)] &= \int \frac{\mathrm{d}^2 k_\perp}{(2\pi)^2} [k_x \operatorname{Re} \chi(\vec{k}_\perp) + k_y \operatorname{Im} \chi(\vec{k}_\perp)] \\
&= -\int \frac{\mathrm{d}^2 k_\perp}{(2\pi)^2} \left[\operatorname{Re} \int \mathrm{d}^2 b e^{-i\vec{k}_\perp \cdot \vec{b}} i \frac{\mathrm{d}\chi(\vec{b})}{\mathrm{d}b_x} + \operatorname{Im} \int \mathrm{d}^2 b e^{-i\vec{k}_\perp \cdot \vec{b}} i \frac{\mathrm{d}\chi(\vec{b})}{\mathrm{d}b_y}\right] \\
&= -\lim_{\vec{b} \to 0} \left[\operatorname{Re}\left(i \frac{\mathrm{d}\chi(\vec{b})}{\mathrm{d}b_x}\right) + \operatorname{Im}\left(i \frac{\mathrm{d}\chi(\vec{b})}{\mathrm{d}b_y}\right)\right] \\
&= \lim_{\vec{b} \to 0} \left[\operatorname{Im} \frac{\mathrm{d}\chi(\vec{b})}{\mathrm{d}b_x} - \operatorname{Re} \frac{\mathrm{d}\chi(\vec{b})}{\mathrm{d}b_y}\right].
\end{aligned}$$

[1] The numerical procedure that we use, however, is different from that proposed in [74, 75]. The method proposed in section E.2 is conceptually a bit clearer and was found to be more reliable.
[2] We use the same symbol to denote the functions ψ, χ and their Fourier transformations.

E. Solving the equation for the LPM effect numerically

For $\psi(b)$ we already used that due to rotational invariance in the transverse plane it can only depend on $b \equiv |\vec{b}|$. A similar simplification can be done for $\chi(\vec{b})$. In fact, we want to relate it to the solutions for $\vec{f}(\vec{b})$ which is the Fourier transformation of the vector quantity that appears in (E.2). Again due to rotational invariance, it must be proportional to $\vec{b}$ and we can introduce a scalar function $h(b)$ by writing

$$\vec{f}(\vec{b}) \equiv h(b)\vec{b},$$

which means that $\chi(b) = \vec{u} \cdot \vec{f} = (b_x + ib_y)h(b)$. Using this form, we can simplify the expression obtained above even further and write it in terms of $h(b)$:

$$\begin{aligned}\int \frac{\mathrm{d}^2 k_\perp}{(2\pi)^2} \operatorname{Re}[(k_x - ik_y)\chi(\vec{k}_\perp)] &= \lim_{\vec{b}\to 0}\left[2\operatorname{Im} h(b) + b_x\left(\frac{\mathrm{d}\operatorname{Im} h(b)}{\mathrm{d}b_x} - \frac{\mathrm{d}\operatorname{Re} h(b)}{\mathrm{d}b_y}\right) + b_y\left(\frac{\mathrm{d}\operatorname{Re} h(b)}{\mathrm{d}b_x} + \frac{\mathrm{d}\operatorname{Im} h(b)}{\mathrm{d}b_y}\right)\right] \\ &= 2\lim_{b\to 0} h(b)\end{aligned}$$

The drastic simplification in the last line can easily be explained. First of all, the terms involving the derivatives of the real part cancel each other because $h = h(b) = h(\sqrt{b_x^2 + b_y^2})$. Furthermore, if the limit $b \to 0$ is supposed to exist at all, then terms involving the derivatives of the imaginary part have to vanish for $\vec{b} \to 0$. That this limit is indeed finite (and in addition nonzero) has to be assumed because otherwise the production rate would be infinite (or zero, respectively). So even without any knowledge on the explicit solution we can already say that only the first term in the brackets survives in the limit $\vec{b} \to 0$. In fact, we will see below that the solutions of the differential equation for $h(b)$ automatically satisfy the property $\lim_{b\to 0} \operatorname{Im} h(b) = C$ with a nonzero constant C. The real part will turn out to be divergent for $b \to 0$, but it is never needed and its singular behaviour for small b is thus irrelevant.
We have now managed to express (4.25) in the much easier form[3]

$$\frac{\mathrm{d}\Gamma_N}{\mathrm{d}^3 p} = -\frac{2N_f|\lambda|^2}{(2\pi)^4 p_0} f_F(p_0) \int_0^\infty \mathrm{d}k_\parallel \frac{f_B(k_\parallel) + f_F(k_\parallel - p_\parallel)}{k_\parallel} \lim_{b\to 0}\left[p_- \operatorname{Re}\psi(b; k_\parallel, p_\parallel) + \frac{p_+}{4(k_\parallel - p_\parallel)^2} \operatorname{Im} h(b; k_\parallel, p_\parallel)\right]. \tag{E.4}$$

The functions ψ and h of course still parametrically depend on the large momentum components $k_\parallel, p_\parallel$ as we have indicated explicitly. The remaining task is to formulate equations for the two unknown functions. They obey second-order differential equations which are of the same form as those written down in [75] for the production of longitudinal and transverse photons in a QGP. In order to find the desired differential equations, we have to write

$$\epsilon(\vec{k}_\perp) \equiv \alpha(k_\parallel, p_\parallel) + \beta(k_\parallel, p_\parallel)k_\perp^2 \to -\beta(k_\parallel, p_\parallel)(\Delta_{\vec{b}} - M_{eff}^2), \quad M_{eff}^2 \equiv \frac{\alpha(k_\parallel, p_\parallel)}{\beta(k_\parallel, p_\parallel)} \tag{E.5}$$

where $\Delta_{\vec{b}}$ is the Laplace operator in Fourier space and we introduced an *effective mass* M_{eff}.[4] The functions α and β can be read off the definition (3.52):

$$\alpha(k_\parallel, p_\parallel) = \frac{M_N^2}{2p_\parallel} + \frac{m_\ell^2}{2(k_\parallel - p_\parallel)} - \frac{m_\phi^2}{2k_\parallel}, \quad \beta(k_\parallel, p_\parallel) = \frac{p_\parallel}{2k_\parallel(k_\parallel - p_\parallel)} \tag{E.6}$$

We have expanded p_- in α to leading order here.
The differential equations for ψ and $\vec{f}$ are now easily found from (4.23) and (E.2) by going to Fourier space:

$$-i\beta(k_\parallel, p_\parallel)(\Delta_{\vec{b}} - M_{eff}^2)\vec{f}(\vec{b}) + \sum_{a=0}^{3} g_a^2 C_2(r_a) T D(m_{D,a} b)\vec{f}(\vec{b}) = -i\vec{\nabla}_{\vec{b}}\delta(\vec{b}) \tag{E.7}$$

$$-i\beta(k_\parallel, p_\parallel)(\Delta_{\vec{b}} - M_{eff}^2)\psi(\vec{b}) + \sum_{a=0}^{3} g_a^2 C_2(r_a) T D(m_{D,a} b)\psi(b) = \delta(\vec{b}) \tag{E.8}$$

[3] Note that the restriction on the integration range that we found in (4.17) does not apply here. The processes which involve multiple scattering off gauge bosons are not restricted to happen only if the masses of the particles are such that the corresponding tree-level process is kinematically allowed. They can always occur and thus open up a new kinematical regime for the decay and recombination processes.

[4] Note that since α and β can have different signs, this mass can also become complex. It should not be thought of as a 'physical mass' but rather as a helpful auxiliary quantity that we introduced only to be in accord with the notation from [75].

In order to obtain the rhs, we have used that the Fourier transformation of a constant gives a delta function. The function $D(x)$ which is the Fourier transformation of the kernel is given by [74, 75]

$$D(x) = \frac{1}{2\pi}\left[\gamma_E + \ln\frac{x}{2} + K_0(x)\right] \tag{E.9}$$

where $\gamma_E \approx 0.577\ldots$ is the Euler-Mascheroni constant and $K_0(x)$ a Bessel function of the second kind.
These two equations are second-order differential equations with a two-dimensional manifold of solutions, out of which we have to pick the one we need. In order to find it, we have to impose two conditions. One of those conditions is easy to find: The Fourier integrals can only be convergent if

$$\lim_{\vec{b}\to\infty} \vec{f}(\vec{b}) = 0, \quad \lim_{b\to\infty} \psi(b) = 0. \tag{E.10}$$

The second condition is less obvious and is related to the behaviour of the solutions at small $\vec{b}$. Physically, only solutions which give a finite and nonzero production rate make sense, which means that $\mathrm{Re}\,\psi(b)$ and $\mathrm{Im}\,\vec{f}(\vec{b})$ should be finite and nonzero for $\vec{b}\to 0$. Unfortunately, this turns out not to be restrictive at all since *all* solutions of (E.7) and (E.8) which vanish at infinity respect this constraint. Imposing the finiteness of either the real or imaginary part for $\vec{b}\to 0$ is not an efficient way to solve the problem. Still, it is possible to find a unique solution of the given problem using both analytical input and numerical computations. This is described in the following section and plots of the numerical results can be found in the main text, in section 4.6.
In summary, we have described how to trade a complicated way to compute a number (a two-dimensional integral over a function that is the solution of an integral equation) by a much easier way to compute a number (the value of a function which solves a differential equation in the limit where its argument goes to zero). In section E.2 we will explain how to get that number.

E.2. Solution of the problem

We now describe how to solve (E.7) and (E.8). For arbitrary b it is not possible to give analytic solutions. As one can easily check, the function $D(x)$ behaves like $x^2\ln x$ for $x \ll 1$, which means that in the small b limit, this function is irrelevant. In the limit $\vec{b}\to 0$, also M_{eff} becomes negligible and we only have to solve the approximate equations

$$\beta(k_\parallel, p_\parallel)\Delta_{\vec{b}}\vec{f}(\vec{b}) = \vec{\nabla}_{\vec{b}}\delta(\vec{b}) \tag{E.11}$$

$$-i\beta(k_\parallel, p_\parallel)\Delta_{\vec{b}}\psi(\vec{b}) = \delta(\vec{b}). \tag{E.12}$$

Both solutions can easily be found from the following theorem:

Let $\vec{b}\in\mathbb{R}^2$ and $\Phi(\vec{b})$ be a weak solution of

$$\Delta_{\vec{b}}\Phi(\vec{b}) = \delta(\vec{b}) \text{ in } \mathbb{R}^2. \tag{E.13}$$

Then $\Phi(\vec{b})$ is (up to an additive constant) uniquely given by

$$\Phi(\vec{b}) = \frac{1}{2\pi}\ln|\vec{b}|. \tag{E.14}$$

The proof is relatively simple and can be found e.g. in [76]. It gives us immediately the small b solution for $\psi(b)$, while the small b solution for $\vec{f}(\vec{b})$ follows by taking a gradient w.r.t $\vec{b}$. This means that

$$\vec{f}(\vec{b}) = \frac{1}{2\pi\beta(k_\parallel, p_\parallel)}\frac{\vec{b}}{b^2} + \mathcal{O}(\vec{b}) \tag{E.15}$$

$$\psi(b) = \frac{i}{2\pi\beta(k_\parallel, p_\parallel)}\ln b + \mathcal{O}(b^0). \tag{E.16}$$

We now see explicitly that both the real part of ψ and the imaginary part of $\vec{f}$ are automatically finite. Their values are not determined yet, however. This is because we still have to use the boundary conditions (E.10).

E. Solving the equation for the LPM effect numerically

Since they are formulated at large b where the function $D(m_{D,a}b)$ cannot be neglected [5], we have to resort to a numerical procedure. For $b > 0$, the delta functions can be dropped and we deal with homogeneous equations. By exploiting the symmetry properties of $\vec{f}$ and ψ, we can even write *ordinary* differential equations by using

$$\Delta_{\vec{b}}\psi(b) = \psi''(b) + \frac{1}{b}\psi'(b) \tag{E.17}$$

and

$$\Delta_{\vec{b}}\vec{f}(\vec{b}) = \left(h''(b) + \frac{3}{b}h'(b)\right)\vec{b}. \tag{E.18}$$

Then we have to solve the two equations

$$-i\beta(k_\parallel, p_\parallel)\left(\psi''(b) + \frac{1}{b}\psi'(b) - M_{eff}^2\psi(b)\right) + \sum_{a=0}^{3} g_a^2 C_2(r_a) T D(m_{D,a}b)\psi(b) = 0 \tag{E.19}$$

$$-i\beta(k_\parallel, p_\parallel)\left(h''(b) + \frac{3}{b}h'(b) - M_{eff}^2 h(b)\right) + \sum_{a=0}^{3} g_a^2 C_2(r_a) T D(m_{D,a}b)h(b) = 0. \tag{E.20}$$

For a numerical treatment, it is convenient to deal with dimensionless quantities. In order to do so, we rescale all momenta and masses by introducing (cf. (4.98))

$$\tilde{k} \equiv \frac{k_\parallel}{T}, \quad \tilde{p} \equiv \frac{k_\parallel}{T}, \quad z_i \equiv \frac{z_i}{T}.$$

We also introduce a dimensionless variable

$$t \equiv Tb.$$

The equations can now be written as

$$-i\tilde{\beta}(\tilde{k}, \tilde{p})\left(\psi''(t) + \frac{1}{t}\psi'(t) - \tilde{M}_{eff}^2\psi(t)\right) + \sum_{a=0}^{3} g_a^2 C_2(r_a) D(z_{D,a}t)\psi(t) = 0 \tag{E.21}$$

$$-i\tilde{\beta}(\tilde{k}, \tilde{p})\left(h''(t) + \frac{3}{t}h'(t) - \tilde{M}_{eff}^2 h(t)\right) + \sum_{a=0}^{3} g_a^2 C_2(r_a) D(z_{D,a}t)h(t) = 0. \tag{E.22}$$

The functions $\tilde{\alpha}$ and $\tilde{\beta}$ are given by

$$\tilde{\alpha}(\tilde{k}, \tilde{p}) = \frac{z^2}{2\tilde{p}} + \frac{z_\ell^2}{2(\tilde{k} - \tilde{p})} - \frac{z_\phi^2}{2\tilde{k}}, \quad \tilde{\beta}(\tilde{k}, \tilde{p}) = \frac{\tilde{p}}{2\tilde{k}(\tilde{k} - \tilde{p})} \tag{E.23}$$

with $z = M_N/T$.
This can now be solved numerically with the boundary condition that the solution vanishes at $t \to \infty$. The procedure is the same for both equations and will be described explicitly for $\psi(t)$. The necessary changes for the solution of $h(t)$ will be described at the very end.
The solution of (E.21) can be written as

$$\psi(t) = c_1\psi_1(t) + c_2\psi_2(t). \tag{E.24}$$

The fundamental solutions $\psi_i(t)$ are of course not known analytically for arbitrary t. However, at *small* t we can neglect the function D and the solution can be given analytically in terms of Bessel functions:

$$\psi(t) = c_1 Y_0(-i\tilde{M}_{eff}t) + c_2 J_0(i\tilde{M}_{eff}t) \tag{E.25}$$

Since for small arguments, the function J_0 goes to a constant while the function Y_0 diverges logarithmically, this is consistent with the limiting behaviour (E.16) which we of course have to reproduce. This means on the one hand that by going from our original equation which was a *partial* differential equation with

[5] Note that due to the boundary condition which is formulated at large b where the Fourier transform of the kernel is important, it plays a role for our solution although we are interested in the limit $b \to 0$ where the kernel is irrelevant.

weak solutions to a homogeneous *ordinary* differential equation with continuous solutions we have neither introduced spurious solutions nor lost any solutions of our original problem. On the other hand, it also allows us to fix already one of the two constants: By comparing (E.25) and (E.16) we can immediately deduce that

$$c_1 = \frac{i}{2\pi\tilde{\beta}(\tilde{k},\tilde{p})}. \tag{E.26}$$

The other constant is still unknown and has to be found from the boundary condition at infinity. For generic values of c_2, the solution will contain growing parts which violate (E.10). We want to find the value of c_2 which makes the growing part of the solution disappear. Due to (E.25), we know the fundamental solutions ψ_i explicitly for small t and we can use this information to find the constant c_2 numerically. The procedure is as follows:

1. Pick a small value t_0, e.g. $t_0 = 10^{-5}$ and solve equation (E.21) twice, both times using one of the fundamental solutions from (E.25) as initial condition. This means, we set

   $$\psi(t_0) = Y_0(-i\tilde{M}_{eff}t_0), \psi'(t_0) = \frac{\mathrm{d}}{\mathrm{d}t}Y_0(-i\tilde{M}_{eff}t_0)\bigg|_{t=t_0}$$

   and solve (E.21). Then we do the same again and only replace the function Y_0 by J_0. The two solutions correspond to the fundamental solutions $\psi_i(t)$ to very good accuracy if t_0 is chosen small enough such that $D(z_{D,a}t_0) \sim t_0^2 \ln t_0$ is strongly suppressed.

2. Once we have those two solutions, we can evaluate them at a large value $t_* \sim \mathcal{O}(10^2 - 10^3)$. The boundary condition $\psi(t_*) = 0$ will give us a relation between c_1 and c_2:

   $$c_1\psi_1(t_*) + c_2\psi_2(t_*) = 0$$

3. With the relation between c_1 and c_2 which is obtained numerically and the result (E.28) for c_1 which was gained from the analytical solution, one can fix c_2 and then take its real part which is needed for (E.4).

The same also works for $h(t)$, only the explicit solution for small t looks a bit different and is given by

$$h(t) = c_1\frac{\tilde{M}_{eff}Y_1(-i\tilde{M}_{eff}t)}{t} + c_2\frac{J_1(i\tilde{M}_{eff}t)}{\tilde{M}_{eff}t}. \tag{E.27}$$

Comparing with (E.15) reveals that the constant c_1 is in this case given by

$$c_1 = \frac{1}{2\pi\tilde{\beta}(\tilde{k},\tilde{p})}. \tag{E.28}$$

The remaining constant c_2 is then determined by the numerical procedure that is explained above.

F. Proof of relations for the production rate of Majorana neutrinos

Here we prove various equations used in section 4.4.

Proof of (4.31)

First, we use general properties of the invariant phase space element to obtain

$$\frac{\mathrm{d}^3 p_1}{2E_1} = \mathrm{d}^4 P_1 \delta(P_1^2)\Theta(E_1) = \frac{\delta(E_1 - |\vec{p}_1|)}{2|\vec{p}_1|}\Theta(E_1)\mathrm{d}^3 p_1 \mathrm{d}E_1.$$

Now we include the delta function and perform the integrals, which results in $E_1 = E + E_3 - E_2$ and $\vec{p}_1 = \vec{p} + \vec{p}_3 - \vec{p}_2 = \vec{q} - \vec{p}_2$ due to the definition (4.28). This leads to

$$\begin{aligned}\frac{\mathrm{d}^3 p_1}{2E_1}\delta(P_1 + P_2 - P_3 - P) =& \frac{\Theta(E + E_3 - E_2)}{2|\vec{q} - \vec{p}_2|}\delta(E + E_3 - E_2 - |\vec{q} - \vec{p}_2|) \\ &= \delta\left((E + E_3 - E_2)^2 - |\vec{q} - \vec{p}_2|^2\right)\Theta(E + E_3 - E_2).\end{aligned}$$

Using (4.29), the argument of the delta function becomes

$$(E + E_3 - E_2)^2 - |\vec{q} - \vec{p}_2|^2 = (E + E_3 - E_2)^2 - E_2^2 - q^2 + 2qE_2\cos\chi.$$

With the help of $\delta(ax) = \frac{1}{|a|}\delta(x)$ we then arrive at (4.31).

Proof of (4.33)

The proof of (4.33) proceeds more or less the same way. Only at the beginning, we need to insert a dummy integration over $\vec{q}$ to get that variable into the game and then integrate over $\mathrm{d}^3 p_3$:

$$\begin{aligned}\frac{\mathrm{d}^3 p_3}{2E_3} = \delta(P_3^2)\Theta(E_3)\mathrm{d}E_3\mathrm{d}^3 p_3 =& \int \mathrm{d}^3 q \delta(\vec{q} - \vec{p} - \vec{p}_3)\delta(P_3^2)\Theta(E_3)\mathrm{d}E_3\mathrm{d}^3 p_3. \\ &= \delta(E_3^2 - |\vec{q} - \vec{p}|^2)\Theta(E_3)\mathrm{d}E_3 q^2 \mathrm{d}q\mathrm{d}\Omega_q.\end{aligned}$$

Now we use (4.29) and arrive at the expression given in (4.33) the same way as we did for (4.31).

Proof of (4.35)

In order to prove (4.35), we need to investigate what restrictions the two delta functions introduce. By demanding that $|\cos\vartheta| \leq 1$, we get two conditions:

$$\begin{aligned}\cos\vartheta \leq 1 \Leftrightarrow & E^2 - E_3^2 + q^2 \leq 2qE \Leftrightarrow |E - q| \leq E_3 \Leftrightarrow E - E_3 \leq q \leq E + E_3 \\ \cos\vartheta \geq -1 \Leftrightarrow & E^2 - E_3^2 + q^2 \geq -2qE \Leftrightarrow E + q \geq E_3 \Leftrightarrow q \geq E_3 - E\end{aligned}$$

It is important to remember that E, q are positive, therefore the absolute value is needed only for the difference. Both conditions together can be summarized by the product $\Theta(q - |E - E_3|)\Theta(E + E_3 - q)$. Now we repeat the same procedure demanding that $|\cos\chi| \leq 1|$. Here we give only the final results for the conditions:

$$\begin{aligned}\cos\chi \leq 1 &\Leftrightarrow 2E_2 - E_3 - E \leq q \leq E + E_3 \\ \cos\chi \geq -1 &\Leftrightarrow q \geq E + E_3 - 2E_2\end{aligned}$$

In this case, both conditions are represented by a single step function, namely $\Theta(q - |2E_2 - E_3 - E|)$. Therefore, all step functions together give

$$\Omega(q, E, E_2, E_3) = \Theta(E_2)\Theta(E_3)\Theta(E + E_3 - E_2)\Theta(q - |E - E_3|)\Theta(E + E_3 - q)\Theta(q - |2E_2 - E_3 - E|).$$

In order to obtain (4.35), we finally use that

$$\Theta(E+E_3-q)\Theta(q-|2E_2-E_3-E|) = \Theta(E+E_3-q)(1-\Theta(|2E_2-E_3-E|-q)) = \Theta(E+E_3-q)-\Theta(|2E_2-E_3-E|-q),$$

since in the second term positivity of one of the arguments implies positivity of the other such that one step function is redundant. Inserting this into $\Omega(q, E, E_2, E_3)$ then finally results in (4.35).

Proof of (4.45)

Again we need to figure out the constraints from the integration over the delta functions. Proceeding like we did for the proof of (4.35), we obtain first of all

$$\begin{aligned}
\cos\vartheta \leq 1 &\Leftrightarrow E_1 - E_3 \leq k \leq 2E + E_3 - E_1 \\
\cos\vartheta \geq -1 &\Leftrightarrow k \geq E_3 - E_1 \\
\cos\chi \leq 1 &\Leftrightarrow E_1 - E_3 \leq k \\
\cos\chi \geq -1 &\Leftrightarrow E_3 - E_1 \leq k \leq E_1 + E_3
\end{aligned}$$

This is summarized by a factor $\Theta(k-|E_1-E_3|)\Theta(2E+E_3-E_1-k)\Theta(E_1+E_3-k)$. All k dependent step functions together then make up a factor of

$$\Theta(k-k^*)\Theta(k-|E_1-E_3|)\Theta(2E+E_3-E_1-k)\Theta(E_1+E_3-k).$$

Now we want to trade as many of the k's for a k^* as possible. For this purpose we first rewrite the product of four step functions as a sum of two products of three step functions:

$$\begin{aligned}
&\Theta(k-k^*)\Theta(k-|E_1-E_3|)\Theta(2E+E_3-E_1-k)\Theta(E_1+E_3-k) \\
&= \Theta(k-k^*)\Theta(k-|E_1-E_3|)\Theta(2E+E_3-E_1-k)[1-\Theta(k-E_1-E_3)] \\
&= \Theta(k-k^*)[\Theta(k-|E_1-E_3|)-\Theta(k-E_1-E_3)]\Theta(2E+E_3-E_1-k)
\end{aligned}$$

where $\Theta(x-a)\Theta(x-|a|) = \Theta(x-a)$ was used. Now we multiply both terms with 1 in the form $1 = \Theta(x)+\Theta(-x)$. The factor $\Theta(2E+E_3-E_1-k)$ will not be further manipulated and we leave it out:

$$\begin{aligned}
&\Theta(k-k^*)\Big[\Theta(k-|E_1-E_3|)-\Theta(k-E_1-E_3)\Big] \\
&= \Theta(k-k^*)\Big[\Theta(k^*-|E_1-E_3|)+\Theta(|E_1-E_3|-k^*)]\Theta(k-|E_1-E_3|) \\
&- \Theta(k-k^*)[\Theta(k^*-E_1-E_3)+\Theta(E_1+E_3-k^*)\Big]\Theta(k-E_1-E_3)
\end{aligned}$$

This can now be simplified to the expression found in (4.45) since one of the step functions in each term is redundant. We have for example

$$\Theta(k-k^*)\Theta(k^*-|E_1-E_3|)\Theta(k-|E_1-E_3|) = \Theta(k-k^*)\Theta(k^*-|E_1-E_3|)$$

Putting it all together we then arrive at (4.45).

Proof of (4.67)

Finally we prove (4.67). The proof uses the Saclay representation (2.19), only that instead of the analogue of (2.20) for HTL resummed propagators, we express the propagators $\Delta(\tau,\vec{p})$ in terms of the corresponding *spectral functions* by using (2.10). The advantage is that we already know the spectral functions explicitly–for the Higgs boson it is given by (2.15) and for the lepton by (2.34). This means that after performing the thermal sum as explained in section 2.1.1, we have

$$S = \int_0^\beta \mathrm{d}\tau e^{i\omega\tau}\Delta(\tau,\vec{k})\Delta(\tau,\vec{q}). \tag{F.1}$$

where

$$\Delta(\tau,\vec{k}) = \int_{-\infty}^{\infty} \frac{\mathrm{d}k^0}{2\pi} e^{-k^0\tau} D^{>}(k^0) = \int_{-\infty}^{\infty} \frac{\mathrm{d}k^0}{2\pi} e^{-k^0\tau}(1+f_B(k^0))\rho(k^0,\vec{k}) \tag{F.2}$$

and analogously

$$\Delta(\tau,\vec{q}) = \int_{-\infty}^{\infty} \frac{\mathrm{d}q^0}{2\pi} e^{-q^0\tau} S^{>}(q^0) = \int_{-\infty}^{\infty} \frac{\mathrm{d}q^0}{2\pi} e^{-q^0\tau}(1-f_F(q^0))\tilde{\rho}(q^0,\vec{q}). \tag{F.3}$$

Inserting this back into (F.1) and performing the integral over τ using $e^{i\omega\beta} = -1$ leads to

$$S = -\left(e^{-(k^0+q^0)\beta}+1\right)\int_{-\infty}^{\infty}\frac{\mathrm{d}k^0}{2\pi}\int_{-\infty}^{\infty}\frac{\mathrm{d}q^0}{2\pi}(1+f_B(k^0))(1-f_F(q^0))\frac{\rho(k_0,\vec{k})\tilde{\rho}(q^0,\vec{q})}{i\omega-k^0-q^0}.$$

The discontinuity is then given by

$$\mathrm{Disc}\, S(p^0) = -2\pi i\left(e^{-(k^0+q^0)\beta}+1\right)\int_{-\infty}^{\infty}\frac{\mathrm{d}k^0}{2\pi}\int_{-\infty}^{\infty}\frac{\mathrm{d}q^0}{2\pi}(1+f_B(k^0))(1-f_F(q^0))\rho(k_0,\vec{k})\tilde{\rho}(q^0,\vec{q})\delta(p^0-k^0-q^0) \tag{F.4}$$

Now we only need to use that

$$\left(e^{-(k^0+q^0)\beta}+1\right)(1+f_B(k^0))(1-f_F(q^0))\delta(p^0-k^0-q^0) = (e^{\beta p^0}+1)f_B(k^0)f_F(q^0)\delta(p^0-k^0-q^0)$$

and we arrive at (4.67).

Bibliography

[1] Besak, D. and Bödeker, D. *Hard thermal loops for soft and collinear external momenta*, JHEP 1005, 007 (2010). arXiv:1002.0022 [hep-ph]

[2] Anisimov, A., Besak, D. and Bödeker, D. *The complete leading order high-temperature production rate of Majorana neutrinos*, in preparation

[3] Landau, L. and Pomeranchuk, I. *Limits of applicability of the theory of bremsstrahlung electrons and pair production at high energies*, Dokl.Akad. Nauk Ser. Fiz. 92, 535 (1953)

[4] Migdal, A. *Bremsstrahlung and pair production in condensed media at high energies*, Phys.Rev. 103, 1811 (1956)

[5] Aurenche, P., Gelis, F. and Zaraket, H. *Landau-Pomeranchuk-Migdal effect in thermal field theory*, Phys.Rev. D 62, 096012 (2000). hep-ph/0003326

[6] Arnold, P., Moore, G. and Yaffe, L. *Photon emission from ultrarelativistic plasmas*, JHEP 0111, 057 (2001). hep-ph/0109064

[7] Arnold, P., Moore, G. and Yaffe, L. *Photon emission from quark-gluon plasma: Complete leading order results*, JHEP 0112, 009 (2001). hep-ph/0111107

[8] Peskin, M. and Schroeder, D. *An introduction to Quantum Field Theory* (Addison-Wesley, Reading, Massachusetts, 1999)

[9] LeBellac, M. *Thermal field theory* (Cambridge University Press, Cambridge, 1st paperback edition, 2000)

[10] Kapusta, J. and Gale, C. *Finite-Temperature field theory* (Cambridge University Press, Cambridge, 2nd edition, 2006)

[11] Kubo, R. *Statistical-mechanical theory of irreversible processes. I. General theory and simple applications to magnetic and conduction problems*, J.Phys.Soc. Japan 12, 570 (1957)

[12] Martin, P. and Schwinger, J. *Theory of many-particle systems. I*, Phys.Rev. 115, 1342 (1959)

[13] Baym, G. and Mermin, N. *Determination of thermodynamic Green's functions*, J.Math.Phys. 2, 232 (1961)

[14] Blaizot, J. and Iancu, E. *The Quark-Gluon Plasma: Collective Dynamics and Hard Thermal Loops*, Phys.Rep. 359, 355 (2002). hep-ph/0101103

[15] Linde, A. *Infrared problem in the thermodynamics of the Yang-Mills gas*, Phys.Lett. B96, 289 (1980)

[16] Braaten, E. *Solution to the perturbative infrared catastrophe of hot gauge theories*, Phys.Rev.Lett. 74, 2164 (1995)

[17] Bödeker, D. *Effective dynamics of soft non-abelian gauge fields at finite temperature*, Phys.Lett. B426, 351 (1998). hep-ph/9801430

[18] Bödeker, D. *From hard thermal loops to Langevin dynamics*, Nucl.Phys. B559, 502 (1999). hep-ph/9905239

[19] Aurenche, P., Gelis, F., Kobes, R. and Petitgirard, E. *Breakdown of the Hard Thermal Loop expansion near the light-cone*, Z.Phys. C75, 315 (1997). hep-ph/9609256

[20] Flechsig, F. and Rebhan, A. *Improved hard-thermal-loop effective action for hot QED and QCD*, Nucl.Phys. B464, 279 (1996)

[21] Bauer, C., Fleming, S., Pirjol, D. and Stewart, I. *An effective field theory for collinear and soft gluons: heavy to light decays*, Phys.Rev. D63, 114020 (2001). hep-ph/0011336

[22] Bauer, C., Pirjol, D. and Stewart, I. *Power counting in the soft-collinear effective theory*, Phys.Rev. D66, 054005 (2002). hep-ph/0205289

[23] Braaten, E. and Pisarski, R. *Soft amplitudes in hot gauge theories: A general analysis*, Nucl.Phys. B337, 569 (1990)

[24] Thoma, M. *Damping of a Yukawa fermion at finite temperature*, Z.Phys. C66, 491 (1995)

[25] Kiessig, C., Plumacher, M. and Thoma, M. *Decay of a Yukawa fermion at finite temperature and applications to leptogenesis*, arXiv:1003.3016v1 [hep-ph]

[26] Braaten, E. and Pisarski, R. *Simple effective lagrangian for hard thermal loops*, Phys.Rev. D45, 1827 (1992)

[27] Frenkel, J. and Taylor, J. *Hard thermal QCD, forward scattering and effective actions*, Nucl.Phys. B374, 156 (1992)

[28] Braaten, E. and Pisarski, R. *Resummation and gauge invariance of the gluon damping rate in hot QCD*, Phys.Rev.Lett. 64, 1338 (1990)

[29] Braaten, E. and Pisarski, R. *Calculation of the gluon damping rate in hot QCD*, Phys.Rev. D42, 2156 (1990)

[30] Baier, R., Nakkagawa, H., Niegawa, A. and Redlich, K. *Production rate of hard thermal photons and screening of quark mass singularity*, Z.Phys. C53, 433 (1992)

[31] Braaten, E. and Thoma, M. *Energy loss of a heavy quark in the quark-gluon plasma*, Phys.Rev. D44, 2625 (1991)

[32] Pisarski, R. *Scattering amplitudes in hot gauge theories*, Phys.Rev.Lett. 63, 1129 (1989)

[33] Peigne, S., Pilon, E. and Schiff, D. *The heavy fermion damping rate puzzle*, Z.Phys. C 60, 455 (1993). hep-ph/9306219

[34] Lee, T. *Abnormal nuclear states and vacuum excitation*, Rev.Mod.Phys. 47, 267 (1975)

[35] Cabibbo, N. and Parisi, G. *Exponential hadronic spectrum and quark liberation*, Phys.Lett. B 59, 67 (1975)

[36] Bolz, M., Brandenburg, A. and Buchmüller, W. *Thermal production of gravitinos*, Nucl.Phys. B606, 518 (2001). hep-ph/0012052

[37] Pradler, J. *Electroweak contributions to thermal gravitino production*, arXiv:0708.2786v1 [hep-ph]

[38] Rychkov, V. and Strumia, A. *Thermal production of gravitinos*, Phys.Rev. D75, 075011 (2007). hep-ph/0701104

[39] Brandenburg, A. and Steffen, F. *Axino dark matter from thermal production*, JCAP 0408, 008 (2004). hep-ph/0405158

[40] Gale, C. and Kapusta, J. *Vector dominance model at finite temperature*, Nucl.Phys. B357, 65 (1991)

[41] Asaka, T., Laine, M. and Shaposhnikov, M. *On the hadronic contribution to sterile neutrino production*, JHEP 0606, 053 (2006). hep-ph/0605209

[42] Kolb, E.W. and Turner, M. *The early universe* (Addison-Wesley, Redwood City, USA, 1990)

[43] Weldon, H. *Simple rules for discontinuities in finite-temperature field theory*, Phys.Rev. D28, 2007 (1983)

[44] Klein, S. *Suppression of bremsstrahlung and pair production due to environmental factors*, Rev.Mod.Phys. 71, 1501 (1999). hep-ph/9802442

[45] Arnold, P. *Quark-gluon plasmas and thermalization*, arXiv:0708.0812v4 [hep-ph]

[46] Moore, G. *Transport coefficients in hot QCD*, hep-ph/0408347

[47] Arnold, P., Moore, G. and Yaffe, L. *Photon and gluon emission in relativistic plasmas*, JHEP 0206, 030 (2002). hep-ph/0204343

[48] Larson, D. et al. *Seven-year Wilkinson Microwave Anisotropy Probe (WMAP) observations: Power spectra and WMAP-derived parameters*, arXiv:1001.4635 [astro-ph]

[49] Komatsu, E. et al. *Five-Year Wilkinson Microwave Anisotropy Probe (WMAP) observations: Cosmological interpretation*, Astrophys.J.Suppl. 180, 330 (2009). arXiv:0803.0547 [astro-ph]

[50] Sakharov, A. *Violation of CP invariance, C asymmetry and baryon asymmetry of the universe*, JETP Letters 5, 24 (1967)

[51] Dine, M. and Kusenko, A. *Origin of the matter-antimatter asymmetry*, Rev.Mod.Phys. 76, 1 (2004). hep-ph/0303065

[52] Cline, J. *Baryogenesis, Lectures at Les Houches Summer School, Session 86: Particle Physics and Cosmology: the Fabric of Spacetime, 7-11 aug. 2006*, hep-ph/0609145

[53] Fukugita, M. and Yanagida, T. *Baryogenesis without grand unification*, Phys.Lett. B174, 45 (1986)

[54] Kuzmin, V., Rubakov, V. and Shaposhnikov, M. *On anomalous electroweak baryon-number non-conservation in the early universe*, Phys.Lett. B155, 36 (1985)

[55] Gell-Mann, M., Ramond, P. and Slansky, R. *Complex spinors and unified theories, in: Supergravity, ed. by P. van Nieuwenhuizen and D.Z. Freedman* (North-Holland Publ. Co, Amsterdam, 1979)

[56] Davidson, S., Nardi, E. and Nir, Y. *Leptogenesis*, Phys.Rep. 466, 105 (2008). arXiv:0802.2962 [hep-ph]

[57] Covi, L., Rius, N., Roulet, E. and Vissani, F. *Finite temperature effects on CP-violating asymmetries*, Phys.Rev. D57, 93 (1998). hep-ph/9704366

[58] Giudice, G. et al. *Towards a complete theory of thermal leptogenesis in the SM and MSSM*, Nucl.Phys. B685, 89 (2004). hep-ph/0310123

[59] Anisimov, A., Buchmüller, W., Drewes, M. and Mendizabal, S. *Leptogenesis from quantum interference in a thermal bath*, Phys.Rev.Lett. 104, 121102 (2010). arXiv:1001.3856v2 [hep-ph]

[60] Garny, M., Hohenegger, A., Kartavtsev, A. and Lindner, M. *Systematic approach to leptogenesis in nonequilibrium QFT: vertex contribution to the CP-violating parameter*, Phys.Rev. D 80, 125027 (2009). arXiv:0909.1559v2 [hep-ph]

[61] Garny, M., Hohenegger, A., Kartavtsev, A. and Lindner, M. *Systematic approach to leptogenesis in nonequilibrium QFT: self-energy contribution to the CP-violating parameter*, Phys.Rev. D 81, 085027 (2010). arXiv:0911.4122 [hep-ph]

[62] Braaten, E. and Yuan, T. *Calculation of Screening in a Hot Plasma*, Phys.Rev.Lett. 66, 2183 (1991)

[63] Besak, D. *Leptogenesis in two different models of the Universe* (Diploma thesis, University of Dortmund, 2007)

[64] Hahn-Woernle, F., Plumacher, M. and Wong, Y. *Full Boltzmann equations for leptogenesis including scattering*, JCAP 0908, 028 (2009). arXiv:0907.0205v2 [hep-ph]

[65] Arason et al., H. *Renormalization-group study of the SM snd its extensions: The SM*, Phys.Rev. D 46, 3945 (1992)

[66] Schrempp, B. and Wimmer, M. *Top quark and Higgs boson masses: Interplay between infrared and ultraviolet physics*, Prog.Part.Nucl.Phys. 37, 1 (1996). hep-ph/9606386

[67] Amsler, C. et al. *Review of Particle Physics*, Phys.Lett. B 667, 1 (2008)

[68] Pilaftsis, A. and Underwood, T. *Resonant leptogenesis*, Nucl.Phys. B692, 303 (2004). hep-ph/0309342

[69] Garny, M., Hohenegger, A. and Kartavtsev, A. *Quantum corrections to leptogenesis from the gradient expansion*, arXiv:1005.5385 [hep-ph]

[70] Strumia, A. *Thermal production of axino Dark Matter*, JHEP 1006, 036 (2010). arXiv:1003.5847 [hep-ph]

[71] Bailly, S., Choi, K., Jedamzik, K. and Roszkowski, L. *A re-analysis of gravitino Dark Matter in the constrained MSSM*, JHEP 0905, 103 (2009). arXiv:0903.3974v2 [hep-ph]

[72] Weldon, H. *Effective fermion masses of order gT in high-temperature gauge theories with exact chiral invariance*, Phys.Rev. D26, 2789 (1982)

[73] Weldon, H. *Structure of the gluon propagator at finite temperature*, Ann.Phys. 271, 141 (1999)

[74] Aurenche, P., Gelis, F. and Zaraket, H. *A simple sum rule for the thermal gluon spectral function and applications*, JHEP 0205, 043 (2002). hep-ph/0204146

[75] Aurenche, P., Gelis, F., Moore, G. and Zaraket, H. *Landau-Pomeranchuk-Migdal resummation for dilepton production*, JHEP 0212, 006 (2002). hep-ph/0211036

[76] Fischer, H. and Kaul, H. *Mathematik fuer Physiker, Bd.2* (Teubner, Wiesbaden, 3.Auflage, 2008)

Acknowledgements

Without any questions, there would never be an answer,
he who was never freezing will not like the heat.
You can't truly be happy without going through disaster,
and only the sunrise is coming for free.

The road towards obtaining a PhD is not an easy one. It is full of potholes and pitfalls and a subliminal worry that you will never arrive is a constant companion along the way. Indeed, one person alone would probably never be able to arrive at the desired goal in a finite amount of time and this is the place to express my gratitude to all people who, in one way or another, contributed to my biggest personal achievement until now.

First and foremost, I'd like to take the opportunity to thank my thesis advisor, Prof.Dr.Dietrich Bödeker. Without his constant guidance, completing this thesis successfully would have definitely been impossible. He was always thoroughly helpful when help was needed and never reluctant to answering my "stupid questions". I learned a lot from our numerous discussions and his comments on my work, and our collaboration was always a pleasant one. In addition, he gave me the opportunity to participate in national and international conferences where I could present parts of my research and I could visit interesting places–the midnight sun in Finland is something I certainly will never forget!

In the last year of my postgraduate studies, Dr.Alexey Anisimov joined our group. Without him, I would most likely still desperately try to get stable numerical results and struggle with solving the differential equations and evaluating integrals. Many thanks for all your effort and the insights you provided for me! As with my thesis advisor, the collaboration with Alexey was always very pleasureable and I enjoyed it very much.

I am further also grateful to Prof.Dr.Mikko Laine for refereeing my thesis and to Prof.Dr.Günter Reiss as well as Prof.Dr.Nicolas Borghini for being part of the examination board. Further thanks go to our secretaries Gudrun Eickmeyer and Susi von Reder who were always glad to help with organisatorial or administrative issues.

In the third year of my postgraduate studies I was given the opportunity to spend six weeks at the LPT Orsay in France and I thank Prof.Dr.Ulrich Ellwanger and Dr.Gregory Moreau for their reception and for reserving some time for discussion.

The quality and efficiency of research is only one aspect of a successful and enjoyable time of postgraduate studies. In order to "survive" this long and stressful time, nice colleagues and a pleasant working atmosphere are equally important. And I was indeed lucky to have great office mates all the time. In the first place I have to thank Tillmann Funke with whom I shared my office during the entire three years. He not only proofread large parts of my thesis, he was also very helpful with computer issues and we had many discussions about all possible things, related to physics and my thesis and also going beyond that. Thanks also for enduring my endless talking about a certain female singer!
What was said about Tillmann largely applies also to my other office mates, in particular Sebastian Schmitz and Ioan Ghisoiu. But also the other people from the physics department contributed to the great atmosphere and I will keep them in good memory. In particular, I want to mention Ervin Bejdakic, Sabine Bönig, Hengtong Ding, Florian Kühnel, Jan Möller, Dirk Rollmann, Marina Seikel, Maik Stuke and Wolfgang Unger. Thanks for a great time!

During nearly the complete time of my postgraduate studies I was financially supported by the DFG funded graduate school GRK 881 "Quantum Fields and Strongly Interacting Matter" which is, last but not least, greatly acknowledged.